Doctoral Dissertation
Doctoral Program in Civil and Environmental Engineering (XXXII cycle)

Development and characterization of capsule-based self-healing cementitious materials

Giovanni Anglani
* * * * * *

Supervisor
Prof. Paola Antonaci

Doctoral Examination Committee:
Prof. Tomoya Nishiwaki, Referee, Tohoku University
Prof. Mercedes Sánchez Moreno, Referee, University of Cordoba
Prof. Vítor M.C.F. Cunha, University of Minho
Prof. Elke Gruyaert, KU Leuven
Dr. Ana María Guerrero Bustos, Spanish National Research Council
Prof. Jean-Marc Tulliani, Politecnico di Torino

Politecnico di Torino
September 25, 2020

I hereby declare that, the contents and organization of this dissertation constitute my own original work and does not compromise in any way the rights of third parties, including those relating to the security of personal data.

. . . . . .

Giovanni Anglani

Turin, September 25, 2020

Summary

Concrete is the most widely used building material on earth. However, concrete structures present several issues that threaten their durability and consequently the safety of their users. One of the major hindrances to the durability of concrete is its susceptibility to cracking. Cracking leads to the reduction of mechanical properties and contributes to create pathways for the penetration of aggressive agents into the bulk material. In order to avoid major durability problems, concrete structures need to be repaired, but repair works can present several issues such as the individuation and access to the damaged zones, the direct cost to realize them, the indirect cost connected to the loss of serviceability, and the environmental impact in terms of carbon dioxide emissions for the production of new cement.

In the last decade, significant advancements have been achieved concerning the enhancement of the longevity of the cementitious structures using preventive repair methods defined as self-healing techniques. These techniques may be implemented based on the autogenous healing mechanisms naturally present in cement-based materials and through strategies aimed to improve it or to built-in new autonomous healing properties. Among these technologies, capsule-based self-healing using macro-encapsulation is being increasingly acknowledged as a promising strategy to improve the durability and resilience of concrete structures.

The focus of this dissertation was the development and characterization of an efficient self-healing system using cementitious capsules filled with a suitable healing agent. The system should be able to provide repair directly at the damage location upon crack occurrence and achieve recovery in both durability-related and mechanical properties, also in presence of large cracks.

The research activities led to the development of a new manufacturing technique, which allowed to produce cementitious capsules with controlled and customizable dimensions using a polymer-modified cement paste. Moreover, the adopted coating and sealing procedures allowed the encapsulation of highly moisture-reactive healing agents. The capsules were used to successfully encapsulate and release several types of healing agents from the main types commonly used for self-healing applications: namely, sodium silicate solutions and water-repellent agents (minerals), highly moisture-reactive polyurethane precursors (polymers), and ureolytic bacterial strain *Bacillus sphaericus* able to precipitate calcium carbonate (bacteria). The

investigation and comparison of the performances of the different healing agents allowed to select the polyurethane precursors as the most promising to realize the desired self-healing system.

Moreover, the cementitious capsules were proven effective in resisting the mixing procedure. This characteristic, combined with their inherent compatibility with the cementitious matrix and the easy customization of the capsules size and shape, makes cementitious capsules equivalent to enhanced aggregates that could be used in the ordinary construction processes.

The development of the final system followed several steps, with the aim to progressively improve it through the inputs offered by the characterization of intermediate tentative systems.

For what concerns the characterization in terms of recovery of durability-related properties, the sealing efficiency was assessed through the reduction of capillary water absorption and water permeability offered by the autonomous healing system. The tests were conducted using both testing techniques present in the relevant literature and novel techniques developed in the frame of this doctoral study. Specifically, a newly developed water permeability test allowed to characterize the system efficiency using stricter testing conditions.

As regards the recovery of the mechanical properties, this was first investigated via three-point bending test in order to apply indirect tensile stresses in static loading conditions, as in most of the scientific literature. Furthermore, the mechanical behavior was also tested in repeated cyclic loading conditions until rupture in order to obtain insights regarding the seldom studied fatigue performance of the self-healing systems. In fact, this is an aspect of paramount importance to develop a reliable autonomous repair system that can be used in real field conditions.

The performances of the self-healing system using cementitious capsules were also compared with those of a system using glass capsules, which is an encapsulation technique thoroughly studied by several research groups and that served as a benchmark for the newly developed system. This comparison was obtained through the application of a test protocol developed in the framework of a European inter-laboratory testing. This allowed also to prove the protocol applicability to different self-healing cementitious materials based on the use of macro-capsules.

Visual analyses of the crack faces were also carried out to estimate the spreading of the healing agent in order to complement the previous characterizations.

In conclusion, the main objective set for this doctoral thesis was achieved, namely the development and characterization of an efficient self-healing system for cementitious materials based on the encapsulation of polyurethane in newly-designed cementitious capsules. The final self-healing system allowed to obtain almost full recovery in both durability-related and mechanical properties after damage occurrence, proving that the system is able to improve the durability of cementitious structures and has a good potential for future scale-up.

Acknowledgements

Although a Doctoral dissertation is a single-authored work, the journey to get to this final goal is surrounded by many people that allowed to reach it and whose contribution must be acknowledged. Therefore, I would like to spend some words on all these people, hoping not to forget anyone.

The first and foremost person I would like to acknowledge is my supervisor, Prof. Paola Antonaci, who was the person that allowed me to start this amazing journey in the world of self-healing concrete, and that followed me in each step of it. In these years, she always embodied what a good leader in my opinion should be: firm without being severe, available for debate and ready to question herself, precise, patient, dedicated, and always ready to spend entire days working hard in the laboratory or discussing ideas, enjoying it and having fun. It was an honor to share the laboratory and its iconic *good smell*, together with many travels around the world. I treasure everything I learned from her in these years and I thank her for making me a better researcher.

I wish to thank Prof. Tomoya Nishiwaki and Prof. Mercedes Sánchez Moreno for acting as referees of this dissertation, their thoughtful comments greatly helped me in improving the initial manuscript and making it this final Doctoral Dissertation. With them, I wish also to thank Prof. Vítor Cunha, Prof. Elke Gruyaert, Dr. Ana Guerrero, and Prof. Jean-Marc Tulliani for their willingness in joining my Doctoral Examination Committee and discuss this work together. The possibility of discussing my work with such an international panel of experts, especially in this particular year in which the COVID-19 pandemic forced all of us to stay apart, was a real honor.

Thanks also to Prof. Giuseppe Lacidogna, Prof. Pietro Cornetti, and the late Prof. Vincenzo Ilario Carbone, which acted as the internal commission in the annual evaluation of my doctoral research activities. Thanks to Prof. Lacidogna also for being the thematic area referent of my scholarship, which financed my studies for the duration of the PhD program, and all the nice conversations about food and history in front of the Departmental coffee machine during breaks. I also wish to thanks Prof. Luca Ridolfi and Prof. Giulio Ventura for being always helpful and available as Coordinators of my PhD Programme in Civil and Environmental Engineering.

Without any doubt, this dissertation would not exist without the essential collaboration that I received from whom I consider the best lab technician that a researcher could wish to meet during his life: Mr. Vincenzo Di Vasto. His dedication to the work in the laboratory is praiseworthy and always reflected his passion for continuously learning and put his knowledge at the service of the others. I always found amazing that each time we discussed how to better perform an experiment or solve a problem in the afternoon, I found him in the lab the morning after with the table full of sketches or already with the best solution on how to tackle each issue. I take with me all our discussion in the lab, all his humble teachings, and all the help he gave me in performing the experiments included in this thesis for which I wish to thank him.

I wish to thank also all the amazing technicians working in the main laboratory of the Department of Structural, Geotechnical and Building Engineering for what concerns the testing of materials and structures, the MASTRLAB, which were always available in helping me when needed: Vincenzo Angilletta, Giovanni Bricca, Davide Carello, Stefano Di Domenico, Franco Grindatto, Piero Provenzano, Dario Varretto, with their coordinator Dr. Antonino Quattrone and the head of the laboratory Prof. Donato Sabia.

I would like to express my gratitude to Prof. Pietro Giovanni Bocca, which was the first head of the labs in which I spent most of my time during these years, namely the Non Distructive Testing Laboratory and the Structural Safety Educational Laboratory (LaDiSSS). It was a pleasure to assist him and Paola during the Testing of materials, models, and structures course, which represented my first teaching experience.

I thanks also Prof. Gabriele Bertagnoli and Prof. Francesco Tondolo, who first introduced me to the amazing world of experimental research during my Master Thesis. It is also thanks to that experience and their guidance if I decided that my life after graduation should have been continually surrounded by bags of cement, testing machines, and data to be analyzed.

The development of this thesis was made possible also thanks to many collaboration from the academic and industrial worlds.

I am willing to acknowledge Prof. Jean-Marc Tulliani from the Department of Applied Science and Technology of Politecnico di Torino for its collaboration in the development of the polymer-modified cement paste and the manufacturing process that allowed to create the cementitious capsules. It was a pleasure to share with him a long trip by car from Turin to Bayonne and back in order to participate in a conference. I thanks also Prof. Antonio Gliozzi and Prof. Marco Scalerandi, also from the Department of Applied Science and Technology of Politecnico di Torino, who first introduced me to the interesting world of non-destructive testing and nonlinear acoustic. It was a pleasure to share many lunches together, another long trip by car and boat to join my first conference together, and spent many days in front of the oscilloscope in their laboratory.

For what concerns the industrial partner, I want to thank Buzzi Unicem SpA for providing cement, Stefano Airoldi from Minova CarboTech GmbH for providing the polyurethane precursor that allowed the creation of the final self-healing system developed in the thesis, and Beniamino Magnaghi from API SpA for providing the epoxy resins that contributed in the creation of the encapsulation technology.

During my PhD journey, I was lucky to take an active part in the activities of the COST Action CA15202 SARCOS (https://www.sarcos.eng.cam.ac.uk), which allowed me to work and develop my research activity in a very stimulating international environment. It was amazing to take part in many meetings, conferences, training schools, and in two very interesting inter-laboratory testings, which allowed me to learn and apply that new knowledge to my study. I wish to acknowledge also the financial support of the SARCOS Action, which supported me through a Travel Grant to participate in the 1st SARCOS Training School in Lisbon. It was a pleasure to meet so many researchers working together towards the same objectives and I will always remember with joy the tourist time around Lisbon with Riccardo, Tim, Estefania, Tarmesh, Brubeck, Martina, Puput, and Xuejiao.

Moreover, the SARCOS COST Action financially supported me with an STSM Grant that I gratefully acknowledge, which allowed me to spend about two months in the amazing Magnel-Vandepitte Laboratory for Building Materials and Structures of Ghent University. I wish to express my gratitude towards Prof. Nele De Belie and Prof. Kim Van Tittelboom for being my supervisor, allowing me to work in an inspiring and efficient work environment, that I will always consider the Wonderland of concrete research. Working with you allowed me to improve myself, my approach towards research and writing, and the collaborations established since those days are always a great source of inspiration. My work there, which converged also in this dissertation, was made possible also thanks to the collaboration with great colleagues: Tim Van Mullem, Xuejiao Zhu, and Prof. Jianyun Wang. I wish also to thank the fundamental contribution of the technical staff of the Magnel-Vandepitte Laboratory, especially Tommy De Ghein, Dieter Hillewaere, Nathan Lampens, and Tom Stulemeijer. With them, I want to thank also the many colleagues with which I shared my time in the laboratory or the canteen during lunch breaks, especially Bjorn, Natalia, Didier, Puput, Roberto, Xiujiao, Kai, Yu, Laurence, Philip, Robin, and Alessandro. It is always a pleasure to meet all of you around the world during conferences.

I wish to thanks also the group from the Microlab of TU Delft for the interesting collaborations that we carried on in these years, in particular with Prof. Erik Schlangen, Prof. Branko Šavija, Claudia Romero Rodriguez and Emanuele Rossi. Your research group is always a hotbed of ideas and every occasion in which I could discuss with you, I found myself enriched with new ideas. I am also grateful to Prof. Schlangen, along with the other organizers of the mini-symposium about "Self healing of concrete" of the 10th International Conference on Fracture Mechanics of Concrete and Concrete Structures (FraMCoS-X), Prof. Liberato Ferrara and

Prof. Tony Jefferson, for granting me the possibility to give one of the keynote lectures of the conference, while being still a PhD student. I always consider that moment as one of the greatest acknowledgment of my PhD journey. I also want to acknowledge Claudia for all the days spent talking about research, sharing our ideas, doubt, enthusiasm, and also talking about less professional aspects of our lives. It is incredible how we spent years in the same classes just to find ourselves in two different countries studying self-healing concrete and starting our friendship at a conference in Germany. I value her as an amazing colleague and I am grateful for having such a good friend.

I would also like to acknowledge several students I have worked with during these years: Luca Salini, Giuseppe Idone, Martina Genovese, Susana Carrillo, Giorgia Paganelli, Luca Mercuri, Rui Ye, Carmela Cioffi, Mattia Giovanni Zoda, Nicole Priante, and all the students of the Testing of materials, models and structures course. You all contributed somehow to my work and to my attempts to learn how to be a good supervisor and teacher, which I hope that were at least sufficient.

The journey towards the conclusion of this PhD was made way more enjoyable also thanks to the presence of the many amazing colleagues I met in our Department, many of which I consider among my best friends nowadays. The first group of people that I want to gratefully acknowledge for their friendship and the many moments spent together greatly contributed in making the third floor of our Department, where we spent most of our days in our offices, a very special place: Alessandra, Alice, Fabio, Fabrizio, Francesco, and Matteo. Some of us are still on that third floor, while some left and started new journeys, but I am happy that our friendship goes beyond sharing a workplace. I treasure every moment, every talk, every laugh that we spent together in these years, thank you very much.

In the past years, I shared the office with two office mates: Gianluca and Marco. It was nice to share the workplace with you, trying to solve each other work issues, learning at least a little bit from your field of studies, and many times stop laughing because we were afraid of being too noisy.

A special thanks goes also to Giorgia, which I met as one of the newest colleagues while I was starting my last year of PhD and that ended up becoming one of my best friends, roaming around the Department and outside of it as Timon and Pumbaa. I thank her and Francesco for our beautiful friendship.

There were many colleagues in these years with whom I shared entire days (and also many nights). I would like to spend some words for everyone, but I will limit myself to say that they all contributed to making all those days (and nights) better and memorable: Alessandra R., Alessandro C., Alessandro L., Alessio, Amedeo, Andrea, Costanza, Domenico, Elena, Erica, Federico A., Federico P., Francesco, Gaetano, Giampiero, Gianfranco, Gianmarco, Gianni, Giulia D.L., Giulia M., Gregorio, Mahesh, Mariana, Marica, Mauro, Nicola, Oliver, Oscar B., Oscar M., Paolo C., Paolo T., Renato, Renzo, Rinto, Sebastiano, and Silvio.

I wish to acknowledge also some colleagues that came to our University from

abroad. The time spent with you was rather limited with respect to other colleagues, but I greatly enjoyed meeting you, learn from your cultures, and spend many beautiful moments together: Soyoun, Margaux, Lili, He Qi, Hamza, and Piotr.

Another group of special people that I met thanks to the life at Politecnico di Torino came from another Department, but it would be reductive to consider them just my friends from DIATI. We shared days, nights, lunches, dinners, weddings, new births, laughs, tears of joy and all of them made my life a little bit more special: Angela, Alessandro, Andrea, Kharen, Miriam, Ruggero, Riccardo, Alberto, Margherita, Nicola, and the little newborn members Giorgio, Asia, and Alma.

Beyond the "academic world", there are some people I must acknowledge for their presence in my life, that gave me joy and support throughout these years.

I wish to thank my dear Pata Team: Cristiano, Luca Bertone, Luca Boltri, Luis, and Paolo. We started as strangers in a big classroom of a University, we ended up scattered throughout the world, but our friendship goes beyond every distance. I want to thank them for these eleven years of friendship and for all the unforgettable memories we share together. I look forward to our next big trip around some foreign country.

I want to thank Elena Clara Maria for all our talk, our laugh, our mutual support, and all I learned from her about recycling and eco-sustainability, even if I do not always put in practice what I learned.

I wish to deeply thank Pamela, whose support was fundamental in the final rush towards this final goal. Although we met from such a short time, her presence made my days and my life much more special, happy, and complete.

I wish to thank my "second family", with whom I shared about half of my life: Ciccio, Marianna, Antonella, Peppe, and Benedetto. Thanks for all these years of friendship, all the laughs, the talk, the quarrels, and all the moments spent together. They really embody the concept that "home" is not a physical place and that a family does not necessarily have to share the same blood.

I want to conclude with a great thanks to my first and real family, that supported me way before this amazing PhD journey. I want to thank my uncle Leonardo, my aunt Claudia, and my cousins Tullio, Giovanni, and Luca. I wish to thank Ignazio, my "big" brother, even if growing up I became way bigger than him. He was always there for me, regardless of the distances. Thanks for looking after me since the moment I was born, you deserve the best that life can give. I am happy that he found a special person, Enrica, which I consider as a sister. A special thanks go to my mother and father (*Mamma and Papà*), Miranda and Adriano. Thanks for allowing me to be here now, concluding this thesis, because if I am here it is just thanks to their support and unconditional love. My final words go to my grandparents, Liliana and Nino (*Nonna and Nonno*). They are the greatest example of love that I met in my life and supported me also from a distance when I first moved to Turin to study for my Bachelor in 2009. It always made me happy to

hear your words, through a phone call or in person during holidays, feeling how proud you always were of your grandson. Unfortunately, Nonno left us one year ago at the venerable age of 97 years. I treasure all his words, all the moment spent together, and everything I learned from him. I am sure that if he was still here with us, regardless of the language in which this dissertation is written, he would have asked a copy of it to watch it carefully, page by page. For all these reasons, I want to dedicate this work to him, in loving memory of his life and my time with him.

Contents

List of Tables

List of Figures

Chapter 1

Introduction

1.1 Background and problem statement

Concrete is the most widely used building material on earth, with an estimated yearly consumption approaching 30 billion tons [1]. However, the cement manufacturing industry is currently under scrutiny because of the large volumes of CO_2 emitted during the production of Portland cement, since the production of cement contributes about 5-10% to the global anthropogenic CO_2 emission, through the calcination process of limestone and combustion of fuels in the kiln [1, 2]. In view of this problem, research in the construction and building materials sector is targeting alternative materials to partly or totally replace the ordinary Portland cement, such as supplementary cementitious materials derived from industrial by-products [3–6]. Moreover, the analysis of the carbon footprint of a structure also involves the estimation of its lifetime and the CO_2 emissions associated with its use, maintenance, and repair. Furthermore, repair works have also a big economic impact, other than environmental. Just in Europe, it is estimated that around half of annual construction budget is spent on rehabilitation and repair [7]. Moreover, indirect costs due to loss in productivity can be much higher than the direct costs involved in maintenance and repair [8].

Indeed, the proper maintenance of a concrete structure and the selection of appropriate repair products and techniques is essential to guarantee and extend the designed lifetime [9], thus limiting the need for demolition and production of new concrete that would further increase the carbon footprint of the structure. Enhancing the longevity of the built environment will undoubtedly reduce the impact of human activities on the stability of the biosphere [10].

One of the major hindrances to the durability of concrete structures is their susceptibility to cracking. It is well-known that all cementitious materials tend to have defects, resulting from incorrect mix design or execution, shrinkage, and other causes. Their low tensile strength, in combination with the presence of such defects, makes them prone to cracking. Cracks can occur all along the service life,

even in the earliest stages, due to several mechanisms, such as plastic and/or drying shrinkage, temperature changes, alkali-silica reaction (ASR), freeze-thaw damage, or structural loading. Because of the possible concurrent or subsequent action of cyclic loading, even micro-cracks can propagate and coalesce into macro-cracks, ultimately leading to a reduction of durability or even collapse [11]. This is especially true for the infrastructure sector, where several bridges and viaducts are at risk due to the severe conditions caused by the increasing demand of traffic volumes [12–14].

Even though cracking is required in order to engage the tensile capacity of the rebars in reinforced concrete, the presence of cracks, along with the intrinsic interconnected porosity of concrete, contributes to create pathways for the penetration of aggressive agents into the bulk material. Therefore, durability is strongly dependent on the ease with which fluids and fluid-borne aggressive substances penetrate through cracks and diffuse into the cementitious matrix. Water is one of the main vehicles for several detrimental substances that may attack either the concrete or the rebars, hence reducing the water ingress, especially from the cracks, will be reflected in a durability improvement of the material.

In order to avoid major durability problems, concrete structures need to be repaired. However, cracks in structures can be almost invisible or inaccessible, which makes repair works very difficult [15], especially when manual repair is involved.

In the last decade, significant advancements have been achieved concerning the enhancement of the longevity of the built environment, by moving from passive repair approaches, that require an external manual intervention, to active methods that are incorporated at the construction stage and are regarded as self-sealing or self-healing techniques [16, 17]. The first implies the filling and sealing of the crack, thus mitigating the ingress of deleterious substances present in the environment, the latter implies the recovery of the material properties as a consequence of the crack sealing [18, 19]. Several self-healing approaches are under study by the scientific community, such as the autogenous or intrinsic healing of traditional concrete, the stimulated autogenous healing via use of mineral additives, crystalline admixtures, or (superabsorbent) polymers, and the autonomous self-healing mechanisms through the application of micro-, macro-, or vascular encapsulated polymers, minerals, or bacteria [16].

1.2 Objectives

Capsule-based self-healing has been proposed as a promising strategy to improve the durability and resilience of reinforced concrete infrastructures [16–18, 20–24]. As regards the macro-encapsulation approaches, several types of capsules were thoroughly investigated [20, 25–31] by varying their shape, dimension, and constituent material. Several requirements must be fulfilled in order to obtain effective

systems: capsules should be compatible both with concrete and the encapsulated healing agent to protect it for a long time; they should be crack-responsive and able to release their content in order to fill and repair the cracks once formed, yet at the same time they should be able to resist the concrete mixing and casting processes. Finally, they should not affect the concrete mechanical properties significantly. In many studies, glass capsules were successfully used [20–22, 26, 29–34]. However, glass capsules may have a negative effect on concrete durability because of the possible onset of undesired alkali-silica reactions [16, 28]. In addition, the likeliness that these stay intact during mixing is low unless proper additional precautions are taken [27, 28, 35–37]. In previous studies, the use of cementitious hollow tubes (CHTs) produced with an extrusion process [38–40] was proven effective in meeting the above-mentioned requirements while presenting an inherent compatibility between the capsules shell and the cementitious matrix.

The extrusion process of a tailor-made polymer-modified cement paste was developed at Politecnico di Torino during the project "DualCEM: Development of self-healing cementitious materials with high durability" (2012-2014). The DualCEM project was financed by Regione Piemonte and was carried out through the cooperation between Politecnico di Torino, as an academic subject, and several companies as additional Research & Development subjects or end-users (Buzzi Unicem S.p.A., NovaRes s.r.l., ARIA s.r.l., Varnish Tech s.r.l., Silvateam S.p.a.). The project aimed to investigate two key technological factors of a self-healing concrete system: on one side the efficiency of different healing agents and, on the other side, the potential of different encapsulation technology approaches [40].

The good results of the project led to another project on these themes at Politecnico di Torino, namely the research project "SHEcrete: Development of advanced Self HEaling concrete systems with improved reliability and durability" (2015-2017), financed by Politecnico di Torino and Fondazione CRT and that was the starting point of this thesis work. The research was based on a multidisciplinary approach, that took its starting point from the study and selection of the optimal healing agents, alongside with the development of a production technology for capsules suitable to store such healing agents and release them at damage occurrence, in order to finally get to the production and physical-mechanical characterization of some prototypes of self-healing cementitious systems, with different performance levels.

Starting from what was done in the framework of these projects and after the complete review of the different strategies adopted in literature to obtain self-healing cementitious materials (as described in Chapter 2), it was decided to focus this doctoral study on the cementitious macro-capsule technology as autonomous healing mechanism. Specifically, the goal of the research was to improve the existing technology in order to obtain a self-healing cementitious system that could allow a high degree of recovery in both durability-related and mechanical properties after damage occurrence. In order to obtain the desired outcome, several intermediate

objectives must be fulfilled.

The first concerns the manufacturing of the self-healing system. Namely, it was necessary to further improve the cementitious capsule technology to allow its use for different manufacturing techniques other than the extrusion, in order to exert a higher control over the capsule final dimensions. Moreover, it was necessary to make the cementitious capsules suitable for the encapsulation of highly reactive healing agents, which require high standards in terms of tightness stability.

Then, the next intermediate objective was to assess the capability of the cementitious capsules to correctly protect and release the healing agents. Following this, it was necessary to assess the efficiency of different types of healing agents in correctly sealing the controlled cracks that were introduced to simulate the damage occurrence. This is an aspect of paramount importance to prevent the ingress of deleterious substances through the crack. Moreover, this allowed to highlight the different healing agents' advantages and disadvantages, in order to select the most suitable type to pursue the development of the final self-healing system.

Once that the most suitable healing agent was selected in order to guarantee a satisfactory self-sealing performance, the next intermediate objective was to test the mechanical recovery that can be offered by its use. This aspect was tested not only in static loading conditions as in most of the literature, but also investigating the seldom studied field of fatigue in self-healing cementitious systems. This represents an important aspect to be studied in order to decide if the system could be used in real field conditions.

The following intermediate objective was to compare the performances of the newly developed system based on cementitious capsules with those of another self--healing system based on the use of macro-capsules, namely glass capsules. This choice was done since this system was thoroughly studied in the past decades by several research groups with positive results, representing a good benchmark for a newly developed self-healing system.

Once that all these objectives were fulfilled, it was possible to bring together all the positive results obtained, in order to realize and test the final self-healing system and check if it could be capable of restoring most of the mechanical and durability-related properties of the damaged system.

In order to pursue these objectives, cement mortar prisms either with or without capsules were used. Cement mortar was selected as a prototypal cementitious material instead of concrete for several reasons. First, the healing agents' reactions usually do not depend on the mortar fraction and the aggregate-cement ratio, hence it is easier to evaluate their effect in a more homogenous matrix as the one offered by mortar. In addition to the fact that mortar is more homogenous with respect to concrete, the main reason for its use is the possibility to do a fast and cost-effective screening of different self-healing techniques before upscaling for use in concrete [41]. For this reason, cementitious mortar is commonly used in the literature on self-healing cementitious materials and consequently using it allows comparability

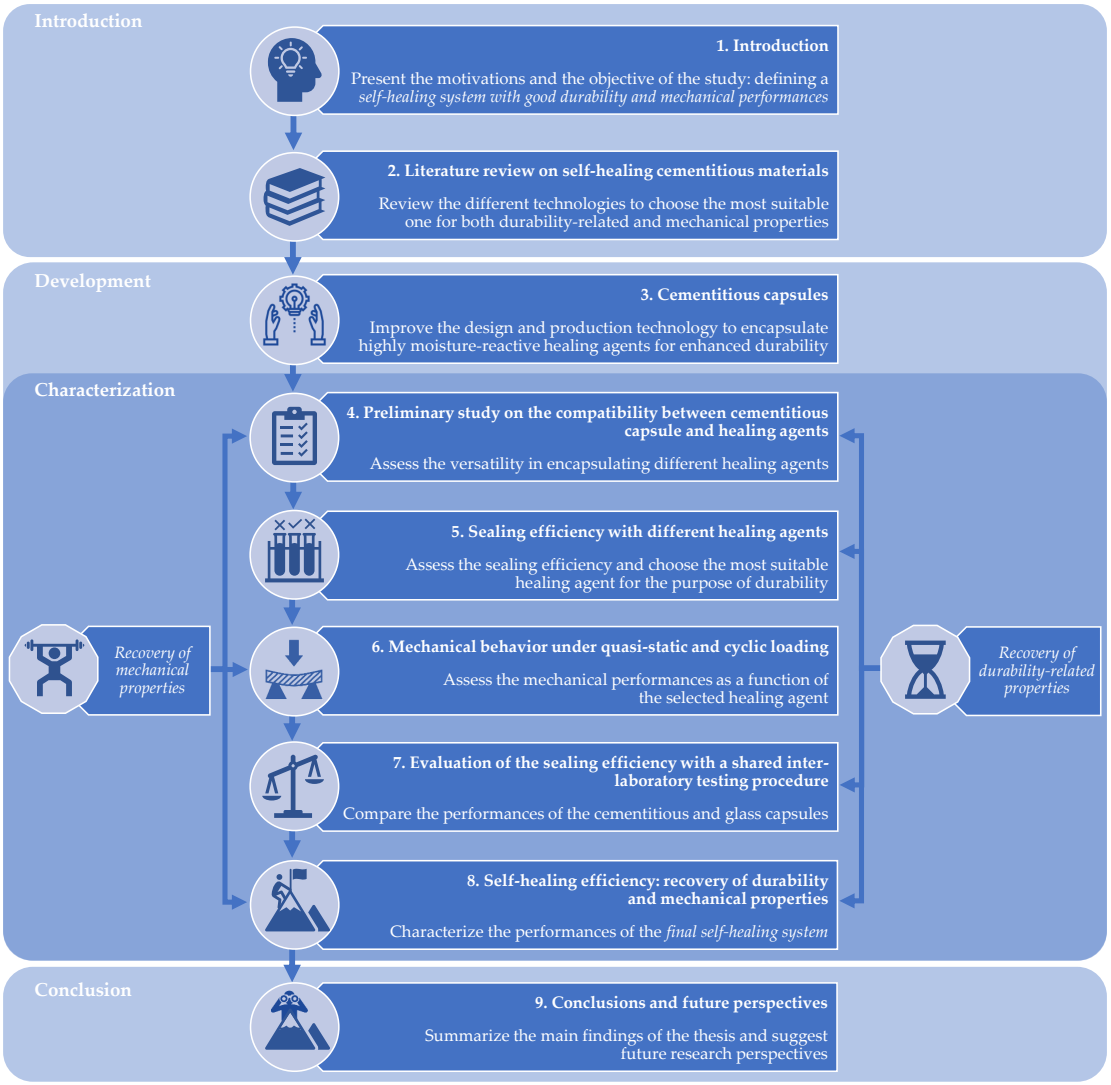

Figure 1.1: Outline of the thesis.

with other techniques and testing methods.

1.3 Outline of the thesis

The thesis is divided into nine chapters, which are organized as in Figure 1.1 and reflect the main objectives set in the previous section. The content of each chapter can be summarized as follows:

Chapter 1 In this first introductory chapter, the motivations and objectives of the research were stated. Moreover, the outline of this thesis is presented here.

Chapter 2 In this chapter, a literature review of the state-of-the-art on the development of self-healing cementitious materials is given, presenting the different self-healing technologies, encapsulation techniques, and healing agents. The analysis of the advantages and limitations of each self-healing technique allowed to select the macro-encapsulation based on the use of cementitious capsules as focus of this thesis.

Chapter 3 This chapter reports on the improvement of the autonomous healing mechanism based on the use of cementitious macro-capsules. The procedures that were developed in order to achieve a functional encapsulation system comprised the manufacturing techniques of the cementitious shell, its mix design, and the coating and sealing techniques to guarantee the correct tightness of the capsules. Moreover, a description of the healing agents that were selected for the study is provided.

Chapter 4 In order to start the characterization of the proposed autonomous healing technology, some preliminary studies were conducted on the compatibility of the cementitious capsules with various types of healing agents, which are presented in this chapter. These preliminary studies provided indications for the further investigation described in the thesis. In particular, it was observed that the cementitious capsules were able to effectively store and release different liquids regardless their chemical nature and reaction mechanisms. Therefore, they offered a high versatility for the purposes of self-healing since they do not impose specific technological limitations on the selection of the healing agent.

Chapter 5 The research activities described in this chapter were focused on the self-sealing capacity, hence the recovery of durability-related properties. For this purpose and to further highlight the flexibility of the encapsulation technique, healing agents from the three main types commonly used for self-healing applications (i.e. minerals, polymers, and bacteria) were encapsulated. The self-sealing capacity was investigated through water flow test, capillary water absorption test, and the visual analysis of the crack faces. This allowed to select the type of healing agent which seemed to be the most promising in counteracting the potential threats offered by the ingress of water and detrimental substances.

Chapter 6 After selecting the most promising healing agent, the research activities described in this chapter investigated the mechanical behavior that could be obtained by encapsulating such a healing agent inside cementitious capsules. This was first investigated via three-point bending test to apply indirect tensile stresses in static loading conditions, as in most of the scientific literature. Furthermore, the mechanical behavior was also tested in cyclic loading

conditions until rupture in order to obtain insights regarding the seldom studied fatigue performance of the self-healing systems. In fact, this is an aspect of paramount importance to develop a reliable autonomous repair system that can be used in real field conditions.

Chapter 7 The objective of the research activities presented in this chapter was to compare the performances of the self-healing system developed so far with those of the system using glass capsules, which is an encapsulation technique thoroughly studied by several research groups. This comparison was obtained through the application of an inter-laboratory testing procedure developed in the framework of the EU COST Action SARCOS. The aim of such procedure was filling the lack of standardized test methods and obtain sound and comparative characterization techniques for performance verification of self-healing cementitious materials. The inter-laboratory test protocol was applied to mortar specimens containing either cementitious or glass capsules filled with the same healing agent, in order to test the effectiveness of the self-healing system here proposed with a shared good-practice and also to prove the SARCOS protocol applicability to different self-healing cementitious materials based on the use of macro-capsules.

Chapter 8 Based on the inputs provided by the intermediate steps of the research, as reported in the previous chapters, the activities described in this chapter concerned the definition of a *final self-healing system* and the demonstration of its full self-healing capacity. Hence, the final outcome of the thesis was a self-healing system that could provide a good recovery of both durability-related properties and mechanical performances after damage occurrence. For the purpose of characterizing the recovery of durability-related properties, the final system was first pre-cracked and then investigated through two types of water flow tests after autonomous healing. The first water flow test is well-established in literature and was used also in the previous chapters. The second one was developed during the study to provide stricter testing conditions and check the system performance in comparison with the previous water permeability test. Subsequently, the mechanical recovery offered by the final system was investigated through static reloading of the healed system. A visual analysis of the crack faces was also carried out to estimate the spreading of the healing agent on the crack faces to complement the previous characterizations.

Chapter 9 To conclude, in this chapter the main research findings of the study are summarized and perspectives for further research are suggested.

Chapter 2

Literature review on self-healing cementitious materials

Natural materials are remarkably efficient and, for this reason, new material development is increasingly being inspired by the emulation of Nature, following a biomimetic approach. Among the properties of natural materials that would be highly beneficial for man-made materials, one of the most fascinating is the self--repair, inspired by biological systems in which damage triggers a healing response [42]. Some materials able to achieve some degree of autogenous healing properties already exist, such as the reoxidation in air of damaged oxide films that provide the corrosion resistance of aluminum, titanium, and stainless steel [42], the recrystallization of metals to restore the pre-deformed properties [42–44], and, of great interest for the construction sector, cementitious materials.

Autogenous self-healing of cement-based materials was noticed since 1836, when the French Academy of Science reported self-healing effect in water retaining structures, culverts, and pipes [18, 45, 46]. However, autogenous healing of cementitious materials has limited capacity, being restricted to small cracks and being effective when water is available [47]. For this reason, in the last decades the scientific community involved in the research of construction material showed increasing interest in developing innovative cementitious materials with built-in improved self-healing properties, with the aim of increasing the durability of this type of materials.

In the last decade, several detailed reviews were produced in order to classify and keep track of the progress in the development of self-healing cementitious materials [16, 18, 46–49]. In this chapter, an overview of the state-of-the-art there presented is given with the inclusion of recent works and examples of real scale applications, starting from the autogenous healing mechanisms and then moving to the strategies aimed to improve it or to built-in new autonomous healing properties.

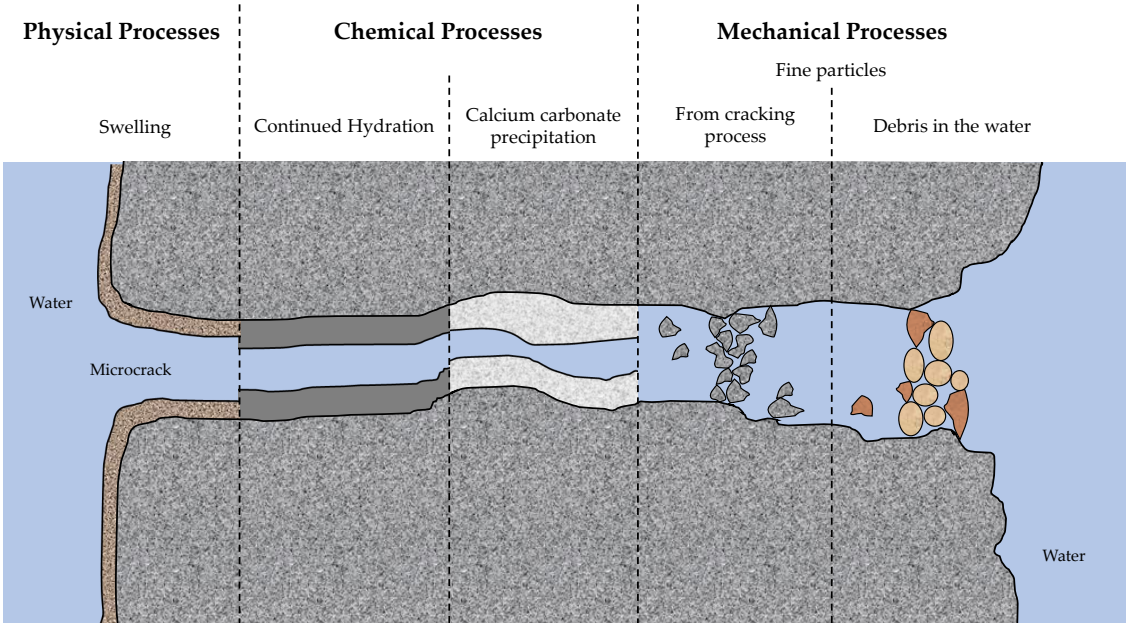

Figure 2.1: Main mechanisms causing autogenous self-healing of cementitious materials. Redrafted after De Rooij et al. (2013) [18] and De Belie et al. (2018) [16].

2.1 Autogenous healing

Autogenous healing of cementitious materials is the basic phenomenon that the intrinsic self-healing capability of cement-based materials [16]. It is considered one of the main reasons of the life extension of ancient structures, such as those built during the Roman Empire [42, 50, 51].

In the last century, research activity established that the autogenous self-healing phenomena are mainly related to physical, mechanical, and chemical mechanisms developing within the cementitious matrix [16, 18, 47, 48, 52], which are summarized in Figure 2.1 and can be classified in:

- Physical processes:
  - Matrix swelling.
- Chemical processes:
  - Continuing hydration of unhydrated cement grains;
  - Precipitation of calcium carbonate crystals ($CaCO_3$) on the crack faces, which can be produced by the chemical reactions between the calcium ions Ca^{2+} present in the concrete matrix with the carbonate ions $CO_3{}^{2-}$

available in the water, or with carbon dioxide CO_2 available in the air entering the crack.

- Mechanical processes:
  - Clogging of the crack by small particles, either produced by the cracking process or debris present in the water, bridging the crack surfaces.

The two most important mechanisms providing the autogenous healing of cementitious materials are the chemical processes. Continuing hydration is beneficial for regaining the mechanical properties [16, 53, 54], since these new hydration products have a strength similar to that of the calcium silicate hydrate (CSH) gels. These products are superior to the $CaCO_3$ precipitation products, however it is to be pointed out that products formed at the crack faces are different from those formed inside the matrix. On the other hand, carbonation was proven to be the most efficient in terms of crack sealing and self-healing performances [16, 18, 46, 47].

Studies aimed at investigating the autogenous healing efficiency [16, 18, 19, 46, 47, 52, 54, 55], defined that the main factors governing it are the availability of water, the age and composition of the cementitious material, and the width and shape of the cracks.

Water is an essential factor governing the autogenous healing, since its presence is necessary to allow the chemical reactions and the transport of fine particles causing the clogging mechanisms, while autogenous healing is limited in air exposure. Also, water temperature, pressure, and pressure gradient can influence the extent of the autogenous healing. Some authors found a better healing in wet–dry cycles compared to water immersion condition, probably due to easier calcium carbonate formation due to the availability of CO_2 in air during the dry phases. High pH environment favors the process of $CaCO_3$ formation, while water hardness is not relevant for the autogenous healing efficiency [55–58].

Regarding the composition, cement type does not have a major importance [56, 59] while the clinker content determines the Ca^{2+} ions content and consequently the ability to develop $CaCO_3$ precipitation [16]. Silicate additions have effects related to the development of their pozzolanic reactions and consumption of $Ca(OH)_2$, which affect the duration of healing mechanisms. Then, a low water to cement ratio (w/c) causes the increase of unhydrated cement grains, which can cause the development of new CSH products due to the ongoing hydration [54]. For what concerns the aggregate type, they have an indirect effect on the healing process by determining the cracking pattern. The age of the cementitious material is an aspect of paramount importance for to the healing mechanism: early age was proven as the most prolific in terms of healing [45, 54, 56, 60–64] due to the higher content of unhydrated binder particles which can develop new CSH gel, while at later ages

$CaCO_3$ deposits are the main cause for crack closing [54]. Also the age of first cracking is an important factor for the autogenous healing [61, 65–67].

Finally, cracks geometry determines the autogenous healing through their width, length, depth, and pattern. Narrower cracks result in more efficient autogenous healing. As a matter of fact, autogenous healing mechanisms were proven effective only for small cracks in the order of 10–100 µm, sometimes up to 200-300 µm in the presence of water [18, 19, 46, 47, 52, 54, 55]. Consequently, a way of improving the intrinsic healing potential is by limiting the crack width, which can be obtained through the addition of fibers in fiber-reinforced concrete (FRC) and high-performance fiber reinforced cementitious composites (HPFRCCs) [55, 68–72]. The addition of natural vegetable fibers, other than contributing to control the crack width, acted also as water reservoirs, absorbing it and releasing it later during dry periods, activating the continuing hydration and carbonation reactions [73, 74].

2.2 Stimulated autogenous healing

From what was discussed in Section 2.1, it is clear that the autogenous healing caused by the intrinsic properties of cementitious materials is rather limited, since cracks must be narrow and the presence of water is essential. For these reasons, methods to improve the autogenous healing by limiting the crack width, providing water, or enhancing hydration or crystallization were developed and are defined as stimulated autogenous healing.

2.2.1 Mineral additions

The use of mineral additions affects the autogenous self-healing through the modification of the hydration kinetics and the material properties. A positive aspect on their use is that many of these additions are already being used in the construction sector due to the growing attention on the use of supplementary cementitious materials (SCMs) to reduce the cement content of cementitious composites, limiting the material costs and its environmental impact related to the carbon dioxide emitted in the production of cement [75, 76].

The main mineral additions studied for their effects on self-healing are blast-furnace slag (BFS) and fly ash (FA). Since these additions remain unhydrated even at later age and thanks to the pozzolanic reaction, they promote autogenous healing due to continuing hydration [53, 77, 78]. It has to be pointed out that a minimum calcium hydroxide content is necessary to allow further reaction of BFS and FA during the healing process [79]. More evident self-healing products have been observed when incorporating BFS, since slag has a mixed cementitious and pozzolanic activity and can undergo delayed hydration reactions in the presence of low $Ca(OH)_2$

unlike pozzolans [75].

However, since the involved hydration kinetics are slow [80], methods have been studied to stimulate the healing process, such as the application of alkaline solutions [53, 81–83], higher curing temperature [84] or blending of different mineral additions [85–87].

Other mineral additions studied for their effect on the autogenous healing includes metakaolin [88], palm oil fuel ash [89] and expansive minerals such as magnesium oxide (MgO), bentonite, and quicklime (CaO) [90, 91]. For what concern the effect of these expansive additions, magnesium oxide stimulated the formation of brucite ($Mg(OH)_2$), bentonite influenced the formation of ettringite and layered microstructures, while quicklime allowed the production of additional portlandite ($Ca(OH)_2$), calcite ($CaCO_3$) and calcium-based hydration products [90].

2.2.2 Crystalline admixtures

The term crystalline admixtures (CA) derives from commercially available products whose constituents are generally not disclosed, consequently it does not reflect their functionality or molecular structure, and ongoing investigation are still carried in order to define what should be named crystalline admixture, based on their composition and their action [16]. In order to distinguish commercial crystalline admixtures from supplementary cementitious materials, it is possible to refer to their admixture dosage, which is typically 1% by cement weight for crystalline admixtures and higher than 5% for SCMs [16]. They share the same advantage of SCMs of being already a common admixture in the construction sector [92, 93].

Crystalline admixtures are classified as a special type of permeability reducing admixtures (PRA), namely among those that are capable to function under hydrostatic pressures (PRAH) [94, 95]. As a product of their reaction and depending on the crystalline promoter, CAs form modified CSH and a precipitate formed from calcium and water molecules. While some studies report that the matrix component that reacts is the tricalcium silicate [94], other studies indicate that crystalline admixtures react with portlandite [93, 96].

For what concern the self-healing efficiency related to the use of CAs, recovery of mechanical properties were proved through their addition to normal strength concrete [92], strain-hardening cementitious composites in combination with a calcium sulfoaluminate expansive agent [96], lime mortars [97] and in High Performance Fiber Reinforced Concrete (HPFRC) [93], where the synergy with the crack-restraining action of the fibers improved their performances. Improved performances were also obtained under exposure to chlorides, probably due the contribution of CAs to chloride binding [98–100]. Also their effectiveness under repeated cracking and healing cycles up to 1 year was tested [101–103].

Other than their mechanical performances, also the healing efficiency in terms of water permeability at high pressure and with visual inspection of the crack closure

was studied [104, 105], but did not show a substantial improvement compared with the control specimens without CAs.

Their efficiency in real scale application is currently under study in a prototype water basin realized in Italy close to an operating geothermal power plant by Enel Green Power in collaboration with Politecnico di Milano, in the framework of the EU H2020 project ReSHEALience [106].

2.2.3 Superabsorbent Polymers

Superabsorbent polymers (SAPs) are natural or synthetic 3D cross-linked homopolymers or copolymers with a high capacity to absorb fluids, with a swelling capacity that depends on the nature of the monomers and the cross-linking density [107] and an absorption behavior that is strongly conditioned by the ionic strength of the swollen medium [71, 108, 109].

The use of SAPs addition in cementitious materials is increasingly being studied, for example as internal curing agents in presence of a low water-to-binder ratio to reduce self-desiccation shrinkage during hardening and to mitigate autogenous shrinkage [110] or to increase the freeze-thaw resistance [111]. As regards their contribution to self-healing of cementitious materials, their addition produces several effects on this aspect.

A first effect caused by SAPs addition to the fresh matrix is the formation of macro-pores, caused by their swelling caused by their absorption of mixing water and successive shrink upon hardening of the matrix [112]. These macro-pores attracts [113] and stimulates multiple cracking [71, 114], acting as weak points in the matrix: these effects facilitate the crack healing since SAPs macro-pores will be crossed by multiple narrow cracks [72], easier to be cured by the internal curing action of the SAPs [115] acting as source of water and stimulus for continuing hydration [116, 117]. However, since macro-pores formation may have a detrimental effect on the mechanical properties [118], ways of reducing the swelling at the upon mixing were studied, either based on coating of the SAPs [119] or the development of synthetic pH-sensitive SAPs [114, 120, 121].

Another important effect of SAPs for the crack sealing and healing is their ability to swell and blocking the cracks upon ingress of liquid substances [113, 122, 123]. A good water permeability reduction due to the sealing effect was proven for cracks up to 150 mu [120, 124].

The efficiency of the SAPs addition was also tested with good results in a large scale lab test conducted by Ghent University on real scale concrete beams [21].

Due to the concern regarding the use of sustainable materials to reduce the impact on the environment, there has been a growing interest in developing natural and semi-synthetic SAPs [125, 126] to substitute the synthetic SAPs, which are mainly made of petroleum-based monomers and synthetic cross linkers [16].

2.2.4 Polymer Additions

Polymer-modified concrete (PMC) or polymer Portland cement concrete (PPCC) are a combination of cement and aggregate mixed with organic polymers, which causes upon hydration a coalescence of the polymer and the formation of a co-matrix of hydrated cement and polymer film [127]. The healing effect caused by the polymer addition is similar to the continuing hydration of normal cementitious materials, but with an extension in time due to the effect of coating of cement grains caused by the polymer films [127].

Various polymers were studied for self-healing application [128], due to this improvement in the delayed hydration and to add other effects to further improve the healing of cracks. For example, some researchers studied the use of epoxy resin, founding that their cross-linking is possible in the environment of cement paste without the presence of hardener due to availability of calcium hydroxide, causing the healing of cracks due to the resin that can remain unhardened in the pores [129–131]. Other researchers studied the use of elastomers to make oil well cements watertight without requiring contact with any type of fluid [132]. A further example of this type of additions is the use of ethylene vinyl acetate (EVA) to fill the cracks upon heating up to 150 °C [133]. Then, another use of the combination of polymers and heating is represented by bitumen-coated steel fibers, which have the twofold effect of restraining the cracks and being able to fill them with melted bitumen upon induction heating [134].

A different use of polymeric materials for self-healing applications is represented by shape memory polymer (SMP) tendons, which are a type of material able to recover their original shape after deformation [135] and that were used to mechanically close cracks [136, 137]. This is obtained by casting the tendons into structural elements and electrically activating them after cracking [138]. The shrinkage of the drawn PET tendons tends to close the cracks crossing them, also causing an increased potential of autogenous healing. The ability of the tendons to maintain the necessary post-activation crack closure force in the long-term was proved by Hazelwood et al. [139]. This technology was further improved by developing a new type of tendons formed from multiple drawn SMP filaments with higher restrained shrinkage potential and is currently being studied in a large scale application using site trial panels realized in the United Kingdom by the collaboration of the Universities of Cardiff, Bath, and Cambridge, in the framework of the EPSRC funded Materials for Life (M4L) project [140]. Another possible technology based on this concept is a hybrid system combining the shape memory properties of the polyethylene terephthalate (PET) with a pre-stressed Kevlar rope [141].

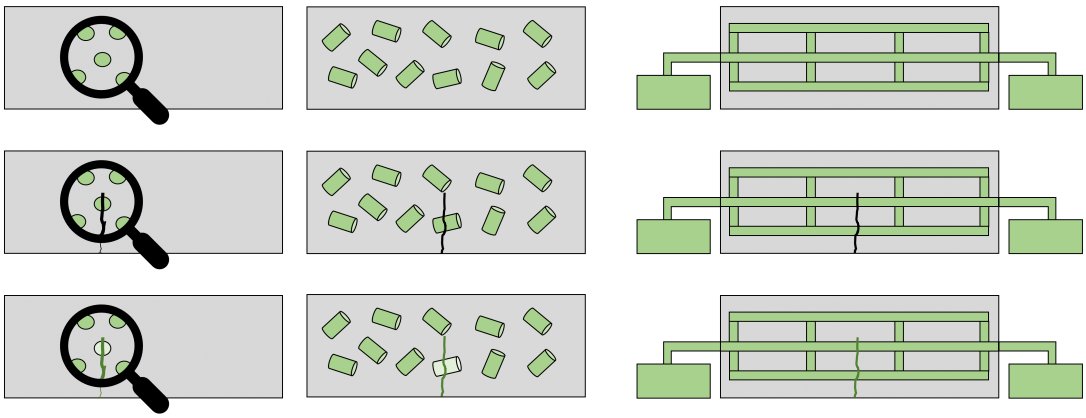

(a) (b) (c)

Figure 2.2: Encapsulated autonomous healing systems in intact, damaged, and healed state: (a) micro-encapsulation; (b) macro-encapsulation; (c) vascular network.

2.3 Encapsulated autonomous self-healing

Autonomous self-healing is based on the concept of embedding unconventional engineered additions in the cementitious matrix to provide self-healing functions [16]. Encapsulation has been widely studied in order to provide a direct delivery of healing agents at the location of crack occurrence. The main types of encapsulation technologies under study for self-healing cementitious materials and that will be described in the following sections are micro-encapsulation (Figure 2.2a), macro-encapsulation (Figure 2.2b), and vascular networks (Figure 2.2c), used in order to store and deliver the appropriate healing agents at the crack site allowing the self-healing effect. The macro-encapsulation is also the technology on which this thesis is focused.

The main triggering mechanism of encapsulated systems is their rupture upon crack occurrence, with the subsequent release and reaction of the healing agent in the region of damage (Figure 2.2). Healing agents react in different ways: some react upon contact with moisture, air or due to heating, others upon contact with the cementitious matrix, while other agents react when making contact with a second component that can be present in the matrix or provided by additional capsules or channels of the vascular network [47].

2.3.1 Micro-encapsulation

Micro-encapsulation is based on the use of healing agents stored in capsules with a maximum diameter of 1 mm [16]. A great number of shell compositions,

properties, production techniques, and healing agents have been researched [16].

For what concern the shell composition and properties, a key factor for to be functional for self-healing application is the durability of both the micro-capsules and their content, which led for example to the development of double-walled shells combining polyurea-urea-formaldehyde [142] or thermally stable polyurea for their use in elevated temperature environments [143]. A great concern when using micro-capsules is their resistance to mixing procedures, hence micro-capsules with switchable mechanical properties were developed in order to exhibit a ductile behavior during mixing and a brittle behavior in the later phase in order to be ruptured and release the healing agent [144–146]. Another aspect of great importance to correctly triggering the rupture and releasing of the agents from the capsules is their bonding with the surrounding matrix, consequently several studies focused on the surface modification of the shell [24, 147, 148] or the use of shell materials (mainly silica-based) able to bond with the hydration products [149–155]. Other than the mechanical trigger caused by the capsules' breakage, the release of the healing agents can be chemically triggered. This is an interesting aspect, since damage is directly connected to decrease of pH, which also causes the depassivation of the steel reinforcement bars with the consequence of making them prone to corrosion caused by the ingress of chlorides. Consequently, pH-sensitive shell materials and chloride binding shell and cargo materials were developed to target the important matter of corrosion-induced damage [156–161].

Many production techniques were proposed in literature, such as emulsion polymerization [161–164], sol–gel reaction [150–155], complex coacervation [145, 146], extrusion [156–159, 165], spray drying [166] or microfluidics [24, 148, 167]. A more complete review is offered in De Belie et al. [16].

For what concern the healing agents, several types were tested, such as the use of adhesive two-part systems which requires the presence of a catalyst within the matrix [164, 167], polymeric agents such as epoxy [151–154] or methyl methacrylate (MMA) [168], or healing agents showing a natural compatibility with the mineral substrate of the cementitious matrix such as encapsulated bacterial strains [165, 169], described also in Sections 2.4 and 3.4.3, or mineral healing agents such as colloidal silica and sodium silicate [142, 143, 145, 146, 170–174]. The reaction mechanisms of the latter are described in depth in Section 3.4.1.

Several healing properties were tested with promising results, comprising the recovery of mechanical properties such as stiffness moduli, fracture energy or compressive and flexural strength, and improvement of durability parameters such as gas and water permeability, chloride diffusion, surface resistivity, and capillary absorption [16].

The use of microcapsules with a polymeric shell made of cross-linked gelatin and acacia gum containing an emulsion of sodium silicate in mineral oil is currently being studied in a large scale application using site trial panels realized in the United Kingdom by the collaboration of the Universities of Cardiff, Bath, and Cambridge,

in the framework of the EPSRC funded Materials for Life (M4L) project [140].

2.3.2 Macro-encapsulation

Since the volume of healing agent provided by micro-encapsulation can be too low to fill large cracks, a possible solution to overcome this issue is the use of macro-capsules. In fact, these types of capsules offer the possibility to store a larger amount of healing agent, which can fill larger cracks while virtually offering multiple healing effects with a single capsule.

Many types of macro-capsules were thoroughly studied by several researchers in the last decades by varying their shape, constitutive materials, and cargo healing agents. The earliest studies involving the use of macro-encapsulation were carried out in the '90s by Dry using polypropylene and glass fibers filled with mono- or multi-component MMA [25, 175]. Other examples on the use of glass capillaries for macro-encapsulation are represented by the studies on hollow glass fibers (0.8 mm inner diameter and 100 mm in length) [176] or long glass capillaries (either 1.5 or 3 mm inner diameter and 100 mm in length) [177] filled with cyanoacrylates.

In many studies, glass capsules with diameters varying from 0.8 to 4 mm were successfully used [20–22, 26, 29–34, 178]. Several healing agents were successfully encapsulated and used for self-healing applications such as polyurethane precursors [21, 26, 29, 30, 32–35, 37, 179–181], (described in Sections 3.4.2), water-repellent agents [15, 17, 182, 183] and other liquid minerals [20] (described in Sections 3.4.1), bacterial agents [31, 182] (described in Sections 2.4 and 3.4.3) or expansive minerals [22]. Positive results were obtained on the recovery of both mechanical properties and durability-related properties. The efficiency of the use of glass capsules filled with polyurethane precursor was also tested with good results in a large scale lab test conducted by Ghent University on real scale concrete beams [21].

However, glass capsules may have a negative effect on concrete durability because of the possible onset of undesired alkali-silica reactions [16, 28]. In addition, the probability that these stay intact during mixing is low unless proper additional precautions are taken [27, 28, 35–37]. A possible alternative to solve these issues was studied using ceramic [26, 32, 182] or polymeric capsules, the latter obtained either by extrusion [27, 28, 36, 184] or additive manufacturing [185, 186]. In order to address the issues connected to the necessity of having a ductile behavior during mixing and a brittle behavior later to trigger the healing mechanism, polymeric capsules with evolving brittleness were produced and studied [36].

Another possible alternative to solve the issues of glass capsules described above was the development of cementitious hollow tubes (CHTs) produced with the extrusion of a polymer-modified cement paste [38, 39]. The capsules, filled either with sodium or potassium silicate solutions showed a good recovery of mechanical properties, hence were proven effective in meeting the requirements of a macro-encapsulation system while presenting an inherent compatibility between the capsules

shell and the cementitious matrix. This type of encapsulation was the starting point for the development of this thesis and is further described in Chapter 3 with the modification of the system that was tested throughout this research study.

A last type of macro-encapsulation is based on the use of lightweight aggregates (LWAs) as container to host self-healing agents by replacement of part of the aggregates. LWAs were either impregnated with a sodium-monofluorophosphate solution under vacuum, covered with cement paste and used in blast-furnace slag cement mortars [187], impregnated with a sodium silicate solution and covered with a polyvinyl alcohol (PVA) solution and used in lightweight concrete [188] or impregnated with bacterial spores and their nutrients and mixed with cement mortar [189] (see also Section 2.4).

2.3.3 Vascular healing

The concept of vascular healing is the clearest example of the biomimetic approach applied to self-healing. Indeed, the majority of natural materials obtain self-healing through some form of vascular networks, such as the human cardiovascular system that transports blood or the plant vascular tissue system that transports food, water, and minerals [16]. Based on the example given by the Nature, vascular self-healing networks can deliver healing agents to damage sites in order to repair them. Moreover, since healing agents are supplied by an external source, healing agents can be continuously supplied and replenished, thus overcoming the issues of micro- and macro-encapsulation related to the stability of the healing agents over time and their limited capacity to allow self-healing [16, 18, 47, 190]. Several researchers focused on the use of this type of biomimetic systems and on solving the issues connected to the scale-up of this method in real structures. Various forms of vascular networks have been used in concrete, ranging from 1D channel to more complex 3D networks.

The early studies made by Dry in the '90s used long thin glass channels [175], which were used also in a trial bridge deck [191]. Other studies focused on the use of glass brittle channels to realize vascular systems than could be externally replenished [177, 192, 193]. An important drawback of the use of glass tubes to realize networks is the brittle nature of these channels, which makes difficult their practical implementation during casting procedures.

Several possible alternatives were proposed by using inorganic phosphate cement (IPC) or alumina tubes [194], by creating channels through embedding and then removing polyurethane terephthalate (PET) tubes [140, 195] or metal rods [196], by the introduction of networks of porous concrete [197] or using more complex 3D printed networks [194, 198, 199].

Vascular networks were also used in combination with another interesting biomimetic approach, namely a self-sensing system, in the study of Nishiwaki et al. [200]. This system was created by the combination of an organic thermoplastic film pipe

used as channel to supply the healing agent and a self-diagnosis composite made of ceramic fibers and a conductive matrix. Upon crack occurrence, the self-sensing system reduces the conductive path and in turn increases its electric resistance, consequently heating the damaged zone. Therefore, the surface of the organic film pipe melts as result of the increased temperature, releasing, and repairing the damaged zone.

The use of 3D printed polylactic acid (PLA) joints was used in combination with the abovementioned removal of PET tubes to obtain 2D networks [140]. This system is currently being studied in a large scale application using site trial panels realized in the United Kingdom by the collaboration of the Universities of Cardiff, Bath, and Cambridge, in the framework of the EPSRC funded Materials for Life (M4L) project [140].

2.4 Bacterial self-healing

Microbially induced calcite precipitation (MICP) has been proposed as environmentally-friendly repairing agent due to its inherent compatibility with the cementitious matrix. MICP was successfully used for the consolidation of sand columns [201] or the surface treatment of limestone [202] and concrete [203]. In 2007, Jonkers and Schlangen [204] started to investigate the possibility to use bacterial $CaCO_3$ for autonomous crack healing, consequently providing all necessary components within the cementitious matrix. The mechanism of bacterial self-healing is similar to that of autogenous healing due to carbonation, since it is based on the precipitation of calcite ($CaCO_3$) to fill the cracks.

Many bacteria can induce the precipitation of $CaCO_3$ in suitable conditions [205], however different bacteria follow different metabolic pathways to cause the precipitation of calcite.

One possibility to obtain $CaCO_3$ precipitation is through the metabolic conversion of organic compounds by microorganisms under aerobic conditions, which is mainly governed by the chemistry of the environment in which the microorganisms are in. Typical requirement for $CaCO_3$ precipitation is that the ion concentration of calcium and carbonate exceeds the solubility product of calcium carbonate [16, 206]. Aerobic degradation of organic compounds does not have a direct effect on the concentration of calcium ions, but it increases the dissolved inorganic carbon concentration (DIC: $CO_2 + HCO_3^- + CO_3^{2-}$) and, especially in alkaline conditions, the carbonate ion concentration. Therefore, in presence of calcium ions, metabolic conversion of organic compounds in alkaline environment will allow calcium carbonate precipitation [207].

These aspects were studied by Jonkers et al. since 2006 [204], leading to the development of a bacterial spore and an organic compound–based healing agent to allow autonomous self-healing of cementitious materials under aerobic conditions

[165, 189, 208–213].

The bacteria, in the form of spores, are alkali-resistant members of the genus *Bacillus* such as *Bacillus cohnii* or *Bacillus pseudofirmus*, while the organic compounds consist in calcium salts of fatty acids such as calcium formate, calcium acetate, calcium glutamate, calcium propionate and calcium lactate or lactate derivatives [16].

Upon crack occurrence, the water ingress activates the spores causing their germination and the organic compounds can be metabolically converted to calcium carbonate and carbon dioxide (Equation 2.1) [214].

$$CaC_6H_{10}O_6 + 6\,O_2 \longrightarrow CaCO_3 + 5\,CO_2 + 5\,H_2O \tag{2.1}$$

Moreover, the metabolically produced CO_2 can further react calcium hydroxide naturally present in the cementitious matrix and produce more $CaCO_3$ (Equation 2.2) [214]

$$5\,CO_2 + 5\,Ca(OH)_2 \longrightarrow 5\,CaCO_3 + 5\,H_2O \tag{2.2}$$

Since microorganisms cause consumption of oxygen [208, 213], a positive side effect could be the reduction of the risk of corrosion in steel reinforcing bars due to their presence.

Another example is given by the alkali-tolerant ureolytic strains, which are commonly been used for application in cementitious materials and to allow self-healing effects [31, 49, 144, 157, 182, 202, 203, 215–218]. Examples of strains belonging to this group are *Sporosarcina pasteurii* (also named *Bacillus pasteurii*), *Sporosarcina ureae* , *Bacillus sphaericus* and *Bacillus megaterium*. These bacteria can decompose urea (CH_4N_2O) into ammonia (NH_3) and carbonate ions (CO_3^{2-}), which is able to react in presence of sufficient Ca^{2+} ions to form $CaCO_3$. The reactions are summarized in Equation 2.3, 2.4 and discussed in depth in Section 3.4.3.

$$CO(NH_2)_2 + 2H_2O \xrightarrow{bacterial\ urease} 2\,NH_4^+ + CO_3^{2-} \tag{2.3}$$

$$Ca^{2+} + CO_3^{2-} \longrightarrow CaCO_3 \tag{2.4}$$

MICP can be achieved also through nitrate reduction by different strains. Examples of strains belonging to this group are *Pseudomonas denitrificans*, *Castellaniella denitrificans*, *Diaphorobacter nitroreducens* or *Pseudomonas aeruginosa* [218–223]. Denitrifiers have been used for self-healing applications due to their ability to function under oxygen limited conditions [221], which is a positive aspect to cure deep crack. In fact in these conditions, denitrifiers can use nitrate (NO_3^-) for oxidation of organic carbon and generate HCO_3^- and CO_3^{2-} ions (Equation 2.5), which further react to generate $CaCO_3$ as discussed above (Equation 2.4).

$$5\,HCOO^- + 2\,NO_3^- \longrightarrow N_2 + 3\,HCO_3^- + 2\,CO_3^{2-} + H_2O \tag{2.5}$$

Another positive aspect of nitrate reduction is that it can also lead to the production of NO_2^-, which is a corrosion inhibitor (Equation 2.6), making the denitrifiers an optimal solution to counteract corrosion in reinforced concrete [222, 224].

$$2\,HCOO^- + 2\,NO_3^- + 2\,H^+ \longrightarrow 2\,CO_2 + 2\,H_2O + 2\,NO_2^- \tag{2.6}$$

The use of axenic cultures in which only a single strain is present, hence requiring sterile production conditions, has the drawback of high production costs [225]. In order to resolve this issue, it was developed a process aimed to obtain an efficient nonaxenic ureolytic microbial community, starting from a side stream of vegetable processing [226]. This mixed culture was defined either "Cyclic En-Riched Ureolytic Powder" (CERUP) or simply Mixed Ureolytic Culture (MUC), it presented high reduction in the production cost while maintaining MICP properties similar to that of axenic *B. sphaericus* and with the additional effect of being able to protect itself from harsh conditions. A similar concept was developed by Ersan et al. by cultivating granules called "activated compact denitrifying core" (ACDC) [223, 227]. ACDC granules were made by denitrifying microbial community protected by various bacterial partners and it was possible to use them as addition in cementitious materials without further protection, granting good results in terms of self-healing properties while presenting also in this case a low cost compared with axenic cultures. Another example of the use of microbial consortia capable of MICP and showing good results in terms of healing was developed by Zhang et al. [228].

Apart the case of self-protected mixed cultures, the direct addition of bacterial strain to cementitious materials presents several issues. In fact, when bacteria are used to heal cracks in concrete, the major hindering factor is the high pH, which may restrict the growth of the bacteria [182]. Moreover, bacteria need to remain active until the moment when cracks appear. Therefore, in order to be suitable for autonomous healing applications, bacterial strains need to be able to form spores. Spores are viable but dormant cells that are able to resist high mechanically and chemically induced stresses and remain viable for periods up to 50 years. However, also bacterial spores added directly to the concrete mixture are subjected to a decrease in lifetime due to the hydration process which causes cell collapse [229]. Therefore, most strains require immobilization of the bacterial cells and protection from the alkaline environment and the reduction in porosity caused by the hydration process. For this reason, several protection strategies were studied in order to introduce in the cementitious matrix both bacteria and the nutrients needed to allow the carbonate precipitation.

Several protection techniques that were used were already discussed in the previous sections, such as micro-encapsulation [144, 230, 231], macro-encapsulation [31, 182] or vascular networks [140].

Many studies focused on the immobilization of bacterial strains such as *B. sphaericus*, *B. subtillis*, *S. pasteurii*, *D. nitroreducens* or *B. pseudofirmus* and their nutrients through the impregnation of many types of lightweight aggregates, such as diatomaceous earth, biochar, metakaolin, expanded clay, expanded perlite, expanded shale, granular activated carbon, ceramsite or zeolite [140, 189, 208, 232–239]. Also magnetic iron oxide nanoparticles were proposed for the protection of bacterial healing agents [240, 241].

Mors and Jonkers recently used a lactate derivative, namely polylactic acid (PLA), to contain bacteria and activation nutrients for self-healing purposes [213, 242]. The effects caused by their addition on the properties of the surrounding matrix, both in terms of chemical reactions and mechanical properties, are currently under study [243, 244].

A last protection strategy is represented by the use of biohydrogels, consisting of hydrophilic polymer gels, that were formed by incorporating a spore suspension into the polymer solution prior to synthesis [169, 217, 245]. Palin et al. applied alginate beads for spores encapsulation [165] and this system was proven effective even in low-temperature marine environments [246], which naturally represent a challenging environment for the use of bacterial self-healing due to the reduction of microbial processes at low temperatures.

Several full-scale demonstrator projects were carried out by several universities using bacterial self-healing cementitious materials.

The research group working at Delft University of Technology realized four full-scale projects situated in different cities of the Netherlands, aimed at demonstrating the performances of bacteria-based self-healing repair mortar and bacteria-based self-healing concrete [247]. The two projects regarding the self-healing repair mortar involved the reparation of the concrete cover of damaged steel reinforced concrete columns of a chemical plant in Limburg and repair of a cracked and leaking parking garage basement walls in Groningen. The two projects regarding the self-healing concrete involved the construction of a wastewater purification tank made of precast concrete elements in Limburg and an in situ cast rectangular concrete water reservoir in Hoogvliet.

The use of *Bacillus pseudofirmus* DSM 8715 infused into lightweight perlite aggregate particles, with yeast extract and calcium acetate infused in separate particles as nutrients, is currently being studied in a large scale application using site trial panels realized in the United Kingdom by the collaboration of the Universities of Cardiff, Bath, and Cambridge, in the framework of the EPSRC funded Materials for Life (M4L) project [140]. A vascular flow network is also provided to supply additional nutrients at later age.

The use of a bacterial mixture called MUC+, made out of the abovementioned Mixed Ureolytic Culture together with anaerobic granular bacteria is currently being studied by Ghent University in a large scale application using the roof slab of an inspection pit realized in Belgium [248, 249].

2.5 Conclusions

The main mechanisms and strategies to obtain self-healing cementitious materials were presented, describing the basic concept for each of these self-healing techniques and highlighting their advantages and limitations.

First, the autogenous healing of cementitious materials was introduced, which is the basic phenomenon that grants the intrinsic self-healing ability of cement-based materials, followed by stimulated autogenous healing that can be obtained through the use of mineral additions, crystalline admixtures, or polymers. Despite the easy applicability of these solutions and the fact that many are already being used in the construction sector also for other purposes, their main limitation is constituted by the reduced crack widths that can be healed, up to 100-150 µm. Moreover, their action is often slow and conditioned by the presence of water.

Subsequently, the autonomous self-healing mechanisms were introduced, which are based on the concept of embedding engineered additions in the cementitious matrix to provide self-healing capabilities. Autonomous self-healing can be obtained through the application of several encapsulation strategies, namely micro-encapsulation, macro-encapsulation, or vascular networks. Encapsulation allows to provide a direct delivery of healing agents at the location of crack occurrence. These healing agents can be polymers, minerals, or bacteria that can allow microbially induced calcite precipitation. Autonomous self-healing mechanisms make it possible to overcome the limitations of autogenous healing and to heal cracks widths of 300 µm or even larger. Moreover, they usually act faster than autogenous healing. On the other hand, the main limitations of the autonomous self-healing technologies are constituted by the additional work, measures, and cost to implement them in the ordinary construction process.

Taking into consideration the advantages and limitations of each self-healing technique, the *macro-encapsulation* was selected as the focus of this thesis. This choice was made due to several benefits offered by this technology. First, the possibility to provide *direct delivery of healing agents* at the crack location. While this is a common aspect in self-healing technologies, the macro-encapsulation also allows to *heal larger crack widths* than other strategies, which consents to offer autonomous repair also in case of cracks that exceed those normally allowed by Model Codes. Moreover, the healing effect can be achieved in a *short time* selecting the appropriate healing agents. Even though the vascular networks could grant the same advantages, the macro-encapsulation does not present the same complexity in the arrangements of the networks inside a structural element. In addition, the use of macro-capsules with a cementitious shell could provide further advantages such as their inherent compatibility with the surrounding cementitious matrix and the possibility to use them in the ordinary construction process in a straightforward manner.

Chapter 3

Cementitious capsules

The extrusion process of a tailor-made polymer-modified cement paste was developed at Politecnico di Torino during the project "DualCEM: Development of self-healing cementitious materials with high durability" (2012-2014). The DualCEM project was financed by Regione Piemonte and was carried out through the cooperation between Politecnico di Torino, as an academic subject, and several companies as additional Research & Development subjects or end-users (Buzzi Unicem S.p.A., NovaRes s.r.l., ARIA s.r.l., Varnish Tech s.r.l., Silvateam S.p.a.). The project aimed to investigate two key technological factors of a self-healing concrete system: on one side the efficiency of different healing agents and, on the other side, the potential of different encapsulation technology approaches [40].

Part of the work described in this chapter has been previously published in:

[**250**] G. Anglani, P. Antonaci, G. Idone, and J.-M. Tulliani. "Self-healing of cementitious materials via embedded macro-capsules". In: *Proceedings of the 4th International Conference on Service Life Design for Infrastructures (SLD4)*. Ed. by G. Ye, Y. Yuan, C. Romero Rodriguez, H. Zhang, and B. Šavija. Delft, the Netherlands: RILEM Publications S.A.R.L., 2018, pp. 385–388

[**251**] G. Anglani, P. Antonaci, J.-M. Tulliani, K. Van Tittelboom, J. Wang, and N. De Belie. "Self-healing efficiency of cement-based materials containing extruded cementitious hollow tubes filled with bacterial healing agent". In: *Final Conference of RILEM TC 253-MCI: Microorganisms-Cementitious Materials Interactions*. Ed. by A. Bertron and H. Jonkers. Toulouse, France: RILEM Publications S.A.R.L., 2018, pp. 425–431

[**252**] G. Anglani, J.-M. Tulliani, and P. Antonaci. "Behaviour of Pre-Cracked Self-Healing Cementitious Materials under Static and Cyclic Loading". *Materials* 13.5 (2020), p. 1149. DOI: 10.3390/MA13051149

[**253**] G. Anglani, T. Van Mullem, X. Zhu, J. Wang, P. Antonaci, N. De Belie, J. M. Tulliani, and K. Van Tittelboom. "Sealing efficiency of cement-based materials containing extruded cementitious capsules". *Construction and Building Materials* 251 (2020), p. 119039. DOI: 10.1016/j.conbuildmat.2020.119039

The cementitious hollow tubes (CHTs) produced with the extrusion process [38–40] were proven effective in meeting the requirements to obtain effective encapsulation system for self-healing purposes, while presenting an inherent compatibility between the capsules shell and the cementitious matrix. In fact, the cementitious tubes were able to protect and release effectively several types of silicate solutions used as healing agents, they showed a flexural strength comparable to that of cementitious mortar and they exhibited the ability to survive the mixing process. Moreover, they offered good performance recovery also in the presence of large cracks (up 800 µm).

Starting from the positive results obtained in the development of the cementitious capsules technology, the aim was to further improve the technology in order to allow its use for different manufacturing techniques other than the extrusion and in order to make it suitable for the encapsulation of highly reactive healing agents, which require high standards in term of tightness stability. In the following Sections, the mix designs, manufacturing techniques, coating, and sealing techniques are described. Moreover, a description of the healing agents that were successfully encapsulated is provided.

The resulting encapsulation system was later used in the experiments performed throughout this research study, in order to characterize the performances of the autonomous self-healing cementitious material realized through its implementation.

3.1 Manufacturing of the shell

3.1.1 Mix design

Cementitious tubular capsules were produced in accordance with previous researches [38–40] using a polymer-modified cement paste, with some modification to the mix design aimed to further improve the workability of the paste. Hence, the powder compounds of the paste were:

- Ordinary Portland cement (CEM I 52.5 R, Buzzi Unicem S.p.A., Italy).
- Calcium carbonate ($CaCO_3$, Sinopia s.a.s., Italy): added as a superfine aggregate in the mixture. Cement containing limestone demands less water and exhibits higher early strength [254, 255]. Calcite functions as an active participant in the hydration process, reducing porosity and permeability of hardened cement pastes, and as a filler [256]. Therefore, calcium carbonate is used to increase the stiffness of the cementitious matrix during the extrusion process, avoiding the collapse of the fresh element.
- Hydroxypropyl methylcellulose (HPMC, Sigma Aldrich, Italy): added to reduce segregation amongst the components, to improve homogeneity, workability, and the hardened product characteristics [257]. It has a strong influence

on the structural breakdown and reconstruction phenomena during the extrusion process [258, 259]. Also, HPMC exerts a retarding action on setting [257].

with the addition also of:

- Metakaolin (MK, halloysite from Applied Minerals Inc., NY, USA, calcined at 650 °C for 3 hours): MK reacts chemically with hydrating cement to form a modified paste microstructure, improving workability, mechanical properties, and durability of the paste [260].

The liquid compounds of the paste were:

- Demineralized water.
- Copolymer of ethyl acrylate (EA) and methyl methacrylate (MMA) (Primal B60A, Sinopia s.a.s., Italy): added to reduce the water to cement ratio, since its addition enhances the workability of the paste [261, 262]. The better flow is due to the presence of surfactants in the polymers and the lower surface tension of polymer molecules. This facilitates a better flow of the mix at the same water content [261, 262]. Moreover, in the case of air-cured samples, the strength is enhanced [262]. Besides enhancing strength, polymer modifications can significantly improve toughness [262]. This is useful to improve the survivability of the capsules during mechanical mixing.
- Polyethylene glycol (PEG, Sigma Aldrich, Italy): glycol compounds possess surface-tension reducing properties, consequently they reduce the shrinkage with a minimal effect on strength [263]. This feature is important since the amount of aggregates in the mixes is very low.

It was chosen to not use superplasticizer as in the previous works [38, 39].

The compounds quantities followed two mix designs: the first, summarized in Table 3.1, was used to extrude the capsules used in Chapter 4-5 and required some adjustment to the workability through small quantities of cement, metakaolin, and demineralized water during the extrusion procedure, since the process is rather sensitive to the ambient temperature and relative humidity (RH). The second mix design, summarized in Table 3.2, was slightly modified with respect to the previous one in order to accommodate both the extrusion process and the new manufacturing procedure described in Section 3.1.2. This mix design was used to produce the capsules used in Chapters 6–8.

Table 3.1: Mix design 1 of the polymer-modified cement paste.

Cement (wt%)	**Water (wt%)**	**w/c (-)**	**$CaCO_3$ (wt%)**	**Metakaolin (wt%)**	**HPMC (wt%)**	**EA/MMA (wt%)**	**PEG (wt%)**
42.5	19.6	0.46	19.6	0.3	0.7	15.7	1.6

Table 3.2: Mix design 2 of the polymer-modified cement paste.

Cement (wt%)	**Water (wt%)**	**w/c (-)**	**$CaCO_3$ (wt%)**	**Metakaolin (wt%)**	**HPMC (wt%)**	**EA/MMA (wt%)**	**PEG (wt%)**
46.2	12.8	0.28	21.3	0.3	0.7	17.0	1.7

3.1.2 Manufacturing techniques

In order to produce the polymer-modified paste, first all solid compounds were manually mixed, while all liquid compounds were separately mixed together with an overhead stirrer (RW 20, IKA, Staufen, Germany). Then, the mixed powder compounds were added progressively to the homogeneously mixed liquid compounds.

The fresh polymer-modified cement paste was used to produce cementitious tubes according to two different manufacturing processes.

In the first manufacturing process, already used in previous works [38, 39], the fresh cement paste was manually extruded (Figure 3.1a) using a low-cost device normally used to prepare fresh homemade pasta (Regina Wellness, Marcato, Italy). The device is composed of a screw extruder having a cylindrical barrel 130 mm long with a diameter equal to 40 mm and replaceable nozzles. The used nozzle allowed to obtain ridged tubes of variable length with a hollow ovoid cross section (external diameter of 10 mm and internal diameter of 7.5 mm). The ovoid cross section is due to the setting of the paste under its own weight.

They were left for 7 days in a moist environment (with temperature T $\approx$ 20 °C and relative humidity (RH) >95%) and subsequently in air (T $\approx$ 20 °C, RH $\approx$ 60%) for complete curing over 28 days, since it is reported in the literature that water curing degrades the mechanical strength of polymer-modified cementitious mortars [262]. The obtained cementitious tubes can be further cut with a saw into smaller tubes of the desired length (Figure 3.2a).

In the second manufacturing process, the fresh cement paste was rolled around an oiled bar with a circular cross section of the desired diameter, until obtaining a smooth cementitious tube with a shell thickness of approximately 1.5 mm (Figure 3.1b). The bar was removed only after setting and first hardening of the cement paste, i.e., after 24 hours storage in a moist environment with T $\approx$ 20 °C and RH $>$ 95%. This allowed to keep a perfectly cylindrical shape of the tubes, unlike the extruded ones in which deformation of the cross section occurred during the first stages of curing because of their own weight. The total duration of curing in moist

(a) (b)

Figure 3.1: Manufacturing techniques used to produce the cementitious tubes: (a) extrusion (b) rolling.

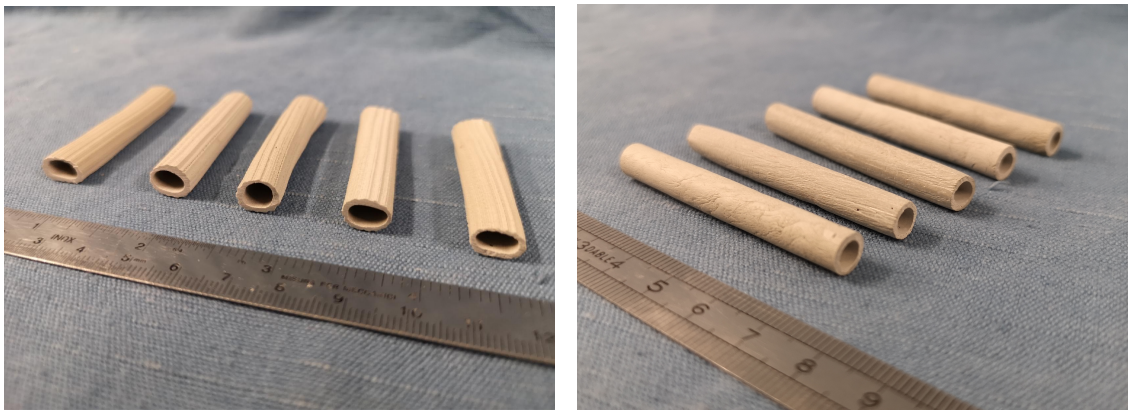

(a) (b)

Figure 3.2: Cementitious tubular shells produced by extrusion (a) and by rolling (b).

environment was of 7 days, after which curing was completed in air (T ≈ 20 °C, RH ≈ 60%) over 28 days for the motivation reported above. Also in this case, the tubes can be further cut with a saw into smaller portions of the desired length (Figure 3.2b).

(a) (b)

Figure 3.3: Premature reaction of the polyurethane core in capsules coated with sodium silicate: (a) inside the capsule; (b) embedded in a cement mortar.

3.2 Coating and sealing

In order to obtain waterproof capsules able to protect the healing agents, the surfaces of the cementitious tubes must be further coated. The application of the coating is necessary because the cement paste cannot guarantee a sufficient protection, since the water is a small molecule that can diffuse through the acrylic macromolecules network of the polymer-modified cement paste and, thus, can enter the shell compromising the healing agent. Similarly, the healing agents could leak from the shell. The coating material must possess an adequate viscosity to be applied and create a film that is brittle and resistant in an alkaline environment. In the previous works [38, 39], sodium silicate and polyester resin cured in the presence of 2% of methyl-ethyl ketone peroxide was used successfully to obtain cementitious capsules capable of protecting different types of silicate solutions as healing agent. However, the sodium silicate coating was proven not effective when using highly reactive healing agents, such as polyurethane precursors (Section 3.4.2). These types of healing agents are highly moisture-reactive and, when encapsulated in cementitious capsules coated with sodium silicate, they reacted prematurely in the capsules, especially when embedded in the moist cementitious environment (Figure 3.3).

In order to overcome this issue, it was decided to move from sodium silicate coating to epoxy coating, which has been demonstrated to be one of the most effective materials to guarantee high standard of sealing and waterproofing [28, 262, 264, 265].

First, a layer of a two-component epoxy primer (Primer AQ, API SpA, Italy)

(a) (b) (c)

Figure 3.4: Premature reaction of the polyurethane core in capsules coated with epoxy resin and sealed with methyl methacrylate glue: (a) capsules after sealing; (b-c) premature reaction of the core when embedded in a cement mortar.

was applied by complete immersion of the tubes to prepare the surfaces of the tubes. Subsequently, a coating layer was applied by using a two-component epoxy resin (Plastigel, API SpA, Italy). This layer (thickness $\approx$ 1 mm) was applied in two ways to the tubes, thus obtaining two types of capsules' shells presenting either an:

1. Internal coating: the epoxy resin was applied only to the internal surface by injection;

2. External coating: the epoxy resin was applied only to the exterior surface with a brush.

The application of an internal coating resulted in the reduction of the internal volume of the capsules, and hence in a reduction in the storable healing agent.

Other than the coating, also the sealing of the capsules end must guarantee the correct tightness of the capsules. Again, the wax sealing used in previous works [38, 39] was found effective to seal capsules containing silicate solutions but not highly reactive polyurethane precursors. The same can be said when methyl methacrylate glue was selected (Schnellklebstoff X60, HBM, Germany) for its rapid curing time and used to seal the capsules coated with epoxy resin, as it can be seen in Figure 3.4.

Also in this case it was decided to an epoxy sealing, namely an epoxy-based two-component thixotropic plaster (Stucco K, API SpA, Italy) which was subsequently coated with the epoxy used for the coating.

In order to produce the cementitious macro-capsules, one end of the coated tube (either internally or externally), was sealed using the epoxy-based plaster and subsequently coated with Plastigel. At this stage, the healing agents were injected with a syringe until complete filling and taking care to limit the amount of entrained air. Finally, the second end of the tube was sealed in the same way as the other,

(a) (b) (c)

Figure 3.5: Cementitious capsules after coating, filling, and sealing: (a) extruded capsules with internal epoxy coating; (b) extruded capsules with external epoxy coating; (c) rolled capsules with internal epoxy coating.

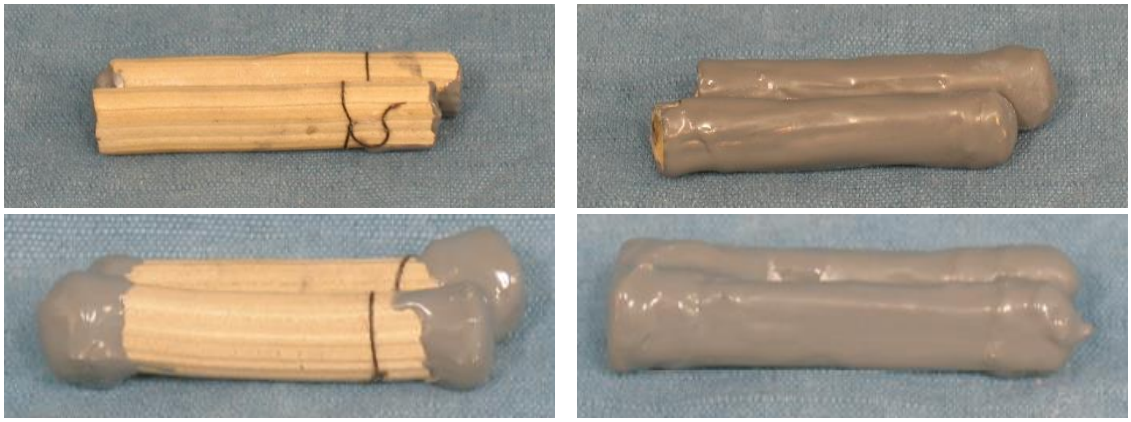

(a) (b)

Figure 3.6: Cementitious capsules coupled to encapsulate two-component healing agents, before and after filling and sealing: (a) extruded capsules with internal epoxy coating; (b) extruded capsules with external epoxy coating.

eventually generating a cementitious tubular capsule. In some cases, both ends or the entire length of the capsules were covered with sand in order to improve their bonding with the surrounding matrix.

Figure 3.5 shows an example of the capsules with their different types of coatings and their cross sections.

In order to make the capsules suitable to encapsulate two-component healing agents (e.g. the bacterial healing agent described in Section 3.4.3), some coated tubes were glued together with cyanoacrylate before filling and sealing (Figure 3.6).

3.3 Resistance to mixing procedure

One of the most challenging issues posed by encapsulation is to find capsules which can be added to fresh concrete during mixing, making them able to withstand the mechanical action of the mixing process, while at the same time being able to be ruptured upon crack occurrence. This is a feature that would be highly beneficial, since capsules could be used in the same way as aggregates and admixtures by adding them during mixing, making them compatible with field practice and the industrial production of concrete.

Most of the existing studies had been performed on proof-of-concept, small scale specimens, using pre-placed capsules and careful molding of specimens [37], mainly using glass capsules. The likeliness that these stay intact during mixing is low unless proper additional precautions are taken [27, 28, 35–37]. For example, Van Tittelboom et al. [35] tried protecting the capsules by embedding them in thicker cement paste bars, but still they did not resist mechanical mixing. Regarding the possibility of using glass capsules during the mixing process, Feiteira [37] showed that this can be obtained by increasing the thicker of the shell (0.80-1.5 mm). Other authors have attempted to develop polymeric capsules, trying also to obtain switchable mechanical properties, so that they could resist the mixing forces while breaking upon crack formation [27, 28, 36].

In order to test the resistance to mixing procedure, cementitious capsules were produced using the rolling procedure (Section 3.1.2). An internal diameter of 12 mm was used and the tubes were cut to a length of 20 mm (Figure 3.7a). These dimensions were selected in order to make the tubes similar to aggregates, having in mind the idea of developing a sort of *enhanced aggregate*. For the sake of simplicity, the epoxy coating was realized by immersion, obtaining tubes with both an internal and external diameter (Figures 3.7b, 3.7c). The capsules were sealed with epoxy using the same procedures described in Section 3.2 and filled with red food dye, in order to detect its release in case of capsule breakage. Finally, the capsules were rolled in sand (Figure 3.7d).

The resistance of the cementitious capsules was tested by directly adding 24 capsules to the fresh concrete (maximum aggregate equal to 8 mm) in the electrical mixer (Figure 3.8a). After some minutes of mixing, water was added to dilute the mixture before casting it into a large plastic container under the mixer (Figure 3.8b).

Then, the capsules were manually searched in order to retrieve them and counting the intact and broken capsules. The survival rate under mixing was defined as the ratio between the intact capsules and the total number of capsules. Extremely positive results were obtained, since all 24 capsules were retrieved intact in the mixture (Figure 3.9), representing a 100% survival rate and the confirmation of the suitability of this configuration of cementitious capsules to be used as addition during the mixing process.

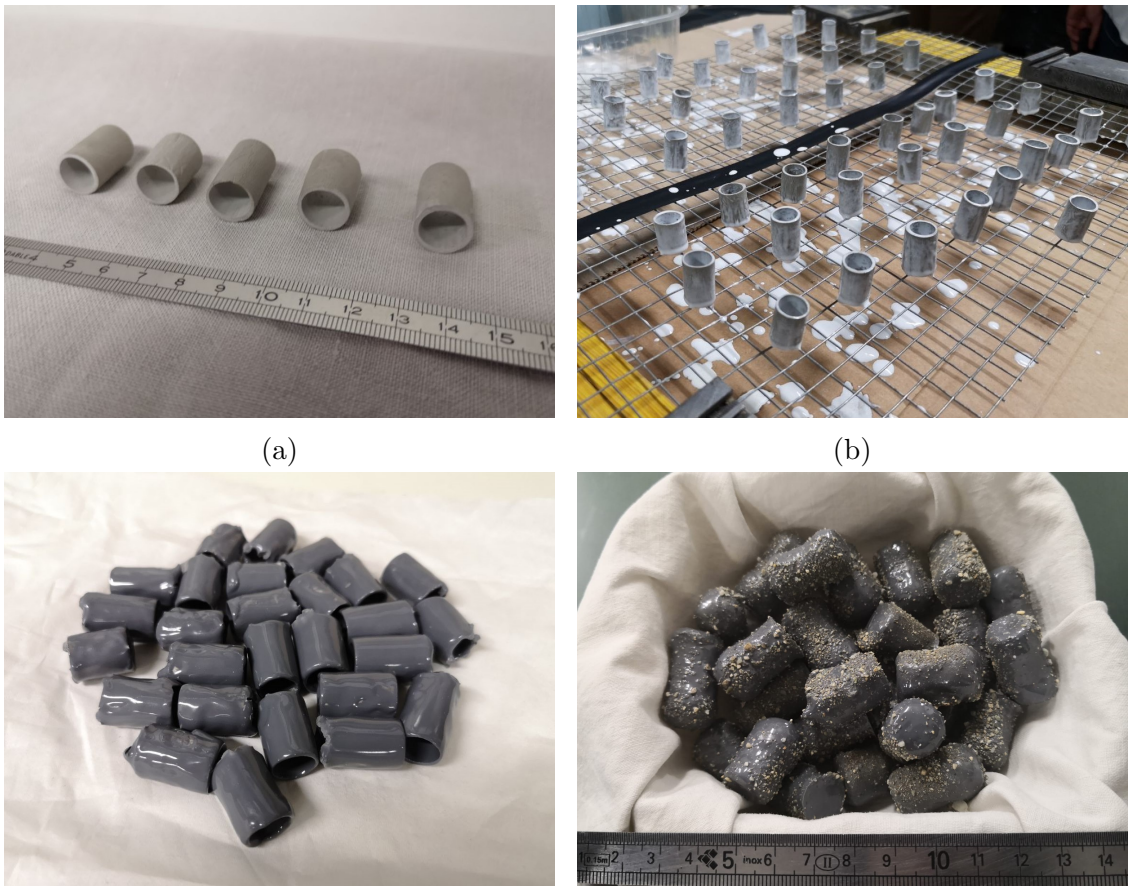

(a) (b)

(c) (d)

Figure 3.7: Cementitious capsules used to test the resistance to mixing: (a) cementitious shell; (b) preparation of the surface with epoxy primer; (c) epoxy coating; (d) capsules after filling, sealing and rolling in the sand.

3.4 Healing agents

The healing agent needs to fulfill several requirements in order to be suitable for application in self-healing concrete. They should present an adequate viscosity and thixotropy. The viscosity should not be too high in order to be able to easily flow out of the capsules and inside the cracks, but at the same time not too low since this could cause leakage of the agent out of the crack or absorption of by the cement matrix. The healing agent should not react too fast upon crack occurrence so that it has the time to flow into the crack before hardening, but fast enough to physically block the crack against penetration of aggressive substances as soon as possible. Moreover, healing agents should be able to remain stable in the capsules until the moment of crack appearance [15]. Finally, also the mechanical properties of the healing agent are very important. The agent should be flexible enough to follow

(a) (b)

Figure 3.8: Resistance to mixing test: (a) capsules inside the mixer; (b) mix poured in a plastic container in order to retrieve intact and broken capsules.

Figure 3.9: Intact capsules after the concrete mixing.

crack movements [37], especially when cracks are expected to open and close due to dynamic loading. Moreover, it is very important to have an adequate adhesive bond strength between the healing agent and the cementitious matrix and that the bond properties remain stable over time, especially in presence of degradation mechanisms such as freeze and thaw cycles, frost scaling, or thermal gradients.

In the following, the main features of the healing agents used throughout this

research study are presented, chosen from the main types commonly used for self-sealing applications (minerals, polymers, and bacteria).

3.4.1 Mineral healing agents

Sodium silicate

Sodium silicate solution (Na_2O 10.6 wt%, SiO_2 26.5 wt%, and H_2O 62.9 wt%, Sigma Aldrich, Italy) was selected considering its low dynamic viscosity (0.141 Pa·s) and its good compatibility with cementitious materials.

Several researchers investigated the application of liquid silicate solutions as mono-component healing agents, such as sodium silicate solution [38, 39, 143, 170, 171, 173, 188] or potassium silicate solution [38, 39]. These healing agents react with the cementitious matrix and promising results were achieved in terms of regain of mechanical properties of a cracked specimen after a healing period. However, their reaction with the cementitious matrix and their healing mechanism show some complexity because these reactions do not develop in a stoichiometrically controlled environment.

Within the cement and concrete industry, soluble silicates, in particular sodium silicate also known as "waterglass", have different uses.

They are used as integral admixtures for construction. An excellent example of this use is shotcreting, raising the pH hence further accelerating hydration and significantly decreasing set time [266].

Another possible use is their incorporation into cementitious waste forms. These stabilization systems are used with a wide range of hazardous materials from heavy metals, organic to nuclear wastes. The objectives of these solidification and stabilization systems are to eliminate all free liquids, improve handling and physical properties of the wastes, reduce mobility, toxicity, and leachability of the hazardous components [266].

They serve also as moisture reducers in the wet kiln process of clinker production [267], as binder for cold consolidation of silica-based aggregates [268], as soil stabilizers [269, 270] or for innovative alkali-activated materials [6, 271, 272].

Finally, one of the foremost uses of soluble sodium silicate is as a concrete sealer. Unlike other sealants, which either repel water (e.g., silanes, silicones, stearates) or function as a physical barrier coating (e.g., epoxies, polyesters, vinyls), soluble silicate sinks into the concrete surface and, theoretically, reacts with portlandite to form C−S−H gel. As a result, the surface has enhanced properties such as decreased permeability, increased hardness, and overall increased durability [267]. In literature, various authors agree that silicate-based concrete sealants do not offer a complete waterproofing protection, but more a densifying action that reduces the porosity of the concrete. Therefore, silicate solutions are generally viewed as pore-blockers.

Sodium silicate is unique in that it can undergo different chemical reactions. For concrete applications, that represent a well-known alkaline environment, it is possible to consider negligible the gelation/polymerization reactions that occur rapidly when the pH of liquid silicate falls below 10.7 and silicate species begin crosslinking to form polymers [273]. Despite the degree of water resistance of the bond formed by the polymerized silicate, it is not desirable for self-healing concrete purposes due to its low strength.

The exact mechanisms by which the silicates act to improve the performance of concretes is unclear. One argument is that sodium silicates are effective and efficient sealers because SiO_2 precipitates in the pores [274]. Another theory is that the active silicates react with excess portlandite ($Ca(OH)_2$) or calcium hydroxide (CH) near the concrete surface to yield relatively insoluble calcium silicate hydrates (C−S−H gels). The reaction of silicate-based compound in concrete can be described, as reported in literature [267, 275–277], by the following chemical equation (3.1):

$$Na_2SiO_3 + y\,H_2O + x\,Ca(OH)_2 \longrightarrow x\,CaO{\cdot}SiO_2{\cdot}y\,H_2O + 2\ NaOH \tag{3.1}$$

A third standpoint is that the silicates form an expansive gel similar to that formed during alkali silicate reactions to fill the concrete voids by swelling [267, 277].

Various authors agree that the main mechanism of self-healing by sodium silicate solution is the reaction with calcium hydroxide in excess, that is a product of cement hydration, to form C−S−H gels, a binding material natural to concrete [39, 170, 171], as reported in Equation (3.1). Calcium silicate hydrate is the main product of the hydration of Portland cement and is primarily responsible for the strength in cement-based materials, due to the dense network of its microcrystals [278].

Another formulation of the relevant chemical reactions is shown below [171]:

$$Na_2{\cdot}SiO_2 + Ca(OH)_2 \longrightarrow x\,(CaO{\cdot}SiO_2){\cdot}H_2O + Na_2O \tag{3.2}$$

$$x\,(CaO{\cdot}SiO_2){\cdot}H_2O + Na_2O + CO_2 \longrightarrow CaCO_3 + SiO_2 + 2NaOH \tag{3.3}$$

In the first reaction (Equation (3.2)) is considered that the product forms rapidly, while the second reaction (Equation (3.3)) is based on a much longer time scale (years). Also sodium-silica-hydrate (N−S−H) is observed in concrete as a result of the reaction between sodium hydroxide and silica [279]. N−S−H is thought to be analogous to C−S−H but has not been well characterized. While the long-term products initiated by the presence of sodium silicate can still be helpful to the integrity of the concrete, it is the newly formed C−S−H gel that will act as a binder and healer in cracks and pores, bridging the gaps in the material and ultimately improving its strength [171].

Moreover, by reacting and reducing the amount of available calcium hydroxide, silicate solutions further improve the acid and sulfate resistance of concrete. Calcium hydroxide tends to crystallize as hexagonal platelets near the cement paste/aggregate interface, resulting in poorly packed and weak areas with high propensity to chemical attacks. Thus, its consumption by sodium silicate is not only beneficial in terms of filling in porosity and cracks with C−S−H gel, reducing the permeability, increasing the hardness and strength of concrete, but also increasing the concrete resistance to acid and other chemical attacks [276].

Another key observation concerning the improved durability that was found in literature [171] is a significant retardation in steel corrosion in samples containing capsules filled with sodium silicate solutions. Two mechanisms for corrosion inhibition were proposed. The first involves the formation of a passive layer to protect the metal. In the second, the ruptured capsule would fill the cracks and reduce porosity and interconnectivity to decrease the solution of sodium chloride imbibition rate. The solution was used to represent the ingress of chlorides to the steel reinforcement bars in concrete.

Some authors conducted ESEM observations and EDS tests on samples with capsules filled with sodium silicate solutions [170]. ESEM images of self-healing behaviors in cracks obviously showed solid phases. Some microcracks form in the healing products during the vacuuming. From EDS analysis, the main chemical elements of the healing products are Si, O, Ca, and Na. What should be mentioned is that there is no Ca in the sodium silicate solution. Since soluble silicates react almost instantaneously with multivalent metal cations to form the corresponding insoluble metal silicate, the chemical element Ca in the healing products reveals that the calcium cations from the matrix react with the sodium silicate solution and thus the C–S–H is formed in the cracks. However, there are not sufficient calcium cations to replace all the sodium cations in the solution. The still available sodium silicate crystallizes when the water of the solution evaporates or transports into the matrixes. As water is removed from liquid silicate, the silicate undergoes the dehydration reaction and progressively becomes tackier and more viscous. The removal of a relatively small amount of water will render the liquid silicate a glassy film [273] with a brittle and fragile nature. Therefore, it can be concluded that the healing products in the cracks are the composites of C–S–H and sodium silicate. The fraction of crystallized sodium silicate in the healing products rises with increasing the concentration of sodium silicate solution and the high fraction of crystallized sodium silicate is able to increase the possibility of propagation of new microcracks in the healing products, which show negative effects on the durability and the recovery of mechanical properties.

The interaction between cement matrix and the sodium silicate solution was investigated during the evolution of the repair through ultrasonic methods [280–282], which highlighted different time scales for the recovery of the linear and the nonlinear elastic properties, further confirming the presence of different ongoing

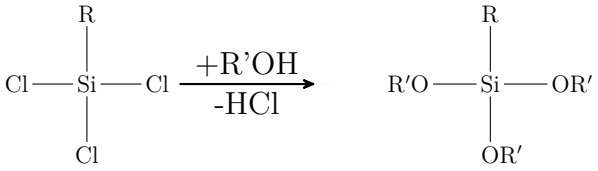

Figure 3.10: Production of silane [283].

mechanisms (i.e. the crystallization of the sodium silicate inside the crack and its reactions with the surrounding matrix).

Water repellent agent

The second healing agent from the mineral group is a commercially available water-repellent agent (Sikagard®-705 L, Sika, Switzerland). It is a 1-component silane-based and solvent-free reactive water repellent with 99% active compounds, with an approximate viscosity of 9 mm^2/s at 25 °C. The water repellent agent (WRA) cures upon penetration in the substrates through chemical reactions that form covalent bonds with the minerals naturally present in the substrate.

In Figure 3.10, the production route of silanes is summarized.

A silane-based agent carries hydrophobic alkyl chains and hydrophilic $Si-OCH_3$ groups. The hydrophobicity mainly depends on the length of the alkyl group. When applied to a substrate, the alkoxy groups of these products react with water or humidity to form a non-stable silanol intermediate which will spontaneously polycondensate to form a hydrophobic film (Figure 3.11). As such, the reactive OH-groups from the silanols can form irreversible bonds with the mineral substrate [283].

The product is commonly used in the construction sector as a water-repellent penetrating sealer for hydrophobic treatment of concrete and cementitious substrates [9, 284–286] and was used also for the treatment of natural fibers to be used in the construction sector [287–289]. This product has been also tested before for its efficiency for self-healing cementitious materials based on encapsulated systems [15, 17, 28, 183]. It is important to point out that the WRA is mainly absorbed by the cementitious substrate at the crack faces due to its low viscosity, resulting in a hydrophobation of the crack faces rather than an actual crack filling as healing mechanism, working mainly on the reduction of the water absorption.

3.4.2 Polymeric healing agents

Polyurethane (PU) precursors have been extensively investigated as possible core agents because of their ability to polymerize rapidly in the presence of humidity. Their ability to restore good water impermeability performances has been widely established in literature [21, 26, 29, 30, 33–35, 37, 179]. In addition, their capability

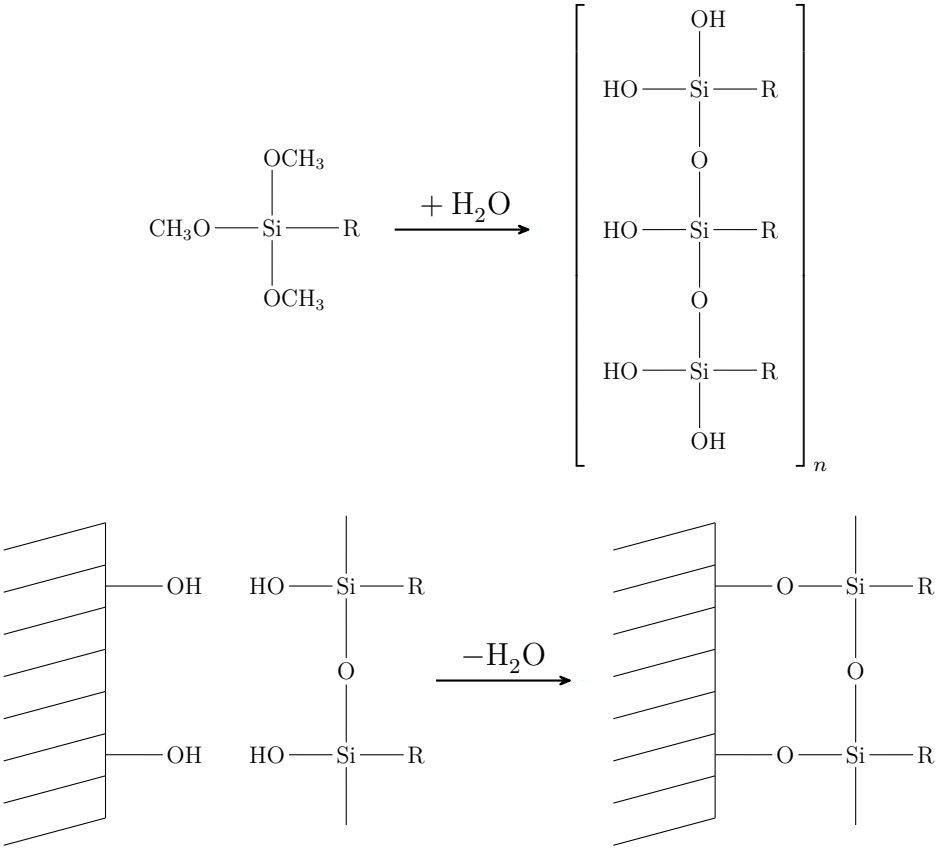

Figure 3.11: Reaction of a silane with a substrate surface [15].

to provide also a mechanical recovery has been highlighted in few studies, mostly under static conditions [26, 29, 32, 37], but also under repeated cracking and healing cycles[29, 37, 181] and cyclic flexural loading [37, 180].

Polyurethanes are sometimes also called "isocyanate polymers" and are characterized by the urethane linkage. The urethane linkages can be produced in polymers by several different routes, which the most common ones are through reactions of the isocyanate groups with compounds bearing hydroxyl groups, such as glycols, dihydroxy-terminated polyethers or polyesters, and others [290].

An example of the reaction between methylene diphenyl diisocyanate (MDI) and a polyether polyol to form a polyurethane precursor is reported in Figure 3.12.

The polyurethane precursors have an excess of isocyanate groups that can cross-link with atmospheric moisture to form insoluble polyurethane. This process is also called the curing of the polyurethane. In the case of polyurethane foams, which are the case of the selected healing agents, gas evolution during the reactions take place simultaneously with chain lengthening and cross-linking, resulting in the formation of cellular structures. The degree of cross-linking determines to a great extent the rigidity of the foam: linear or only slightly branched polymers produce

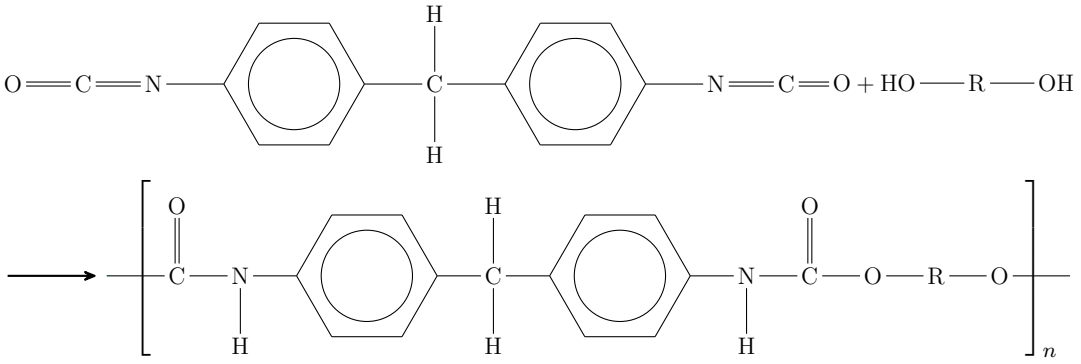

Figure 3.12: Chemical reaction between a MDI and a diol to form a polyurethane precursor [15].

flexible foams, while more highly branched polymers form rigid ones [290]. The healing agents react upon contact with moisture in the matrix and the reaction causes foaming due to the release of CO_2 which causes expansion of the healing agent inside the crack (Equation 3.4).

$$\begin{aligned} \mathrm{R{-}NCO} \quad &+ \quad \mathrm{H_2O} \quad \longrightarrow \quad \mathrm{R{-}NH_2} \quad + \quad \mathrm{CO_2} \\ \mathrm{R{-}NH_2} \quad &+ \quad \mathrm{R{-}NCO} \quad \longrightarrow \quad \mathrm{R{-}NH{-}CO{-}NH{-}R} \end{aligned} \tag{3.4}$$

Two polyurethane precursors yielding to polyurethane foams upon contact with moisture were selected for this research study and described below.

Highly expansive polyurethane precursor (Carbostop U)

The first polymeric healing agent was a commercially available polyurethane precursor (CarboStop U, Minova CarboTech GmbH Branch Italy, Milan, Italy). It is a single-component resin that consists of modified polyisocyanates with additives that rapidly cures by reaction with ambient water yielding a polyurethane/polyurea foam. The precursor is free of chlorofluorocarbons (CFCs) and phthalate plasticizers. Its expansion rate depends on the backpressure exerted by the propagation of the resin into the structure to be sealed: wide cracks result in a high foaming factor, while narrow cracks in a low expansion rate and higher strength. At 25 °C and in presence of 10% of water, it starts foaming in (20±5) seconds and end foaming in (120±15) seconds. The polyurethane precursor is characterized by high expansion rate, with a foam factor in the range of 30-60, measured on the free rise of the precursor mixed with the addition of 10% water to the freshly prepared blend. In Figure 3.13 it is shown an example of the free rise of the polyurethane foam after contact of the precursor with water.

Its viscosity range at 25 °C is 270–1,000 mPa·s. The product is commonly used in the construction sector for stopping water inflow, water ingress in cracks, and sealing of tunnel construction or of drill holes.

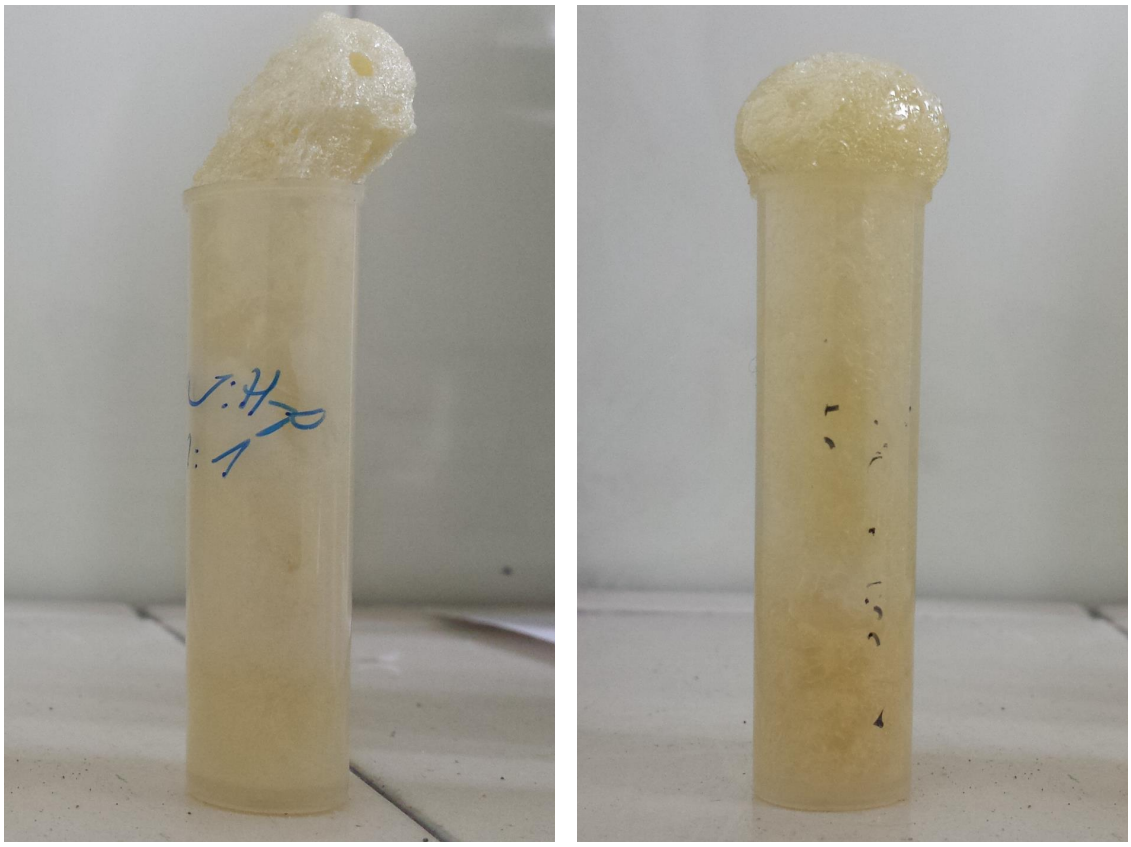

(a) (b)

Figure 3.13: Free rise of the polyurethane foam obtained after 24 hours of curing in air: (a) water added to the precursor and mixed (1:1 ratio); (b) water added to the precursor without mixing (1:1 ratio)

Low viscosity polyurethane precursor (HA Flex SLV AF)

The second healing agent was a commercially available polyurethane precursor (HA Flex SLV AF, De Neef Conchem, Belgium). It is a 1-component methylene diphenyl diisocyanate (MDI) and polyether-polyol-based prepolymer, which contains inert hydrophobic compounds that control the viscosity and rheological behavior, with an approximate viscosity of 200 mPa·s at 25 °C, which makes it characterized by its low viscosity among the studied polymeric healing agents. The healing agent is free of volatile organic compounds, does not contain catalysts or any water-soluble products.

The product is commonly used in the construction sector for grouting joints or stopping water leaks in concrete structures, which are subject to settlement and movement, and for stopping water leaks through joints between tunnel segments.

This PU precursor cures upon contact with moisture to a tough, flexible, closed-cell polyurethane foam. The expansion rate, which is the volume of finished foam divided by the initial volume of precursor, ranges between 12 and 18, depending on temperature and the amount of accelerator if present. This product has been tested before for its efficiency for self-healing cementitious materials based on encapsulated systems [15, 29, 30, 34, 37, 179–181].

3.4.3 Bacterial healing agents

Ureolytic bacterial strain (*Bacillus Sphaericus*)

Bacterially induced calcium carbonate ($CaCO_3$) precipitation has been widely proposed as environmentally-friendly repairing agent due to its inherent compatibility with the cementitious matrix. Gollapudi et al. [201] were the first that, in 1995, introduced this novel biological crack repair technique.

Microbial $CaCO_3$ precipitation can be caused by different metabolic pathways among which the hydrolysis of urea. The precipitation is determined by several factors: the concentration of dissolved inorganic carbon, the pH and the concentration of calcium ions are provided by the metabolism of the bacteria, and the presence of nucleation sites which are constituted by the cell wall of the bacteria [291].

The advantage of urea hydrolysis is that this process is easily regulated and the process results in the production of large amounts of $CaCO_3$ in a short time span [182]. According to literature [202], ureolytic micro-organisms produce urease which catalyzes the hydrolysis of urea ($CO(NH_2)_2$) into ammonium (NH_4^+) and carbonate (CO_3^{2-}). First, 1 mole of urea is hydrolyzed intracellular to 1 mole of carbamate and 1 mole of ammonia (Equation 3.5). Carbamate spontaneously hydrolyzes to form additionally 1 mole of ammonia and carbonic acid (Equation 3.6). These products subsequently form 1 mole of bicarbonate and 2 moles of ammonium and hydroxide ions (Equations 3.7, 3.8). The last 2 reactions give rise to a pH increase, which in turn shifts the bicarbonate equilibrium, resulting in the formation of carbonate ions (Equation 3.9).

$$CO(NH_2)_2 + H_2O \longrightarrow NH_2COOH + NH_3 \tag{3.5}$$

$$NH_2COOH + H_2O \longrightarrow NH_3 + H_2CO_3 \tag{3.6}$$

$$H_2CO_3 \longleftrightarrow HCO_3^- + H^+ \tag{3.7}$$

$$2\,NH_3 + 2\,H_2O \longleftrightarrow 2\,NH_4^+ + 2\,OH^- \tag{3.8}$$

$$HCO_3^- + H^+ + 2\,NH_4^+ + 2\,OH^- \longleftrightarrow CO_3^{2-} + 2\,NH_4^+ + 2\,H_2O \tag{3.9}$$

Since the cell wall of the bacteria is negatively charged, the bacteria draw cations from the environment, including calcium ions (Ca^{2+}), to deposit on their cell surface. The Ca^{2+} ions subsequently react with the CO_3^{2-} ions, leading to the precipitation of $CaCO_3$ at the cell surface that serves as a nucleation site (Equations 3.10,

3.11).

$$Ca^{2+} + Cell \longrightarrow Cell{-}Ca^{2+} \tag{3.10}$$

$$Cell{-}Ca^{2+} + {CO_3}^{2-} \longrightarrow Cell{-}CaCO_3\downarrow \tag{3.11}$$

Microbial $CaCO_3$ precipitation was successfully used for the consolidation of sand columns [201] or the surface treatment of limestone [202] and concrete [203]. In 2007, Jonkers and Schlangen [204] started to investigate the possibility to use bacterial $CaCO_3$ for autonomous crack healing, consequently providing all necessary components within the cementitious matrix.

When bacteria are used to heal cracks in concrete, the major hindering factor is the high pH, which may restrict the growth of the bacteria [182]. Moreover, bacteria need to remain active until the moment when cracks appear. Therefore, in order to be suitable for autonomous healing applications, bacterial strains need to be able to form spores. Spores are viable but dormant cells that are able to resist high mechanically and chemically induced stresses and remain viable for periods up to 50 years. However, also bacterial spores added directly to the concrete mixture are subjected to a decrease in lifetime due to the hydration process which causes cell collapse [229]. Therefore, most strains require immobilization of the bacterial cells and protection from the alkaline environment and the reduction in porosity caused by the hydration process. For this reason, encapsulation is necessary.

The bacterial healing agent used in this research study consists of an ureolytic bacterial strain, namely *Bacillus Sphaericus* (*Bacillus sphaericus* LMG 22257, Belgian coordinated collection of microorganisms, Ghent), coupled with a suitable deposition medium, referred to as DM, in order to allow the hydrolysis of urea. The sealing promoted by the microbially $CaCO_3$ needs some time and it is obtained through the activation of the bacteria with water. This strain has a high urease activity (40 mM urea hydrolyzed. $OD_1^- h_1^-$), long survival time, and can produce $CaCO_3$ in a simple and controllable way [31]. Bacterial cells were used as a first proof of their compatibility with the extruded cementitious capsules instead of spores. The medium used to grow *B. sphaericus* consisted of yeast extract and urea. The yeast extract medium was first autoclaved for 20 min at 120 °C and the urea solution was added, which was sterilized by means of filtration through a sterile 0.22 µm Millipore filter (Millipore, USA). The final concentrations of yeast extract and urea were 20 g/L. Cultures were incubated at 28 °C on a shaker at 100 rpm for 24 h. Bacterial cells were harvested by centrifuging (7000 rpm, 7 min, Eppendorf MiniSpin, Hamburg, Germany) the 24 hours-old grown culture, and the cells were resuspended in saline solution (NaCl, 8.5 g/L). The concentration of bacterial cells in the bacterial suspension (BS) was 109 cells/mL, determined by flowcytometry (Accuri C6, BD Biosciences, USA). In order to provide a suitable carrier to immobilize bacteria and to protect them from the harsh environment of

the cementitious matrix, following previous works [31, 182], the BS was mixed before encapsulation (volume ratio 1:1) with a colloidal silica-sol (Levasil®CS30-316P, Obermeier, Germany) with a viscosity lower than 20 mPas at 20 °C. Additionally, a deposition medium (DM) consisting of 20 g/L urea and 79 g/L $Ca(NO_3)_2 \cdot 4\,H_2O$ was provided separately, in order to allow the carbonate precipitation induced by the urease activity. The BS mixed with silica-sol and the DM were provided in separate capsules which were coupled as explained in Section 3.2.

3.5 Conclusions

The manufacturing of the cementitious shell of the capsules was made possible through the development of a polymer-modified cement paste, which allowed the shaping of cementitious tubes that can be cut at different lengths. Two manufacturing techniques were investigated in order to shape the tubes. The first was based on an extrusion process, which allowed to obtain ridged tubes with an ovoid hollow cross section. The ridged surface has the potential to increase the bond between the capsule and the surrounding matrix. However, the setting of the paste under its own weight causes a variability in the dimensions of the cross section of the capsules. The second manufacturing technique was based on the manual shaping of the tubes by rolling the polymer-modified cement paste around an oiled bar with a circular cross section of the desired diameter. In this way, the setting of the paste on the bar allows to obtain a higher control over the dimensions of the cross section. Both procedures were manually realized in the laboratory but have good potential to be scaled-up through the use of industrial procedures.

Another aspect of paramount importance to obtain an efficient encapsulation system was the coating and subsequent sealing of the capsules. Epoxy resin was selected after several unsuccessful trials to encapsulate highly moisture-reactive healing agents, which could easily react prematurely inside the capsules if the latter do not present high standards of waterproofing and tightness. Two types of coating procedures were studied in order to cover the shell either externally or internally. The external coating procedure allows to isolate both the core and the cementitious shell. On the other hand, the internal coating allows to protect the core while maintaining the contact between the cement matrix and the cementitious shell, which are inherently compatible. The proper functioning of the two different coating procedures and their effect on the healing agents' protection and release is further studied in Chapters 4 and 5. Finally, epoxy was also successfully used to seal the capsules ends.

The capsules produced in accordance to the above-mentioned procedures allowed to encapsulate several healing agents from the main types commonly used for self-healing encapsulated systems, namely minerals (sodium silicate solutions and water repellent agents), polymers (two highly moisture-reactive polyurethane

precursors), and bacteria (alkali-tolerant ureolytic bacterial strain *Bacillus Sphaericus*). Moreover, the system was proven effective in resisting the mixing procedure. This characteristic, combined with their inherent compatibility with the cementitious matrix and the easy customization of the capsules size and shape, makes cementitious capsules equivalent to *enhanced aggregates* that can be perspectively used in the ordinary construction processes.

Chapter 4

Preliminary study on the compatibility between cementitious capsule and healing agents

The research activities described in this chapter concern preliminary studies conducted on the compatibility of the cementitious capsules produced with the new mix design, coating, and sealing procedures with various types of healing agents.

For reasons of continuity with the previous studies on the extruded cementitious capsules [38, 39], a sodium silicate solution was selected from the mineral healing agent type in order to test the compatibility of the capsules with very low viscosity healing agents, which can easily flow out from capsules without the necessary waterproofing. The expansive polyurethane precursor was selected from the polymer healing agent type in order to test the compatibility of the capsules with highly moisture-reactive healing agents, which is a challenging issue for the encapsulation

---

Part of the work described in this chapter has been previously published in:

[250] G. Anglani, P. Antonaci, G. Idone, and J.-M. Tulliani. "Self-healing of cementitious materials via embedded macro-capsules". In: *Proceedings of the 4th International Conference on Service Life Design for Infrastructures (SLD4)*. Ed. by G. Ye, Y. Yuan, C. Romero Rodriguez, H. Zhang, and B. Šavija. Delft, the Netherlands: RILEM Publications S.A.R.L., 2018, pp. 385–388

[251] G. Anglani, P. Antonaci, J.-M. Tulliani, K. Van Tittelboom, J. Wang, and N. De Belie. "Self-healing efficiency of cement-based materials containing extruded cementitious hollow tubes filled with bacterial healing agent". In: *Final Conference of RILEM TC 253-MCI: Microorganisms-Cementitious Materials Interactions*. Ed. by A. Bertron and H. Jonkers. Toulouse, France: RILEM Publications S.A.R.L., 2018, pp. 425–431

system. In fact, while for the low viscosity healing agents the problem is the leakage of the agent from the capsule, in this case the main issue is to prevent the ingress of moisture that could cause a premature reaction of the agent inside the capsule. Finally, a bacterial strain was selected in order to test the compatibility of the cementitious capsules with this type of bio-based healing agents and in order to assess the positive effect of the addition of the bacterial strain to its carrier (i.e. a silica solution), which could cause healing effects also in absence of the strain. Moreover, the different curing condition effect on the efficiency was investigated.

These tests are considered as preliminary studies mainly due to the small number of specimens on which they were performed, not allowing to have statistically significant results, but provided indications for the further investigation described in this thesis.

4.1 Compatibility with mineral and polymeric healing agents

4.1.1 Mortar prisms

Mortar prisms (40 mm × 40 mm × 160 mm) were made by using ordinary Portland cement CEM I 52.5 N, tap water, and normalized sand (0-2 mm grading), with a water to cement ratio of 0.5 and a sand to cement ratio of 3, in accordance with the standard UNI EN 196-1.

Extruded cementitious macro-capsules, produced as described in Chapter 3 (Mix design 1) were produced to carry the healing agents, namely the sodium silicate solution (Na_2O 10.6 wt%, SiO_2 26.5 wt%, and H_2O 62.9 wt%, Sigma Aldrich, Italy) and the highly expansive polyurethane precursor (CarboStop U, Orica) described respectively in Section 3.4.1 and 3.4.2. The capsules had a length of 5 cm, were externally coated (Section 3.2), and were rolled into sand all along their length to improve the bonding with the surrounding mortar matrix. The capsules were manually embedded in the middle of the specimens during casting, without any additional device to fix their position. Both self-healing mortar prisms, either with the encapsulated sodium silicate solution (SSL series) or the highly expansive polyurethane precursor (EPU series), and reference mortars prisms without capsules (REF series), were produced. Upon casting, specimens were covered with plastic foils. After 24 hours, specimens were demolded and stored in water for 28 days, a curing condition representing a hard challenge for the stability of the capsules, especially those containing the highly reactive PU precursor.

Figure 4.1: Visual observation of the leakage of the polyurethane precursor, causing the formation of hardened polyurethane foam.

4.1.2 Crack creation and curing

At an age of 28 days, a discrete crack was created in the middle of the specimens by a three-point bending test, using a 250 kN closed-loop servo-controlled hydraulic press (MTS Systems Corporation, USA) in crack mouth opening displacement (CMOD) control mode, with a constant rate of 1.5 µm/s and a loading span of 100 mm. Tests were performed at room temperature (≈ 23 °C). A clip-on gauge was used to measure the displacement at the notch during loading, limiting the crack mouth aperture to 800 µm. A U-shaped notch was created a day before cracking by wet saw-cutting, measuring 4 mm in width and 5 mm in height.

During the cracking process, it was possible to observe the leakage of the healing agents from the cracked specimens, especially in the case of the EPU series were the yellow foam formation was clearly visible from the crack mouth (see Figure 4.1) apart one case (specimen EPU_4).

Figure 4.2 shows some of the load versus CMOD curves recorded during the crack creation for the different series.

It should be pointed out that during the crack creation, the presence of the cementitious capsules did not have a substantial detrimental effect on the peak load that the specimens could withstand. Furthermore, the capsule breakage was accompanied by an audible sound and could be related to the observed drop in loads that happened for CMOD lower than 250 µm (Figure 4.2). As for the leakage of PU foam, no load drops were detected for the specimen EPU_4.

To allow proper curing of the healing agents, all specimens were stored in the lab at about 20 °C before testing for mechanical regain and water permeability/absorption, for a time well beyond the curing time of the healing agents: 5 weeks for the sodium silicate and 10 days for the polyurethane (which has a foaming time lower than 5 minutes with 10% of water respect with its volume).

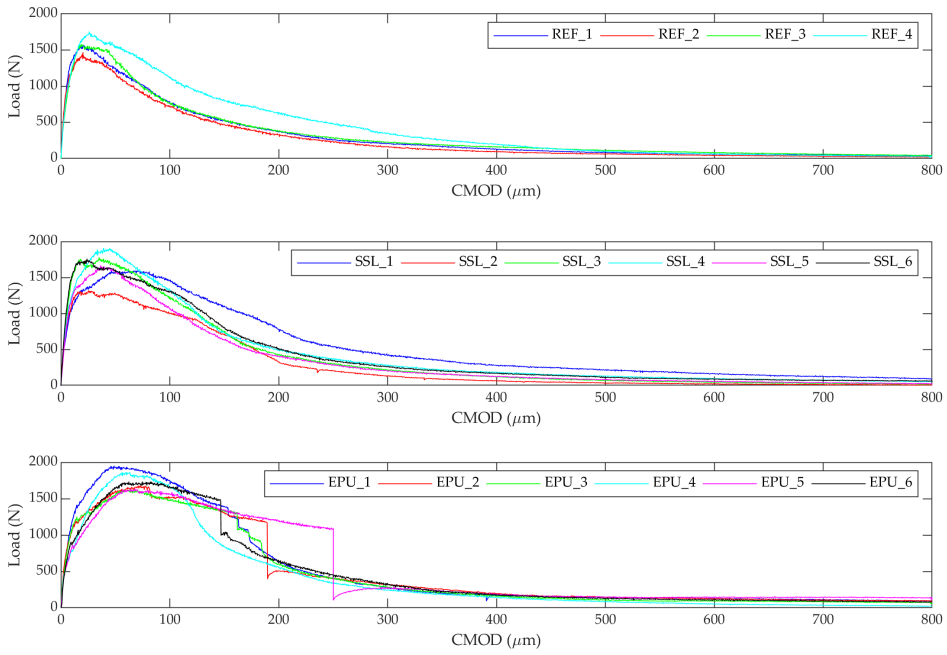

Figure 4.2: Load versus CMOD curves during the pre-cracking for the different series.

4.1.3 Evaluation of the healing process

Mechanical recovery

After the curing of the healing agents, specimens from each series were statically reloaded following the same procedure used for pre-cracking. This allowed to evaluate the mechanical recovery through a load recovery index (LRI) [19, 26, 38, 39, 57, 92] as described in Chapter 6. The LRI was expressed as a function of the maximum load-bearing capacity of the specimens during pre-cracking (L_{peak}) and reloading (L_{reload}) and as a function of the residual load-bearing capacity at the end of pre-cracking (L_{unload}). Its definition is reported in Equation (4.1):

$$LRI(\%) = \frac{L_{reload} - L_{unload}}{L_{peak} - L_{unload}}, \tag{4.1}$$

Figure 4.3 shows the load versus CMOD curves recorded during the pre-cracking and the static reloading for the different series.

Good and repeatable results were obtained on the reloaded specimens. The specimen EPU_4 which did not show any PU release did not show any recovery, as it was expected. The average LRI of the self-healing specimens were (39 ± 10)% for the six specimens of the SSL series and (42 ± 14)% for the five specimens

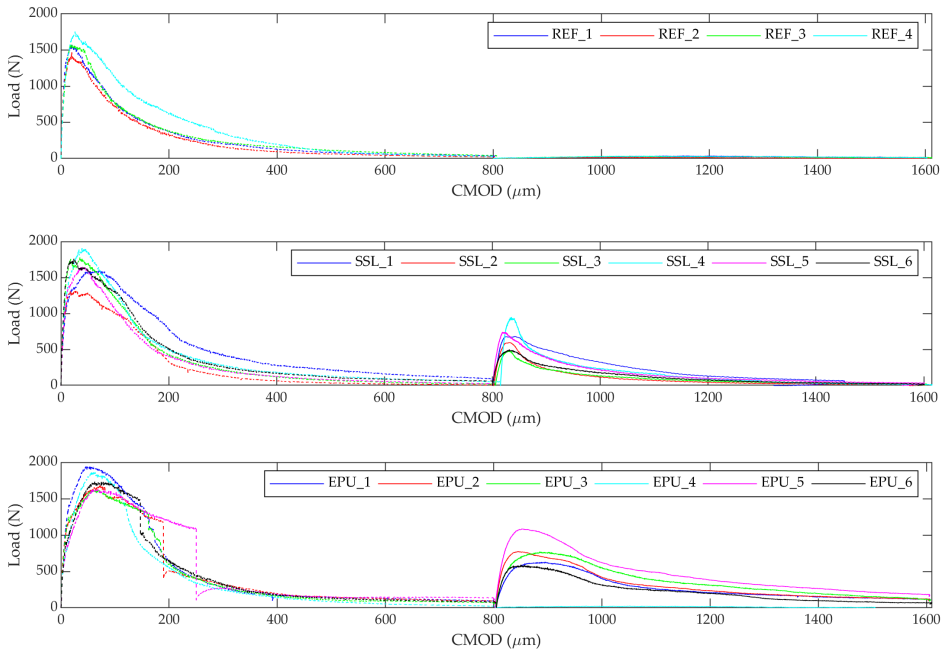

Figure 4.3: Load versus CMOD curves during the pre-cracking (dashed line) and the subsequent static reloading (continuous line) for the different series.

of the EPU series, while the reference plain mortar specimens did not show any mechanical recovery.

Splitting the specimen SSL_1 after reloading, it was noticed that not all the sodium silicate was released, most likely due to the large volume of the cementitious capsules. Since some silicate could have been released during the reloading, after 8 months the other 5 specimens of the SSL series were reloaded (see Figure 4.4).

A second healing effect was detected, with an increase of the maximum load-bearing capacity with respect to the residual load-bearing capacity at the end of the first reloading. This new load bearing capacity was on the average equal to the $(27 \pm 4)\%$ of the maximum load bearing capacity L_{reload} measured during the first reloading, meaning that multiple healing could be possible due to the presence of unreacted healing agent inside the capsules.

Durability recovery

Since the ability of polyurethane healing agents to restore good water impermeability performances has been widely established in literature [21, 26, 29, 30, 33–35, 37, 179], the EPU series was tested in order to have an indication of its self-sealing efficiency.

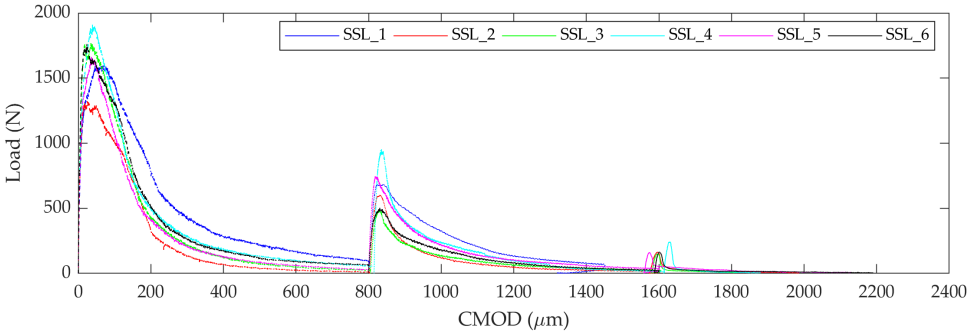

Figure 4.4: Load versus CMOD curves during the pre-cracking (dashed line), the first static reloading (dotted line) and the second static reloading (continuous line) for the SSL series.

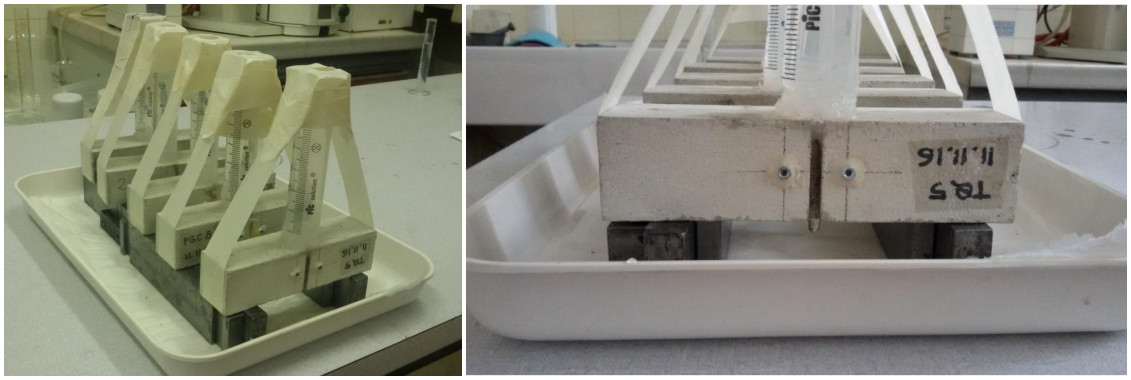

Figure 4.5: Setup of the water permeability test.

The sealing efficiency during water permeability tests was evaluated with a procedure analogous to the one adapted from the Japanese standard JIS A 6909 for water permeability through coating materials for textured finishing of buildings and other adopted in literature to measure the reduction of water ingress through realistic cracks in self-healing cementitious systems [21, 200, 292] and sharing similarities with the RILEM Test Method II.4 for water absorption under low pressure.

The testing method consisted in monitoring in time the water leakage from a pipette (50 mL capacity) with a funnel with a progressive smaller diameter. The pipette was positioned above the crack on the lateral face of the specimens and the funnel was sealed with silicone to avoid lateral leakage (Figure 4.5).

In Figure 4.6, it is possible to see the water leakage in terms of water content of the pipette in time.

A substantial tightness recovery of the self-healing mortar specimens was observed, since the cracked REF specimen allowed a complete leakage of the pipette content during the first minutes of the test, while the EPU series did not show a

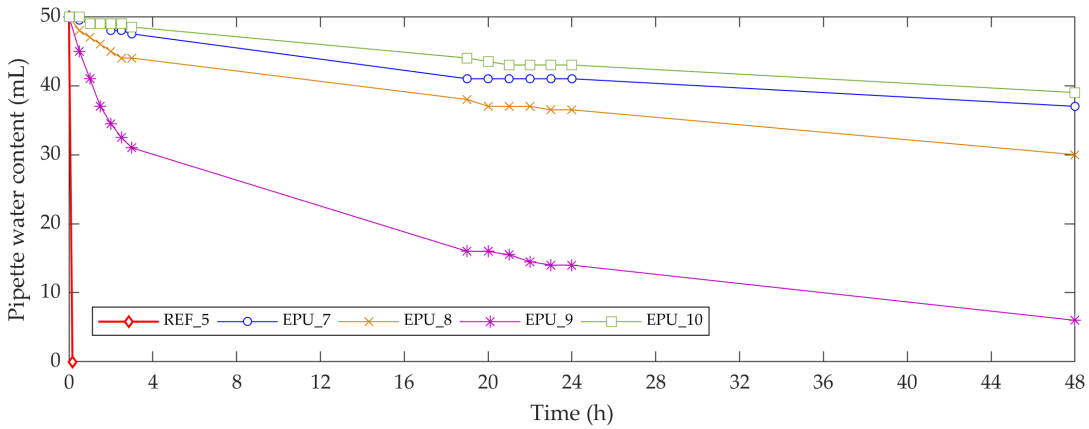

Figure 4.6: Pipette water content versus time.

complete water leakage after 48 hours.

The sealing efficiency was also evaluated via gravimetrical water absorption tests [15, 18, 20, 29, 34]. The specimens were dried at 40 °C and then stored for one day at around 20 °C and 40% RH in the laboratory. Subsequently, they were sealed with adhesive aluminum foil (except the zone of 4 mm × 40 mm in the middle of the specimen, i.e. the notch) and weighed. The test procedure is based on the method described in EN 13057 and consists of bringing the cracked face of the specimens into contact with water (up to 5 mm, i.e. the tip of the notch) and monitoring the mass of absorbed water. The percent change in mass due to the absorbed water (PC_w) is defined as:

$$PC_w\,(\%) = \frac{m_w - m_d}{m_d} \cdot 100 \tag{4.2}$$

where m_w is the mass of the specimen absorbing water (g) and m_d is the mass of the dry specimen (g). In Figure 4.7 the percent change in mass PC_w is plotted in time.

It is possible to see that after 48 hours of immersion, the mass increase of the REF series was higher than that of the EPU series. In order to evaluate the sealing efficiency with respect to the reference specimens, the percent change of mass during the water absorption tests after 48 hours of immersion was considered to define a sealing efficiency index (SE_{wa}):

$$SE_{wa} = \frac{PC_{w,REF} - PC_{w,EPU}}{PC_{w,REF}} \cdot 100 \tag{4.3}$$

The sealing efficiency resulted in an average value of (53 ± 11)%.

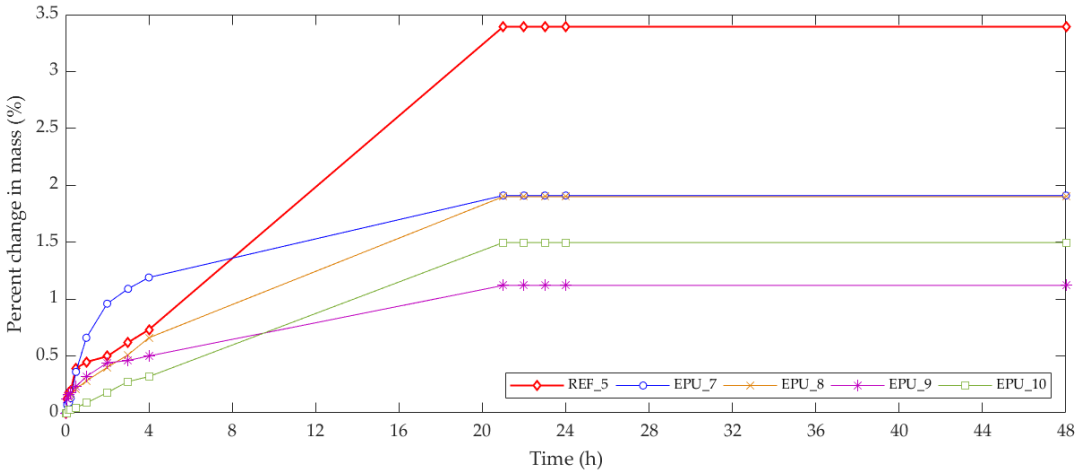

Figure 4.7: Percent change in mass due to the absorbed water PC_w versus time

4.2 Compatibility with bacterial healing agents

4.2.1 Mortar prisms

In order to test the self-healing efficiency of the bacteria-incorporated specimens (dimensions: 40 mm x 40 mm x 160 mm) were produced by using ordinary Portland cement CEM I 52.5 N, tap water, and normalized sand (0-2 mm grading), with a water to cement ratio of 0.5 and a sand to cement ratio of 3, in accordance with the standard UNI EN 196-1.

Extruded cementitious macro-capsules, were produced as described in Chapter 3 (Mix design 1)to carry the healing agent, namely the ureolytic bacterial strain *Bacillus Sphaericus* (*Bacillus sphaericus* LMG 22257, Belgian coordinated collection of microorganisms, Ghent), mixed before encapsulation (volume ratio 1:1) with a colloidal silica-sol (Levasil®CS30-316P, Obermeier, Germany) and provided with a deposition medium (DM) consisting of 20 g/L urea and 79 g/L $Ca(NO_3)_2 \cdot 4\,H_2O$, as described in Section 3.4.3. The capsules had a length of 5 cm and were either externally or internally coated (Section 3.2) and were not rolled into sand. The BS mixed with silica-sol and the DM were provided in separate capsules which were coupled as explained in Section 3.2 (Figure).

In order to demonstrate the improvement in the sealing performances due to the presence of the bacterial strain with respect to the effect exerted by the use of the only silica-sol, capsules were produced with only silica-sol without bacteria. A total of 8 mortar prisms were produced:

- 2 with BS mixed with silica-sol and DM, externally coated (BAC_EXT series);

Figure 4.8: Capsules after filling and sealing, either with external or internal coating.

- 2 with BS mixed with silica-sol and DM, internally coated (BAC_INT series);
- 2 with silica-sol and DM, externally coated (SIL_EXT series);
- 2 with silica-sol and DM, internally coated (SIL_INT series).

The capsules were manually embedded in the middle of the specimens during casting, without any additional device to fix their position. After 24 hours from casting, they were demolded and cured in water for one week.

4.2.2 Crack creation and curing

At an age of 7 days, a discrete crack was created in the middle of the specimens by a three-point bending test, using a 100 kN closed-loop servo-controlled hydraulic press (MTS Systems Corporation) in crack mouth opening displacement (CMOD) control mode, with a constant rate of 1.5 µm/s and a loading span of 100 mm. Tests were performed at room temperature (≈ 23 °C). A clip-on gauge was used to measure the displacement at the notch during loading, limiting the crack mouth aperture to 400 µm. In all samples a U-shaped notch was created one day before cracking by wet saw-cutting, measuring approximately 4 mm in width and 6 mm in height.

Figure 4.9 shows some of the load versus CMOD curves recorded during the crack creation for the different series.

The residual CMOD, as detected by the displacement sensor upon complete unloading was about 383 µm on average. It has to be noted that specimen SIL_INT_2 underwent a smaller crack opening with respect to the other samples, due to an accident which occurred during the cracking procedure (maximum CMOD equal to 273 µm, residual CMOD equal to 271 µm, Figure 4.9).

During the cracking process, it was possible to observe the leakage of the healing agent up to the external surfaces of the specimens (see Figure 4.10).

After crack creation, half of the specimens were cured for a week in demineralized water, the other half in a solution (UYE solution) of demineralized water, urea (12 g/L), and yeast extract (2 g/L) (see Table 4.1).

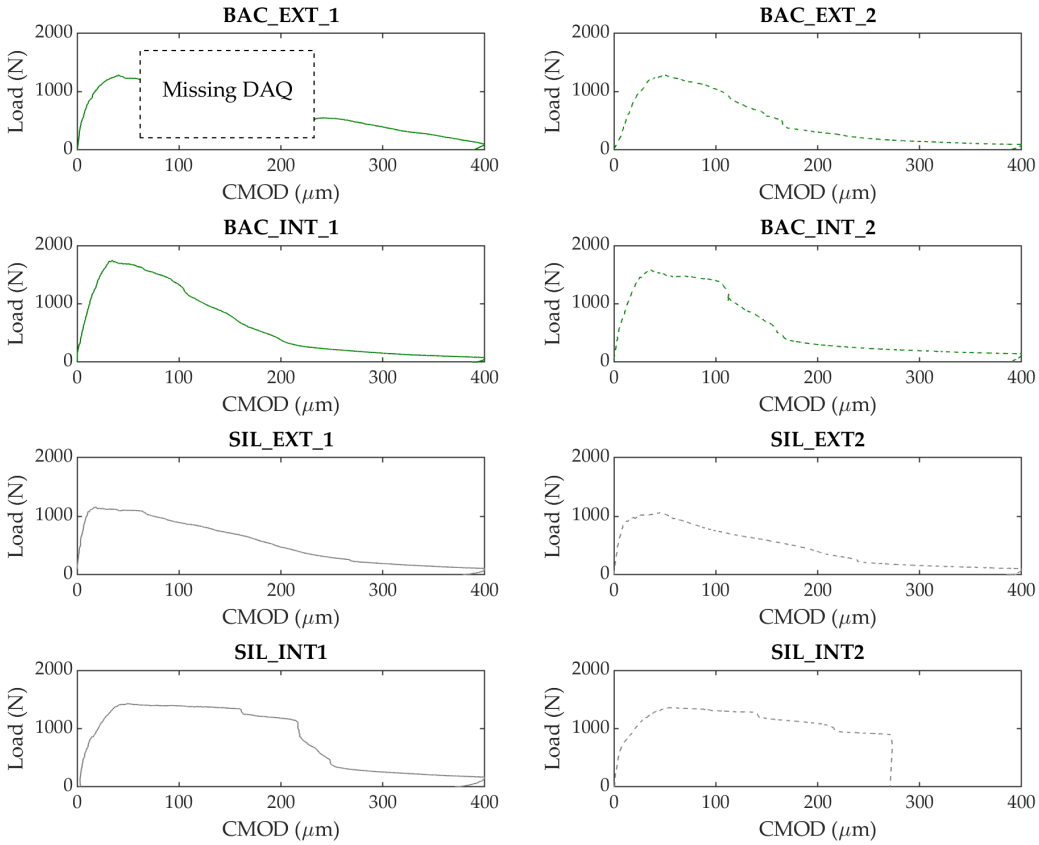

Figure 4.9: Load versus CMOD curves during the pre-cracking for the different specimens.

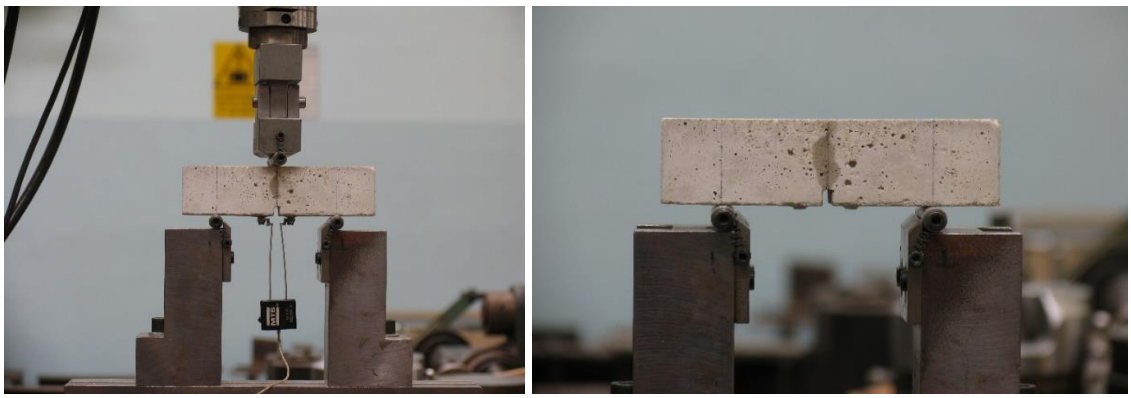

Figure 4.10: Visual observation of the agent leakage during crack creation.

Table 4.1: Curing conditions after cracking.

Demineralized water	**UYE solution (H_2O+urea+yeast)**
BAC_EXT_1	BAC_EXT_2
BAC_INT_1	BAC_INT_2
SIL_EXT_1	SIL_EXT_2
SIL_INT_1	SIL_INT_2

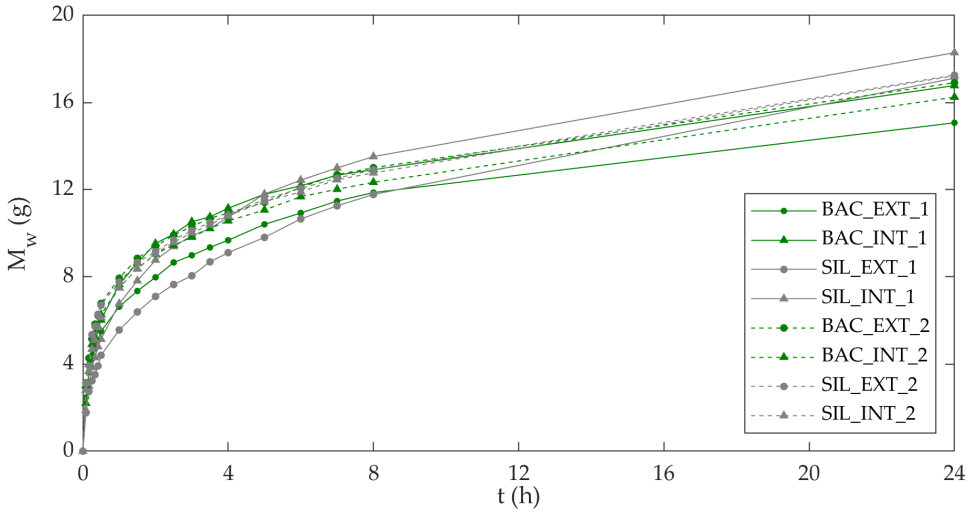

Figure 4.11: Water uptake of each series plotted in time.

4.2.3 Evaluation of the healing process

Water absorption

Water absorption was evaluated via gravimetrical water absorption tests [15, 18, 20, 29, 34]. After curing, the specimens were dried at 40°C for 10 days, until constant mass was achieved (i.e. mass change less than 0.1% in 24 h). Before the test started, the specimens were stored for one day at around 20°C and 60% RH in the laboratory, subsequently sealed with adhesive aluminum foil (except the zone of 4 mm × 40 mm in the middle of the specimen, i.e. the notch) and weighed. The test procedure is based on the method described in EN 13057 and consists of bringing the cracked face of the specimens into contact with water (in this case, up to the tip of the notch) and monitoring the mass of absorbed water (M_w). In Figure 4.11 the mass of absorbed water M_w is plotted in time.

Based on the data of water absorbed after 1 hour and 24 hours of immersion ($M_{w,1h}$ and $M_{w,24h}$ respectively) it is possible to calculate a sorptivity index (S, in g/$\sqrt{}$ h), as defined in Equation 4.4:

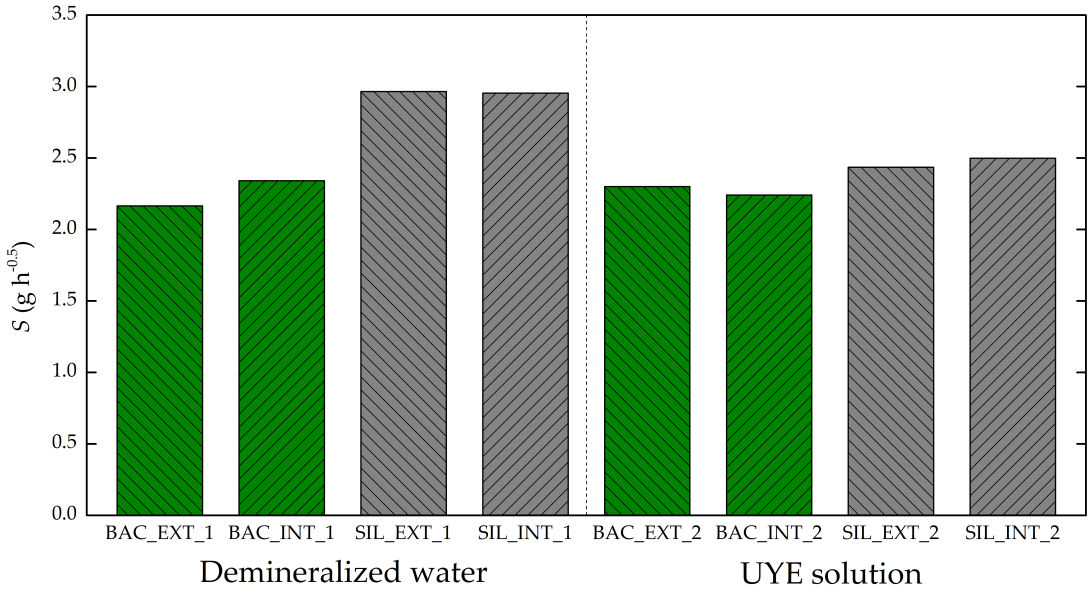

Figure 4.12: Sorptivity index S of each specimen.

$$S = \frac{M_{w,24h} - M_{w,1h}}{\sqrt{24h} - \sqrt{1h}} \tag{4.4}$$

Accordingly, the results of the water absorption tests performed on the different specimens are shown in Figure 4.12.

Overall, the water absorption test did not show remarkable differences among the specimens with incorporated bacteria, though the evidence has low statistical significance due to the limited number of samples per coating and curing condition. As expected, the uptake of water is higher in the specimens with just silica-sol than in the bacterial ones, indicating that bacteria were able to precipitate $CaCO_3$ that had positive effect on decreasing the water absorption. To quantify this effect, the bacterial efficiency in reducing the water absorption was calculated with Equation 4.5:

$$BE_{wa}\,(\%) = -\frac{S_{BAC\_i} - S_{SIL}}{S_{SIL}} \cdot 100 \tag{4.5}$$

Here, the quantity BE_{wa} is defined as the decrease of the sorptivity coefficients in the bacterial self-healing specimens (S_{BAC_i}) with respect to the silica-sol ones (S_{SIL}). For the sake of comparison, the term S_{SIL} was set as the average of the results obtained for all the specimens containing only silica-sol. The minus sign in Equation 4.5 was introduced to obtain positive performance indexes when there were improvements with respect to the silica-sol specimens' performance (i.e. reduction of the S). Results are reported in Table 4.2, showing the positive effect of

Table 4.2: Bacteria efficiency on the water absorption reduction.

Specimen	BE_{wa} (%)
BAC_EXT_1	+20.23
BAC_INT_1	+13.71
BAC_EXT_2	+15.22
BAC_INT_2	+17.39

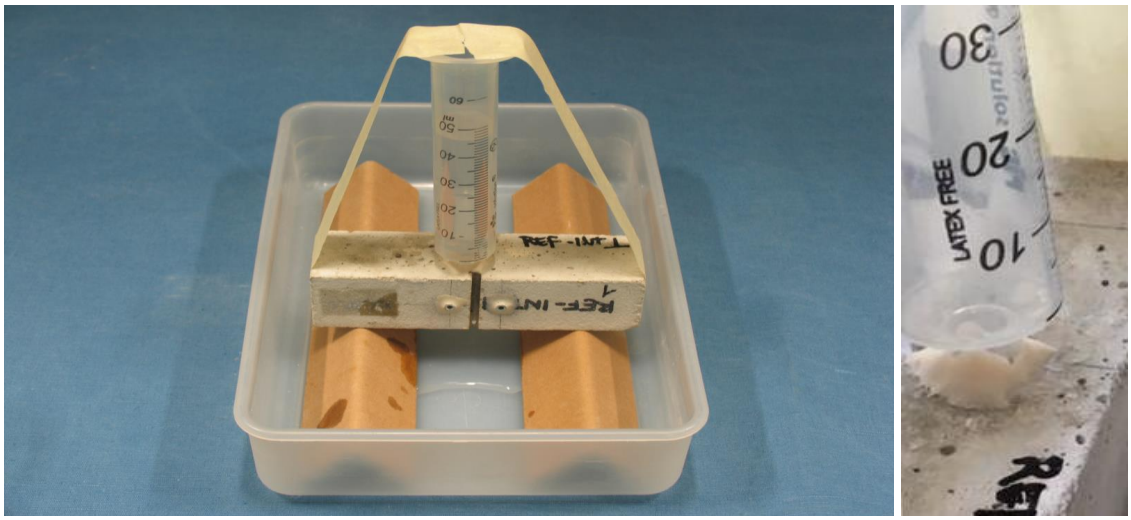

Figure 4.13: Setup of the water permeability test.

the addition of the bacterial strain.

Water permeability

The sealing efficiency during water permeability tests was evaluated with a procedure analogous to the one adapted from the Japanese standard JIS A 6909 for water permeability through coating materials for textured finishing of buildings and other adopted in literature to measure the reduction of water ingress through realistic cracks in self-healing cementitious systems [21, 200, 292] and sharing similarities with the RILEM Test Method II.4 for water absorption under low pressure.

The testing method consisted in monitoring the water leakage from a pipette (50 mL capacity) with a funnel with a progressive smaller diameter, positioned above the crack on the lateral face of the specimens. The interface gap between the funnel and the specimens was sealed with a methyl methacrylate resin (X60, HBM) (see Figure 4.13).

The test was carried out until penetration of a water volume of 50 mL through the crack, detecting the elapsed time. The test was performed twice, respectively on specimens in a dry state (same conditioning as the previous water absorption test)

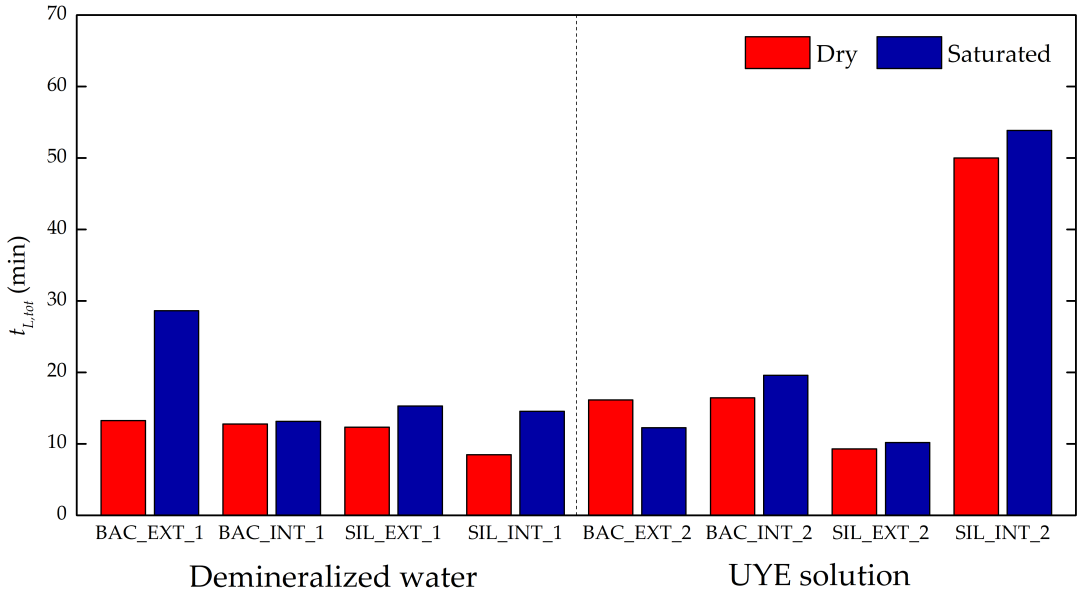

Figure 4.14: Time required for a total leakage of 50 mL to occur for the different specimens.

and on specimens in saturated condition (after four days of immersion in water).

In Figure 4.14, results for the water permeability test are reported in terms of time required for a total leakage of 50 mL to occur on the different specimens.

It is important to point out the unexpected behavior observed in the specimen SIL_INT2. Here, a much longer time was detected for a complete leakage, meaning that the permeability performance was superior with respect to the other samples, either with bacteria or not. This may depend on the smaller residual crack opening (see Figure 4.9) that, further than reducing the leakage rate, can enhance the autogenous healing promoted by the humid environment.

The bacterial efficiency on the water permeability (increase of time required for total leakage, BE_{wp}) was calculated with Equation 4.6:

$$BE_{wp}\,(\%) = \frac{t_{L,tot\,BAC} - t_{L,tot\,SIL}}{t_{L,tot\,SIL}} \cdot 100 \tag{4.6}$$

For the sake of comparison, the normalization factor in the denominators was set as the average of the results obtained for all the silica-sol specimens in the same state ($t_{L,tot\,SIL}$), except for the results obtained for specimen SIL_INT2 that were considered anomalous. Results are reported in Table 4.3. All the tests conducted in dry state showed the positive effect of the bacterial strain on the water permeability reduction.

Table 4.3: Bacteria efficiency on the water permeability reduction.

Specimen	$BE_{wp,dry}$ (%)	$BE_{wp,saturated}$ (%)
BAC_EXT_1	+32.13	+114.73
BAC_INT_1	+27.45	-1.55
BAC_EXT_2	+60.91	-8.1
BAC_INT_2	+63.84	+46.96

4.3 Conclusions

The cementitious capsules, either with external or internal coating, appear to be suitable to contain and release several types of healing agents, also the highly moisture-reactive ones, as shown by the occurrence of visible leakage during crack creation. The effect of the different coating configuration on the recovery efficiency will be further investigated in Chapter 5.

The potential self-healing effect in the preliminary configuration studied in this chapter was evaluated in terms of sealing efficiency during water permeability and absorption tests, and in terms of strength regain after reloading in three-point-bending. Promising results were achieved: a substantial tightness and strength recovery was observed, even in specimens presenting large crack widths. In the case of the silicate solution, the high internal volume of the cementitious capsules allowed to obtain a second healing effect. For what concerns the bacterial healing agent, the addition of the bacterial strain to the silica sol improved the sealing efficiency of the system. Moreover, the curing condition in the urea and yeast extract did not show a remarkable increase in the sealing efficiency, proving that the system can work simply in presence of water and that the nutrients provided inside the capsules are enough to allow the microbial precipitation of calcium carbonate.

These promising results served as a basis to further assess the effectiveness of cementitious capsules, by expanding the statistical sample and using different testing protocols as it will be shown in the next chapters.

Chapter 5

Sealing efficiency with different healing agents

The main focus of the research activities explained in this chapter was the investigation of the self-sealing capability provided by the use of cementitious capsules filled with different healing agents. The sealing efficiency can be classified as recovery in durability-related properties, since durability can be increased when self-sealing of cracks results in retrieval of water tightness, thus preventing the penetration of aggressive liquids along these cracks into the matrix, which could cause further damage [47].

Based on the preliminary successful findings, it was decided to encapsulate one healing agent for each of the main groups of healing substances in order to investigate their different effect of the sealing efficiency: namely, a silane-based water repellent agent (WRA) [28] for the group of mineral substances, a one-component polyurethane (PU) precursor [34] for the group of polymeric substances and a ureolytic bacterial strain (i.e. *Bacillus sphaericus*) dispersed in silica sol (BS) and its deposition medium (DM) [31] for the group of biological substances. Different coating configurations were used.

The efficiency was assessed by evaluating the self-sealing of pre-cracked mortar specimens with the embedded cementitious capsules. The sealing efficiency was evaluated by means of water permeability and water absorption tests, in combination with the visual inspection of the cross sections after final rupture. A novel active crack control technique [41] was implemented in order to reduce the variability on

---

Part of the work described in this chapter has been previously published in:

[253] G. Anglani, T. Van Mullem, X. Zhu, J. Wang, P. Antonaci, N. De Belie, J. M. Tulliani, and K. Van Tittelboom. "Sealing efficiency of cement-based materials containing extruded cementitious capsules". *Construction and Building Materials* 251 (2020), p. 119039. DOI: 10.1016/j.conbuildmat.2020.119039

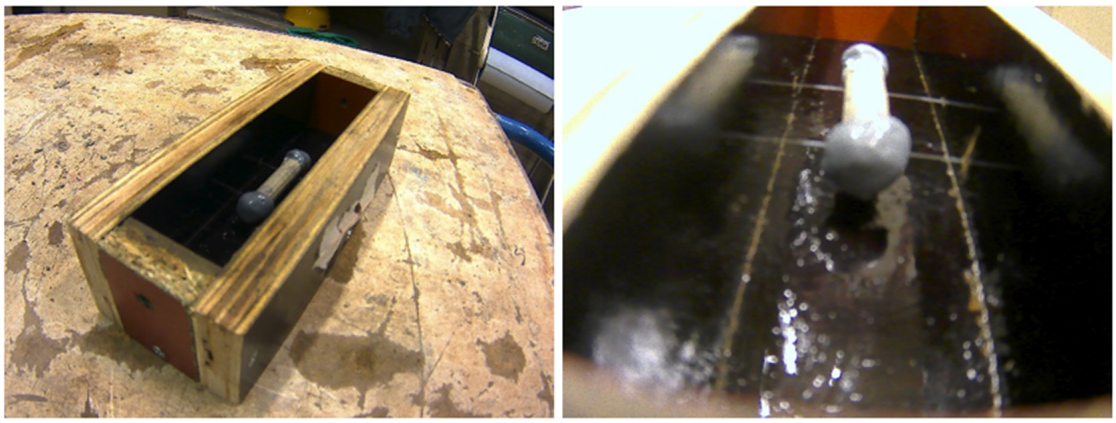

Figure 5.1: Cementitious capsule fixed at its position at the bottom of the molds with nylon threads before the positioning of the oiled bar and casting (cross section in Figure 5.2).

the crack width obtained during the pre-cracking procedure and consequently the variability on the water permeability and absorption tests, which are highly affected by this geometrical parameter [56].

5.1 Materials and methods

5.1.1 Mortar prisms

The self-sealing efficiency of the different healing agents encapsulated in the cementitious capsules was evaluated by using mortar specimens. The mortar was made with a water-to-cement ratio of 0.5 and a sand-to-cement ratio of 3, by using tap water, standardized sand (grading 0/2, DIN EN 196–1), and ordinary Portland cement (CEM I 52.5 N, Holcim, Belgium). The mixing procedure was in accordance with EN 196-1. The fresh conglomerate was used to fill prismatic molds covered with demolding oil (40 by 40 by 160 mm^3), which contained the capsules and a smooth steel bar (diameter of 5 mm) also covered with demolding oil. The bar was positioned centrally, with its center at 12.5 mm from the top side of the specimen, and it was covered with demolding oil in order to ensure its easy removal after casting, in such a way to create a longitudinal hole in the specimen.

Extruded cementitious macro-capsules, produced as described in Chapter 3 (Mix design 1) were produced to carry the healing agents, either with internal or external epoxy coating (see Section 3.2). The capsules had a length of 5 cm and were not rolled into sand. The capsules were placed at 7.5 mm from the bottom side of the specimens by gluing them on two thin nylon threads connected to the lateral side of the molds, to fix their position (Figure 5.1).

Table 5.1: Summary of the characteristics of capsules used for the different series.

		***Series*_INT**	***Series*_EXT**
Manufacturing process		Extrusion	Extrusion
Mix design		Mix design 1	Mix design 1
Surface of the tubular shell coated with epoxy		Internal	External
Average internal diameter of the tubular shell	(mm)	7.5	7.5
Average external diameter of the tubular shell	(mm)	10	10
Average length of the capsule	(mm)	50	50
Average thickness of the epoxy coating	(mm)	1	1
Average internal diameter after epoxy coating	(mm)	5.5	7.5
Volume of cargo healing agent	(mL)	≈1	≈1.5

After the specimens were cast, they were covered with plastic foil and stored in an air-conditioned room at a temperature of (20 ± 2) °C. The day after casting, the steel bar was removed from the specimens when they were demolded. The specimens were then wrapped again in plastic foil and stored at (20 ± 2) °C until the age of 7 days.

Four different series were made: two series containing a single capsule filled with the water-repellent agent (Sikagard®-705 L, Sika, Switzerland) described in Section 3.4.1 (WRA series) or the low viscosity PU precursor (HA Flex SLV AF, De Neef Conchem, Belgium) described in Section 3.4.2 (PUR series); one series containing two coupled capsules, one filled with the bacterial suspension and silica-sol mix and the other capsule filled with the deposition medium as described in Section 3.4.3 (BAC series); one final series consisting of reference specimens without capsules/healing agent (REF series). Each series containing capsules consisted of 8 specimens, 4 of which had capsules with external coating and 4 with internal coating (see Section 3.2), while the REF series consisted of 6 specimens.

The main characteristics of the cementitious capsules used are summarized in Table 5.1.

Table 5.2 summarizes the test series, while Figure 5.2 shows the schematic cross section of all the prepared specimens.

5.1.2 Crack creation and crack width control technique

In order to evaluate the sealing efficiency provided by the use of cementitious capsules filled with different healing agents, a preliminary cracking has first to be

Table 5.2: Test series used to evaluate the self-sealing efficiency.

Series	**Healing agent**	**Number of capsules per specimen**	**Capsule coating**	**Number of specimens**
REF	None	None	-	6
WRA	Water-repellent agent	One capsule	Internal	4
			External	4
PUR	Polyurethane precursor	One capsule	Internal	4
			External	4
BAC	*B. Sphaericus* in silica-sol + Deposition Medium	Two coupled capsules	Internal	4
			External	4

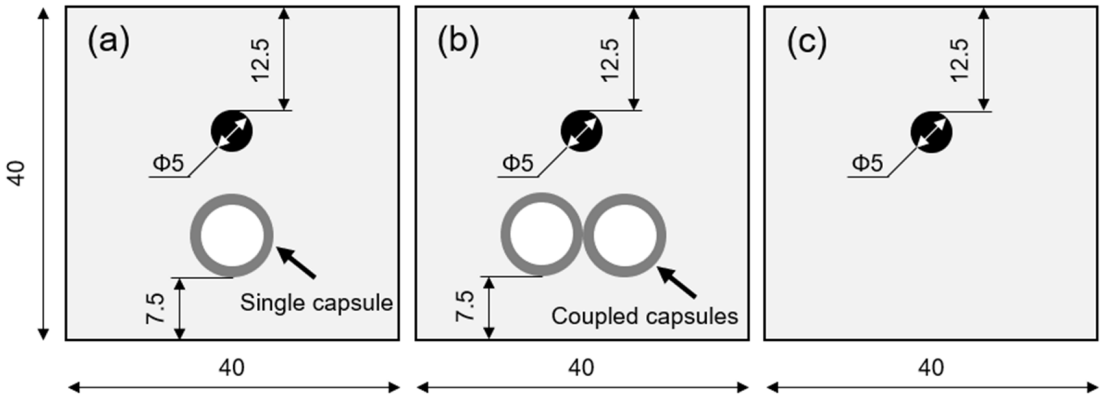

Figure 5.2: Schematic cross section of the specimen containing either (a) one capsule (WRA and PUR series), (b) two coupled capsules (BAC series) or (c) no capsules (REF series). Dimensions expressed in mm.

induced in the specimens [19]. In the attempt to reduce the variability of the crack widths produced by pre-cracking in 3-point bending, and consequently the variability on the sealing results, a novel active crack width control technique was adopted [41]. A Carbon Fiber Reinforced Polymer (CFRP) strip (PC®CARBOCOMP UNI, TRADECC, Belgium) with dimensions of 40 mm by 160 mm was glued on the top side of the mortar specimens a day before pre-cracking by using an epoxy adhesive (Sikadur®-30, Sika, Switzerland). The CFRP strip consisted of unidirectional carbon fibers embedded in epoxy resin. At the age of 7 days from casting, the specimens were cracked until failure in a 3-point bending test setup with a span of 10 cm and at a load rate of 50 N/s. Due to the presence of the CFRP strip, both halves of the mortar specimens divided by the through-going crack created via the 3-point bending test remained connected on top by the laminate, presenting however a large crack between them. As a result of the stiffness of the CFRP, the two halves could

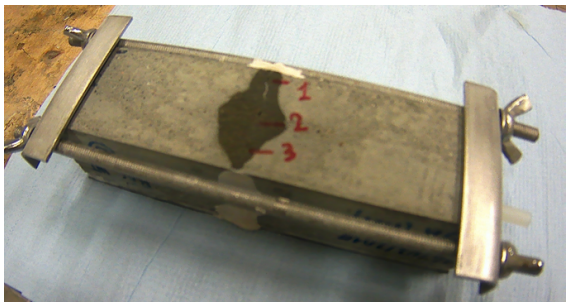

Figure 5.3: Typical sample for which the crack width was controlled using the active crack width control technique. In the figure it is possible to see the healing agent released from the ruptured capsule and spread around the crack mouth (dark colored zone).

only move with one degree of freedom, that was the rotation around the line on top of the through-going crack connected by the laminate. Hence, the crack could be narrowed but the two halves could not rotate relative to each other around their longitudinal axis. Immediately after cracking, the specimens were placed with their crack face upwards and the crack width was restrained using screw jacks using an iterative procedure of measuring and restraining until a desired crack width of 300 µm. The crack width was determined using an optical stereo microscope (Leica S8APO mounted with a DFC295 camera). Along the length of the crack 3 locations were chosen randomly. For each location, the crack width was determined by 4 to 5 measurements. The reported crack width w (µm) is the average of all the measurements of the three locations (in total 12-15 measurements). Fig. 5.3 shows a specimen restrained with the active crack control technique.

Minimally 3 hours after crack creation, the cracks at the sides of the specimens were sealed with a methyl methacrylate glue (Schnellklebstoff X60, HBM, Germany) in order to subsequently perform the water flow and capillary water absorption tests (see Section 5.1.4). Specimens were then placed for one day in a curing room (at 20 ± 2 °C, >95% RH) so as not to affect the curing of the healing agents in the first 24 h; subsequently they were immersed in demineralized water for 6 days. The one-day storage at 20 ± 2 °C and >95% RH was done in order to avoid either washing away the uncured water-repelling agent (WRA series) or, on the contrary, facilitating the reaction of the unpolymerized polyurethane (PUR series) upon continuous contact with water, which could result in an additional filling of the crack. The specimens of the BAC series were directly immersed in demineralized water 5 hours after crack creation for 7 days.

5.1.3 Visual examination of the healing agents in the crack

After the crack creation and at different times after curing and testing, pictures of the crack mouths were taken using the optical stereo microscope. After completion of the sealing efficiency testing (see Sections 5.1.4 and 5.1.4), the samples were split at the location of the crack in order to evaluate the healing agent coverage on the crack faces [15, 29, 30, 39, 293]. This visual evaluation allowed to gain qualitative information on the ability of the healing agents to fill the cracks. In order to quantitatively determine the surface area of the spread region of the healing agents inside the crack, the crack faces of each sample were placed next to each other and a picture of the total crack surface was taken. For each of the crack faces, the area covered by the healing agent was determined using the photo editing software GIMP. The ratio between the crack faces covered by the healing agent and the total crack faces area was then denoted as the surface coverage of the crack faces.

5.1.4 Water flow test

Before crack creation, one side of the specimens was provided with a plastic tube (with external diameter of 6 mm) in order to connect the specimen to the water flow setup. In order to do this, the diameter of the cast-in hole was enlarged over a length of (25 ± 5) mm using a drill. The tube was inserted in the hole and a watertight connection was ensured by using silicone. At the other side of the specimens, the cast-in hole was sealed using the same silicone. Seven days after crack creation, the sealing efficiency of the self-sealing mortar was first assessed by measuring the water flow passing through the specimen, using a test procedure developed in the European project HEALCON [19, 120, 189]. The test requires the use of specimens which have to be saturated for at least 2 days by water submersion, in order to remove as much air bubbles out of the crack as possible and to prevent water absorption through the pores of the mortar matrix during testing. This requirement was fulfilled due to the curing of the specimens in demineralized water for 6 or 7 days after crack creation. One side of the specimen was connected with a plastic tube to a water reservoir at a height of 500 mm with respect to the cast-in hole, while the other side of the specimen was completely sealed with silicone and the crack was sealed at the side surfaces with methyl methacrylate glue (Schnellklebstoff X60, HBM, Germany) after crack creation, so that the water could only leak out from the bottom of the crack (see Figure 5.4).

The water flow test was carried out one time on each specimen at a temperature of (20 ± 2) °C and a relative humidity of (60 ± 5)%. The amount of leaked water was recorded over time for a minimum of 5 minutes on a scale with an automated registration system. However, the first 30 s of testing were not recorded to ensure that the error induced by the initial presence of air bubbles was removed

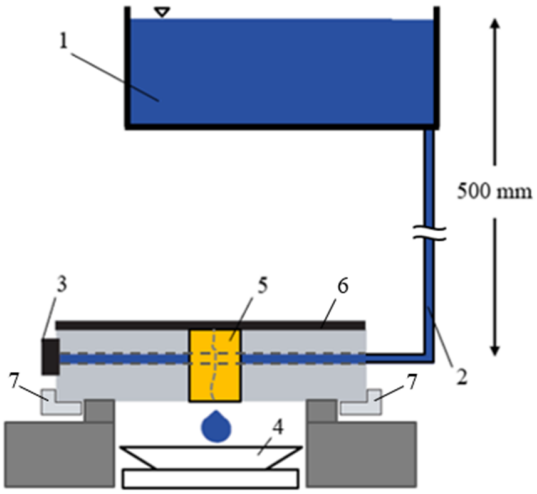

Figure 5.4: Test setup for the water flow test: (1) water reservoir, (2) plastic tube, (3) silicone sealing, (4) scale, (5) sealing with methyl methacrylate glue, (6) CFRP strip, (7) screw jacks.

by the flow of water through the crack and only a stable fully developed flow (i.e. linearly dependent on time) was studied. Out of this data, the flow rate q (g/min) was calculated. The sealing efficiency of a certain type of self-sealing specimens, containing the extruded cementitious capsules, was calculated with respect to the reference specimens, without capsules, using Equation 5.1:

$$SE_{wf}\,(\%) = \frac{q_{REF} - q_i}{q_{REF}} \times 100, \tag{5.1}$$

where SE_{wf} is the sealing efficiency assessed through the water flow test, q_{REF} the average water flow rate (g/min) of the reference specimens (REF, 6 specimens), and q_i the average water flow rate (g/min) of the self-sealing specimens containing capsules (4 specimens per series, distinguished according to the different healing agent used (WRA, PUR or BAC) and capsule coating (INT or EXT)).

5.1.5 Water absorption test

Measuring the capillary water absorption for cracked specimens with and without sealing can also be used to evaluate the crack sealing efficiency [15, 18, 20, 29, 34]. To this aim, the specimens previously used for the water flow test were first placed in an oven at 40 °C to remove moisture (6 reference specimens, 4 specimens for the different self-sealing series distinguished according to the different healing agent used and capsule coating). Specimens were dried until constant mass (mass change less than 0.1% in 24 h) was achieved. After the drying period, the specimens were stored at (20 ± 2) °C and (60 ± 5)% RH for 24 h. Then, the

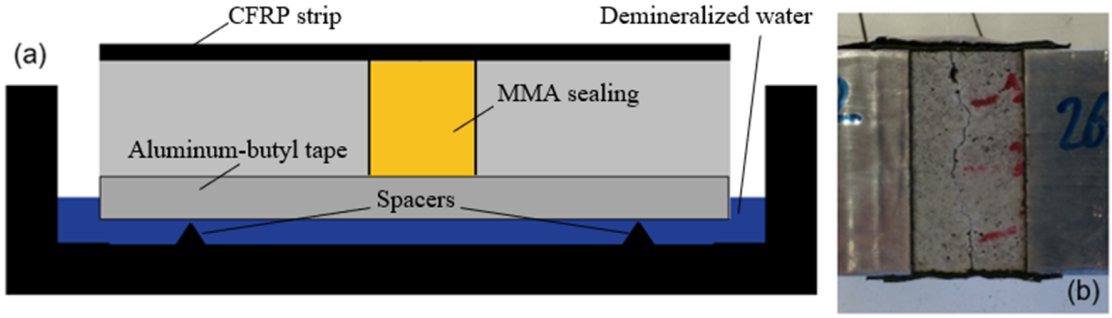

Figure 5.5: Test setup for the water absorption test: (a) schematic illustration; (b) surface exposed to water (20×40 mm^2).

screw jacks used for the active crack width control technique (Section 5.1.2) were removed. The removal did not significantly affect the crack width and was done in order to cover the sides of the specimens over a height of 15 mm with a self-adhesive aluminum-butyl tape so that the water could only enter the samples through a predefined test surface around the crack. The bottom surface was also covered with the aluminum-butyl tape so that only a 20 mm wide zone around the crack was exposed to water during the absorption test (Fig. 6). The specimens were weighed and then placed on two rigid non-porous supports in a container with demineralized water and with only the lower 5 mm of the specimens immersed in water. After the start of the water absorption test, the specimens were all removed at the same time and then weighed at 5 min interval for the first half an hour, then at 30 min intervals until 4 h and every hour until 8 h, following the removal of the excess of water on their faces with absorbing paper. Time correction due to the removal was taken into account, stopping the time at each removal for the duration of the weighing procedures.

The test was carried out at a temperature of (20 ± 2) °C and a relative humidity of (60 ± 5)%. The cumulative absorbed volume of water per unit area i (mm^3/mm^2), defined as the change in mass (mg) divided by the density of water at the recorded temperature (mg/mm^3) and by the water exposed area of the specimen (mm^2), is generally plotted against the square root of time. The slope of the obtained line gives the sorptivity index S ($mm/s^{0.5}$) of the specimen. However, recent studies questioned the calculation of the sorptivity index of cementitious materials by using the square root of time t (seconds), highlighting the lack of linearity that is often found using it [294]. The use of the fourth root of time was then demonstrated to be more effective in showing a linear evolution in the water uptake of non-cracked mortars due to the hygroscopicity of cementitious materials and swelling caused by the interaction with water (Equation 5.2). This model was adopted also in this study.

$$i = S \cdot t^{0.25}. \tag{5.2}$$

The sealing efficiency of the self-sealing specimens, containing the extruded cementitious capsules, was calculated as a reduction of sorptivity with respect to the cracked reference specimens, without capsules, using Equation 5.3:

$$SE_{wa}\,(\%) = \frac{S_{REF} - S_i}{S_{REF}} \times 100, \tag{5.3}$$

where SE_{wa} is the sealing efficiency assessed through the water absorption test, S_{REF} the average sorptivity index (mm/s$^{0.25}$) of the reference specimens (REF, 6 specimens) and S_i the sorptivity index (mm/s$^{0.25}$) of the self-sealing specimens containing capsules (4 specimens per series, distinguished according to the different healing agent used (WRA, PUR or BAC) and capsule coating (INT or EXT)).

5.2 Crack creation and crack width control technique

Figure 5.6 shows the average crack width w (µm) and the related standard deviation bars measured for the different series, distinguished according to the different healing agent used (REF, WRA, PUR, and BAC) and the capsule coating (INT or EXT).

An analysis of variance (ANOVA) test was applied and it showed that the mean crack widths of the different test series were not significantly different from each other (level of significance=0.05, p=0.45), making them comparable in terms of crack width.

Table 5.3 summarizes the average crack width w, the standard deviation σ_w and the resulting coefficient of variation CV of each series after the active crack width control. The highlighted variations are quite small if compared with the literature where other crack control techniques were used. For instance, coefficients of variation ranging from 6% to 20% were obtained for cylinders cracked through their depth and tied back together with spacers [295], while ranges of variation up to 40 µm on the average crack width were measured on prismatic specimens cracked by using a crack-width controlled 3-point bending test [120].

These findings indicate that the active crack control technique can effectively reduce the variability of the crack width, which is a very important parameter when specimens should be subjected to permeability tests. Indeed, Edvardsen [56] stated that the permeability of a crack is related to the third power of the crack width. Nevertheless, it should be noted that permeability and absorption are strongly affected also by the internal geometry of the crack, on which no control can be exerted [19, 41].

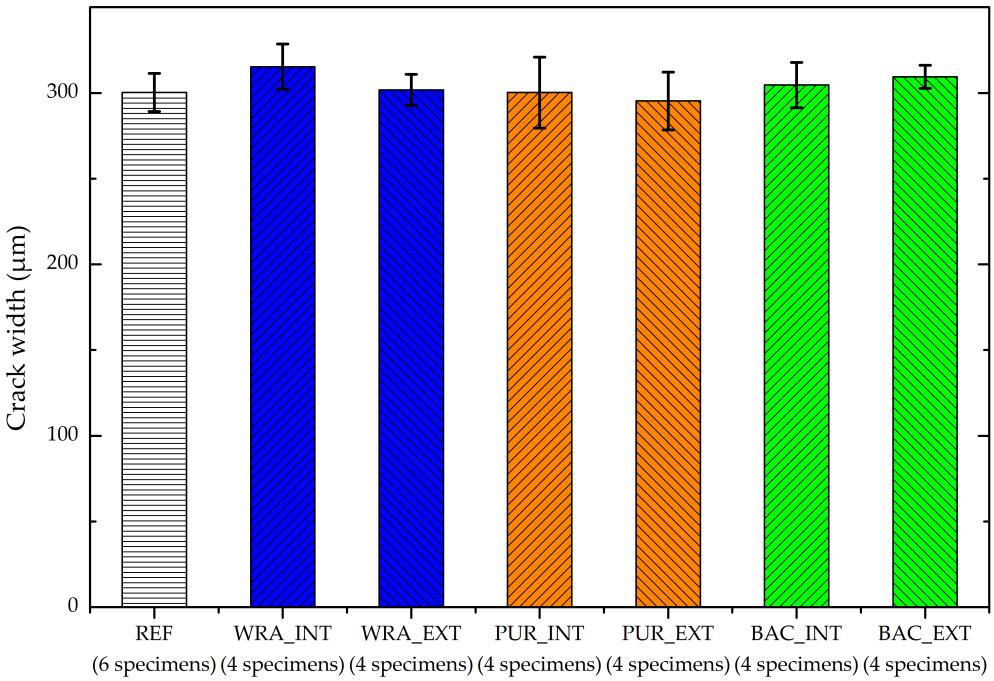

Figure 5.6: Average crack width w of each series after the active crack width control (error bars refer to ± one standard deviation).

Table 5.3: Overview of average crack width w, standard deviation σ_w and coefficient of variation CV of each series after the active crack width control.

Series	**Coating**	$\boldsymbol{w}$ **(µm)**	$\boldsymbol{\sigma_w}$ **(µm)**	$\boldsymbol{CV}$ **(-)**
REF	-	300	11	4%
WRA	INT	315	13	4%
	EXT	302	9	3%
PUR	INT	300	21	7%
	EXT	295	17	6%
BAC	INT	305	13	4%
	EXT	309	7	2%

5.3 Visual examination of the healing agents in the crack

After the crack creation and at different times after curing and testing, pictures of the crack mouth were taken using an optical stereo microscope. Figure 5.7 shows a comparison between the crack mouth at one fixed location for each series,

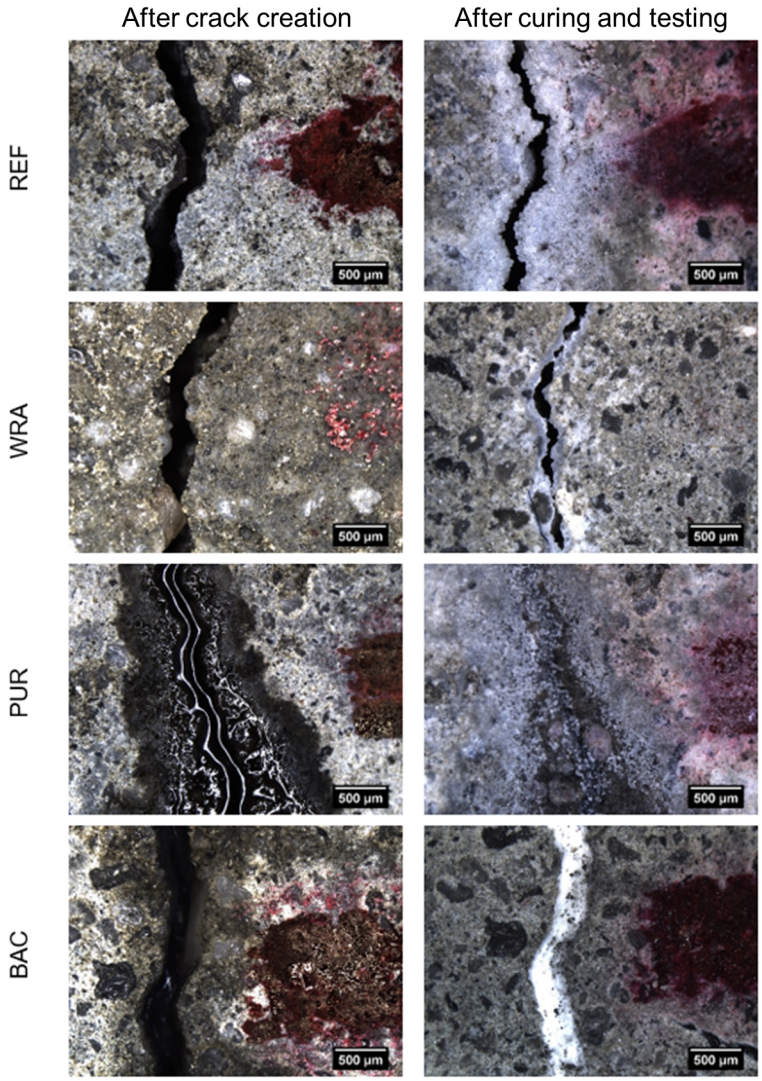

Figure 5.7: Visualization of the crack mouths filled with the different healing agents, after crack creation, and after curing and testing, for some of the best cases observed.

immediately after crack creation and after curing and testing.

It should be noted that also for the REF series, a crack sealing due to autogenous healing was identifiable at the crack mouth. The WRA was mainly absorbed by the matrix due to its low viscosity and was not able to grant a real crack filling, leaving the crack mouth open. On the contrary, the PU and the silica gel with the subsequent precipitation of $CaCO_3$ provided a good crack filling, creating a barrier of healing agent that sealed the crack along its length, in some case completely.

To complement the information gained from the micrographs of the crack mouth,

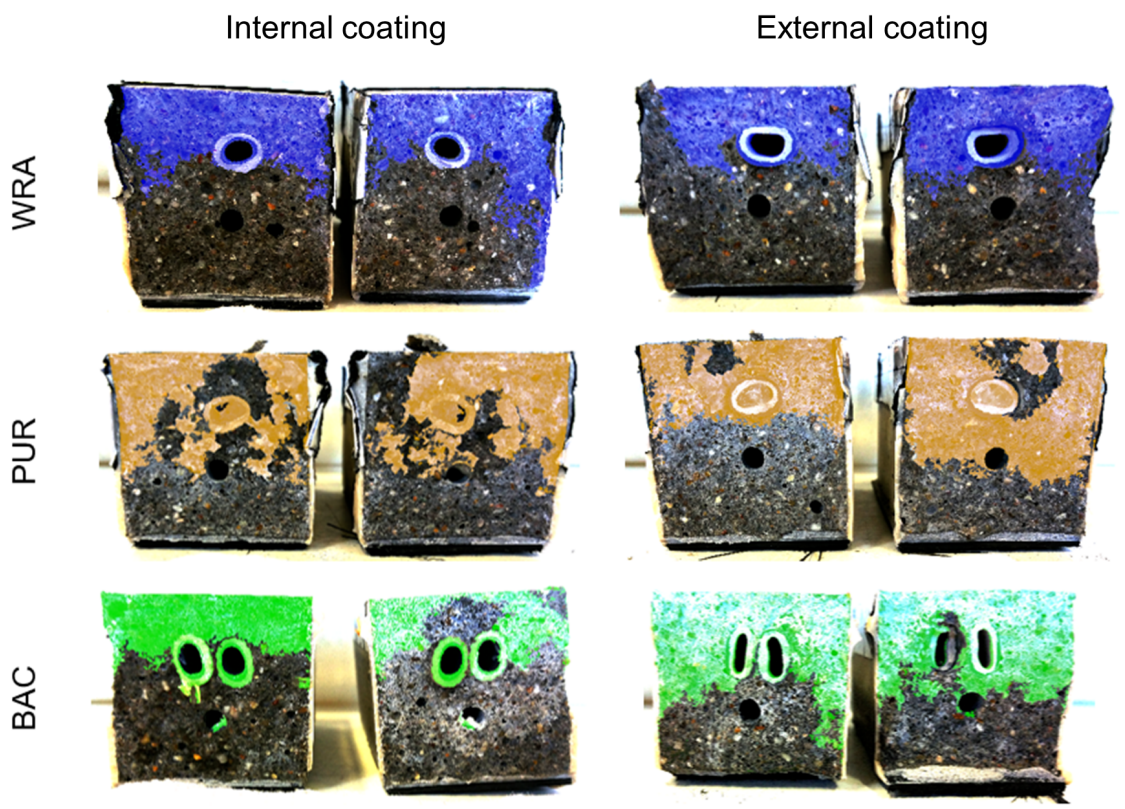

Figure 5.8: Visualization of the spreading region of the healing agents in the crack for mortar prisms containing capsules with internal or external coating.

the specimens were split at the location of the crack, after performing the test described in Section 5.1.4 and Section 5.1.5. The crack faces were then placed next to each other and a picture of the crack faces was taken. The total area covered by the healing agents was determined using a photo editing software. The ratio between the area of the crack faces covered by the healing agents and the total area was then denoted as the surface coverage of the crack faces, so to determine the spreading region of the healing agents inside the crack. The area of the capsules was taken into account for the calculation of the total area of the crack faces. Figure 5.8 shows some representative crack faces and spread regions for each series containing capsules, while Figure 5.9 shows the average surface coverage (%).

As it can be expected and preferred for sealing purposes, the portion of the crack faces that was mainly covered by the healing agents was the bottom part, above the crack mouth. In general, for a given healing agent, a slightly higher surface coverage was detected in the case of the specimens containing the capsules with the external coating, most likely due to the higher amount of healing agent carried by these capsules (see Section 5.1.1). Best spread over the crack faces was obtained when

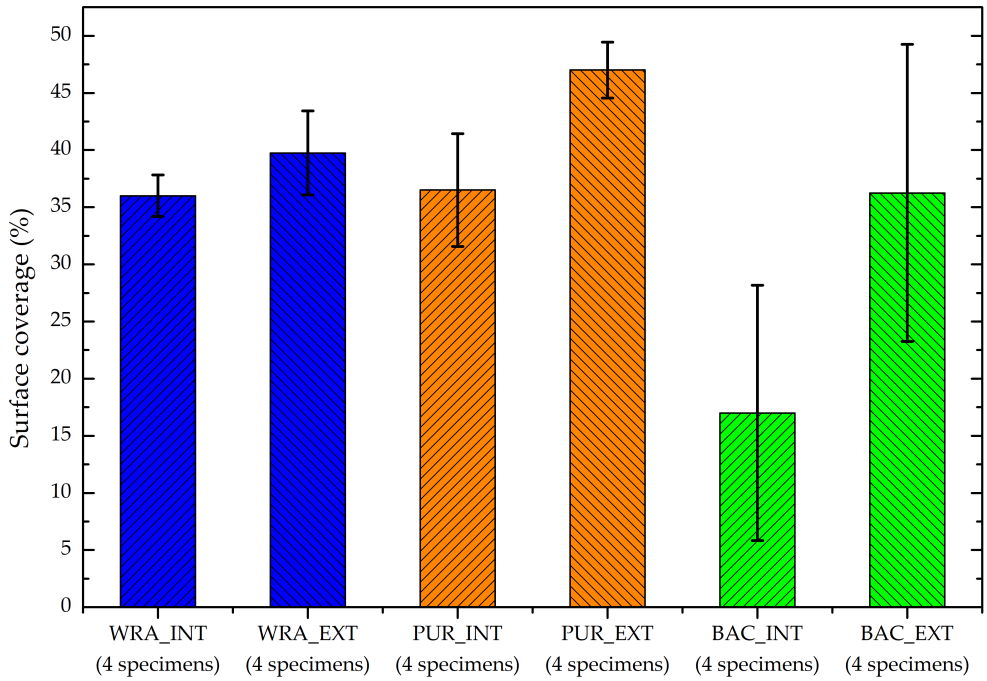

Figure 5.9: Average surface coverage of the healing agent on the crack faces for each series containing capsules (error bars refer to ± one standard deviation).

the PU precursor was used. Crack filling was also noticeable due to the presence of a thick PU foam over the crack faces. Moreover, the PU was able in most of the cases to seal also the cavity left by the capsules. The WRA series also showed a good spread over the crack faces, even if part of the water-repellent agent was lost during the pre-cracking procedure due to the very low viscosity of the healing agent. It is most likely that a large part of the WRA was absorbed by the mortar substrate at the crack faces due to its low viscosity, resulting in a hydrophobation of the crack faces rather than an actual crack filling, as already mentioned. In fact, it should be pointed out that the WRA was commercially designed to work as a cementitious substrate sealer by being absorbed in the superficial part of the matrix. The results of the BAC series showed a higher dispersion. This can be ascribed to the fact that the BAC series is based on a two-component healing agent. Hence, while in some cases an even distribution of the silica gel that immobilized the bacteria was recognizable, in other cases there was a clear separation of the portion covered by the gel and the portion covered by the deposition medium. Just the surface portion that presented the silica gel was taken in consideration for assessing the surface coverage. Last, it is to be underlined that, even though the BAC series with the capsules with an internal coating were those with the smaller

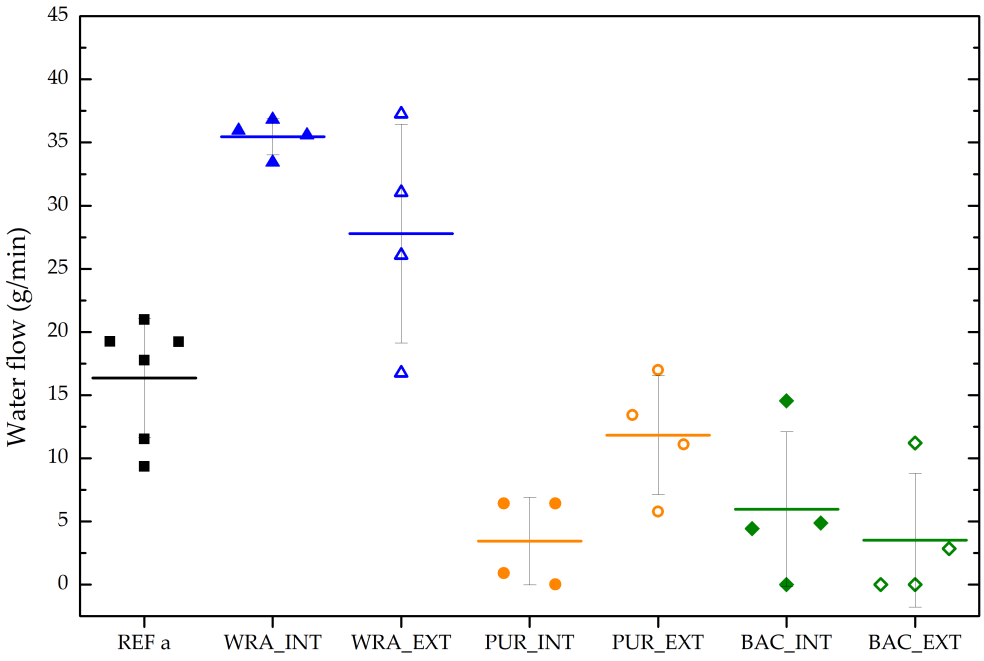

Figure 5.10: Water flow rate q of each series: individual samples results (symbols) and mean value of the series (solid line, error is ± one standard deviation).

surface coverage, the spreading area consisted of a thick white gel that filled the zone adjacent to the crack mouth along its length.

5.4 Water flow test

After curing in demineralized water for 7 days, the pre-cracked specimens were subjected to the water flow test, as reported in Section 5.1.4. Figure 5.10 shows the flow rate q (g/min) measured for the different series, distinguished according to the different healing agent used (REF, WRA, PUR, and BAC) and the capsule coating (INT or EXT).

An analysis of variance (ANOVA) test was applied and it showed that the mean values of the water flows of the different test series were significantly different from each other (level of significance=0.05, $p = 1.52 \cdot 10^{-8}$). After normality was assumed by means of a Shapiro-Wilk test ($p = 0.977$) and homogeneity of variance was assumed by means of a Levene's test (level of significance=0.01, $p = 0.26$), a Tukey test (level of significance=0.05) was used as post-hoc test in order to highlight which series were statistically different or equal in terms of water flow. When comparing two series with the same healing agent but different coating, the

difference of their means was never significant at the 0.05 level of significance. Moreover, the test highlighted that the REF and WRA series (either with internal or external coating), being the series with the worst results in terms of water flow (high flow rate), were not significantly different from each other. Similarly, the PUR and BAC series (either with internal or external coating), being the series with the best results (low flow rate), turned out to be statistically indistinguishable. In fact, some specimens from these two series showed outstanding results, since absent or negligible water flow was detected, consequently presenting a 100% sealing efficiency SE_{wf} (Eq. 5.1), compared to the average flow rate of the REF series. Namely, 3 specimens from the BAC series showed a 100% sealing efficiency (1 with internal and 2 with external coating), while for the PUR series one specimen showed a 100% and one specimen a 95% sealing efficiency (both with internal coating).

On the contrary, as mentioned above, poor results in terms of water flow (high flow rate) were obtained when the water-repellent agent was used. In fact, the use of this healing agent showed even detrimental effects on the performance of the series, with an average flow rate higher than that of the REF series. As already stated in Section 5.3, the WRA was most likely able to spread over the crack faces rather than fill the crack. In addition, for the WRA series the capsules were empty after releasing the low viscosity water repellent agent, contrary to what happened for the PUR series where also the cavities created by the capsules where sealed. The result was just the hydrophobation of the crack faces due to the curing mechanism of the WRA described in 3.4.1.

The effect of such hydrophobation is essentially to prevent the water absorption at low pressure, rather than stop a pressurized water leakage, as in the case of the water flow test. Hence, the water could leak downwards through the open crack during the water flow test without a substantial impediment.

This could have led to a further issue: it shall be considered that the specimens were pre-cracked at an early age (i.e. 7 days), when the autogenous healing mechanism is most relevant due to the presence of unhydrated binder particles and to the ongoing development of new CSH gels [16, 45, 56, 60, 64, 296]. Water is an essential factor for autogenous healing and the water immersion has been reported as the best exposure for this type of self-sealing effect. Thus, by reducing the water absorption on the crack faces, the WRA could have reduced the continued hydration of unhydrated cement grains, hence the autogenous self-sealing, that might have been higher in the REF series, as it is suggested by Figure 5.7 comparing the microscopic images of the crack mouths of these two series immediately after healing.

Table 5.4 summarizes the results of the water flow test, showing the best recovery for the series that used the PU as healing agent and the internal coating of the capsules ($SE_{wf} = 79\%$) and the BAC series with external coating ($SE_{wf} = 78\%$).

Table 5.4: Overview of average water flow rate q, standard deviation σ_q and average sealing efficiency SE_{wf} of each series after the water flow test.

Series	Coating	q (g/min)	σ_q (g/min)	SE_{wf} (-)
REF	-	16	5	-
WRA	INT	35	1	-117%
	EXT	28	9	-70%
PUR	INT	3	3	79%
	EXT	12	5	28%
BAC	INT	6	6	64%
	EXT	4	5	78%

5.5 Water absorption test

After complete oven drying (T=40 °C), the specimens were subjected to a water absorption test, as reported in Section 5.1.5. Figure 5.11 shows the weight gained due to water uptake plotted versus the fourth root of time for each series.

For each series, the coefficients of determination R^2 by using linear regression were respectively 0.9963, 0.9564, 0.9449, 0.9943, 0.9978, 0.9901, and 0.9904, showing that the linear regression fits the data very well. It is possible to notice that the WRA series with internal and external coating showed an almost identical behavior, characterized by a low water uptake and a small scattering between different specimens.

The sorptivity index S (mm/s$^{0.25}$) was calculated using Eq. 5.2, considering the cumulative absorbed volume of water per unit area i (mm^3/mm^2) between 5 minutes and 8 hours of water absorption. Figure 5.12 shows the S values measured for the different series, distinguished according to the different healing agent used (REF, WRA, PUR and BAC) and the capsule coating (INT or EXT).

From the moment that it was not possible to assume normality by means of a Shapiro-Wilk test ($p = 0.977$), a One Way ANOVA on Ranks by means of a Kruskal-Wallis test was applied and it showed that there was a statistically significant difference between the different test series medians ($p < 0.001$). A Dunn's test (level of significance=0.05) was used as a post-hoc test to highlight which series were statistically different or equal in terms of sorptivity. Again, when comparing two series with the same healing agent but different coating, the difference was never significant at the 0.05 level of significance.

Positive results were obtained using the PU and the WRA. The WRA showed outstanding results, contrary to those obtained during the water flow test (Section 5.4). Indeed, a very slow absorption rate was detected, with almost perfect repeatability on each specimen of the series. This excellent performance can be

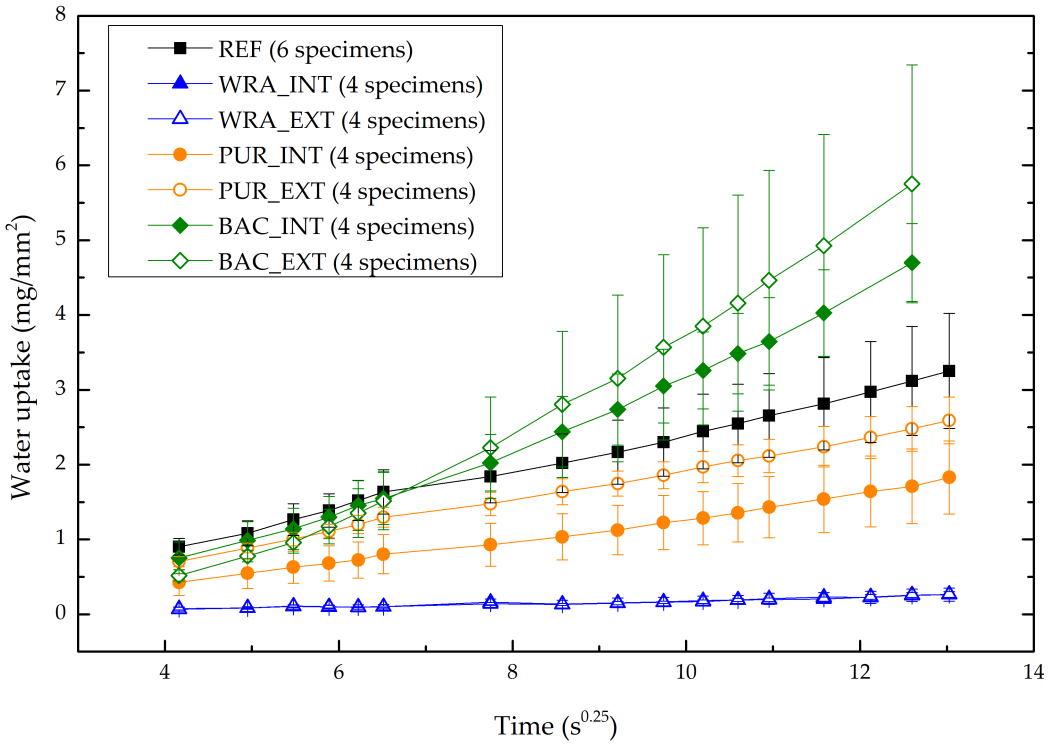

Figure 5.11: Average water uptake of each series plotted versus the fourth square of time (error bars refer ± one standard deviation).

explained by the water-repellent agent characteristics, since it is designed exactly with the aim of reducing the water absorption of cementitious substrates. Moreover, during the pre-cracking procedure, the WRA was spread both on the crack faces, thus penetrating in the mortar matrix, and also on the area adjacent to the crack mouth, which was the area in contact with water during the test (Figure 5.13a). This allowed to obtain an almost perfect protection against the water absorption. The PUR series showed good results because of the good filling of the crack offered by the closed cell PU foam. However, a larger contribution of the matrix absorption rate can reasonably be considered for this series, because the healing agents did not cover the complete area adjacent to the crack as in the previous case (Figure 5.13b).

On the other hand, poor results were obtained for the BAC series. In fact, the use of this healing agent showed even detrimental effects on the performance of the series, with a sorptivity index more than double of that of the REF series. This behavior could be attributed to several causes. The first cause could be ascribed to an intrinsic drawback of the water absorption used on self-sealing systems that is often debated. For instance, a partially healed crack could have a smaller crack width and thus a higher capillary force, resulting in a possible larger amount of

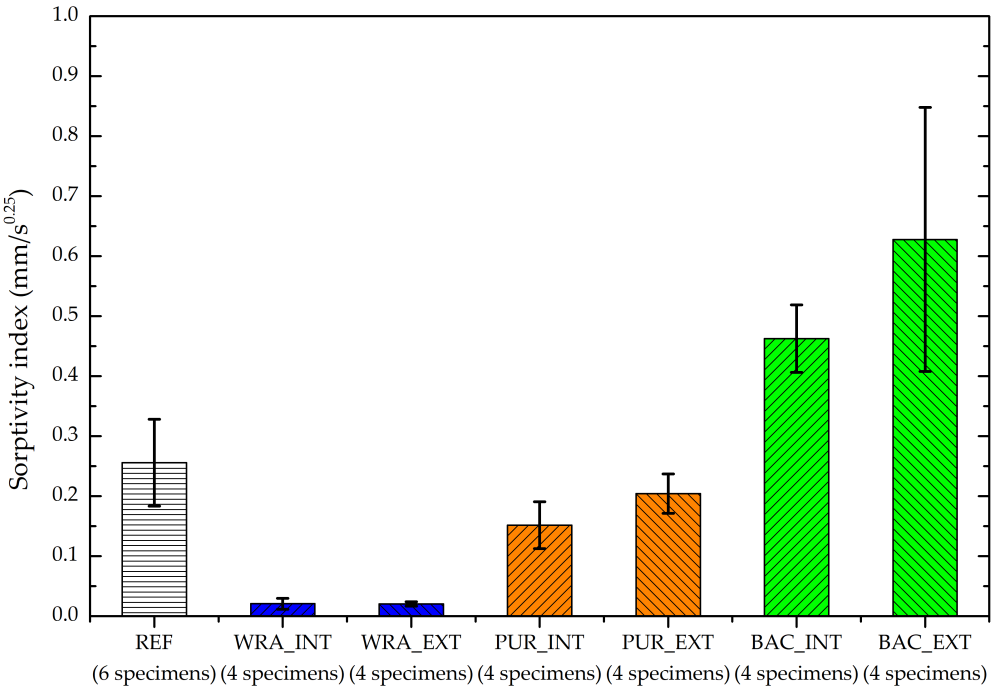

Figure 5.12: Mean sorptivity index S of each series (error is ± one standard deviation).

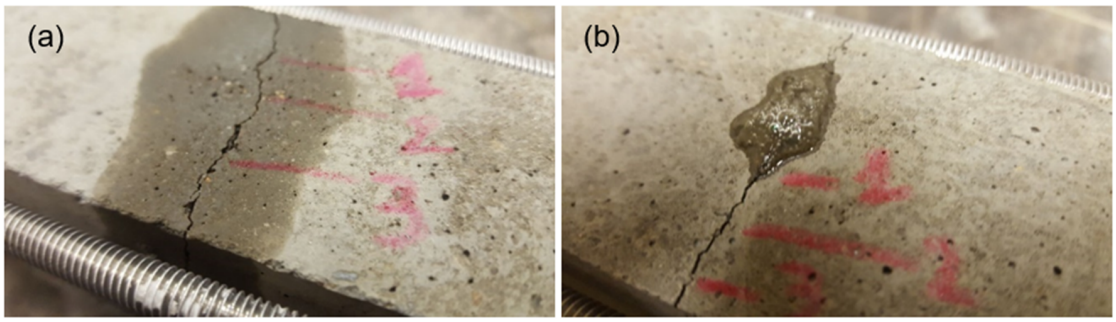

Figure 5.13: Spread of the healing agent on the area adjacent to the crack mouth for (a) WRA and (b) PUR series after crack creation. The water-repellent agent covered the complete area in contact with water during the water absorption test.

water uptake compared to an unhealed crack [19, 41]. This could be the case for the BAC series, were the partially closed crack could promote higher capillary forces if compared with the crack sealed just by the contribution of autogenous healing in the REF series. This partial closure and the opposite results if considering the good behavior showed by the BAC series during the water flow test, could be partially

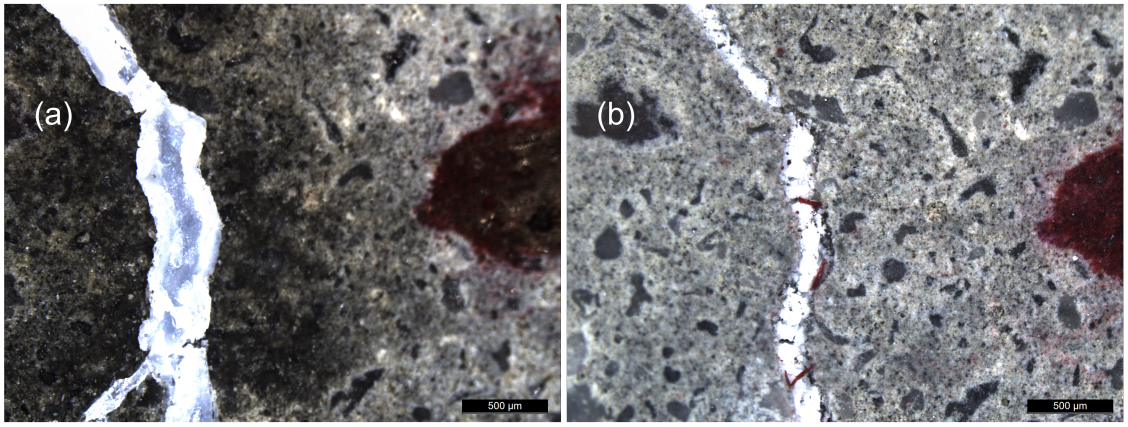

Figure 5.14: Visualization of one fixed crack mouth location filled with the silica-sol of the BAC series: (a) after crack creation and (b) after the drying process, where it is possible to notice partial detachment and damaged zone that could have caused a partial re-opening of the crack before the water absorption test.

attributed to the drying procedure, that could have caused the shrinkage of the silica gel and partial detachment from the crack faces and internal damage in the sealing material (see Figure 5.14).

Lastly, it should be noted that the cementitious capsules act in a way similar to the aggregates in concrete, therefore it is reasonable to consider the existence of an interfacial transition zone (ITZ) between the capsules and the surrounding matrix. This zone leads to a local increase in porosity, with microcracking, that may appear at the interface due to shrinkage or mechanical loading [297, 298]. Therefore, microcracking can be expected for the BAC series in contrast to the REF series, also due to the mechanical action exerted by the capsule breakage. For the sake of completeness, it should be noted also that in the case of the BAC series the silica gel immobilized bacteria were not spread extensively on the area adjacent to the crack mouth, similarly to the PUR series, while the deposition medium was spread on the adjacent area, similarly to the WRA series.

Table 5.5 summarizes the results of the water absorption test, showing the best recovery for the series that used the WRA as healing agent ($SE_{wa} = 92\%$), regardless the coating of the capsules. It has to be noted that the sealing efficiency was calculated just as a reduction in terms of sorptivity with respect to a cracked plain mortar matrix, without taking in consideration uncracked reference specimens in order to neutralize the intrinsic matrix sorptivity. It has to be expected that, taking it into account, the behavior of the WRA series would be even better than that of the pristine mortar specimens in terms of absorption properties.

Table 5.5: Overview of average sorptivity index S, standard deviation σ_S and average sealing efficiency SE_{wa} of each series after the water absorption test.

Series	Coating	S ($mm/s^{0.25}$)	σ_S ($mm/s^{0.25}$)	SE_{wa} (-)
REF	-	0.26	0.07	-
WRA	INT	0.02	0.01	92%
	EXT	0.02	0	92%
PUR	INT	0.15	0.04	41%
	EXT	0.2	0.03	20%
BAC	INT	0.46	0.06	-81%
	EXT	0.63	0.22	-145%

5.6 Conclusions

Extruded cementitious capsules with two different coating configurations were used to encapsulate different healing agents, with the aim of deepening the analysis and expanding the statistical sample with respect to the preliminary study reported in Chapter 4. The used healing agents were chosen again from the main types commonly used for self-sealing applications, namely a water-repellent agent, a polyurethane precursor, and a solution of silica gel immobilized bacteria.

The cementitious capsules were successfully able to sequester and release the healing agents with both coating configurations, showing no substantial differences in the performance of the healing system for a given healing agent. In fact, the findings obtained throughout the investigation were not significantly affected by the different configurations of the position of the epoxy coating layer (i.e. applied to the internal or external surface of the tubular capsule). The reason for that should rely on the cementitious shell preparation and coating procedure. In fact, the primer applied both to the internal and the external surfaces of the tubes was sufficient to isolate the healing agents from contact with the hardened capsule shell, and hence with the low residual humidity that might be present in it. The primary function of the epoxy coating was to offer protection solely against the high humidity and high alkalinity of the fresh mortar mix, which represents a major threat for the healing agents retention. Therefore, applying it either to the internal or the external surfaces of the tubes did not significantly change its performance and allowed to provide a good barrier between the healing agents and the harsh environment of the matrix.

As regards the sealing efficiency evaluated with water permeability and water absorption, good results were obtained in both tests using the polyurethane precursor. When water-repellent agent was used, excellent results were obtained in

preventing the water absorption, while detrimental effects were shown against water permeability. On the contrary, silica gel immobilized *B. Sphaericus* showed the inverse behavior, with good results against water permeability and bad results during water absorption. It can be assumed from these results that, while the polyurethane precursor is well suited in mitigating both mechanisms, the water repellent agent is well suited when the self-sealing structure will mainly be exposed to the ingress of deleterious substances governed by capillary forces, but not when the pressure is the driving force. On the other end, the bacterial healing agent seems more suited when the water leakage, also in pressure, could be the cause of the ingress of deleterious substances and losses of serviceability. For instance, this is the case of submerged structures, water tanks, or tunnel segments.

In light of these considerations, it can be concluded that the self-sealing systems should be tailor-made for the real operating conditions that the structure will meet during its service life, by choosing the correct healing agent, the correct location for the self-sealing system, and by taking advantage of the synergy between different self-sealing mechanisms. Nevertheless, it has to be underlined that the polyurethane precursor allowed to obtain always positive results both in terms of reduction of water permeability and water absorption, never showing detrimental effects such as in the case of the other type of healing agents. Moreover, the polyurethane allows a very fast curing in presence of humidity, without requiring high quantity of water as for the bacterial healing agents. In addition, several types of polyurethane precursors can cause the formation of expansive foam, allowing the autonomous repair of larger cracks. Due to these positive aspects, this type of healing agent was selected as the most promising to obtain the desired self-healing system and it was decided to focus the subsequent study presented in the following chapters on its use.

Chapter 6

Mechanical behavior under quasi-static and cyclic loading

The capability of the self-healing cementitious materials to provide a mechanical recovery has been highlighted in a many studies, mostly under static conditions [26, 29, 32, 38, 39, 57, 92]. Also, the effectiveness of different self-healing techniques under repeated cracking and healing cycles has been analyzed in several studies [29, 101, 103, 181, 289, 299, 300]. However, as far as cyclic loading and fatigue performances are concerned, the mechanical behavior of these materials has not been fully reported in the scientific literature, apart from few studies regarding self-healing systems under cyclic flexural loading [180] or under cyclic compressive loading [301]. Yet, the response to cyclic loading is particularly relevant from the mechanical point of view especially for the infrastructure sector, hence the importance of improving the behavior of the materials commonly used in the sector, for example by adding different types of fibers [69, 302, 303] that can increase their performances in the event of cyclic loads [304–306]. In fact, the main sources of stress on infrastructures can be ascribed to dynamic actions, almost cyclically repeated over short periods of time, or occurring with increasing intensity over longer periods of time. Moreover, cyclic loading can cause additional detrimental effects on self-healing cementitious materials. Specifically, the cyclic actions cause the continuous opening and closing of healed and unhealed cracks. In the case of healed cracks, the composite materials formed by the cementitious matrix and the repairing agent is subjected to strains that could cause not only damages in the matrix or in the repairing material, but also debonding between these two different

---

Part of the work described in this chapter has been previously published in:

[**252**] G. Anglani, J.-M. Tulliani, and P. Antonaci. "Behaviour of Pre-Cracked Self-Healing Cementitious Materials under Static and Cyclic Loading". *Materials* 13.5 (2020), p. 1149. DOI: 10.3390/MA13051149

materials. For this reason, it is of great importance to fill this knowledge gap by deepening the study of the behavior of self-healing cementitious materials with respect to cyclic loading and fatigue. This is an issue of fundamental importance for understanding and characterizing the behavior of these materials in real field conditions, and consequently allowing their use by ensuring the structural safety.

Based on the above considerations, the objective of the activities carried out and explained in this chapter was to investigate the mechanical behavior that could be obtained by encapsulating the polyurethane precursor (as selected in the previous chapter) inside cementitious capsules. This aspect was investigated, after pre-cracking, under both static and cyclic flexural loading, and allowed also to evaluate the influence of some capsule parameters and specimen configurations on the mechanical behavior.

The mechanical behavior was investigated via three-point bending test in order to test the system under indirect tensile stresses and for the sake of comparison with the existing literature, since it has been, so far, the most commonly employed test to assess the healing capacity of cementitious composites through the recovery of mechanical properties [19] under static loading conditions. Furthermore, the force-controlled three-point bending test conducted by using a sinusoidal loading made it possible to investigate the mechanical behavior until rupture of the pre-cracked and subsequently healed system in dynamic condition. This allowed to obtain useful insights regarding the seldom studied fatigue performance of the self-healing systems, which is an aspect of paramount importance to develop a reliable autonomous repair system that can be used in field conditions.

6.1 Materials and Methods

6.1.1 Mortar prisms

Mortar prisms, with a volume of 40 by 40 by 160 mm^3, were produced according to standard UNI EN 196-1. Ordinary Portland cement (CEM I 42.5 N, Buzzi Unicem S.p.A., Italy), tap water, and normalized sand (grain size between 0.08 and 2.00 mm) were used, with a water-to-cement ratio of 0.5 and a sand-to-cement ratio of 3.

Both rolled cementitious macro-capsules (Mix design 2), characterized by a relatively smaller diameter, with a length of 60 mm and with internal coating or extruded cementitious macro-capsules (Mix design 2), characterized by a relatively larger diameter, with a length of 45 mm, either with internal or external epoxy coating, were produced accordingly to what was described in Chapter 3. Capsules ends were rolled into sand to improve their bonding with the surrounding matrix. The highly expansive PU precursor (CarboStop U, Minova CarboTech GmbH Branch Italy, Milan, Italy) described in Section 3.4.2 was selected as healing agent.

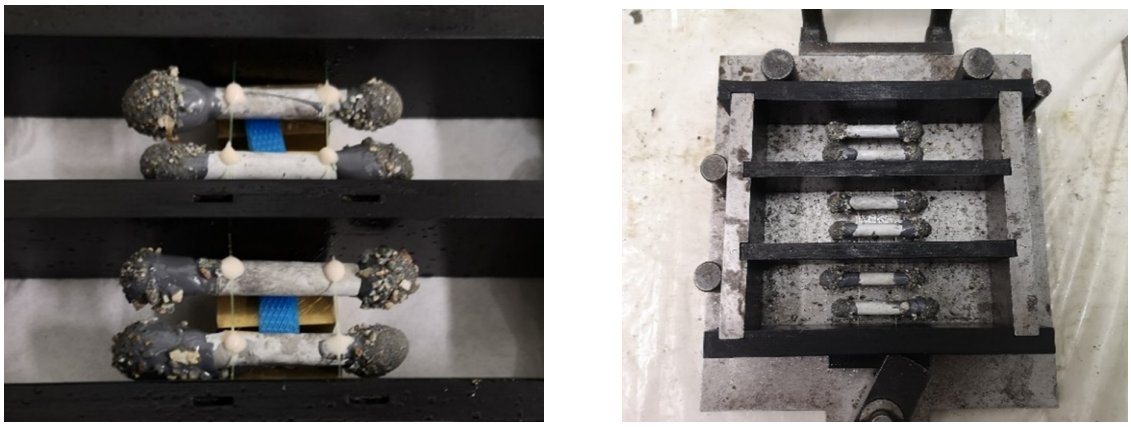

(a) (b)

Figure 6.1: Mold used to produce the self-healing mortar prisms, before casting: (a) Bottom-up view of the capsules glued on the nylon threads with a methyl methacrylate (MMA) glue (X60, HBM, Darmstadt, Germany); (b) assembled and oiled mold with capsules in fixed position.

Reference specimens with no capsules (REF series) were produced along with self-healing specimens, in which the capsules filled with the PU precursor were embedded manually before casting, in fixed positions. Accurate control of the capsules position was achieved by gluing them on top of two thin nylon threads passing through the lateral faces of the mold, at a height of 10 mm from the bottom side of the specimen (see Figure 6.1).

Different series of self-healing specimens were produced: the CEM_SI series contained two small-diameter capsules with internal epoxy coating, the CEM_LI series contained one large-diameter capsule with internal epoxy coating, and finally, the CEM_LE series contained one large-diameter capsule with external epoxy coating. CEM_SI and CEM_LI specimens contained the same volume of healing agent ($\sim$ 0.6 mL) but had different geometric configurations since the healing agent was distributed in two capsules or concentrated in one capsule, respectively. Conversely, CEM_LI and CEM_LE specimens had the same geometric configuration, with a single capsule horizontally centered in the specimen cross-section, but contained a different amount of healing agent ($\sim$ 0.6 mL and $\sim$ 0.9 mL, respectively). For each series, 12 specimens were produced, for a total of 48 specimens.

The main characteristics of the cementitious capsules used are summarized in Table 6.1.

After casting, the molds were covered with plastic foils to maintain a humid environment (T $\approx$ 20 °C). The samples were demolded after 24 hours from casting and cured for two weeks still wrapped in plastic foils (T $\approx$ 20 °C). Then, a U-shaped notch (width = 4 mm, height = 4 mm) was created by means of wet sawing.

Table 6.1: Summary of the characteristics of capsules used for the different series.

		CEM_SI	**CEM_LI**	**CEM_LE**
Manufacturing process		Rolling	Extrusion	Extrusion
Mix design		Mix design 2	Mix design 2	Mix design 2
Surface of the tubular shell coated with epoxy		Internal	Internal	External
Average internal diameter of the tubular shell	(mm)	5	7.5	7.5
Average external diameter of the tubular shell	(mm)	8	10	10
Average length of the capsule	(mm)	60	45	45
Average thickness of the epoxy coating	(mm)	1	1	1
Average internal diameter after epoxy coating	(mm)	3	5.5	7.5
Volume of cargo healing agent	(mL)	≈0.3	≈0.6	≈0.9

Figure 6.2 shows the schematic cross section of all the series.

6.1.2 Pre-cracking

In order to evaluate the effectiveness of the autonomous self-healing system, a controlled localized crack was first induced in the specimens using a mechanical pre-cracking procedure. At an age of 14 days from casting, all the specimens were pre-cracked via a crack-width controlled three-point bending test with a span of 10 cm using a 250 kN closed-loop servo-controlled MTS hydraulic press (MTS 810, MTS Systems Corporation, USA) equipped with a digital controller (FlexTest® 40, MTS Systems Corporation, USA). It was possible to control the crack mouth opening displacement (CMOD) by using a strain-gauge-based displacement transducer (DD1, range ± 2.5 mm, HBM, Germany) mounted on the bottom face of the specimen upon the notch. Figure 6.3 shows the setup of the pre-cracking procedure.

The test was conducted by imposing a CMOD rate of 1.5 µm/s. Upon reaching a maximum value of 800 µm, the specimens were unloaded at the same CMOD rate. The target value for the maximum CMOD was set at 800 µm in order to test the ability of the system to heal large cracks and in order to inhibit the influence of the autogenous healing, that could be significant for smaller cracks because of the young age of the specimens at pre-cracking. The CMOD and load were recorded

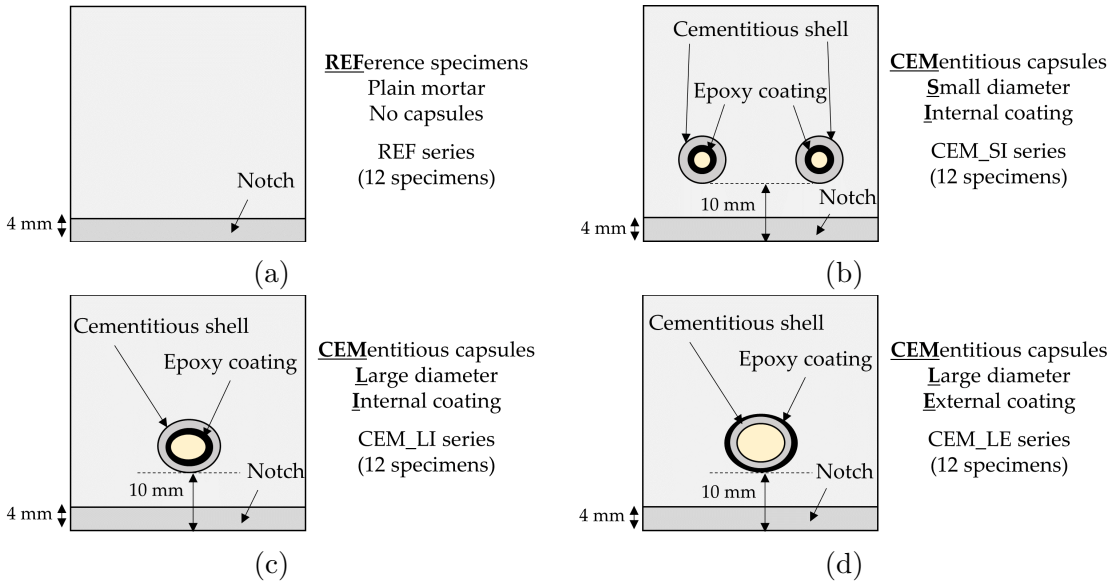

Figure 6.2: Schematic cross section of the specimens: (a) without capsules, REF series; (b) with two small-diameter capsules, CEM_SI series; (c) with one large-diameter capsule with internal epoxy coating, CEM_LI series; (d) with one-large diameter capsule with external epoxy coating, CEM_LE series.

throughout the execution of the test.

Immediately after pre-cracking, the specimens were stored in a curing cabinet (T = 20 °C, 60% RH) for one week and then in the lab, with no temperature and humidity control, for another week. Two supports with a span of 10 cm allowed to keep the specimens in the same geometric configuration during pre-cracking, with their bottom face pointing downward. The duration of the curing cabinet conditioning definitely exceeded the time required for the PU to react with air humidity and form a rigid foam (normally ranging from less than one hour up to a few hours, depending on ambient conditions). This ensured that the healing agent released from the capsules during pre-cracking was fully cured at the time of successive testing.

6.1.3 Quasi-static reloading

After 2 weeks from pre-cracking, the recovery of the mechanical properties was first evaluated by assessing the load-bearing capacity under static conditions.

Half of the specimens from each series were statically reloaded following the same procedure described in Section 6.1.2 for pre-cracking.

This allowed to evaluate the mechanical recovery through a load recovery index in accordance with common approaches reported in literature [19, 26, 38, 39, 57, 92, 250]. The load recovery index (LRI) was expressed as a function of the

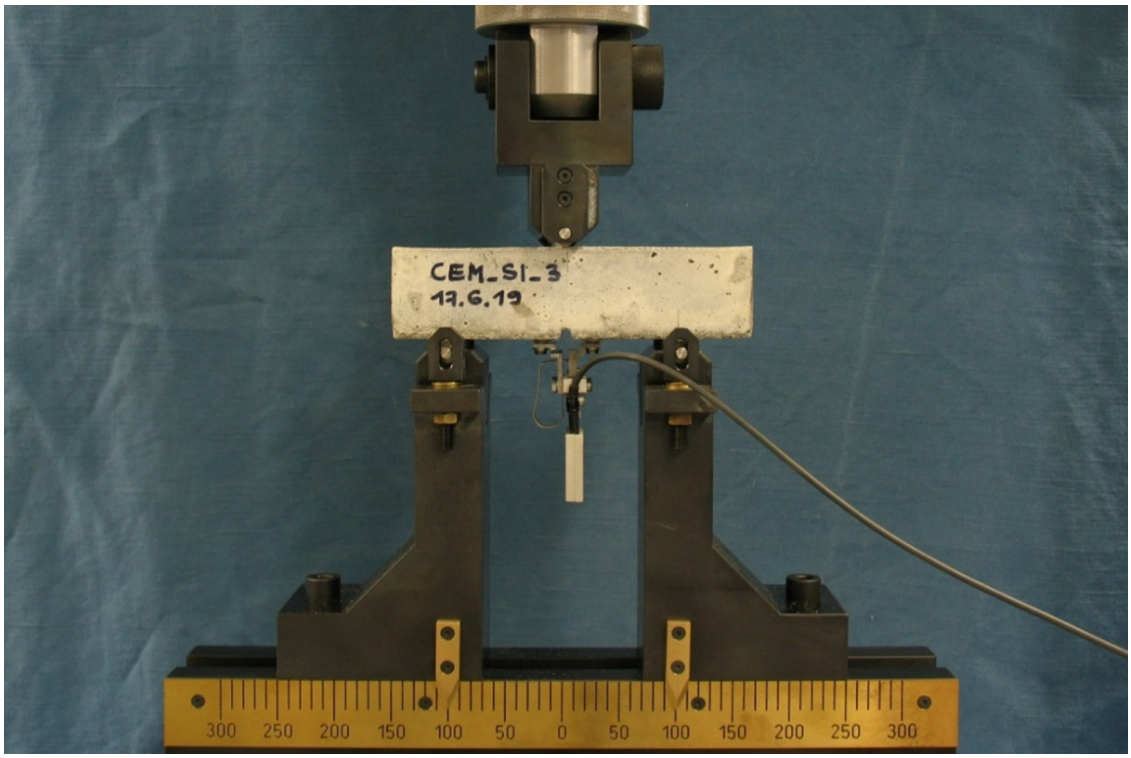

Figure 6.3: Setup of the pre-cracking procedure.

maximum load-bearing capacity of the specimens during pre-cracking (L_{peak}) and reloading (L_{reload}) and as a function of the residual load-bearing capacity at the end of pre-cracking (L_{unload}). Its definition is reported in Equation (6.1):

$$LRI(\%) = \frac{L_{reload} - L_{unload}}{L_{peak} - L_{unload}}, \tag{6.1}$$

The static reloading allowed also to subsequently define the parameters to perform the cyclic reloading procedure (Section 6.1.4).

Figure 6.4 reports the setup for the static reloading procedure and a graphical illustration of how the maximum and residual load-bearing capacities were calculated for the purposes of LRI determination.

6.1.4 Cyclic reloading

After the static reloading of half of the pre-cracked specimens (Section 6.1.3), the mechanical behavior under cyclic flexural loading was evaluated.

In order to investigate the behavior in cyclic conditions, the remaining specimens were reloaded through a force-controlled three-point bending test with the same span used for the pre-cracking and static reloading (10 cm) and using the

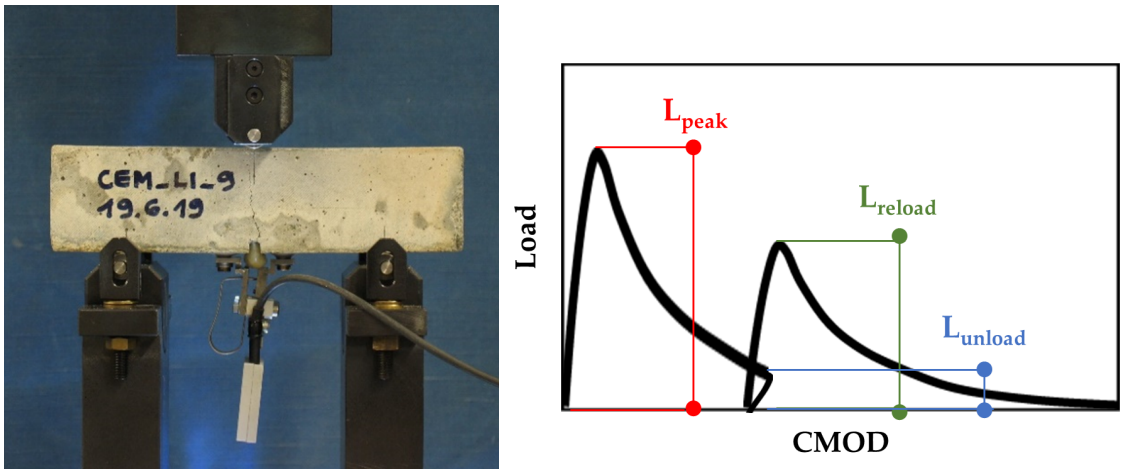

(a) (b)

Figure 6.4: (a) Experimental setup for the static reloading procedure; (b) schematic load versus crack mouth opening displacement (CMOD) curves related to pre-cracking and reloading, with indication of maximum and residual load-bearing capacities.

same closed-loop servo-controlled hydraulic press. In order to measure the damage evolution during the cyclic loading in terms of increment of crack opening displacement (COD), an inductive displacement transducer (WI, range 0–5 mm, HBM, Germany), connected to the digital controller through a measuring amplifier (SCOUT55, HBM, Germany), was mounted on the lateral surface of the tested specimen, just above the tip of the notch. It was not possible to mount the WI displacement transducer on the bottom face to measure the CMOD as in the pre-cracking and reloading setup because of the lack of space between the supports.

The force-controlled three-point bending test was conducted by first reloading the specimens up to a maximum load value L_{max} with a load rate of 50 N/s. Upon reaching L_{max}, a sinusoidal loading with a frequency of 4 Hz was applied, where the peaks were set to L_{max} and the valleys to a lower load value L_{min}.

Figure 6.5 reports the experimental setup and a graphical illustration of the loading procedure used for the cyclic reloading.

The limits L_{min} and L_{max} of the cyclic reloading were defined as a fraction of the average load-bearing capacity L_{reload} obtained during static reloading for each series. Specifically, L_{min} and L_{max} were set according to Equation (6.2):

$$\begin{cases} L_{min} = 0.1 \cdot L_{reload} \\ L_{max} = S \cdot L_{reload} \end{cases} \tag{6.2}$$

where the value of S was initially set to 0.7 for the first 10,000 cycles; if the specimen did not fail within the first 10,000 cycles, then the value of S was increased in steps of 0.05 for additional reloading series of 10,000 cycles each, until eventual

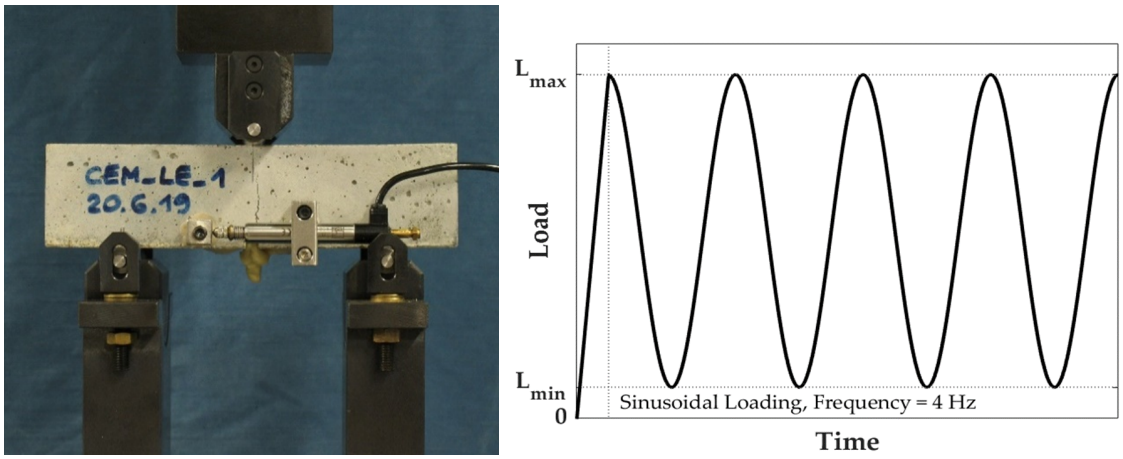

(a) (b)

Figure 6.5: Cyclic reloading procedure: (a) experimental setup; (b) graphical illustration of the loading procedure for the cyclic reloading.

failure of all the specimens.

Such settings were adopted in order to impose a high stress, equal to or higher than 70% of the expected strength of the healed material. Indeed, after release and curing of the PU in the crack, the material properties changed in correspondence of the most stressed cross-section with respect to their initial values. They depended not only on the mechanical characteristics of the hardened PU, but also on its crack filling ratio and interaction with the surrounding cementitious matrix. The flexural strength of the healed material could only be estimated experimentally based on the load-bearing capacity L_{reload} obtained during static reloading. Testing the specimens cyclically with a cyclic peak value close to L_{reload} was meant to check their performances under severe conditions, in such a way to provide a first feedback on how this type of self-healing materials could behave during their remaining service life after they have produced their autonomous repair action. The number of cycles sustained until failure as a function of the maximum force applied during cyclic reloading was analyzed as a representative parameter to describe their cyclic behavior.

6.2 Pre-cracking

All specimens from each series (REF, CEM_SI, CEM_LI, and CEM_LE), namely 12 specimens per series for a total of 48 specimens, were pre-cracked at an age of 14 days via a controlled three-point-bending test as described in Section 6.1.2.

Figure 6.6 shows some of the load versus CMOD curves recorded during the

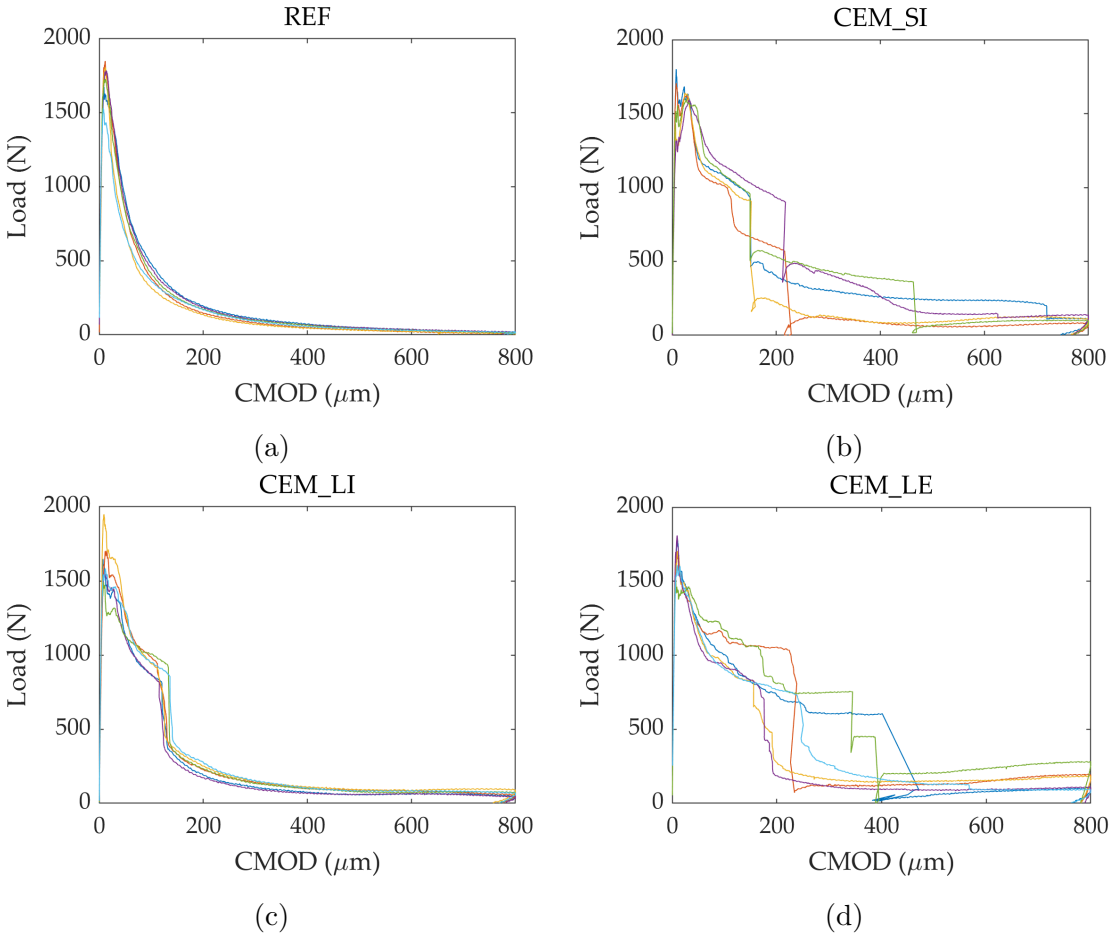

Figure 6.6: Load versus CMOD curves due to pre-cracking: (a) REF series; (b) CEM_SI series; (c) CEM_LI series; (d) CEM_LE series. The specimens are distinguished by different color lines.

tests for the different series. For the sake of clarity, only the curves related to the specimens that were later subjected to static reloading (see Section 6.3) are displayed.

During the controlled crack formation, first the load increased until reaching the peak value with a very low increase in terms of displacement because of the high stiffness of the intact material. After reaching the peak load, crack formation and subsequent propagation occurred, with progressive load decrease as a function of increasing CMOD due to the material post-peak softening behavior. The specimens were unloaded upon reaching a CMOD of 800 µm, with a consequent small CMOD decrease due to recovery of the elastic deformation. While for the series without capsules (REF series) the softening phase had a continuous and gradual advancement, the self-healing series showed sudden load drops during this phase.

These drops are attributable to the breakage of the capsules upon crack creation, being these drops accompanied with an audible acoustic energy release. These results are confirmed in literature, where the same behavior was shown during crack creation using glass capsules [26, 32, 307].

In all the specimens of the CEM_LI series, the drop was highly repeatable at a CMOD around 135 µm. In the case of the CEM_SI series, which contained two capsules per specimen, there were usually double load drops due to non-simultaneous breakage of the capsules. The first drop was always detected for a CMOD smaller than 215 µm. The highest scattering in the CMOD value corresponding to the load drop was shown by the CEM_LE series, for which such CMOD value did not exceed 240 µm on average: the higher scattering could be attributed to a higher variability in the coating thickness due to its manual application over the ridged surface of the capsule.

It is worth recalling here that the capsules were positioned 10 mm above the bottom face of the specimens, while the CMOD measuring points were situated some millimeters below it because of the experimental setup adopted. Therefore, the actual crack opening at the capsule level in correspondence of the aforementioned load drops was surely lower than the corresponding CMOD value experimentally detected. This results in the possibility of using the cementitious capsules to trigger the healing also for cracks smaller than 135–240 µm. This range of crack size is particularly relevant from a durability point of view, as confirmed by the structural design codes, where the limit for the maximum acceptable crack width is fixed to no more than 400 µm, depending on the exposure conditions [39, 184, 308].

A further evidence of the relationship between the load drops, the acoustic emission, and the breakage of the capsules was that they were followed by leakage of the foaming polyurethane released by the capsules in the crack (see Figure 6.7).

The expansive foaming reaction is triggered by the capsule breakage, which makes it possible for the polyurethane precursor to get in contact with the humidity present in the air at the crack site and to start its polymerization reaction. Such reaction induces gas formation and consequent expansion of the polyurethane precursor, that progressively passes from a viscous fluid state to a plastic foam and then hardened foam state. For equal conditions in terms of humidity, amount of reagent, and relative contact surface, the expansion is governed by the crack width. It was possible to notice that in the case of the CEM_SI series containing two capsules, the PU leakage was most often visible both on the lateral faces and at the crack mouth, covering nearly the entire notch area. Despite that the amount of healing agent was the same, in the case of the CEM_LI series the PU leakage was mainly visible at the crack mouth, concentrated in the central part of the notch area in correspondence of the single capsule position. The CEM_LE series, containing 50% more healing agent with respect to the other two series, showed a behavior in between, with the expansion zone mainly concentrated in the central part of the notch area in correspondence of the single capsule position, but with some visible

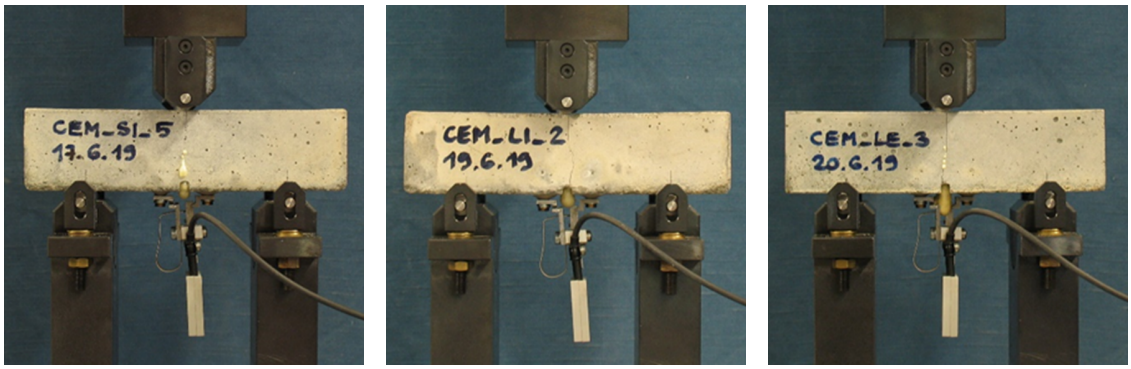

(a) (b) (c)

Figure 6.7: Leakage of polyurethane upon capsule breakage during pre-cracking: (a) Polyurethane (PU) visible both at the crack mouth inside the notch and on the lateral faces for a CEM_SI specimen; (b) PU visible at the crack mouth inside the notch for a CEM_LI specimen; (c) PU visible both at the crack mouth inside the notch and to a lesser extent on the lateral faces for a CEM_LE specimen.

leakage also from the lateral face. This releasing mechanism had consequences on the mechanical performance recovery which are dealt with in the following sections.

Considering the peak load L_{peak}, it should be pointed out that the presence of the cementitious capsules did not have a strong detrimental effect on the load-bearing capacity that the specimens could withstand. It is possible to assess the reduction of the load-bearing capacity $L_{reduction}$ of the self-healing specimens with respect to the plain mortar specimens without capsules as:

$$L_{reduction} = \frac{L_{peak,REF} - L_{peak,i}}{L_{peak,REF}}, \tag{6.3}$$

where $L_{peak,REF}$ is the average load-bearing capacity L_{peak} calculated over the 12 specimens of the REF series and $L_{peak,i}$ is the average load-bearing capacity L_{peak} calculated over the 12 specimens of each self-healing series. Respectively, the percentage reductions were equal to 8% for the CEM_SI series, 13% for the CEM_LI series and 6% for the CEM_LE series. This result showed that the flexural strength is not significantly influenced by the presence of the cementitious capsules, at least for the capsule proportion here used.

Table 6.2 summarizes the results of the pre-cracking phase, with the average values and standard deviation of L_{peak} and L_{unload} per each series and the percentage load reduction $L_{reduction}$ of each self-healing series with respect to the reference series.

Table 6.2: Overview of the average L_{peak} and L_{unload} (with respective standard deviation) and $L_{reduction}$ for each series (12 specimens per series) after the pre-cracking procedure.

Series	L_{peak} (N)	L_{unload} (N)	$L_{reduction}$ (%)
REF	1844 ± 140	14 ± 5	-
CEM_SI	1694 ± 86	88 ± 24	8
CEM_LI	1611 ± 147	59 ± 15	13
CEM_LE	1737 ± 125	143 ± 58	6

6.3 Quasi-static reloading

After the pre-cracking and the complete curing of the PU in a controlled environment (T = 20 °C, 60% RH), half of the specimens (6 per series, for a total of 24 specimens) were selected to be reloaded in static condition to evaluate the self-healing efficiency in terms of strength regain. The specimens were selected based on a visual inspection in order to always have another specimen with a comparable PU release to be tested later in cyclic condition (Section 6.4).

Figure 6.8 shows the load versus CMOD curves recorded during the pre-cracking and the static reloading for the different series. It is important to point out that the curves for the CEM_SI series are 5 because one specimen was accidentally broken during the positioning operations.

Upon reloading, the reference specimens without capsules could only reach at max the residual load-bearing capacity after pre-cracking ($L_{reload} \leq L_{unload}$) and then kept following the same softening branch of the pre-cracking phase. Conversely, the autonomously healed specimens showed a higher maximum load compared to the residual load-bearing capacity before healing ($L_{reload} > L_{unload}$). The load versus CMOD curves were sufficiently repeatable and highlighted a slightly less brittle behavior if compared to the intact specimen behavior. The possibility to improve the ductility as a side effect of the self-healing through polyurethanic agents is a positive aspect in order to prevent brittle failure in the remaining life and to sustain higher deformation in service conditions.

The maximum load obtained during reloading was used to set the cyclic loading limits, as anticipated in Section 6.1.4, and to assess the load recovery in static condition according to the load recovery index definition reported in Equation (6.1). The reference specimens had negligible healing, in some cases even negative performance. On the contrary, the self-healing specimens from all the series had satisfactory healing performances, with average LRI of about 36% for the CEM_SI series, 31% for the CEM_LI series, and the best result of about 47% for the CEM_LE series (see Table 6.3 for a detailed overview). This positive result is in good agreement with literature data concerning the use of cementitious capsules.

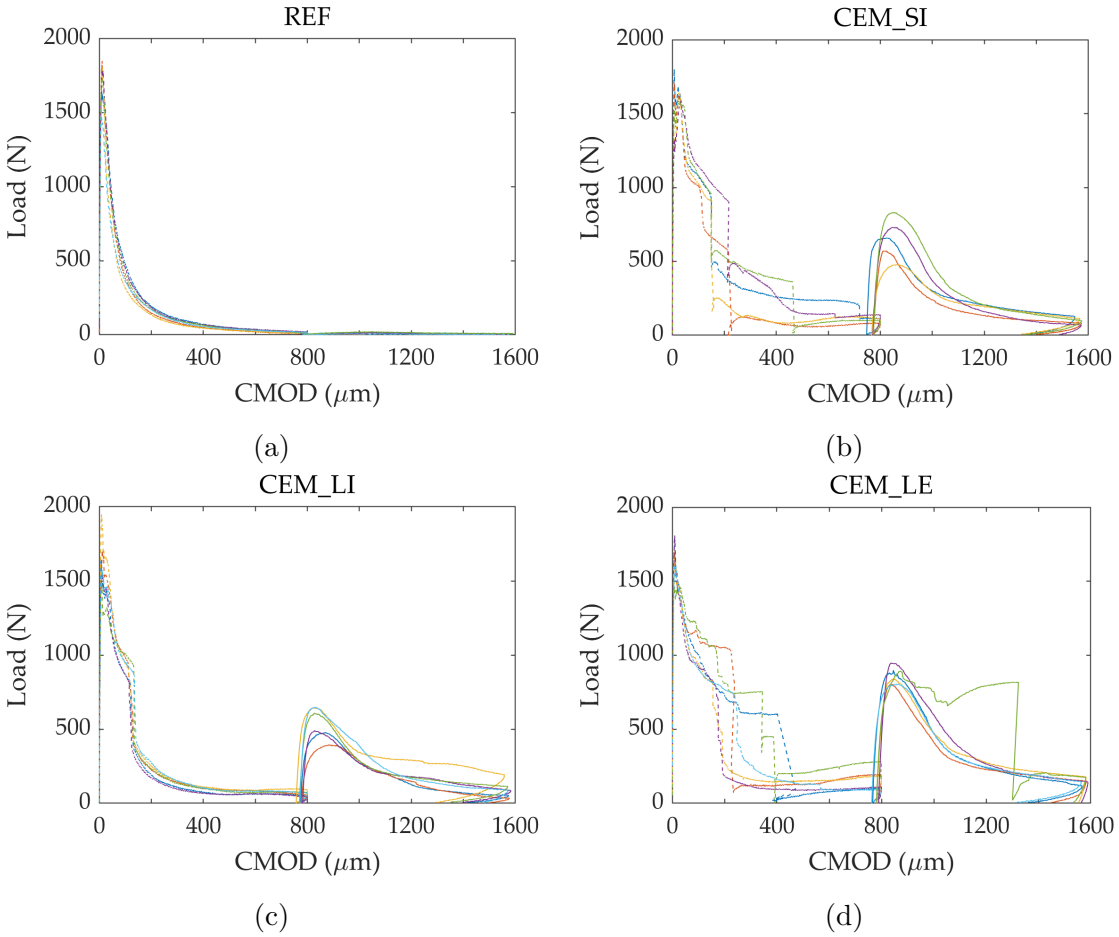

Figure 6.8: Load versus CMOD curves during the pre-cracking (dashed line) and the subsequent static reloading (continuous line) for the different series: (a) REF series; (b) CEM_SI series; (c) CEM_LI series; (d) CEM_LE series. The specimens are distinguished by different color lines.

Table 6.3: Overview of L_{peak} and L_{unload} (average values and standard deviations over 12 specimens per series), L_{unload} and LRI (average values and standard deviations over six specimens per series apart CEM_SI[1]).

Series	$\boldsymbol{L_{peak}}$ **(N)**	$\boldsymbol{L_{unload}}$ **(N)**	$\boldsymbol{L_{reload}}$ **(N)**	$\boldsymbol{LRI}$ **(%)**
REF	1844 ± 140	14 ± 5	15 ± 9	0.1 ± 0.4
CEM_SI	1694 ± 86	88 ± 24	659 ± 137[1]	35.9 ± 17.4[1]
CEM_LI	1611 ± 147	59 ± 15	547 ± 105	30.8 ± 6.7
CEM_LE	1737 ± 125	143 ± 58	869 ± 57	46.5 ± 3.6

[1]Estimated on five reloaded samples.

The manufacturing procedure of the cementitious capsule shells does not seem to influence the overall outcome of the system, since the load reduction during pre-cracking was negligible for all cases, as reported in Section 6.2. Also, the capsule breakage mechanism, with consequent polyurethane release, occurred in similar ways for either the capsules produced by extrusion or by rolling.

Similarly, applying the epoxy coating to the internal or to the external surface of the tubular capsules does not appear to be a relevant factor of influence, considering that in both cases it allowed adequate waterproofing of the capsules and protection of the moisture-reactive healing agent, as confirmed by the abundant release of polyurethane during the pre-cracking stage for all the self-healing series.

The volume proportion of healing agent seems to be correlated to the mechanical recovery under static condition, since better results were observed for the CEM_LE series, which contained 50% more polyurethane with respect to the other series. However, the increase in mechanical performance recovery is not directly proportional to the increase in healing agent volume, probably because in reality not all the polyurethane contained in the capsules reacted with ambient moisture upon crack formation, as it will be further discussed and exemplified in the following. Therefore, the increase in the mechanical performance recovery could be correlated to the internal diameter of the capsule more than to the overall internal volume. A larger internal diameter could be responsible for a better release in the cracked cross-section due to a more favorable ratio between capsule area and capsule perimeter, considering that the walls of the capsule inevitably cause a retaining action over the polyurethane.

For equal cumulative volume of healing agent, even if the capsule internal diameter is slightly smaller, the distribution of the capsules inside the specimen plays a more prominent role. Specifically, the use of more capsules increases the number of points from which the PU can be released and from which is allowed to expand, hence allowing a more even spreading of the PU over the crack surfaces, rather than a concentrated release in the central part of the section. This mechanism improves the overall crack filling and consequently should be reflected on the mechanical recovery during static reloading. This could explain the slightly superior performance of the CEM_SI series with respect to the CEM_LI series, although such conclusion needs to be further confirmed from a statistical point of view.

To conclude the analysis of the static behavior, one interesting case to be pointed out concerns one specimen of the series containing one large-diameter capsule with external epoxy coating, namely the specimen labeled as CEM_LE_9. Upon reloading, a hardening behavior was detected after the peak value L_{reload}, followed by a second load drop and a further polyurethane release. This event could be possibly ascribed to a self-protecting action of the polyurethane that sealed both the crack and the core of the capsule, protecting the unpolymerized precursor and allowing a second healing effect.

In order to analyze this second healing, after complete curing of the PU the

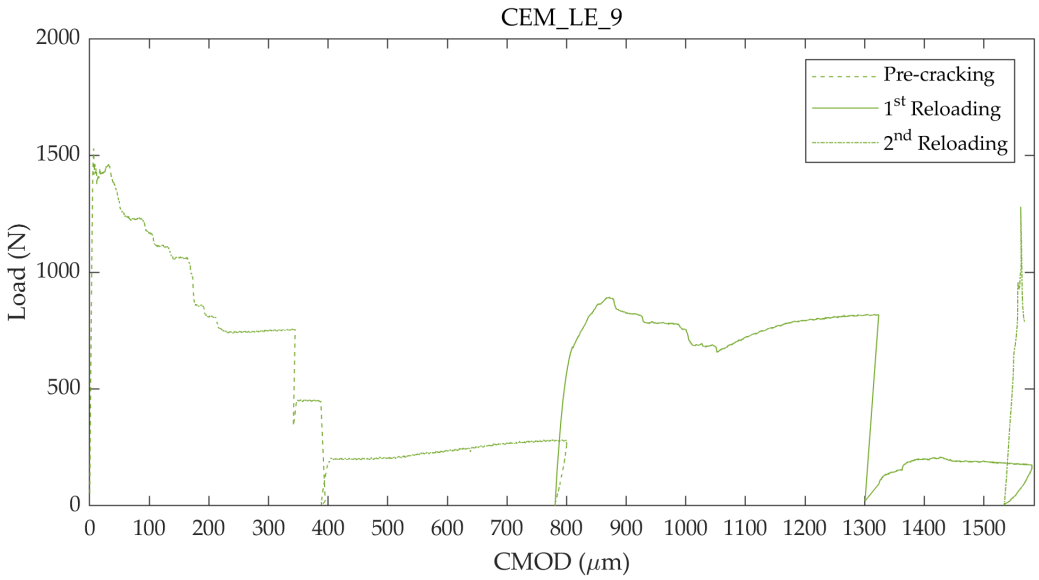

Figure 6.9: Load versus CMOD curves for the specimen CEM_LE_9 during the pre-cracking (CMOD up to 800 µm), the first static reloading in which there was a drop in load followed by a new PU release and the subsequent second static reloading after PU curing.

specimen was further reloaded following the same procedure used for the pre-cracking. Figure 6.9 shows the load versus CMOD curves acquired for the pre-cracking, first reloading, and second reloading procedures. It is to be pointed out that soon after reaching the new maximum load, the specimen was unloaded due to a malfunctioning in the control system of the testing machine.

Surprisingly, the new maximum load L_{reload} was higher than the one obtained in the previous reloading. It is possible to compare the two successive reloading in terms of LRI, comparing their maximum load with the peak load obtained during pre-cracking:

$$LRI_1(\%) = \frac{L_{reload,1} - L_{unload,p}}{L_{peak} - L_{unload,p}}, \tag{6.4}$$

$$LRI_2(\%) = \frac{L_{reload,2} - L_{unload,1}}{L_{peak} - L_{unload,1}}, \tag{6.5}$$

where L_{peak} is the load-bearing capacity obtained during pre-cracking, $L_{unload,p}$ the residual bearing capacity after unloading during the pre-cracking, $L_{reload,1}$ the maximum load carrying capacity obtained during the first static reloading, $L_{unload,1}$ the residual bearing capacity after unloading during the first static reloading and $L_{reload,2}$ the maximum load carrying capacity obtained during the second static

Table 6.4: Overview of the parameters characterizing the static flexural behavior of the CEM_LE_9.

Series	No.	L_{peak} (N)	$L_{unload,p}$ (N)	$L_{reload,1}$ (N)	LRI_1 (%)	$L_{unload,1}$ (N)	$L_{reload,2}$ (N)	LRI_2 (%)
CEM_LE	9	1531	258	896	50	165	1280	82

reloading. The self-healing efficiency in terms of load carrying capacity regain increased in the second reloading to 82%, while in the first was equal to 50%.

Table 6.4 summarizes these results regarding the static flexural behavior of the specimen CEM_LE_9 during the pre-cracking and the successive two reloading stages.

6.4 Cyclic reloading

After defining the limits of the cyclic flexural load as a function of the average load carrying capacity upon reloading L_reload per each series, the cyclic reloading itself was performed, in accordance with the procedure reported in Section 6.1.4.

As expected, it was not possible to test the specimens without capsules under cyclic conditions. This was due to the fact that the selected pre-cracking procedure was used to simulate a severe condition of damage, resulting in a residual load carrying capacity after pre-cracking substantially nil for all the specimens. The plain mortar specimens without reinforcement of the REF series could not sustain any further load after pre-cracking because the contribution of the autogenous healing was insufficient to restore an adequate load carrying capacity, so that they failed immediately before the beginning of the actual cyclic test, during the positioning operations. On the contrary, the autonomous repair action provided by the polyurethane in the self-healing series allowed to perform the cyclic reloading in most cases. Specifically, all the specimens of the CEM_LI series were tested, (six in total) while in the case of the CEM_SI and CEM_LE series respectively three and two specimens failed in the initial part of the procedure, before reaching the prescribed cyclic peak load. It is worth reminding that the latter was defined as 70% of their estimated load-bearing capacity after healing. Clearly, the estimation based on the results of the static reloading test was not very accurate in these cases.

For all the self-healing specimens that could undergo the cyclic reloading, a three-stage curve was detected. A typical example of it is reported in Figure 6.10, where the evolution of the crack opening at the peak of each cycle (i.e., at maximum load L_{max}) is reported for the specimen CEM_SI_4.

This three-stage behavior is typically observed in plain or fiber-reinforced concrete under compressive, tensile, and flexural fatigue loading [304, 309–314].

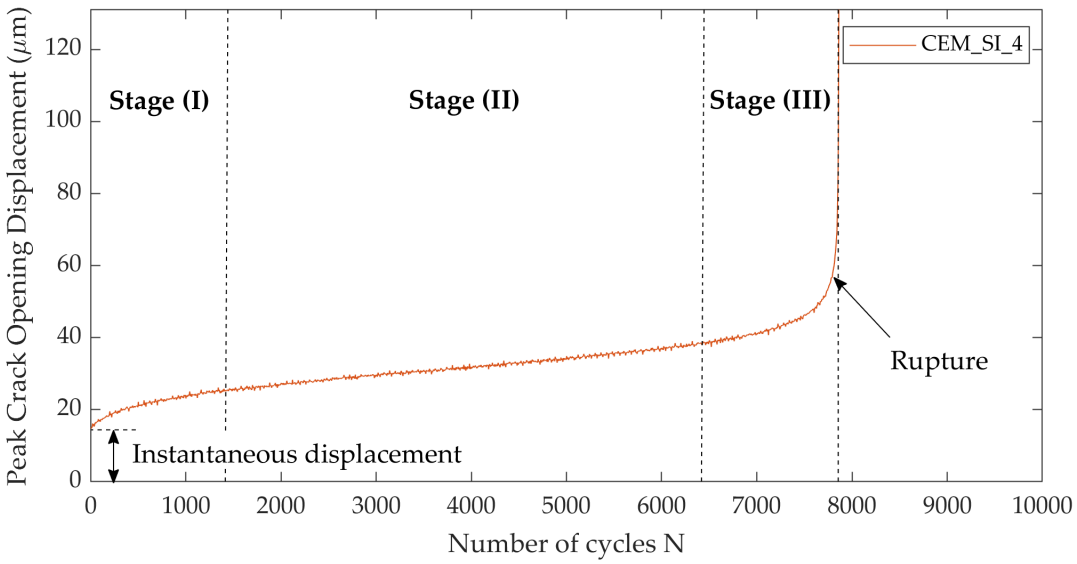

Figure 6.10: Three-stage fatigue evolution of the peak crack opening with increasing number of cycles.

After an almost instantaneous crack opening displacement increase upon loading, there was a first rapid development denoted as flaw initiation, or Stage (I). In concrete, this stage involves the defects within the matrix; in the case of the self-healing system here studied, it most likely involved the defects at the interface between the PU and the crack faces and inside the PU foam, rather than the defects in the mortar matrix surrounding the crack, though it cannot be excluded that they also provided a contribution. It is worth noting that, in literature, tests conducted over pre-cracked fiber reinforced concrete under flexure lacked this stage, because the initial loading already caused the opening of the crack [315]. So, the experimental evidence of Stage (I) in cementitious mortar autonomously healed by PU is a further confirmation of the important role of the presence of the healing agent in restoring a behavior similar to the one of an intact material.

The Stage (II) is a stable development stage that involves slow and progressive growth of damage, most likely concentrated in the bonding interface formed by the PU, and the progressive elongation and rupture of the foam cells. By comparison, in fiber-reinforced concrete this phase is mainly associated to the fiber/matrix bond deterioration [82, 316] and fiber rupture [317].

Finally, the Stage (III) is the failure stage, in which damage develops unsteadily until fatigue failure occurs, with a complete failure of the bonding PU interface and detachment of the crack faces.

Figure 6.11 shows the curves that represent the relationship between the crack opening measured at the maximum load with the increasing of number of cycles

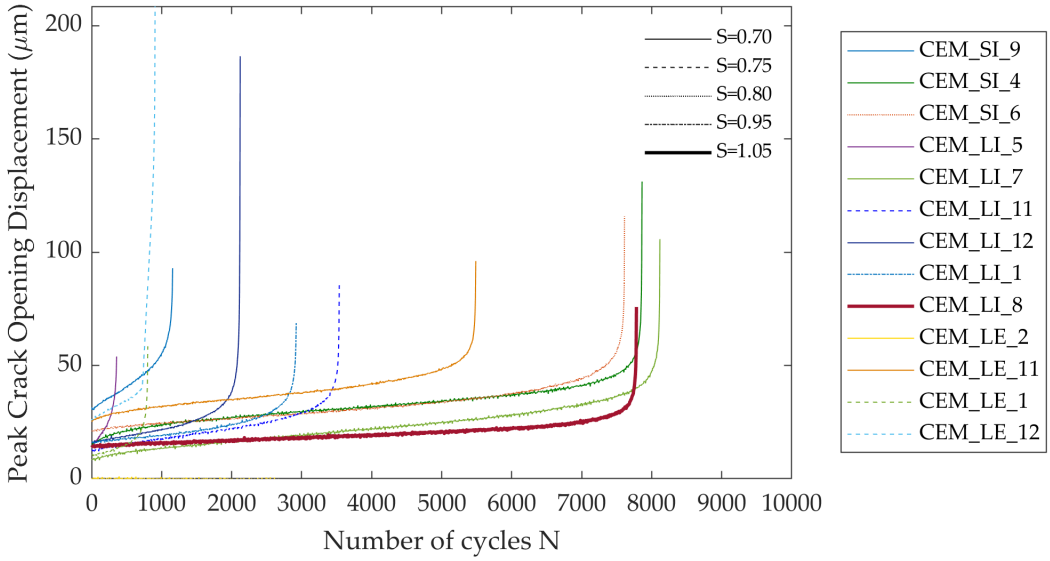

Figure 6.11: Peak crack opening versus number of cycles until complete failure, which occurred at different load level S among the specimens.

Table 6.5: Number of cycles sustained by the specimens at each load level S.

Load Level S		**0.70**	**0.75**	**0.80**	**0.85**	**0.90**	**0.95**	**1.00**	**1.05**
Series	**No.**	**Number of cycles N**							
REF	all	0	-	-	-	-	-	-	-
CEM_SI	9	1177	-	-	-	-	-	-	-
	4	7881	-	-	-	-	-	-	-
	6	10000	10000	7625	-	-	-	-	-
CEM_LI	5	381	-	-	-	-	-	-	-
	7	8138	-	-	-	-	-	-	-
	11	10000	3557	-	-	-	-	-	-
	12	10000	10000	10000	2141	-	-	-	-
	1	10000	10000	10000	10000	10000	2940	-	-
	8	10000	10000	10000	10000	10000	10000	10000	7797
CEM_LE	2	2732	-	-	-	-	-	-	-
	11	5503	-	-	-	-	-	-	-
	1	10000	816	-	-	-	-	-	-
	12	10000	921	-	-	-	-	-	-

N until complete failure, that occurred at different load level S, while Table 6.5 summarizes the number of cycles sustained by each specimen at a given load level S.

The self-healing specimens were able to sustain a satisfactory amount of cycles

Table 6.6: Comparison between the load-bearing capacity of the intact self-healing specimens and their residual load-bearing capacity after pre-cracking with the applied maximum load in cyclic condition.

		Load Level S							
	Series	**0.70**	**0.75**	**0.80**	**0.85**	**0.90**	**0.95**	**1.00**	**1.05**
$\frac{L_{max}}{L_{unload}}$	CEM_SI	13	14	15	-	-	-	-	-
	CEM_LI	6.5	7	7.5	8	8.5	9	9.5	10
	CEM_LE	4.5	5	-	-	-	-	-	-
$\frac{L_{max}}{L_{peak}}$	CEM_SI	0.27	0.29	0.31	-	-	-	-	-
	CEM_LI	0.24	0.25	0.27	0.29	0.31	0.32	0.34	0.36
	CEM_LE	0.35	0.38	-	-	-	-	-	-

before failure, both for the lower and the higher load levels. This result, compared to the performance of the reference specimens, strongly underlines the contribution of the autonomous self-healing system in restoring the mechanical properties of the damaged cementitious materials, especially in severe conditions of damage and also when cyclic loads are involved, improving the resilience of the system during its remaining service life.

In terms of number of cycles and maximum load level, the best performance was expressed by the CEM_LI series. On the other hand, it is important to point out that this result deeply depends on the estimation of the load-bearing capacity after self-healing that was made based on the static reloading data (Section 6.3).

Comparing the initial load-bearing capacity of the intact self-healing specimens and their residual load-bearing capacity after pre-cracking with the applied maximum load in cyclic condition, it is possible to see that the specimens sustained a maximum load in cyclic condition much higher than the residual bearing capacity after unloading in the pre-cracking phase (L_{unload}): up to 15 times this residual capacity for the CEM_SI series, 10 times for the CEM_LI series and 5 times for the CEM_LE series (see Table 6.6).

The comparison with the peak load of the intact specimens indicates that the system possesses a good recovery ability under cyclic conditions, being able to sustain cyclic loads up to 31% of the intact load-bearing capacity for the CEM_SI series, up to 36% for the CEM_LI series and up to 38% for the CEM_LE series (see Table 6.6). This is in good agreement with the performance regain observed under static conditions, where the values of the load recovery indexes were approx. 36%, 31% and 47% respectively.

As a general tendency, looking at Table 6.5 it is possible to notice an overall decrease in the number of cycles to failure with increasing load levels. Figure 6.12 shows the relationship between the evolution of the crack opening at the maximum load with increasing number of cycles N, at each load level S at which they were

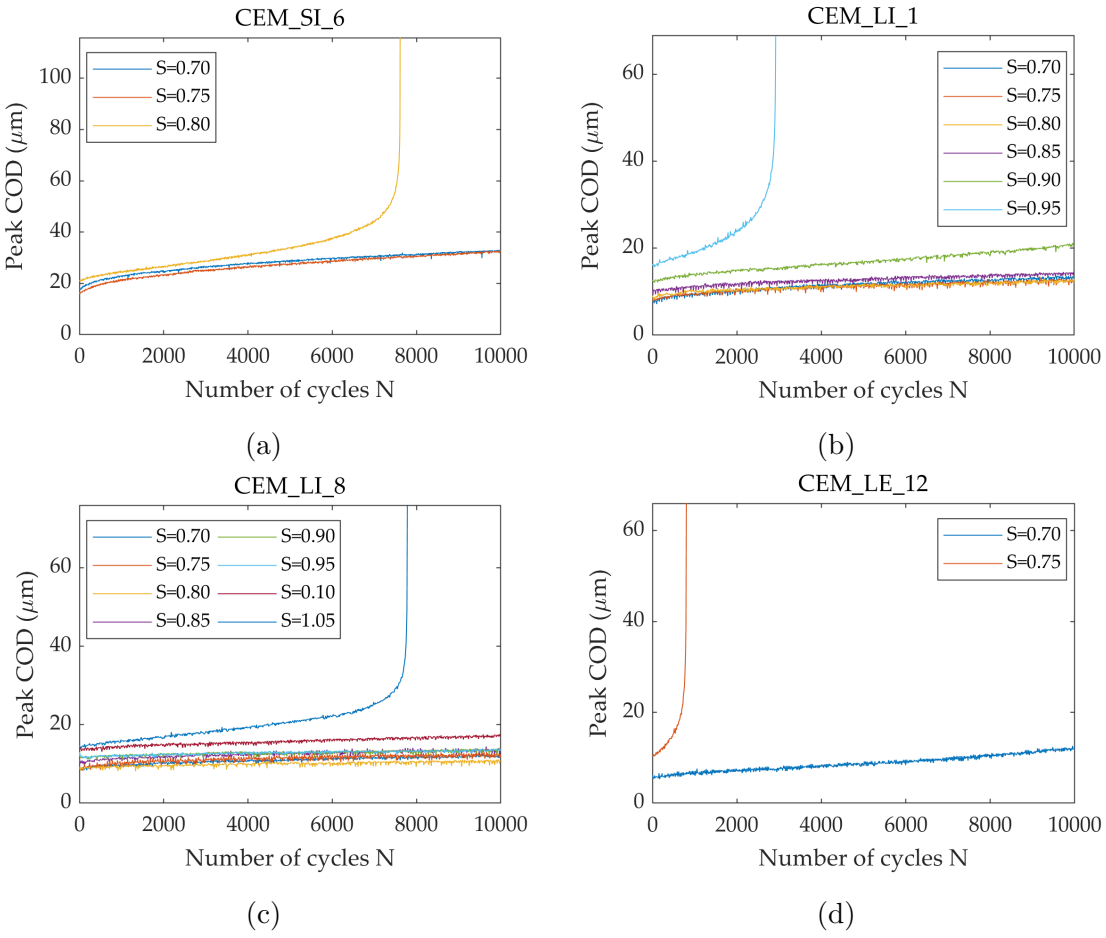

Figure 6.12: Evolution of the crack opening displacement at the maximum load with increasing number of cycles N with increasing load level S: (a) CEM_SI_6; (b) CEM_LI_1; (c) CEM_LI_8; (d) CEM_LE_12.

tested before complete failure. In the figure, four of seven specimens that underwent the cyclic testing at increasing load levels are displayed, as a way of example.

Looking in detail at these curves, it is possible to notice that with increasing S an increase of the slope in the Stage (II) curves occurs and a progressive deviation from linearity as a function of the number of cycles is displayed. The latter is a typical feature of the Stage (III) and is evidenced for example in Figure 6.12b for $S = 0.90$, after about 7000 cycles. This feature is directly correlated to a faster increase in the damage rate evolution. Further studies would be needed to better investigate this change of slope in correlation with the load level S, for the purpose of characterizing the fatigue life of the self-healing cementitious materials, in comparison with ordinary and fiber reinforced concrete. Nevertheless, these results represent a step forward with respect to the limited literature concerning the

fatigue performances of self-healing cementitious systems, which is an important knowledge gap that needs to be filled in order to ensure the reliability of these systems in real field conditions.

6.5 Conclusions

Self-healing mortars were produced adding cementitious tubular capsules filled with a polyurethane precursor in the mortar mix. The capsules were manufactured according to the two different procedures described in Section 3.1.2, and were also characterized by different waterproofing coating configurations, size, and distribution within the mortar specimens. Their self-healing effect was evaluated in terms of mechanical recovery under static flexural loading and number of cycles to failure under repeated cyclic flexural loading.

The results were not significantly affected by the capsule manufacturing procedure and by the sequence of application of the epoxy coating layers as highlighted in Chapter 5; conversely, the internal diameter of the capsules and their distribution within the specimen may have influenced the release of the polyurethane precursor upon pre-cracking and hence the final mechanical performance.

In all cases, the mechanical regain was very satisfactory in comparison with the behavior of reference plain mortars, both under static and cyclic loading. A maximum load recovery index in static condition of more than 40% and a maximum number of cycles to failure of more than 70000 were observed, confirming the potential of the proposed capsule-based self-healing system for the purposes of improving the structures durability and mechanical performances also when subjected to dynamic actions.

Chapter 7

Evaluation of the sealing efficiency with a shared inter-laboratory testing procedure

The critical nature of the increasing sustainability and safety requirements of structures is pointed out by their inclusion as priority challenges in the European Research Program. In this context, the growing importance of research on self-healing cementitious materials has been highlighted in the last decade by the funding of several FP7 and Horizon 2020 projects concerning the use of these technologies, such as the HEALCON project[1] (2013 - 2016), the SHeMat project[2] (2012 - 2015), the EnCoRe project[3] (2012 - 2014), the CAPDESIGN project[4] (2013 - 2017), the LORCENIS project[5] (2016 - 2020), the ReSHEALience project[6] (2018 - 2022) or the SMARTINCS project[7] (2019 - 2023).

Within the projects concerning self-healing funded by the European Union, there is also the COST Action SARCOS (Self-healing As preventive Repair of COncrete Structures) CA15202[8] (2016 - 2021). The project is funded by the European Cooperation in Science and Technology (COST), which is a funding organization

[1]HEALCON: https://cordis.europa.eu/project/id/309451

[2]SHeMat: https://cordis.europa.eu/project/id/290308

[3]EnCoRe: https://cordis.europa.eu/project/id/295283

[4]CAPDESIGN: https://www.era-learn.eu/network-information/networks/m-era-net/m-era-net-joint-call-2012/encapsulation-of-polymeric-healing-agents-in-self-healing-concrete-capsule-design

[5]LORCENIS: https://cordis.europa.eu/project/id/685445

[6]ReSHEALience: https://cordis.europa.eu/project/id/760824

[7]SMARTINCS: https://cordis.europa.eu/project/id/860006

[8]SARCOS: https://www.cost.eu/actions/CA15202/, https://www.sarcos.eng.cam.ac.uk/

for the creation of research networks (COST Actions). These networks offer an open space for collaboration among scientists across Europe (and beyond) and thereby give impetus to research advancements and innovation.

The first focus of the SARCOS COST Action is to compare the use of self-healing capabilities of concrete [16] with the use of external healing methods [9] for repairing existing concrete elements. Despite the promising potential of the developed healing technologies, they will be real competitive alternatives only when sound and comparative characterization techniques [19] for performance verification are developed, being this SARCOS's second focus. The third focus deals with modeling the healing mechanisms taking place [318] for the different designs and with predicting the service life increase achieved by these methods. In order to achieve these objectives, SARCOS brings together researchers from academia, industry, and regulators from 31 countries, including EU, Near Neighbor and International Partner Countries.

With the aim of achieving the second focus of SARCOS of filling the lack of standardized test methods and develop sound and comparative characterization techniques, six different inter-laboratory tests are running to evaluate test methods to assess the efficiency of self-healing cementitious materials. Each test focuses on a different healing technology.

One of the inter-laboratory tests in which the research group of Politecnico di Torino is involved and which is in close relation to the topic here described focuses on self-healing mortar and concrete with macro-capsules, filled with polymeric healing agents [319]. Glass capsules were chosen due to their well-documented successful use throughout the last decade [20–22, 26, 29–34], and considered as representative also for other types of brittle capsules. Six laboratories participated in this inter-laboratory test:

- Ghent University,
- *Politecnico di Torino*,
- Riga Technical University,
- Cracow University of Technology,
- Cambridge University,
- KU Leuven (Ghent Technology Campus).

For the inter-laboratory test program, two different tests are under evaluation: a water permeability test and a capillary water absorption test. To execute the water permeability test, mortar specimens were cast, and concrete specimens were cast to perform the water absorption test. All specimens were produced by Ghent University and then shipped to the participating laboratories.

Following the opportunity to participate in this inter-laboratory testing, it was decided to use the results obtained for the glass capsules as a benchmark to compare the performances of the newly developed cementitious capsules filled with polyurethane precursor. This allowed to fulfill an important objective of the research activities, namely to compare the cementitious capsules with another macro-encapsulation technology that obtained positive results through the last decades in its applications by several research groups. This also allowed to prove the SARCOS protocol applicability to different self-healing cementitious materials based on the use of macro-capsules.

7.1 SARCOS Inter-laboratory test protocol

7.1.1 Mortar prisms with glass capsules

Specimens preparation

Unreinforced mortar prisms (40×40×160 mm^3) were cast using a mortar mix composition deduced from the concrete composition (concrete equivalent mortar). Ordinary Portland cement (CEM I 42.5 N, ENCI, the Netherlands), sieved sand (grading 0-2 mm), limestone filler, and tap water were used. The water to cement ratio was 0.50. Superplasticizer was added in a dosage of 0.16 m% relative to the weight of cement. For each laboratory, a separate batch was made to cast all specimens.

The mortar prisms remained unreinforced. Yet, the specimens were provided with a cast-in-hole in order to perform the water flow test (as in Section 5.1.4). This cast-in-hole was created by placing an oiled smooth steel bar (Φ 5 mm) along the length of the molds. When the specimens were demolded, the day after casting, the steel bar was pulled out of the mortar prisms, creating a hollow core along the longitudinal axis of the specimens. The cast-in hole was located with its center at 15 mm from the bottom side of the specimens (Figure 7.1). After demolding, the specimens were sealed in plastic foil in groups of 3 to prepare them for shipping (6 specimens per series, for a total of 12 specimens).

For the self-healing specimens, two capsules were placed at a height of 5 mm above the bottom side of the specimen so that the vertical distance between the cast-in hole and the capsule, and the distance between the capsule and the bottom side of the specimen was approximately equal. The macro-capsules were made from borosilicate glass (Φ_{ext} =3.35 mm, Φ_{int} =3 mm). The length of the capsules used for the mortar prisms was equal to 55 mm. To estimate the volume of healing agent in a capsule, an effective length of the capsule 5 mm shorter than the total length was assumed (i.e. 50 mm). This was done to account for a small amount of air in the capsule, as well as the sealing of the capsules with a two-component epoxy glue (PC 5800, Tradecc, Belgium). One side of the glass capsules was first sealed

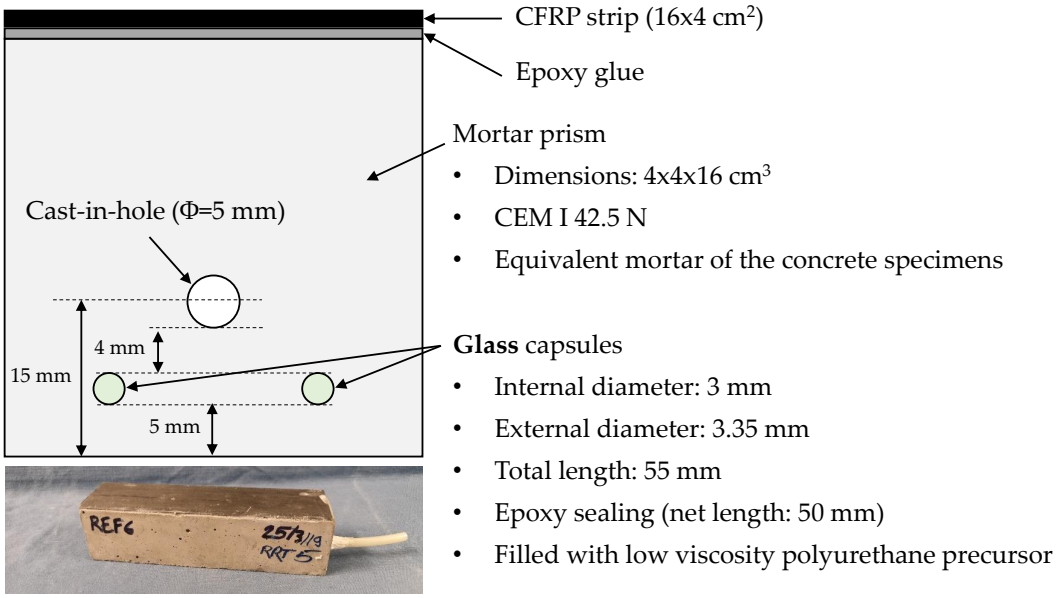

Figure 7.1: Specimens containing glass capsules.

with epoxy glue. Subsequently, the capsules were filled with the low viscosity PU healing agent described in 3.4.2 (HA Flex SLV AF, GCP Construction Products N.V., Belgium) using a syringe with needle. Care was taken to limit the amount of entrained air. To make the leakage of PU from the cracked specimens more visible, a small amount of bright yellow fluorescent powder dye (EpoDye, Struers, the Netherlands) was mixed into the PU prior to filling the capsules. After filling the capsules with PU, the open side of the capsules were also sealed using epoxy glue.

Specimens which contained glass capsules are denoted in this chapter as GLASS specimens, as opposed to their reference specimens without capsules which are denoted as REF_G specimens.

Test procedure

The test procedure shares similarities with the tests described in Chapter 5. It is reported below and summarized in Figure 7.2. Some results of the test performed on the specimens at Politecnico di Torino in the framework of the inter-laboratory testing will be used as comparison for the results using cementitious capsules.

Crack creation and active crack width control Prior to shipping, a carbon fiber reinforced polymer (CFRP) strip (PC®Carbocomp UNI, Tradecc, Belgium) with dimensions 40×160 mm^3 was glued on the top of the specimens using an epoxy

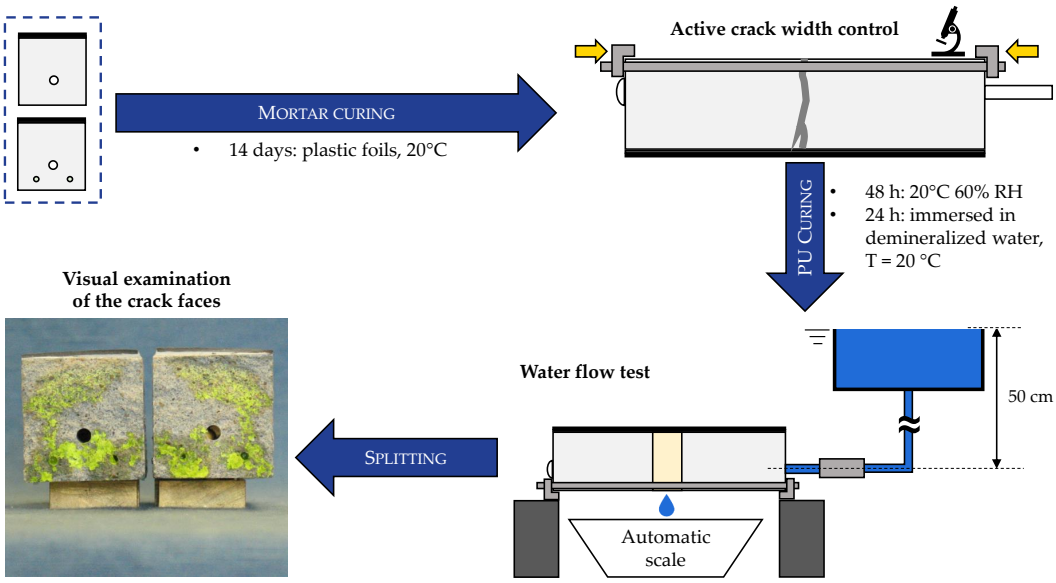

Figure 7.2: Summarization of the SARCOS inter-laboratory test protocol.

resin (Sikadur®-30, Sika, Belgium) (see Figure 7.1). At an age of 14 days, the specimens were cracked in a three-point bending test with a span of 100 mm and a loading rate of 50 N/s (similar to the bending test prescribed by EN 196-1). Due to the fact that there was no tensile reinforcement in the specimens, they failed suddenly; however, both halves remained connected due to the CFRP, which allowed to widen or close the cracks and to apply the active crack width control [41, 124, 179] (as described in Section 5.1.2). Immediately after cracking the specimens were placed with their crack mouth facing upwards and the crack width was restrained using screw jacks (shipped by Ghent University) to a nominal value of 400 µm. The crack width was then further restrained under an optical microscope using an iterative procedure of measuring and restraining until the average crack width fell within the desired crack width range of 290 to 310 µm.

Along the crack path, three different locations were chosen to measure the crack width. The locations were not fixed to avoid the risk of studying a location with a defect (e.g., a missing aggregate or sand particle, (semi) loose particles, missing pieces of the cementitious matrix, parallel cracks, etc.), resulting in the measurement of a local phenomenon, instead of a global description of the crack. Consequently, the operator chose locations representative of the crack, taking into account to avoid borders and spread equally the locations along the crack length. In each location, the crack width was measured 5 times. Hence, the average crack width was calculated as the average of the 15 crack width measurements.

The specimens were then turned so that the crack mouth was facing downwards

(i.e. CFRP facing upwards), in order to limit the influence of the specimen orientation on the outflow of PU from the capsules. The active crack width control was executed in less than 30 minutes.

Water flow test to assess sealing efficiency The water permeability of the specimens was measured using a water flow test [19, 120, 189] (as in Section 5.1.4). Prior to executing the test, specimens were stored in an indoor climate with their crack facing downwards for at least 1 day, to allow the PU to polymerize. Afterward, specimens were submersed in demineralized water for 24 to 48 h to prevent the influence of water absorption by the matrix on the results. The specimens were then taken out of the water and were surface dried. To connect the specimens to the water flow setup, the cast-in hole was enlarged to a diameter of 6 mm over a length of 25 ± 5 mm using a drill. This was done prior to cracking to prevent the vibrations from influencing the crack. A short plastic tube (length of ±60 mm, $\Phi_{external}$ 6 mm, $\Phi_{internal}$ 4 mm) was then inserted in the cast-in hole and sealed using silicone. Also the other side of the cast-in hole was sealed completely with silicone (see Figure 7.3). The inserted tube was then connected to a tube in contact with an open water reservoir. The water head, measured from the tube in the specimens up to the water level, was kept constant throughout the test at 50 ± 2 cm by topping up with demineralized water, in order to maintain a constant pressure (≈ 0.05 bar). In order to measure only the water leaking out of the crack mouth, the sides of the specimens were sealed prior to saturation. Sealing could be achieved by the different laboratories using aluminum tape, silicon sealant, or a viscous glue. In the case of our laboratory, viscous methyl methacrylate glue was used (Schnellklebstoff X60, HBM, Germany). The first 60 seconds of water leakage was not recorded in order to measure only a fully developed flow and to allow the removal of water bubbles from the system. Subsequently, the weight of the water which leaked from the crack was recorded for a minimum of 6 minutes.

The sealing efficiency SE_{wf} of the self-healing specimens containing the glass capsules was calculated with respect to the reference specimens, without capsules, using Equation 7.1:

$$SE_{wf}\,(\%) = \frac{\bar{q}_{REF\_G} - \bar{q}_{GLASS}}{\bar{q}_{REF\_G}} \times 100, \tag{7.1}$$

where $\bar{q}_{REF\_G}$ the average water flow rate (g/min) of the reference specimens and $\bar{q}_{GLASS}$ the average water flow rate (g/min) of the self-healing specimens containing glass capsules.

Visual examination of healing agent on the crack surfaces After performing the water permeability test, the GLASS specimens were split at the location of the crack to determine the healing agent coverage [15, 29, 30, 39, 293]. Pictures were taken from both crack faces of each specimen. The PU spread was

determined via machine learning by using the Trainable Weka Segmentation [320] plugin in the open source software ImageJ, distribution Fiji (version 1.52) [321]. After manually training the machine learning algorithm, it was able to produce a pixel-based segmentation of the zones with and without PU. The segmented images were then filtered to remove outliers, after which the images were manually checked for misidentified zones (e.g. a sand particle being identified as PU due to similar color). The application of the Trainable Weka Segmentation to analyze images has also been used for self-healing applications to segment swollen SAP particles in tomography images of cracked mortar [322, 323]. The surface coverage was defined as the quotient of the area with PU over the total area and reported as the average from both crack faces of a specimen, as it was noted that the spread was similar on each crack face.

7.1.2 Mortar prisms with cementitious capsules

Specimens preparation

Unreinforced mortar prisms (40×40×160 mm^3) were cast using standardized mortar mix composition, as described in EN 196-1. Ordinary Portland cement (CEM I 42.5 N, Buzzi Unicem S.p.A., Italy), normalized sand (grading 0-2 mm, DIN EN 196-1), and tap water were used. The water to cement ratio was 0.50, the sand to cement ratio was 3.

In this case, for the self-healing specimens, cementitious capsules were used. It was decided to manufacture two series of specimens using either extruded (Φ_{ext} =10 mm, Φ_{int} =7.5 mm) or rolled (Φ_{ext} =8 mm, Φ_{int} =5 mm) cementitious capsules, manufactured as described in Chapter 3. An epoxy coating was applied only internally (see Section 3.2), with a thickness of about 1 mm, reducing the internal diameter of the capsules to 5.5 mm for the extruded capsules and 3 mm (as the glass capsules) for the rolled capsules. For this reason, the lengths of the capsules were chosen respectively equal to 45 mm and 60 mm. The reason for these lengths was that, taking into account the reduction of the effective length due to the sealing with a two-component epoxy plaster (Stucco K, API SpA, Italy) and a small amount of air in the capsules, it was possible to encapsulate in the rolled capsules the same volume of healing agent of the glass capsules, while double of this volume in the extruded capsules.

Taking this into account and in order to have the same amount of healing agent as in the case of glass capsules, two self-healing series of specimens were produced: one containing one extruded capsule (CEM_L series, 6 specimens), one containing two rolled capsules (CEM_S series, 6 specimens). The capsules were filled with the same PU healing agent modified with the fluorescent dye described in Section 7.1.1, using a syringe with needle and limiting the amount of entrained air.

The main characteristics of the cementitious capsules used are summarized in

Table 7.1: Summary of the characteristics of capsules used for the different series.

		CEM_L	**CEM_S**
Manufacturing process		Extrusion	Rolling
Mix design		Mix design 2	Mix design 2
Surface of the tubular shell coated with epoxy		Internal	Internal
Average internal diameter of the tubular shell	(mm)	7.5	5
Average external diameter of the tubular shell	(mm)	10	8
Average length of the capsule	(mm)	45	60
Average thickness of the epoxy coating	(mm)	1	1
Average internal diameter after epoxy coating	(mm)	5.5	3
Volume of cargo healing agent	(mL)	≈0.6	≈0.3

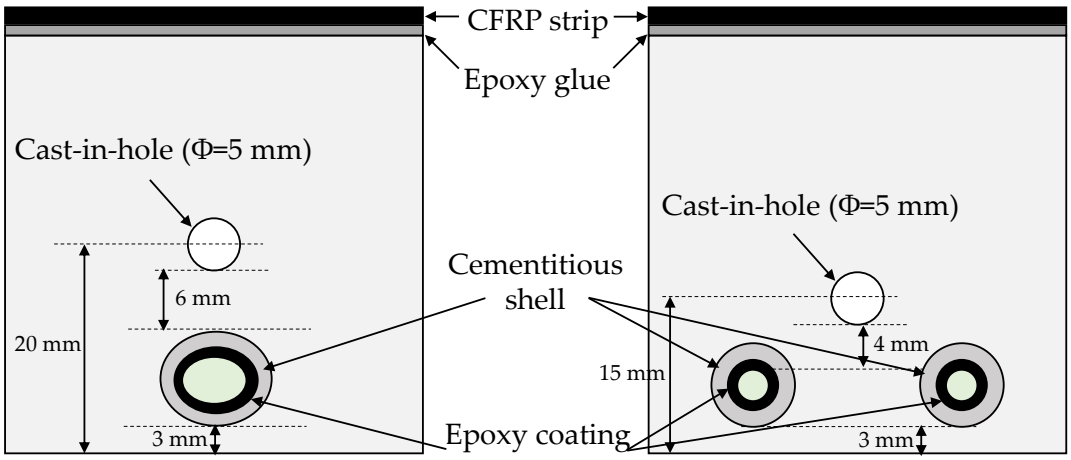

Figure 7.3: Specimens containing cementitious capsules.

Table 7.1.

The capsules were placed at a height of 3 mm above the bottom side of the specimen (Figure 7.3) so that, taking into account the shell and coating thicknesses, the vertical distance between the internal core of healing agent and the bottom side of the specimen was approximately equal to that of the glass capsules (≈5 mm).

Also in this case, the specimens were provided with a cast-in-hole in order to perform the water flow test. The cast-in hole was located with its center at 15 mm from the bottom side of the specimens in the case of the CEM_S series, keeping the testing conditions of the inter-laboratory testing. However, due to the dimension of

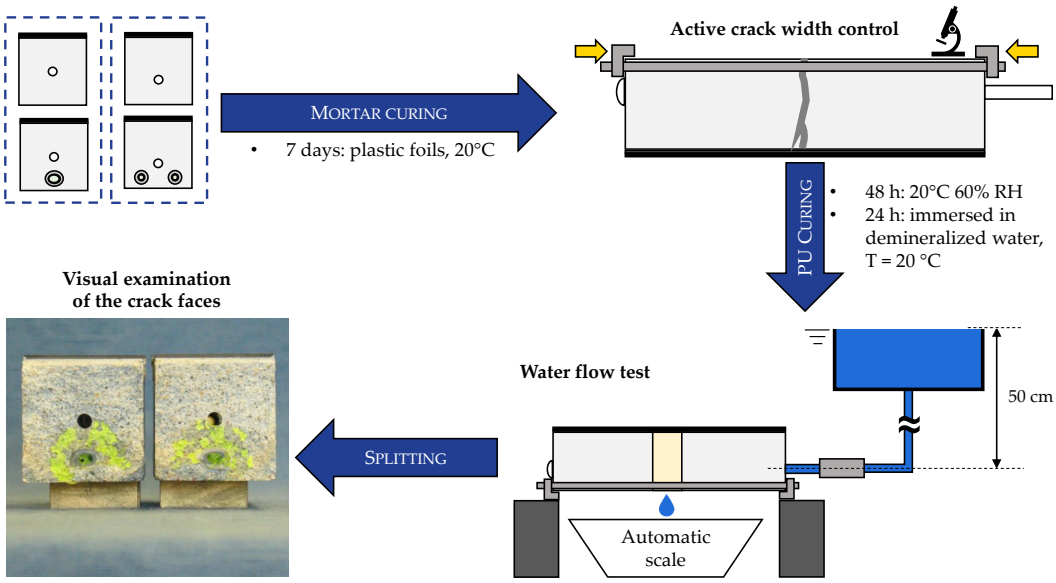

Figure 7.4: Summarization of the test protocol used for the self-healing specimens containing cementitious capsules.

the extruded capsules, it was necessary to move upwards the cast-in-hole to a height of 20 mm (see Figure 7.3). This height was chosen also in order to keep constant in the two series the distance between the center of the capsules and of the cast-in-hole. To take into account the influence different position of the cast-in-hole, two series of reference mortar specimens without capsules were produced to be compared with their respective self-healing series: one with the higher cast-in-hole (REF_L series, 6 specimens) and one with the lower cast-in-hole (REF_S series, specimens).

After demolding, the specimens were sealed in plastic foil in groups of 3 to maintain the same curing condition of the GLASS series.

Test procedure

The test procedure for the self-healing specimens containing cementitious capsules is summarized in Figure 7.2. The procedure was the same as described in Section 7.1.1, apart the differences reported below.

Crack creation and active crack width control Also in this case, a carbon fiber reinforced polymer (CFRP) strip (Sika CarboDur®, Sika, Italy) with dimensions 40×160 mm^3 was glued on the top of the specimens using an epoxy resin (Sikadur®-30, Sika, Belgium) (see Figure 7.3). At an age of 7 days, instead of 14 days due to technical organization reasons, the specimens were cracked in a three-point bending test with a span of 100 mm and a loading rate of 50 N/s. The same active crack width control technique described in Section 7.1.1 was applied.

Water flow test to assess sealing efficiency The water permeability of the specimens was measured using the same water flow test and the same procedures described in Section 7.1.1.

The sealing efficiency SE_{wf} of each series of self-healing specimens containing cementitious capsules was calculated with respect to the reference specimens, without capsules and with the same cast-in-hole configuration, using Equation 7.2:

$$SE_{wf}\,(\%) = \frac{\bar{q}_{REF\_i} - \bar{q}_{CEM\_i}}{\bar{q}_{REF\_i}} \times 100, \tag{7.2}$$

where $\bar{q}_{REF\_i}$ the average water flow rate (g/min) of the reference specimens and $\bar{q}_{CEM\_i}$ the average water flow rate (g/min) of the self-healing specimens containing glass capsules. i indicates either the L or S that identifies the type of capsules and the position of the cast-in-hole.

Visual examination of healing agent on the crack surfaces After performing the water permeability test, the self-healing specimens were split at the location of the crack to determine the healing agent coverage [15, 29, 30, 39, 293]. Pictures were taken from both crack faces of each specimen. Prior to the segmentation of the zones with and without PU, the crack faces were overlapped using the open source software GIMP [324]. One crack face was flipped horizontally, overlapped to the other face in order to have a correct matching of the side of the crack faces and the cast-in-hole. Taking into account that the pixels corresponding to PU have a higher pixel value (i.e. higher brightness) than those of the matrix, the two faces were merged comparing each single pixel in the same position composing the two faces:

$$P_{merged} = max(P_1, P_2) \tag{7.3}$$

where P_{merged} is the final pixel value after merging, while P_1 and P_2 are the pixel value of the two crack faces in the same position after overlapping.

The PU spread was then determined via machine learning as described in Section 7.1.1 by using the Trainable Weka Segmentation [320] plugin and filtering the outliers and misidentified zones. The surface coverage was defined as the quotient of the area with PU over the total area on the final merged image.

7.2 Crack creation and active crack width control

Figure 7.5 shows the average crack width $\bar{w}$ (µm) and the related standard deviation bars measured for the different series. It has to be noted that for all series, 6 specimens were produced and tested. However, for the CEM_S series, one specimen was erroneously broken during the crack creation and for this reason only 5 specimens were available for the crack width measuring and further testing.

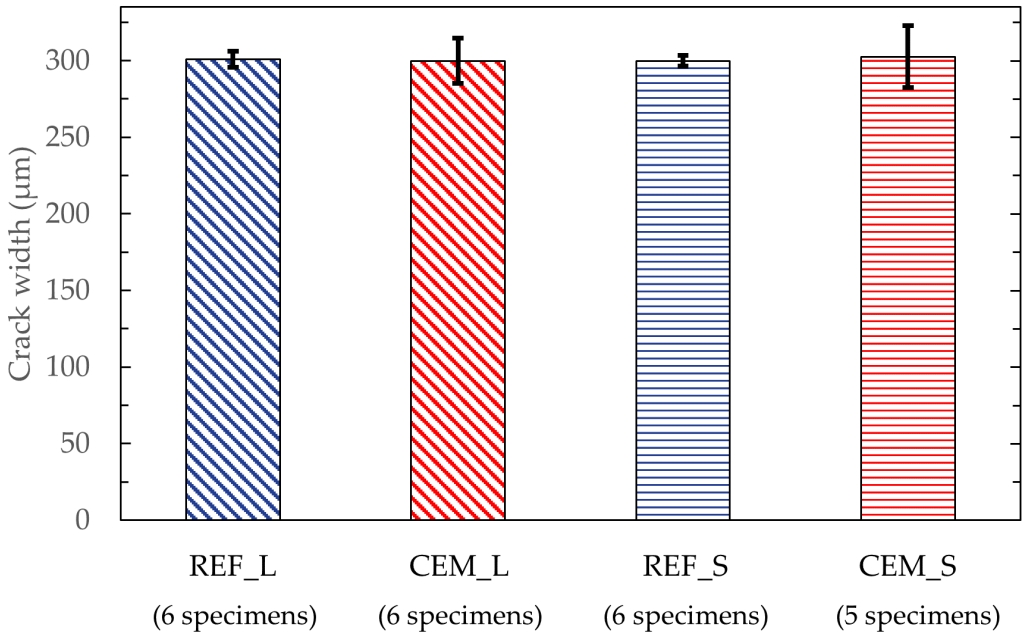

Figure 7.5: Average crack width $\bar{w}$ of each series after the active crack width control (error bars refer to ± one standard deviation).

Overall, the application of the active crack width control technique was successful for obtaining crack widths within the desired range of 290-310 µm. A one-way analysis of variance (ANOVA) test was applied and it showed that the mean crack widths of the different test series were not significantly different from each other (level of significance=0.05, p=0.98), making them comparable in terms of crack width. The same is true considering in the ANOVA test the results of the REF_G and GLASS series (level of significance=0.05, p=0.96), making the 6 series comparable.

Both the reference series were characterized by a very low variability in the crack widths, combined with a clean appearance, that is without many ramifications or loose particles (Figure 7.6a, 7.6e). For the specimen with embedded extruded capsules, it was possible to notice an abundant release of PU, that was clearly visible over the crack mouth (Figures 7.6b). However, the influence of the capsule stiffness caused crack toughening mechanisms such as bifurcation or deviation of the crack path (Figures 7.6c, 7.6d), resulting in a higher variability of the crack widths. It is important to highlight that the young age of the mortar in comparison to the already hardened capsules played an important role and that the cementitious capsules, both for their size and mechanical properties, are much closer to a concrete aggregate, rather than a mortar grain. Hence, it has to expect that it should work better when upscaled to a concrete mix. In the case of the small diameter

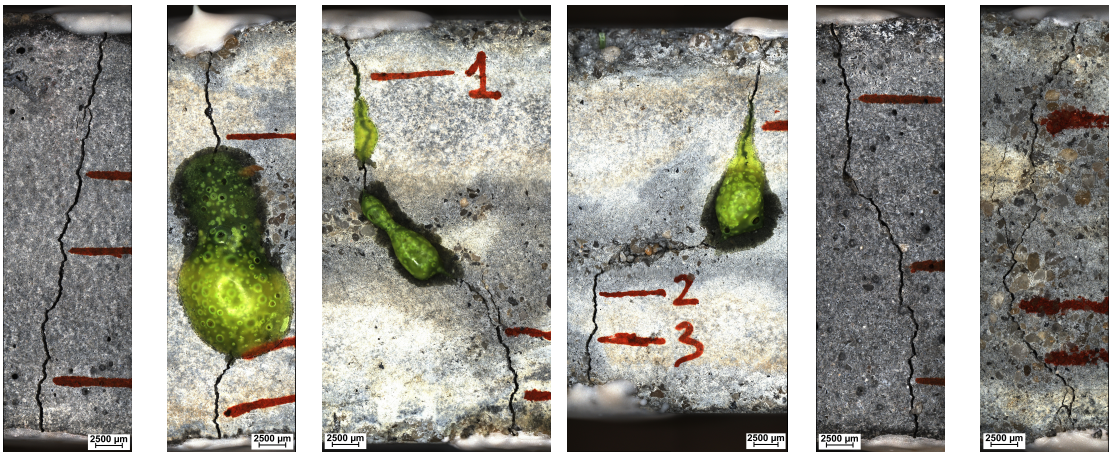

(a) (b) (c) (d) (e) (f)

Figure 7.6: Crack mouths after the active crack width control technique: (a) REF_L series; (b-d) CEM_L series; (e) REF_S series; (f) CEM_S series. The locations used for the crack width measuring are visible.

Table 7.2: Overview of average crack width $\bar{w}$, standard deviation σ_w and coefficient of variation CV_w of each series after the active crack width control.

Series	$\bar{w}$ **(µm)**	σ_w **(µm)**	CV_w **(-)**
REF_G	302	5	2%
GLASS	304	2	1%
REF_L	301	5	2%
CEM_L	300	15	5%
REF_S	300	4	1%
CEM_S	303	20	7%

cementitious capsules, there were again similar issues in the crack development and hence its variability. However, this time it was not possible to observe an external release of polyurethane (Figure 7.6f), presumably due to the smaller quantity of healing agent for each capsule and the higher capillary forces exerted by the capsule.

Table 7.2 summarizes the average crack width $\bar{w}$, the standard deviation σ_w and the resulting coefficient of variation CV of each series after the active crack width control. The highlighted variations are quite small, confirming the efficacy of the active crack width control technique as stated in Chapter 5.

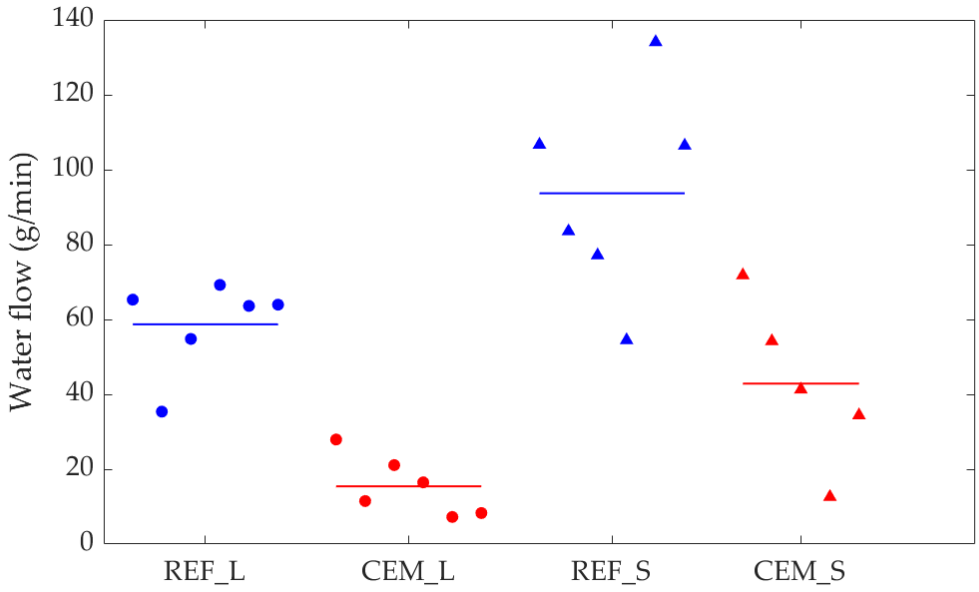

Figure 7.7: Water flow rate q of each series: individual samples results (symbols) and mean value $\bar{q}$ of the series (solid line).

7.3 Water flow test to assess sealing efficiency

After submersion in demineralized water for 1-2 days, the pre-cracked specimens were subjected to the water flow test. Figure 7.7 shows the flow rate q (g/min) measured for the different series.

The good release of PU from the specimens containing extruded capsules (Figure 7.6) resulted in a low measured water flow, as opposed to the higher water flow measured on their corresponding reference specimens. While for the latter a steady and heavy flow was detected once that the specimens were connected to the reservoir, in the majority of the self-healing specimens just a constant slow dripping was visible (Figure 7.8a). As might be expected, the dripping was visible just from the zone of the crack that was not covered by the PU (Figure 7.8b). Consequently, a good sealing efficiency was obtained of about 74% with respect to the corresponding reference specimens. It is interesting to point out the close value of sealing efficiency measured in Section 5.4 using also in that case extruded cementitious capsules with internal coating, the low viscosity PU as healing agent and similar procedures for testing ($SE_{wf} = 79\%$). This result further underlines the importance of repeatable procedures to obtain repeatable results.

In the case of the specimens with the cast-in holes in a lower position, the water flow was overall higher than that of the previous configuration and showed a higher variability. The self-healing specimens containing small capsules showed

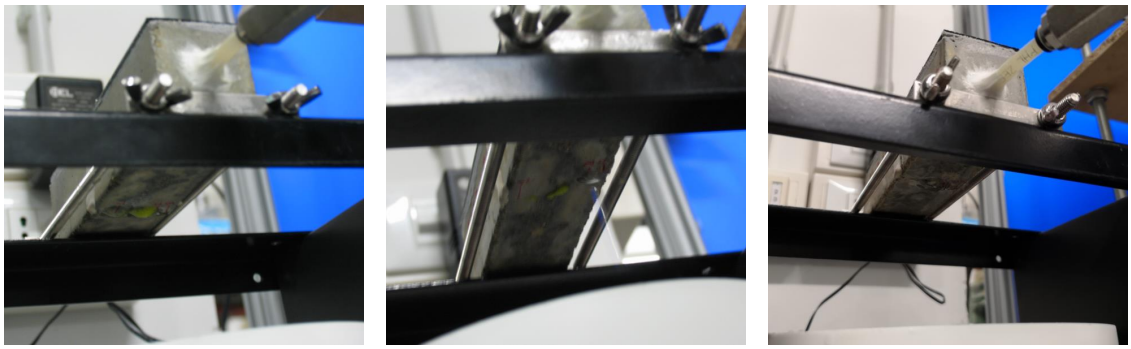

(a) (b) (c)

Figure 7.8: Leakage : (a,b) CEM_L series; (c) CEM_S series

Table 7.3: Overview of average water flow rate $\bar{q}$, standard deviation σ_q, coefficient of variation CV_q, average sealing efficiency SE_{wf} and standard deviation $\sigma_{SE_{wf}}$ of each series after the water flow test.

Series	$\bar{q}$ **(g/min)**	σ_q **(g/min)**	CV_q **(-)**	SE_{wf} **(-)**	$\sigma_{SE_{wf}}$ **(-)**
REF_G	108	19	18%	-	-
GLASS	54	42	78%	50%	39%
REF_L	59	12	21%	-	-
CEM_L	15	8	52%	74%	14%
REF_S	94	28	30%	-	-
CEM_S	43	22	52%	54%	24%

also in this case a water flow lower than that of the corresponding reference specimens and a dripping behavior (Figure 7.8c), compared with the steady flow of the reference specimens. A satisfactory sealing efficiency was assessed, but lower if compared to that of the large capsule specimens. This could be possibly ascribed to a lower release of healing agent, later confirmed by the splitting of the specimens (Section 7.4). Comparing the water flow measured on the specimens of the CEM_L and CEM_S series through a one-way ANOVA test, it was showed that the means of the two test series were significantly different from each other (level of significance=0.05, p=0.02).

Table 7.3 summarizes the results of the water flow test, including both the results using glass and cementitious capsules with their respective reference specimens.

Comparable coefficients of variation for the CEM_L and CEM_S series were obtained, as well as those of their reference specimens. Comparing the coefficients of variation on the crack width (Table 7.2) and on the water flow (Table 7.3) it is possible to notice that even with low variability on the crack width, the variation

on water flow is almost an order of magnitude higher, as reported in literature [41]. Indeed, Edvardsen [56] stated that the permeability of a crack is related to the third power of the crack width, hence also small variability on the crack width will result in higher variability on the permeability. Moreover, permeability is strongly affected also by the internal geometry of the crack, on which no control can be exerted [19, 41].

The best results were obtained using the extruded cementitious capsules (CEM_L series), which also present the lower variability in terms of sealing efficiency.

Similar to the consideration of the comparable results between the use of extruded cementitious capsules in the present Section and in Section 5.4, the same can be said for the CEM_S (SE_{wf} = 54%) and GLASS (SE_{wf} = 50% series, which were tested with the same setup (i.e. position of the cast-in-hole and of the capsules). This was confirmed by applying a one-way ANOVA test on the two series, which showed that the mean water flows of the different test series were not significantly different from each other (level of significance=0.05, p=0.60). These similar results are most likely dependent from the similarities of the two self-healing systems, which presented comparable internal diameter, length, and volume of cargo healing agent, resulting in similar release mechanisms and consequently sealing efficiency.

7.4 Visual examination of healing agent on the crack surfaces

After performing the water permeability test, the specimens were split at the location of the crack to analyze the spread of the healing agent. Figure 7.9 shows the example of two specimens from the two self-healing series (CEM_L and CEM_S) after splitting and segmentation of the PU to identify the spreading of the healing agent on the crack faces.

After binarization, the area covered by PU was compared to the total area of the crack face, including the area occupied by the capsules and the hole for the water flow test. An average surface coverage of 13.1% for the CEM_L series and of just 2.4% for the CEM_S series was obtained. For what concern the surface coverage obtained for the GLASS series using the procedure described in 7.1.1, an average surface coverage of 47.2% was calculated.

From the visual observation of the crack faces and the result obtained in the surface coverage of the CEM_S series, it is clear that they suffered from a high capillary action that did not allow a good releasing of healing agent. This is a useful indication for the improvement of the system, that will probably benefit from a slightly change in the capsules dimensions. Moreover, when using small diameter cementitious capsules, the use of a polyurethane precursor with a higher expansion rate of the foam, hence a higher production of CO_2, would further help to

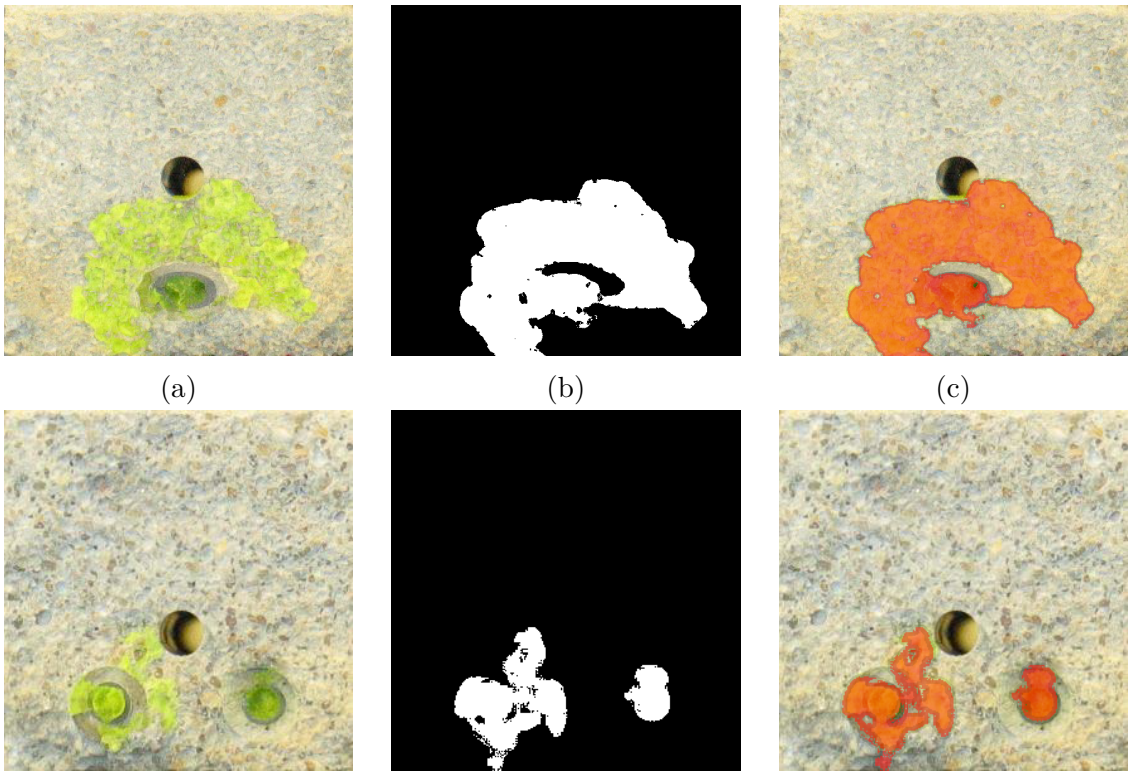

Figure 7.9: Process of segmentation of one specimen from the CEM_L (a-c) and the CEM_S (d-f) series: (a,d) overlay of the two crack faces; (b,e) picture after segmentation, binarization and removal of the outliers; (c,f) area of the spread PU overlapped on the crack face.

boost the healing-agent release. A clear example of this was provided in Chapter 6 where the use of a highly expansive polyurethane precursor allowed a visible leakage of PU.

Another aspect to be pointed out is that, while the sealing efficiency measured through water flow test for the CEM_L series and the PUR_INT series in Chapter 5 were similar (respectively 74% and 79%), the average surface coverage was different (respectively 13.1% and 36%). The same can be said for the CEM_S series and the GLASS series, which also presented similar sealing efficiency (respectively 54% and 50%) with a striking difference in the average surface coverage (respectively 2.4% and 47.2%).

Consequently, it can be concluded that a higher surface coverage does not necessarily translate into a better sealing efficiency. This can be seen for example in Figure 7.10 where it is possible to observe the crack faces of a specimen from the GLASS series. Even though the spreading of the PU on the crack faces is visible,

Figure 7.10: Crack faces after splitting of a specimen from the GLASS series.

it is possible to observe an empty zone below the cast-in hole that should have allowed the leakage of water from the crack mouth.

Therefore, unless the healing agent provided is sufficient to seal the crack mouth or to seal all the possible paths for the water to leak out of the specimen, the water flow will be possibly slowed down but not stopped. This highlights the importance of how the healing agent is spread, other than the area covered by the polyurethane itself.

7.5 Conclusions

In this chapter, the self-healing performances obtained with cementitious capsules filled with a polyurethane precursor were compared with those obtained using glass capsules filled with the same healing agent. This comparison was performed by applying an inter-laboratory testing procedure developed in the framework of the EU COST Action SARCOS, which involved six European Universities including Politecnico di Torino. The use of such testing procedure offered the advantage of adopting a shared good practice and consequently making the results easily comparable and reproducible.

Two series of self-healing mortar prisms were produced: one with a single large capsule manufactured by extrusion and comparable to those used in Chapter 5, the other with two smaller capsules manufactured with the rolling procedure developed in the framework of this thesis. The latter were comparable with the glass capsules

used in the inter-laboratory testing in terms of internal diameter and volume of cargo healing agent.

The application of the active crack width control technique allowed the reduction of variability in the crack width, as already mentioned in Chapter 5. The water flow testing showed positive results in terms of sealing efficiency for both the series. The best average result was shown by the use of the specimens containing a single cementitious capsule, which allowed to obtain a reduction of 74% in terms of water flow rate with respect to the average water flow measured on the reference series without capsules. Positive results were obtained also for the series using the smaller diameter capsules, with an average reduction in the order of 54%. In general, cementitious capsules offered comparable or better performance with respect to glass capsules, for the same healing agent type and content. Specifically, the average sealing efficiency for the glass macro-capsules was equal to 50%.

The analysis of the spreading region of the healing agent on the crack surfaces did not show a strong relationship between the surface coverage and the water flow rate, highlighting that a high surface coverage does not guarantee a crack sealing as long as the possible pathways for the water leakage are stopped by the healing agent. Moreover, the visual inspection suggested that a higher capillary action was exerted by the smaller diameter capsules on the release of the healing agent. This is a useful indication to design the system modifying its dimensions (i.e., length and internal diameter) to allow a reduction in the capillary action. Moreover, using healing agents with a lower viscosity, or with a higher expansion in the case of foaming agents, would improve their release and filling of the crack.

Finally, it can be observed that when applying the SARCOS protocol to test specimens with a single macro-capsule containing the same amount of polyurethane, substantially the same results are obtained in different repetitions of the test. Indeed, the results shown in this chapter and in Chapter 5 highlighted an average sealing efficiency respectively of 74% and 79% for comparable capsule configurations. This result further contributes to validate the robustness of the SARCOS protocol.

Chapter 8

Self-healing efficiency: durability and mechanical properties recovery

The activities described in this chapter concerned the definition of the *final self-healing system* and the demonstration of its full self-healing capacity, hence the possibility to obtain the recovery of both durability-related and mechanical properties.

The self-healing system was manufactured taking in consideration the inputs provided by the intermediate steps of the research, which are reported in the previous chapters. For this reason, it was decided to use the newly manufactured rolled capsules, which allows a higher control over the capsule dimensions (Chapter 3), by increasing their internal diameter after the evidence of capillary action in Chapter 7. As it was decided in Chapter 5, it was decided to use a polyurethane precursor for the good sealing efficiency offered by this type of healing agents (Chapters 4, 5 and 7). Namely, it was decided to use the highly expansive polyurethane precursor for its good tested performances (Chapters 4 and 6) and to boost the release of the healing agent.

For the purpose of characterizing the recovery of durability-related properties, the final system was first pre-cracked and then investigated through two types of water flow tests after autonomous healing. The first water flow test is well-established in literature and was used also in the previous chapters. The second one was developed during this study to provide stricter testing conditions and check the system performance in comparison with the previous water permeability test. Subsequently, the mechanical recovery offered by the final system was investigated through static reloading of the healed system. A visual analysis of the crack faces was also carried out to estimate the spreading of the healing agent on the crack faces to complement the previous characterizations.

Table 8.1: Summary of the characteristics of capsules used for the different series.

		CEM_A & CEM_B
Manufacturing process		Rolling
Mix design		Mix design 2
Surface of the tubular shell coated with epoxy		Internal
Average internal diameter of the tubular shell	(mm)	6
Average external diameter of the tubular shell	(mm)	8.5
Average length of the capsule	(mm)	50
Average thickness of the epoxy coating	(mm)	1
Average internal diameter after epoxy coating	(mm)	4
Volume of cargo healing agent	(mL)	≈0.7

8.1 Materials and Methods

8.1.1 Mortar prisms

Unreinforced mortar prisms (40×40×160 mm^3) were cast using standardized mortar mix composition, as described in EN 196-1. Ordinary Portland cement (CEM I 42.5 N, Buzzi Unicem S.p.A., Italy), normalized sand (grading 0-2 mm, DIN EN 196-1), and tap water were used. The water to cement ratio was 0.50, the sand to cement ratio was 3.

Cementitious capsules were used, manufactured using the rolling procedure (Φ_{ext} =8.5 mm, Φ_{int} =6 mm) as described in Chapter 3. The internal diameter was slightly incremented to reduce the capillary action exerted by the capsule, as described in Chapter 7. An epoxy coating was applied only internally (see Section 3.2), with a thickness of about 1 mm, reducing the internal diameter of the capsules to 4 mm. The length of the capsules was chosen equal to 50 mm. The capsules were filled with a syringe with the highly expansive polyurethane precursor (CarboStop U, Orica), described in Section 3.4.2 and used in Chapters 4 and 6, limiting the amount of entrained air. After sealing, the capsules were further coated with sand to improve the bonding with the surrounding matrix. The main characteristics of the cementitious capsules are summarized in Table 8.1.

Two self-healing series of specimens were produced, both containing two capsules at a height of 10 mm above the bottom side of the specimen (Figure 8.1): one was provided with the cast-in-hole required for the water flow test described in Sections 5 and 7 at a depth of 15 mm from the top side of the specimen (CEM_A series, 6 specimens, Figure 8.1a), one without the cast-in-hole (CEM_B series, 6 specimens, Figure 8.1c). Reference specimens without capsules were produced for both the series (REF_A series, 6 specimens, Figure 8.1b; REF_B series, 6 specimens, Figure 8.1d). For all the specimens, a cast-in U-shaped notch measuring 4 mm in width and 4 mm in height was provided in the molds.

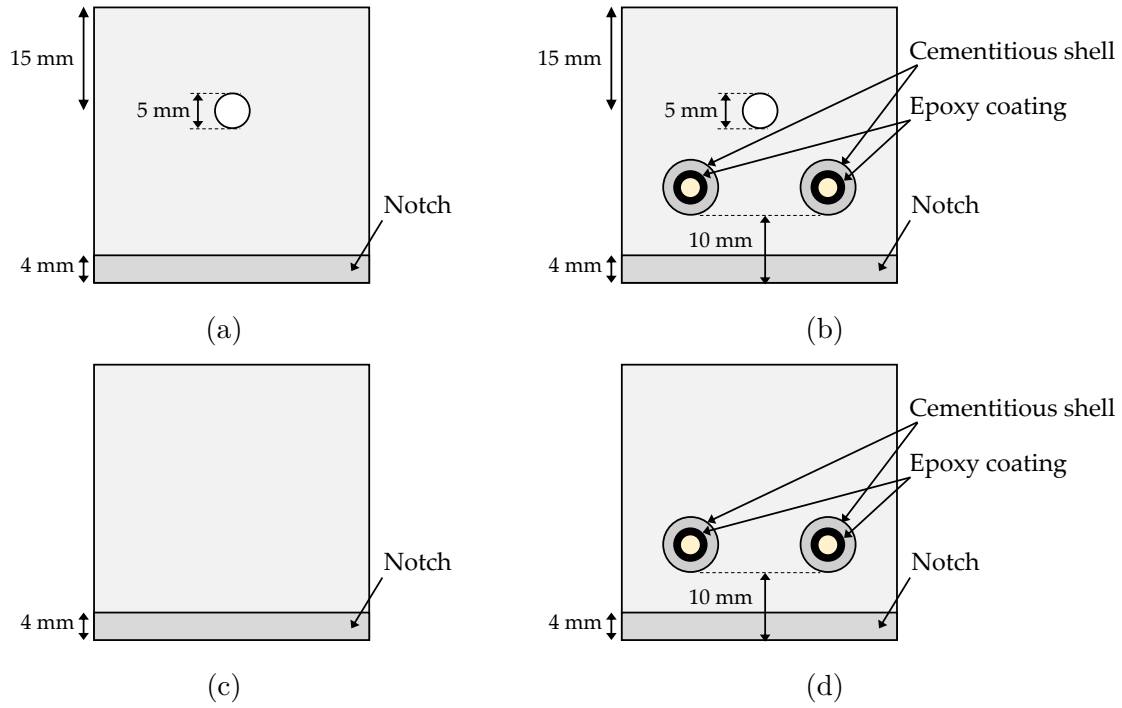

Figure 8.1: Schematic cross section of the specimens: (a) without capsules and with cast-in-hole, REF_A series; (b) with two rolled capsules and with cast-in-hole, CEM_A series; (c) without capsules and no cast-in-hole, REF_B series; (d) with two rolled capsules and no cast-in-hole, CEM_B series.

Upon casting, the specimens were covered with plastic foil. After 24 hours, the specimens were demolded, the oiled bars used to obtain the cast-in-hole removed, and the specimens were wrapped in plastic foils for 14 days.

8.1.2 Pre-cracking

In order to evaluate the effectiveness of the autonomous self-healing system, a controlled localized crack was first induced in the specimens using a mechanical pre-cracking procedure as in Chapter 6. It was decided to not use the active crack control technique used in Chapters 5 and 7, since the experiences with the use of the highly expansive PU precursor (Chapters 4 and 6) suggested that it would have posed some issues, such as the fast coverage of the crack mouth by the expansion of the PU foam that would not allow the iterative measurement and restriction, and the risk to cause a too high expansion of the foam during the sudden crack creation due to the back-pressure (see Section 3.4.2).

At an age of 14 days from casting, all the specimens were pre-cracked via a crack-width controlled three-point bending test with a span of 10 cm using a 250

kN closed-loop servo-controlled MTS hydraulic press (MTS 810, MTS Systems Corporation, USA) equipped with a digital controller (FlexTest® 40, MTS Systems Corporation, USA). It was possible to control the crack mouth opening displacement (CMOD) by using a strain-gauge-based displacement transducer (DD1, range ± 2.5 mm, HBM, Germany) mounted on the bottom face of the specimen upon the notch.

The test was conducted by imposing a CMOD rate of 1.5 µm/s. Upon reaching a maximum value of 800 µm, the specimens were unloaded at the same CMOD rate. The target value for the maximum CMOD was set at 800 µm in order to test the ability of the system to heal large cracks. The CMOD and load were recorded throughout the execution of the test.

Immediately after pre-cracking, the specimens were stored in a curing cabinet (T = 20 °C, 60% RH) for three weeks. Two supports with a span of 10 cm allowed to keep the specimens in the same geometric configuration during pre-cracking, with their bottom face pointing downward. The duration of the curing cabinet conditioning definitely exceeded the time required for the PU to react with air humidity and form a rigid foam, ensuring that the healing agent released from the capsules during pre-cracking was fully cured.

8.1.3 Water flow tests

Water flow via cast-in-hole

The water permeability of the series CEM_A was measured using the same water flow test and the same procedures described in Chapters 5 and 7. To connect the specimens to the water flow setup, the cast-in hole was enlarged to a diameter of 6 mm over a length of 25 ± 5 mm using a drill. This was done prior to cracking to prevent the vibrations from influencing the crack. A short plastic tube (length of ±60 mm, $\Phi_{external}$ 6 mm, $\Phi_{internal}$ 4 mm) was then inserted in the cast-in hole and sealed using silicone. Also the other side of the cast-in hole was sealed completely with silicone. Before testing, specimens were submersed in demineralized water for 24 hours to prevent the influence of water absorption by the matrix on the results. In order to measure only the water leaking out of the crack mouth, the sides of the specimens were sealed prior to saturation using silicon sealant. Figure 8.2 shows the test setup for the water flow test.

The first 60 seconds of water leakage were not recorded in order to measure only a fully developed flow and to allow the removal of water bubbles from the system. Subsequently, the weight of the water which leaked from the crack was recorded for a minimum of 6 minutes.

The sealing efficiency $SE_{wf,h}$ of the self-healing specimens containing cementitious capsules and the cast-in-hole was calculated with respect to the reference specimens, without capsules and with the same cast-in-hole configuration, using

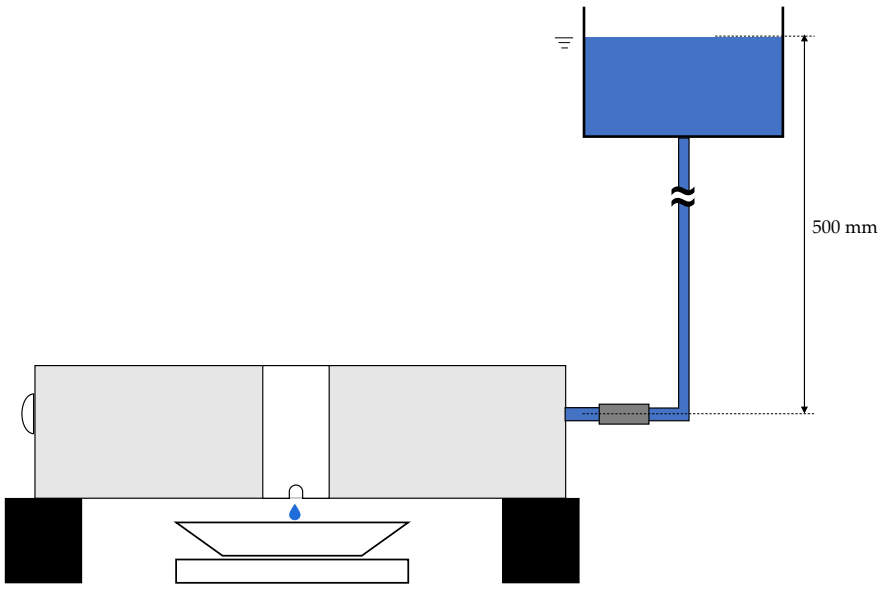

Figure 8.2: Test setup for the water flow test using the cast-in-hole.

Equation 8.1:

$$SE_{wf,h}\,(\%) = \frac{\bar{q}_{REF\_A} - \bar{q}_{CEM\_A}}{\bar{q}_{REF\_A}} \times 100, \tag{8.1}$$

where $\bar{q}_{REF\_A}$ is the average water flow rate (g/min) of the reference specimens and $\bar{q}_{CEM\_A}$ is the average water flow rate (g/min) of the self-healing specimens.

Water flow via funnel

Other than the water flow test widely used throughout this research study, other permeability tests aimed at investigating the amount of water passing through a crack in order to assess the healing efficiency using water pressure as driving force were developed during years. Some were based on measuring the water drop in a reservoir connected to the crack [21, 57, 71, 200, 292, 325, 326], other researchers determined the permeability by monitoring the weight of the leaked water instead of the water drop, keeping the hydraulic water head constant (i.e. constant pressure) [83, 295] or through pressurized water ingress [104, 120, 327].

Drawing inspiration from the literature and the quick water permeability assessment test described in Chapter 4, a new testing procedure is here presented. The idea behind the development of a new water permeability test was to provide comparisons to other types of water permeability tests by using stricter testing conditions that could confirm or disprove results that could depend on the testing

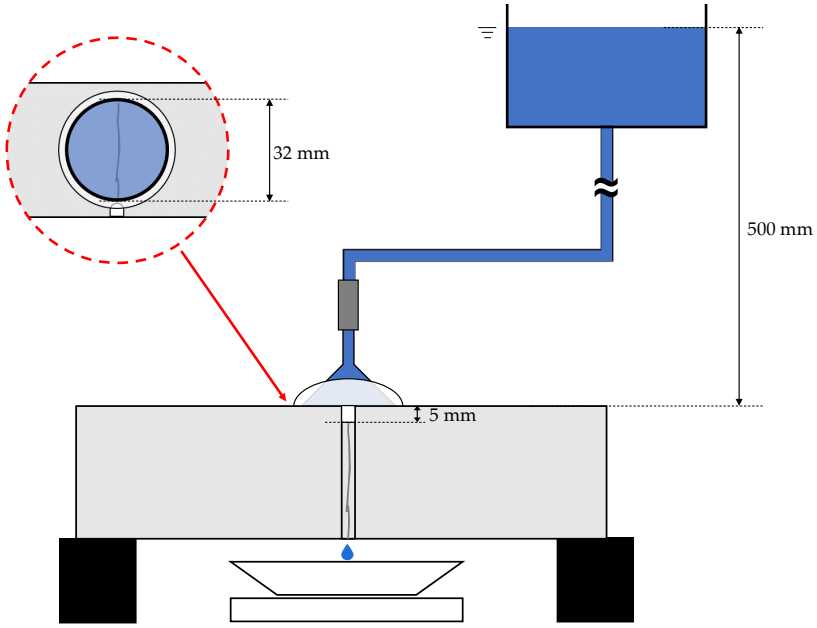

Figure 8.3: Test setup for the water flow test using the laterally glued funnel.

condition rather than the effective sealing. At the same time, the developed test should be easily applicable to commonly used specimens.

It was chosen to develop a constant head test to be applied on prismatic specimens in order to compare the procedure with the results obtained by the water flow test using the cast-in-hole, which is a test that was thoroughly investigated during this research activity and in literature [41, 120, 124, 189]. Moreover, the constant head test has been often applied for specimens having a relatively large crack width [295, 328], which is the crack width investigated throughout this study and usually addressed by autonomous encapsulated systems.

After crack creation and the healing agent curing, the prismatic specimens were turned by 90 degrees. A plastic funnel with an internal diameter of 32 mm was positioned on the lateral surface of the specimen, tangent to the notch tip, so that all the crack on the lateral face was contained in the funnel area. The interface between the funnel side and the surface of the specimen was sealed with silicone, as well as the first 5 mm of the crack mouth below the funnel. This was done to prevent edge effects. The funnel was then connected to a tube in contact with an open water reservoir. The water head, measured from the base of the funnel up to the water level, was kept constant throughout the test at 50 ± 2 cm by topping up with demineralized water, in order to maintain a constant pressure (≈ 0.05 bar) equal to the one used for the previous water flow test. Figure 8.3 shows the test setup used for the water flow test.

Before testing, specimens were submersed in demineralized water for 24 hours

to prevent the influence of water absorption by the matrix on the results. Also in this case, the first 60 seconds of water leakage were not recorded in order to measure only a fully developed flow and to allow the removal of water bubbles from the system. Subsequently, the weight of the water which leaked from the crack was recorded for a minimum of 6 minutes.

The stricter condition of the testing is represented by the fact that the water could leak from different directions, namely from the crack mouth or from the lateral side of the crack opposite to the one with the funnel, requiring a sealing that could stop the leakage from both directions.

The sealing efficiency $SE_{wf,f}$ of the self-healing specimens containing cementitious capsules and the sealed funnel was calculated with respect to the reference specimens, without capsules and with the same configuration, using Equation 8.2:

$$SE_{wf,f}\,(\%) = \frac{\bar{q}_{REF\_B} - \bar{q}_{CEM\_B}}{\bar{q}_{REF\_B}} \times 100, \tag{8.2}$$

where $\bar{q}_{REF\_B}$ is the average water flow rate (g/min) of the reference specimens and $\bar{q}_{CEM\_B}$ is the average water flow rate (g/min) of the self-healing specimens.

8.1.4 Quasi-static reloading

After the water flow test, the silicone used to seal the lateral side of the specimens (CEM_A series) or the funnel side (CEM_B series) was completely removed and the recovery of the mechanical properties was evaluated by assessing the load-bearing capacity under static conditions as in Chapters 4 and 6.

The specimens from each series were statically reloaded following the same procedure described in Section 8.1.2 for pre-cracking.

The mechanical recovery was evaluated through a load recovery index (LRI), expressed as a function of the maximum load-bearing capacity of the specimens during pre-cracking (L_{peak}) and reloading (L_{reload}) and as a function of the residual load-bearing capacity at the end of pre-cracking (L_{unload}). Its definition is reported in Equation (8.3):

$$LRI(\%) = \frac{L_{reload} - L_{unload}}{L_{peak} - L_{unload}}, \tag{8.3}$$

8.1.5 Visual examination of the healing agents in the crack

After reloading, the self-healing specimens were split at the location of the crack to determine the healing agent coverage [15, 29, 30, 39, 293]. Pictures were taken from both crack faces of each specimen. The crack faces were overlapped using the open source software GIMP [324] and the open source software ImageJ, distribution Fiji (version 1.52) [321]. One crack face was flipped horizontally and overlapped to

the other face to have a correct matching of the side of the crack faces and, for the CEM_A series, the cast-in-hole.

The PU spread was then determined via machine learning as described in Section 7.1.1 by using the Trainable Weka Segmentation [320] plugin and filtering the outliers and misidentified zones using MATLAB.

The surface coverage was defined as the quotient of the area with PU over the total area on the final merged image. Also, the moment of inertia of the area covered by polyurethane was defined using a MATLAB algorithm to define the horizontal centroidal axis of the section and to divide the entire area covered with PU in n sub-areas a_i (mm^2). The moment of inertia I (mm^4) was then defined as:

$$I = \sum_{i=1}^{n} a_i \cdot y_i^2 \tag{8.4}$$

where y_i (mm) is the distance between the sub-areas a_i and the horizontal centroidal axis.

8.2 Pre-cracking

At an age of 14 days, all specimens from each series (REF_A, CEM_A, REF_B, and CEM_B), namely 6 specimens per series for a total of 24 specimens, were pre-cracked via the controlled three-point-bending test described in Section 8.1.2.

Figure 8.4 shows the load versus CMOD curves recorded during the tests for the different series.

The specimens were unloaded upon reaching a CMOD of 800 µm as it was done in Chapter 6, with a small CMOD decrease due to recovery of the elastic deformation. The series without capsules showed a repeatable behavior, apart some difference for the specimen REF_B_6 (Figure 8.4c) which presented some damages in the demolding phase. Moreover, the maximum bearing capacity of the REF_B series was slightly higher, due to the fact that the cross section of the REF_A series was reduced by the presence of the cast-in hole.

While both the reference series showed a continuous and gradual advancement during the softening phase, the self-healing series showed sudden load drops during this phase. As mentioned in Chapter 6, these drops are caused by the capsules breakage and were accompanied by an audible acoustic energy release, as shown also in literature [26, 32, 307].

For the series CEM_A these drops were more scattered, while the CEM_B series showed a more repeatable mechanical behavior and the drops were detected for a CMOD smaller than 160 µm. A further evidence of the relationship between the load drops, the audible sound, and the capsules breakage was that they were followed by leakage of the foaming polyurethane in the crack, apart the case of the specimen CEM_B_6 which showed just a small trace of PU from one lateral side

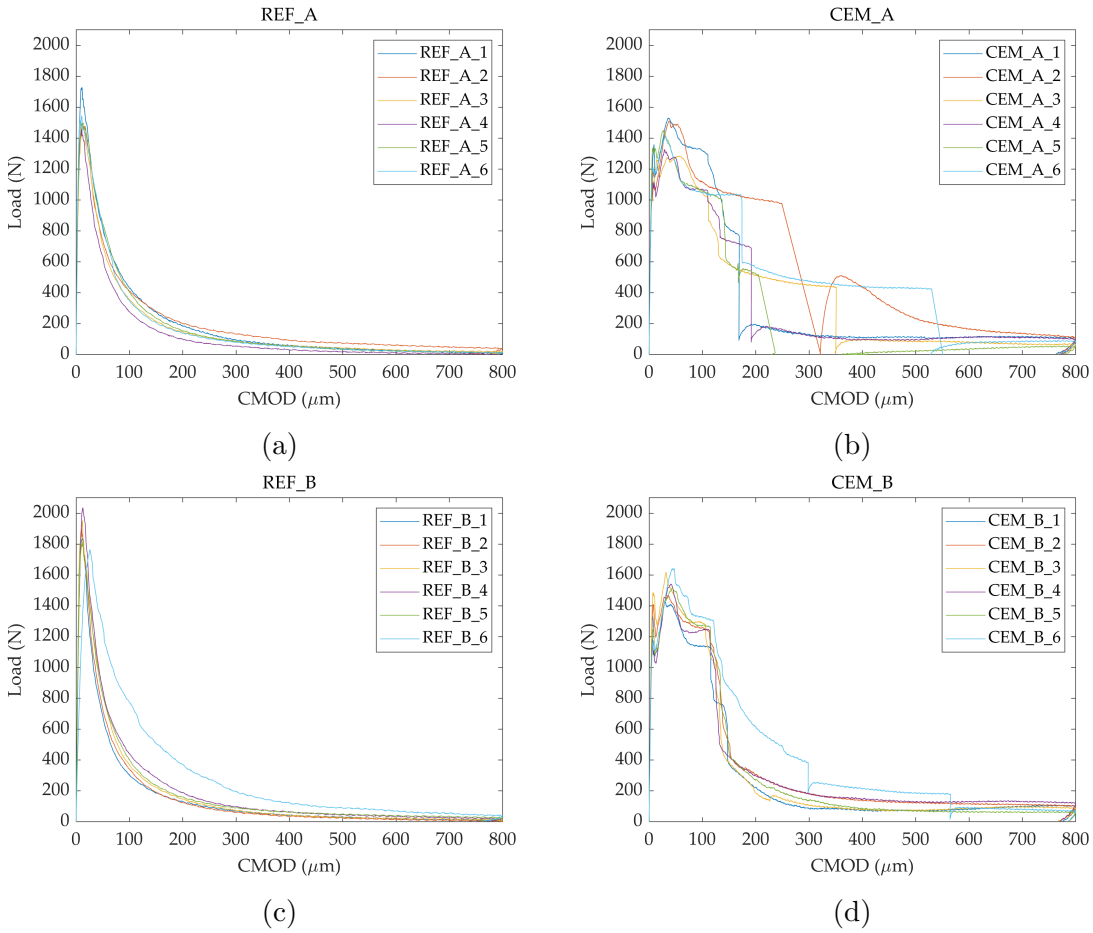

Figure 8.4: Load versus CMOD curves due to pre-cracking: (a) REF_A series; (b) CEM_A series; (c) REF_B series; (d) CEM_B series.

of the specimen. Moreover, also its mechanical behavior and the load drops differed from the other specimens, as showed in Figure 8.4d.

In order to assess the effect of the presence of the capsules on the maximum load bearing capacity, the peak load L_{peak} of the specimens with and without capsules in the same configuration (with or without cast-in hole) were compared and the reduction of the load-bearing capacity $L_{reduction}$ was defined as:

$$L_{reduction} = \frac{\bar{L}_{peak,REF\_i} - \bar{L}_{peak,CEM\_i}}{\bar{L}_{peak,REF\_i}}, \tag{8.5}$$

where $\bar{L}_{peak,REF\_i}$ is the average load-bearing capacity L_{peak} calculated over the 6 specimens of each reference series without capsules and $\bar{L}_{peak,CEM\_i}$ is the average load-bearing capacity L_{peak} calculated over the 6 specimens of each self-healing series. i indicates either the A or B that identifies the specimen configuration. The

Table 8.2: Overview of the average L_{peak} and L_{unload} (with respective standard deviation) and $L_{reduction}$ for each series (6 specimens per series) after the pre-cracking procedure.

Series	$\boldsymbol{L_{peak}}$ **(N)**	$\boldsymbol{L_{unload}}$ **(N)**	$\boldsymbol{L_{reduction}}$ **(%)**
REF_A	1535 ± 99	17 ± 12	-
CEM_A	1420 ± 99	88 ± 23	7.5
REF_B	1886 ± 99	18 ± 14	-
CEM_B	1536 ± 83	91 ± 20	18.5

percentage reductions were equal to 7.5% for the CEM_A series and slightly higher for CEM_B series, where it was equal to 18.5%.

Table 8.2 summarizes the results of the pre-cracking phase.

Immediately after pre-cracking, the specimens were stored in a curing cabinet (T = 20 °C, 60% RH) for three weeks. During this time, when the PU foam was hardened, the pictures of the crack mouths of all the specimens were acquired with a stereo microscope (Nikon SMZ18, Nikon, Japan) in order to define their width. The pictures of all the specimens' crack mouths of the series REF_A and CEM_A are shown in Figure 8.5 while those of the series REF_B and CEM_B are shown in Figure 8.6.

From the picture it was clear that the crack mouths of the self-healing specimens were well sealed by the hardened PU foam, apart the specimen CEM_B_6 (Figure 8.6l), which did not show a good release of PU as mentioned above.

The crack width of the REF specimens was measured using the open source software ImageJ, distribution Fiji (version 1.52) [321], and was defined as the average of 16 linear measurements equally spread across the entire length. On the contrary, due to the presence of the PU, it was impossible to measure the crack width of the CEM series, apart for the above-mentioned specimen that did not show PU leakage and a small visible zone of the specimen CEM_A_2 (Figure 8.5h). The results of the crack width measurements on the reference series with their standard deviations are reported in Figure 8.7.

The specimen REF_B_2 showed a much higher value and variability along the crack if compared to the other specimens. This caused effects that will be discussed in the following Section. Excluding this unusual value, the two series showed an average crack width of (322 ± 44) µm for the REF_A series and (311 ± 42) µm for the REF_B series. The measurement on the CEM_A_2 and CEM_B_6 resulted in values equal to (513 ± 23) µm and (563 ± 14) µm, respectively. This difference in term of crack width was most likely caused by the fact that, while the reference series could recover some elastic deformation while being unloaded since they did not have any reinforcement, the presence of the capsules and the PU foam should have caused some locking effect that maintained the cracks more open.

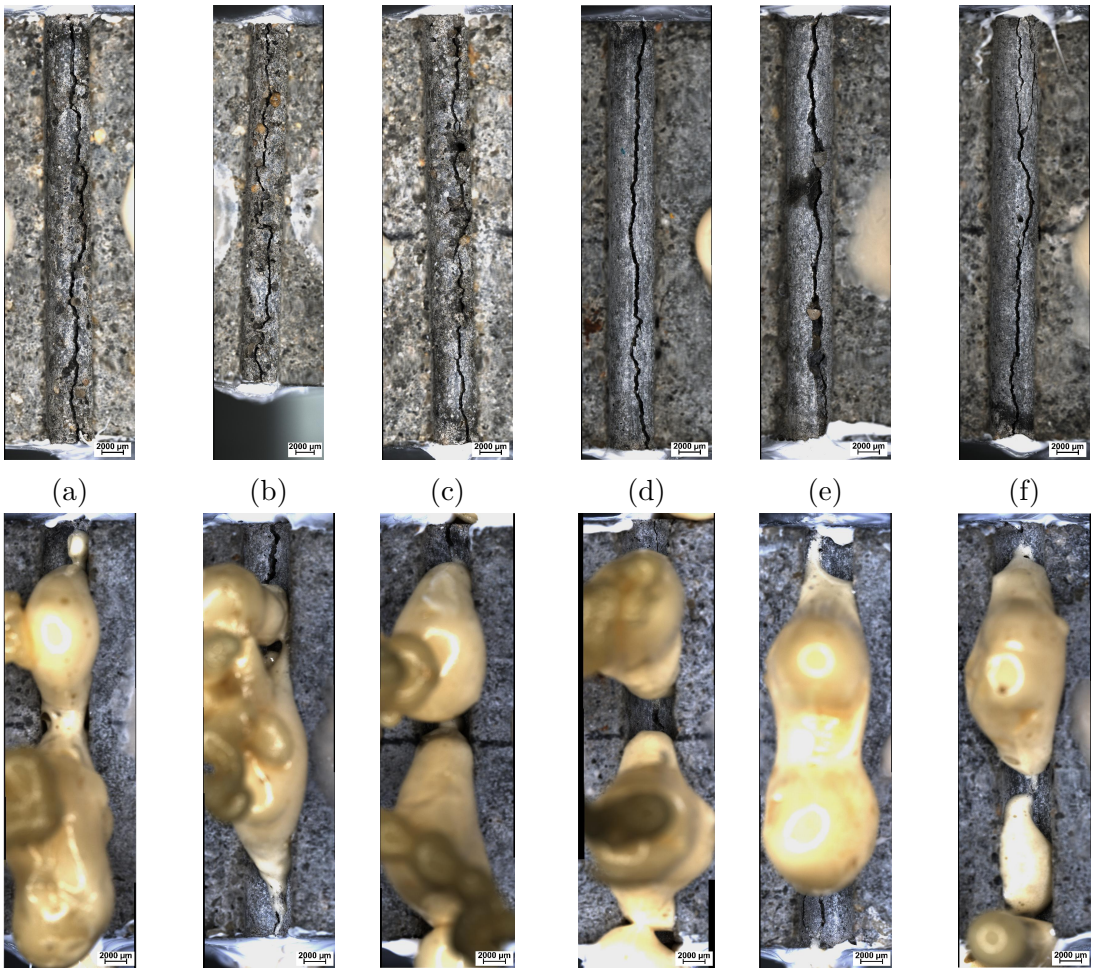

Figure 8.5: Crack mouth of the all specimens acquired through the stereo microscope: (a-f) REF_A series; (g-l) CEM_A series.

8.3 Water flow tests

Before submerging the specimens in demineralized water, the pre-cracked specimens were prepared for the test. The lateral sides of the specimen with the cast-in hole were sealed with silicone, while for the series without it, the funnel was glued on one of the lateral faces using silicone, as can be seen in Figure 8.8.

After preparing the specimens, pictures of the lateral faces opposite to the ones with the funnel were acquired using the stereo microscope (Figure 8.9).

The specimen REF_B_2 presented a much larger crack width (Figure 8.9b) as already mentioned for the crack mouth. However, it was decided to test it. Also, the lateral view of the CEM_B_6 did not show any PU leakage (Figure 8.9l). The

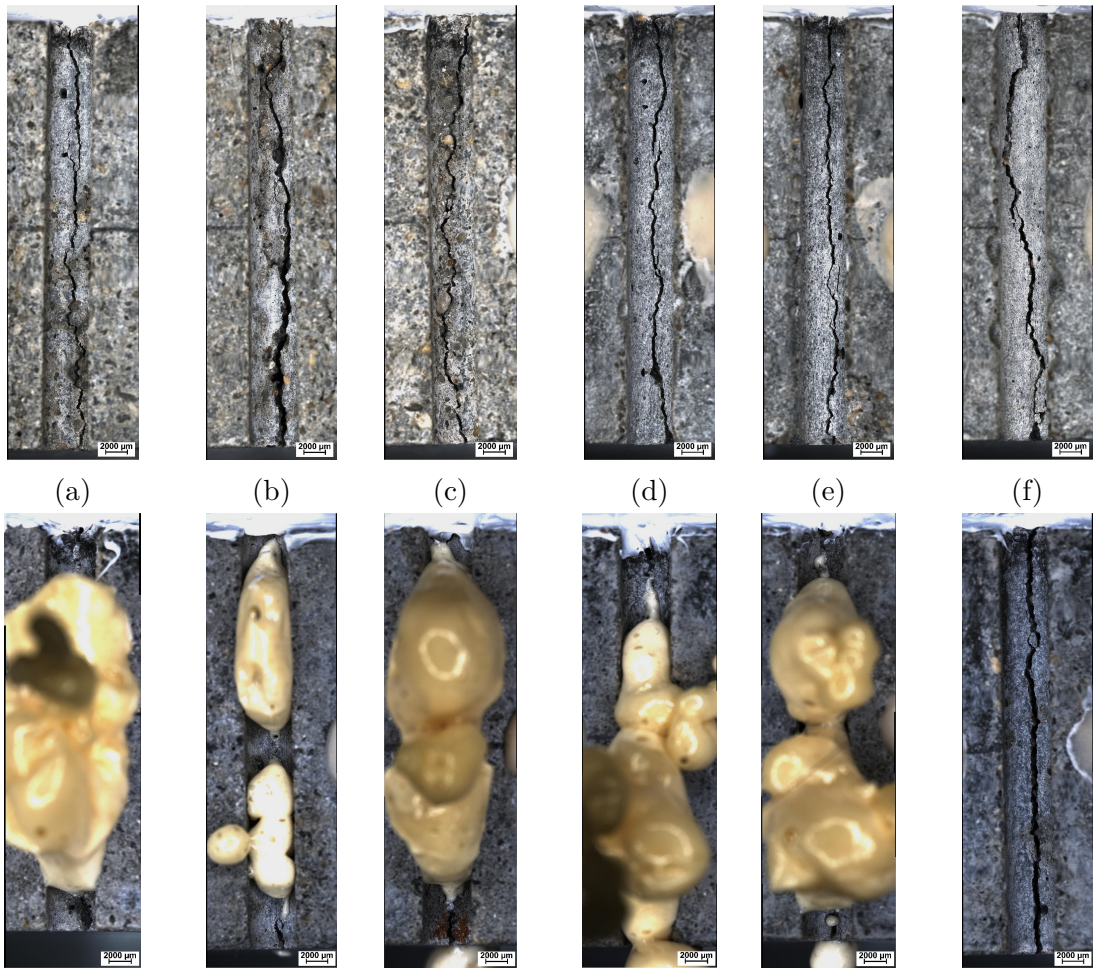

Figure 8.6: Crack mouth of the all specimens acquired through the stereo microscope: (a-f) REF_B series; (g-l) CEM_B series.

pictures of the lateral crack were not used to measure the width since it changes along the height of the specimen. However, they served to confirm that the crack height was comparable to the funnel diameter and that the specimens were kept together just by a small ligament.

After 24 hours of submersion in demineralized water to exclude the matrix absorption contribution, the excess water on the surface was wiped with a wet cloth and the specimens were connected to the setup through the tube in the cast-in hole or the plastic funnel as in Figure 8.10.

After the first 60 seconds from the connection to the water reservoir, the next 6 minutes of water leakage were recorded with the automatic scale and used to calculate the water flow rate of each specimen. Figure 8.11 shows the results in

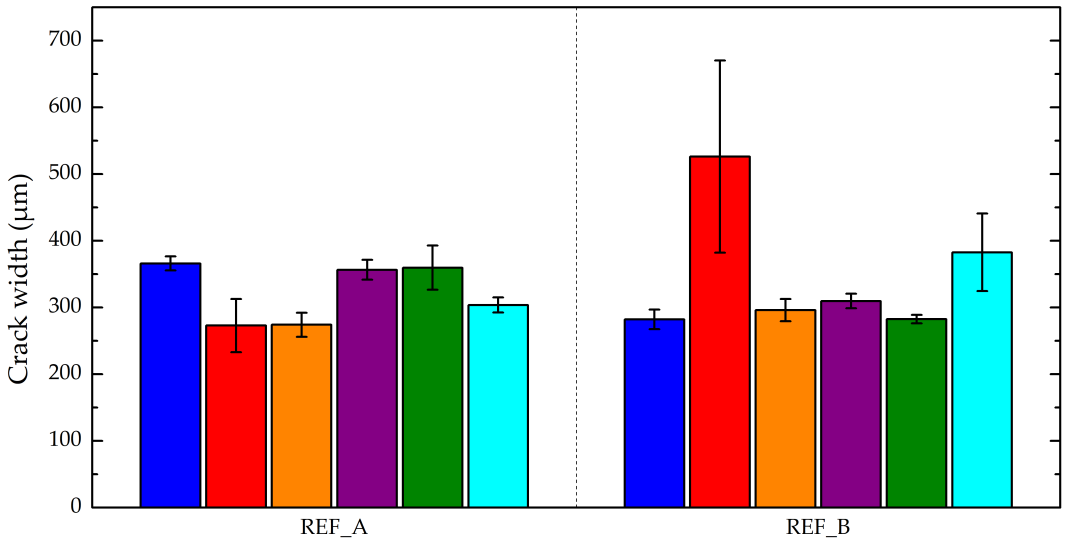

Figure 8.7: Average crack width of each specimen of the REF_A and REF_B series (error bars refer to ± one standard deviation).

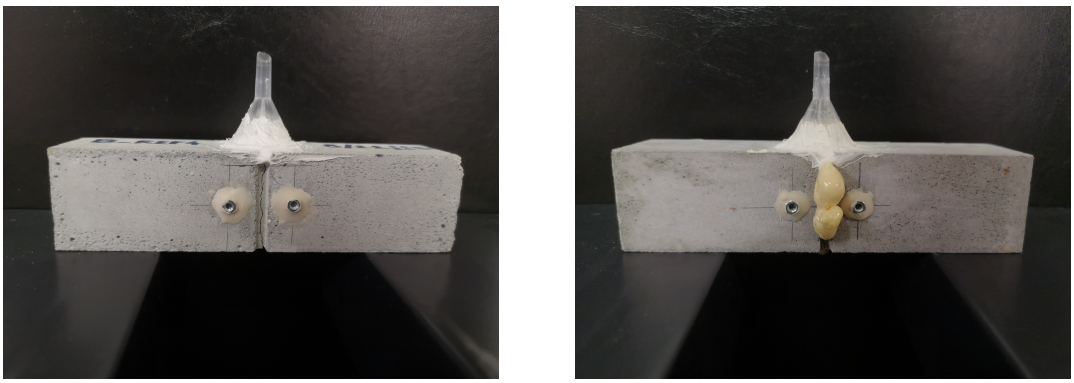

(a) (b)

Figure 8.8: Specimens prepared for the water flow test using the funnel: (a) reference specimen without capsules (REF_B series); self-healing specimen with visible PU foam leakage (CEM_B series).

terms of water flow rate of each specimen overlapped by the box plots of each series. The limits of the box represent the 25th and 75th percentile while the line inside the box represents the 50th percentile. The whiskers extend up to the value not considered as outliers (Upper Limit = 75th Percentile + Interquartile Range; Lower Limit = 25th Percentile - Interquartile Range). Both the results of the series with the cast-in hole setup and the funnel setup are shown in the Figure.

Three values were considered outliers. Two outlier values were already expected,

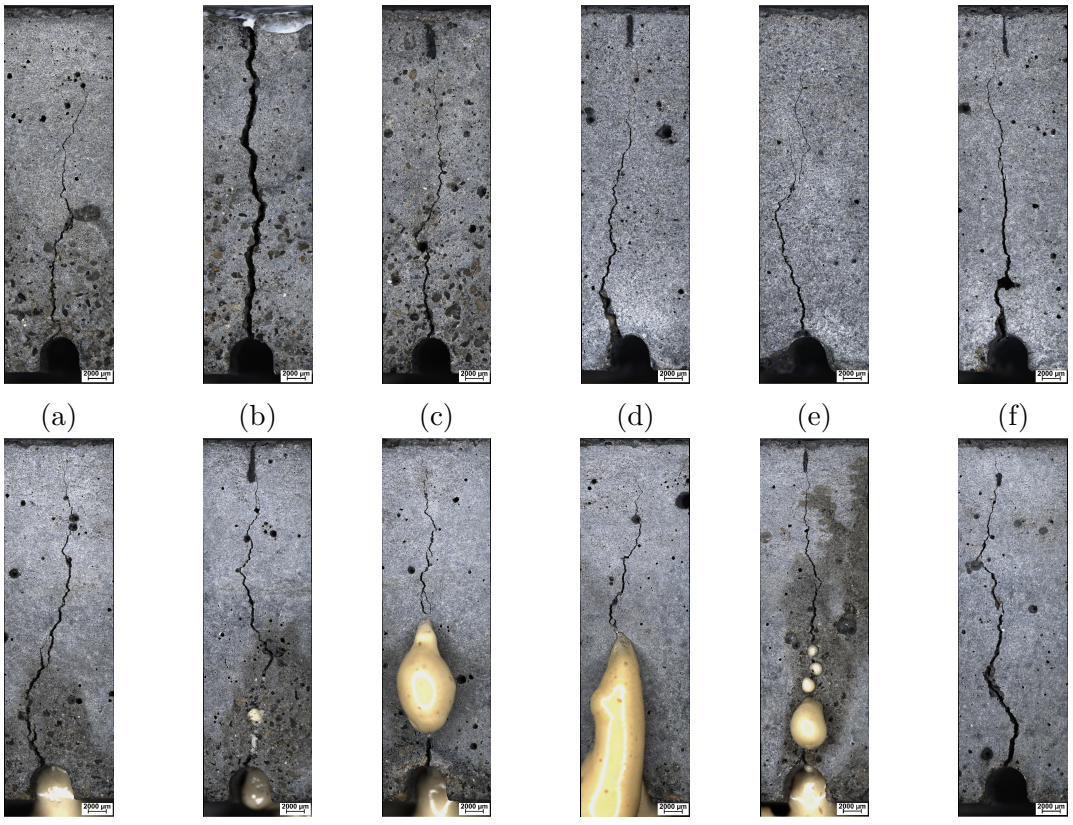

(a) (b) (c) (d) (e) (f)

(g) (h) (i) (j) (k) (l)

Figure 8.9: Lateral cracked face opposite to funnel acquired through the stereo microscope: (a-f) REF_B series; (g-l) CEM_B series.

(a) (b)

Figure 8.10: Specimen connected to the water flow setup using the funnel.

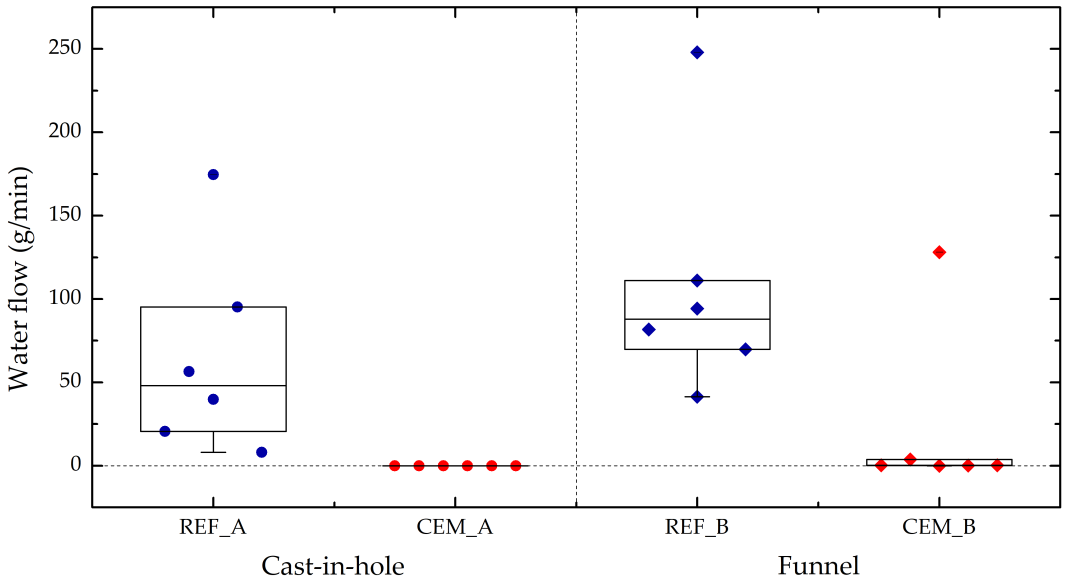

Figure 8.11: Water flow rate q of each specimens (dots) with the box plot of each series, measured with the two water flow setups.

namely the one that was caused by the higher and not comparable crack width of the specimen REF_B_2 (Figure 8.7) and one by the specimen CEM_B_6 that did not show PU release. Another outlier was caused by the specimen REF_A_5 that presented an unexpected leakage also from the top face, due to the small ligament that was most likely damaged during the positioning of the specimen. However, it is to be considered that disregard the highest value of water flow in the reference specimen is a condition that has a negative effect in the calculation of the sealing efficiency, hence it is a safe condition to apply in the assessment of the self-healing performance.

The average water flow rate of the REF_A series was equal to (44 ± 34) g/min, while for the REF_B series tested with the novel water flow testing was equal to (80 ± 26) g/min. As it was expected, the stricter condition of the new water flow test was reflected by this higher water flow rate. For what concerns the performance of the self-healing specimens, the results were highly positive even if they presented a higher crack width as evidenced by the visual examination of the crack mouths. The self-healing specimens tested with the setup presenting the cast-in hole (CEM_A) showed outstanding results since all the specimens did not show any water leakage, meaning a perfect sealing efficiency of 100% for all the series. The specimens tested with the funnel showed as well highly positive results, since apart the specimen that did not show any PU leakage and was disregarded (128 g/min), the specimens showed an efficiency close to the complete sealing. Specifically, the water flows

measured on the other five specimens were equal to 0.1 g/min, 0.3 g/min for two specimens, 3.7 g/min, and a perfect sealing with no water leakage for one specimen. This resulted in an average water flow rate $\bar{q}_{CEM\_B}$ of 1 g/min for the series and a sealing efficiency $SE_{wf,h}$ of 99%.

The sealing efficiency results with both testing configuration were in good accordance with each other, highlighting the good performance of the proposed system with a well-established technique and also with the novel technique which presented stricter testing conditions.

8.4 Quasi-static reloading

After the water flow testing that assessed the positive self-sealing efficiency of the self-healing series, the specimens were reloaded in static condition to evaluate the self-healing efficiency in terms of strength regain. It was not possible to reload all the reference specimens since two specimens per series (REF_A and REF_B) were broken during the removal of the silicone. This was the consequence of the severe damage introduced in the specimens, which were unreinforced and presented just a small ligament as active resistant section.

Figure 8.12 shows the load versus CMOD curves recorded during the pre-cracking and the static reloading for the different series.

Upon reloading, the reference specimens were only able to reach a bearing capacity close to the residual load-bearing capacity after pre-cracking ($L_{reload} \leq L_{unload}$). Consequently, they had negligible healing, in some cases even negative performance. On the contrary, the autonomously healed specimens showed an increase of load bearing capacity after healing ($L_{reload} > L_{unload}$). The load versus CMOD curves were sufficiently repeatable and, as pointed out in Chapter 6, showed a more ductile behavior if compared to the intact specimen behavior, with a residual load bearing capacity upon unloading, after reaching an increase of other 800 mu, higher than the one after pre-cracking. The most noticeable results were shown by the specimen of the CEM_A series, in which three specimens reached a maximum loading close and even slightly higher than the one obtained during the pre-cracking. In Figure 8.13 the LRI calculated for each specimen using Equation 8.3 are summarized, overlapped by the box plots of each series. The limits of the box represent the 25th and 75th percentile while the line inside the box represents the 50th percentile. The whiskers extend up to the value not considered as outliers (Upper Limit = 75th Percentile + Interquartile Range; Lower Limit = 25th Percentile - Interquartile Range).

Also in this case, the specimen CEM_B_6 which did not show a good PU leakage was disregarded as an outlier. However, even if low, a load recovery was detected with a LRI equal to 17%, while both the REF series did not show any recovery as mentioned above.

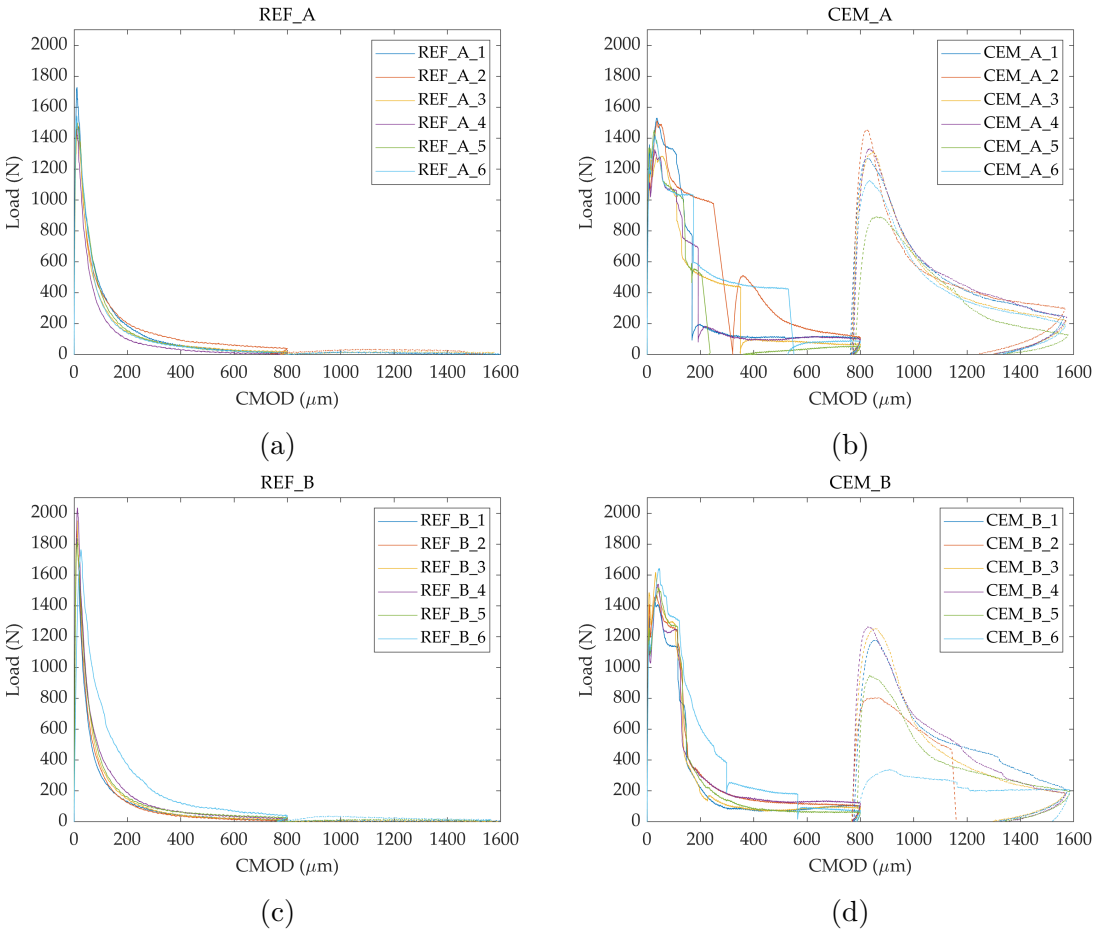

Figure 8.12: Load versus CMOD curves during the pre-cracking (continuous line) and the subsequent static reloading (dashed line) for the different series: (a) REF_A series; (b) CEM_A series; (c) REF_B series; (d) CEM_B series.

The most outstanding results were shown by the CEM_A series, with three specimens showing a LRI of 96%, 101%, and 102%, meaning that the mechanical behavior was even better than the intact specimen, as a sort of super healing [329–331]. In this case, this result was probably caused by the combined effect of the mechanical resistance offered by the bonding action exerted on the crack faces by the polyurethane with the increase of the resisting section, since a large portion of the notch was filled and bonded by the PU foam after expansion. Most likely, the same can be said for the zone of the cast-in-hole and later confirmed by the visual inspection of the crack faces (see Section 8.5). The average LRI of the series was equal to $(86 \pm 16)\%$.

Positive results were obtained also by the CEM_B series, where it was measured an average LRI of $(70 \pm 13)\%$. This result showed an improvement in the behavior

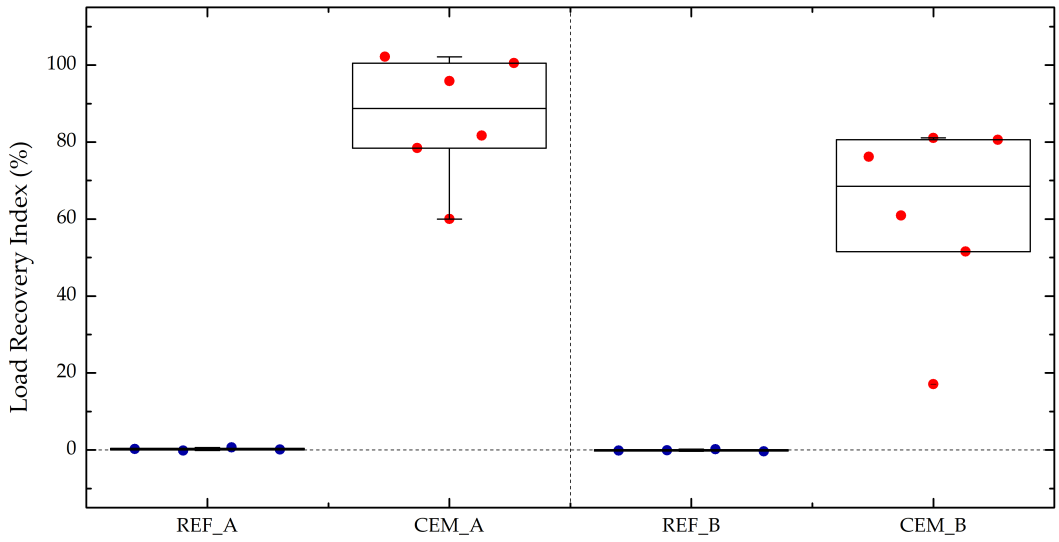

Figure 8.13: Load Recovery Indexes LRI of each specimens (dots) with the box plot of each series.

Table 8.3: Overview of L_{peak} and L_{unload} (average values and standard deviations over 6 specimens per series), L_{unload} and LRI (average values and standard deviations over six specimens per series apart specified cases.

Series	$\boldsymbol{L_{peak}}$ **(N)**	$\boldsymbol{L_{unload}}$ **(N)**	$\boldsymbol{L_{reload}}$ **(N)**	$\boldsymbol{LRI}$ **(%)**
REF_A	1535 ± 99	17 ± 12	25 ± 8[a]	0[a]
CEM_A	1420 ± 99	88 ± 23	1232 ± 196	86 ± 16
REF_B	1886 ± 99	18 ± 14	21 ± 13[a]	0[a]
CEM_B	1536 ± 83	91 ± 20	1090 ± 204[b]	70 ± 13[b]

[a]Estimated on four reloaded samples since two could not be reloaded.
[b]Estimated on five reloaded samples after disregarding one outlier.

of the series when compared with the CEM_SI series used in Chapter 6, which had a similar specimen configuration and the same healing agent. In that case, the average LRI was equal to (35.9 ± 17.4)%, showing that the slight modification of the capsules used in the CEM_B series (shorter length, slightly higher diameter) resulted in a better release of the same polyurethane agent.

Table 8.3 summarizes the results obtained in the mechanical recovery.

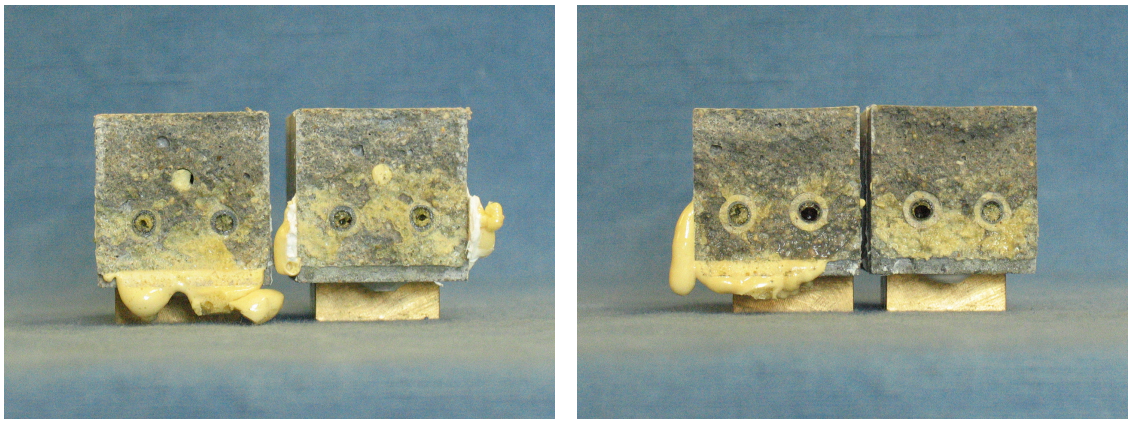

(a) (b)

Figure 8.14: Crack faces after splitting: (a) CEM_A_1; (b) CEM_B_4.

8.5 Visual examination of the healing agents in the crack

After performing the mechanical reloading, the specimens were split at the location of the crack to analyze the spread of the healing agent. From a first visual observation, it is clear that both series presented a very good release of polyurethane on the crack faces and along the crack mouth (Figure 8.14).

In the case of the CEM_A series, other than the spreading over the crack faces and the crack mouth, it was possible to also observe the sealing of the hole. These three aspects explain the perfect sealing observed during the water flow test. Also the CEM_B series showed a very good spreading of the healing agent on the lower half of the specimen with the inclusion of the crack mouth. This means that the water could flow just from the upper part of the cracked cross section, if finding a pathway to flow from there. However, the upper part presents the narrower part of the crack due to the method used to introduce it, which created a V-shaped bending crack varying from the crack mouth (larger width) to the crack tip, explaining the good behavior in terms of water flow reduction.

From the splitting of the CEM_B_6 specimens, which did not show a visible PU leakage and presented values that differed from those of the series both in terms of water flow and mechanical recovery, it was possible to assess the motivation of this unusual behavior. After splitting, it was possible to observe only few traces of PU above the crack faces. Moreover, upon splitting, there was a small foaming action from one of the capsules as highlighted in Figure 8.15. These effects could be probably addressed to a bad filling and/or sealing of the capsules used for this specimen, which caused a premature reaction inside the capsules and the polymerization just when the unreacted core had a sufficiently back-pressure and there was

Figure 8.15: Crack faces after splitting of the specimen CEM_B_6. The PU inside the red circle was released after splitting.

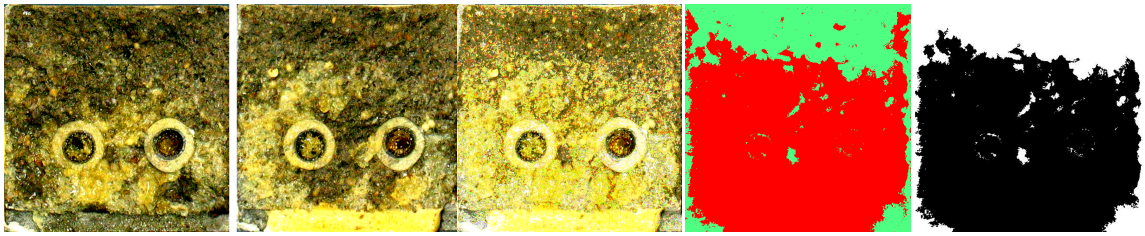

(a) (b) (c) (d)

Figure 8.16: Segmentation process: (a) crack faces with enhanced contrast, the right face was flipped horizontally; (b) crack face after overlay; (c) picture segmented with Trainable Weka Segmentation; (d) outliers removal and binarization.

contact between the environment humidity and the precursor.

Also in this case, the pictures were analyzed in order to segment the areas with and without polyurethane, using the softwares GIMP, Fiji, and MATLAB. An example of the segmentation process is reported in Figure 8.16.

After the binarization, the area covered by PU was compared to the total area of the crack face, including the area occupied by the capsules and the hole in the case of the CEM_A series. An average surface coverage of 62% for the CEM_A series and of 61% for the CEM_B series (without taking in consideration the specimen CEM_B_6) was calculated. These were the best results in terms of surface coverage

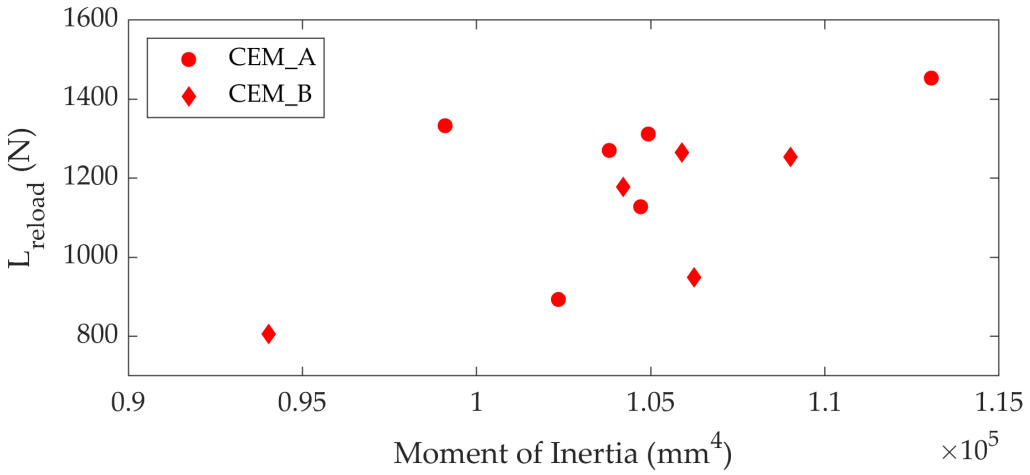

Figure 8.17: Load bearing capacity during reloading plotted against the calculated moment of inertia of the covered area.

obtained throughout the investigation conducted for the research study. Following the consideration in Chapter 7, these surface coverages were not put in correlation with the results of the water flow tests since the correlation between these values is not straightforward.

For what concern the effect of the spreading of the healing agent on the mechanical performances, the first consideration that can be done was already mentioned in Section 8.4: the PU foam, other than bridging the crack faces, increased the resistant section by filling the notch and the hole in the case of CEM_A series. A second consideration comes from Figure 8.17, where the load bearing capacity after reloading L_{reload} of the different specimens is plotted in function of the moment of inertia of the PU area calculated as reported in Section 8.1.5.

From Figure 8.17 it is not possible to find a straightforward relation between these two values, however it is noticeable a trend showing an increase in the L_{reload} with the moment of inertia I. This result would confirm the importance also for the mechanical regain of how the healing agent is spread, other than the area covered by the polyurethane itself.

8.6 Conclusions

The activities described in this chapter were the last research activities of the experimental campaign on cementitious capsules carried out in the framework of this doctoral research. The positive and negative aspects highlighted throughout the campaign were taken as basis for the further improvement and testing of the *final autonomous self-healing system*.

The cementitious capsules were manufactured using the rolling procedure developed in order to achieve a controllable internal and external diameter. In order to reduce the effect of capillary action that was highlighted in Chapter 7, the dimensions of the capsules were modified. Namely, shorter capsules (50 mm versus 60 mm) with a slightly larger diameter (6 mm versus 5 mm before coating) were used. Moreover, the highly expansive polyurethane precursor described in Section 3.4.2 was selected in order to boost the release of the healing agent due to its expansive action. Further reasons for selecting such a healing agent are the good results obtained in Chapters 4 and 6 in terms of durability-related and mechanical properties.

In order to characterize the self-healing performances of the system, first a controlled pre-cracking method in CMOD control was adopted. It was decided not to adopt the active crack control technique used in Chapters 5 and 7 for different reasons. The first is that the fast coverage of the crack mouth caused by the expansion of the PU foam would hinder the iterative measurement and restriction; the second is that an excessive foam expansion could be caused by the sudden crack creation due to the back-pressure, which would not be sufficiently representative of realistic release conditions. The capsule breakage was clearly identifiable by load drops and visual PU leakage for CMOD inferior to 160 mu.

The durability improvement against the ingress of fluid-borne substances was investigated through two types of water flow tests. The first is well-established in literature and was used in the previous chapters (Chapters 5 and 7). The second one was developed during this thesis to provide stricter testing conditions and check the system performance in comparison with the previous water permeability test. The results with both testing configurations were highly positive and comparable, since an average sealing efficiency of 100% and 99% were obtained in the two configurations, showing a perfect sealing offered by the polyurethane.

Subsequently, the mechanical recovery was investigated through the quasi-static reloading of the healed system. Also in this case, the results were positive, showing in some cases a complete recovery of the mechanical properties, with load-bearing capacity even slightly higher than that of the intact system. Average Load Recovery Indexes LRI of 86% and 70% were obtained for the self-healing specimen configurations adopted for the two water flow tests mentioned above.

An analysis of the spread of the polyurethane on the crack surfaces was also performed, showing a high surface coverage and suggesting that a connection exists between the healing performances and the way in which the healing agent is spread, other than the quantity of spread healing agent itself.

These positive results mark the achievement of the desired outcome, namely the development of an autonomous repair system for cementitious materials obtained through the encapsulation of polyurethane in newly-designed cementitious capsules. The final system allowed to obtain a high degree of recovery in both durability-related and mechanical properties after damage occurrence.

Chapter 9

Conclusions and future perspectives

9.1 Conclusions

The use of cementitious macro-capsules to develop autonomous self-healing cement-based materials was investigated in this thesis.

This was done since capsule-based self-healing has been proposed as a promising strategy to improve the durability and resilience of cementitious structures, which constitute the vast majority of the built environment. This choice was also supported by a thorough review of the existing self-healing technologies for cementitious materials. Taking into consideration the advantages and limitations of each self-healing technique, the *macro-encapsulation* was selected as the focus of this thesis due to several benefits offered by this technology. First, the possibility to provide *direct delivery of healing agents* at the crack location. While this is a common aspect in self-healing technologies, the macro-encapsulation also allows to *heal larger crack widths* than other strategies, which consents to offer autonomous repair also in case of cracks that exceed those normally allowed by Model Codes. Moreover, the healing effect can be achieved in a *short time* selecting the appropriate healing agents. Even though the vascular networks could grant the same advantages, the macro-encapsulation does not present the same complexity in the arrangements of the networks inside a structural element. In addition, the use of macro-capsules with a cementitious shell could provide further advantages such as their inherent compatibility with the surrounding cementitious matrix and the possibility to use them in the ordinary construction process in a straightforward manner.

Based on these premises, the objective was to improve the cementitious capsule technology in such a way to develop a novel self-healing cementitious system that could allow a high degree of recovery in both durability-related and mechanical properties after damage occurrence. In order to reach this goal, several intermediate objectives had to be fulfilled, as stated in Chapter 1. The outcomes of the

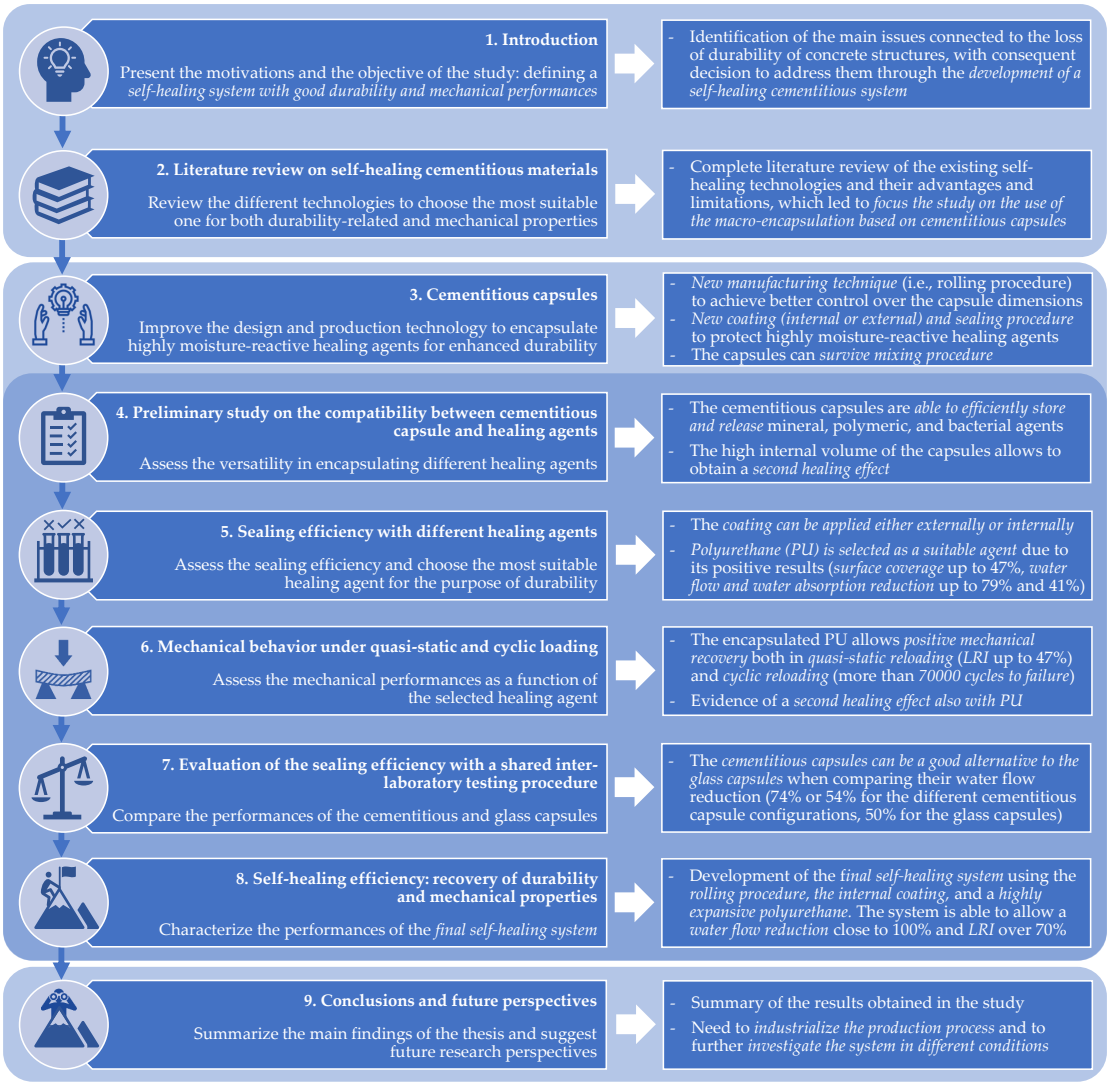

Figure 9.1: Objectives and main outcomes of the research steps described in each chapter of the dissertation.

different research steps that comprise this dissertation contributed in meeting these objectives and in defining the resulting final self-healing system, as outlined in Figure 9.1.

The improvement of the production of the cementitious capsules concerned the mix design, the manufacturing techniques of the cementitious shell, and the further coating, filling, and sealing.

The mix design of the polymer-modified cement paste was kept very similar in terms of components to the original mix design proposed in literature to allow the extrusion of cementitious capsules. The main changes regarded the proportion

of these components, in order to improve the workability and make the modified cement paste suitable also for manufacturing by rolling. This latter manufacturing procedure allowed to solve the issues connected to the uncontrolled deformation of the cementitious capsules realized by extrusion, with the consequent possibility to achieve a better control over the final dimensions of the capsules. Both procedures were manually realized in the laboratory but have good potential to be scaled-up through the use of industrial procedures.

Concerning the coating, epoxy resin was selected after several unsuccessful trials to encapsulate highly moisture-reactive healing agents. Indeed, some of the most effective healing agents show a high reactivity in the presence of humidity. On one hand, this makes them suitable to be activated fast by crack occurrence, thus preventing the further ingress of water. On the other hand, this makes them also susceptible to premature hardening inside the capsules, if the latter do not present high standards of waterproofing and tightness. To deal with this issue, two types of coating procedures were studied in order to cover the shell either externally or internally. The external coating procedure allows to isolate both the core and the cementitious shell. On the other hand, the internal coating allows to protect the core while maintaining the contact between the cement matrix and the cementitious shell, which are inherently compatible. Finally, epoxy was also successfully used to seal the capsules ends.

The capsules allowed to encapsulate several healing agents from the main types commonly used for self-healing systems, namely minerals (sodium silicate solutions and water repellent agents), polymers (two highly moisture-reactive polyurethane precursors), and bacteria (alkali-tolerant ureolytic bacterial strain *Bacillus Sphaericus*). Moreover, the system was proven effective in *resisting the mixing procedure*. This characteristic, combined with the inherent compatibility with the cementitious matrix and the easy customization of the capsules size and shape, makes cementitious capsules equivalent to *enhanced aggregates* that can be used in the ordinary construction processes.

Some preliminary studies were conducted in order to prove the possibility to fill the capsules with the above-mentioned healing agents. The cementitious capsules either with external or internal coating, appeared to be suitable to contain and release several types of healing agents, also the highly moisture-reactive ones, as shown by the occurrence of visible leakage during crack creation. The potential self-healing effect in the preliminary configuration was evaluated in terms of sealing efficiency during water permeability and absorption tests, and in terms of strength regain after reloading in three-point-bending. Promising results were achieved, showing a substantial tightness and strength recovery, even in specimens with large crack widths. Moreover, the high internal volume of the cementitious capsules allowed to obtain a second healing effect. However, these promising results needed to be expanded, further validated, and corroborated by using a more significant statistical sample.

To do so, several self-healing cement mortar prisms were produced and tested according to the objectives that were set for this study and following the advancements of the research steps. Their performances were compared with those of reference plain mortar prisms. An overview of the main characteristics of each self-healing series that was tested during the study and of the results obtained during their characterization is shown in Table 9.1.

It was confirmed that the cementitious capsules were successfully able to sequester and release different healing agents. The findings obtained throughout the investigation were not significantly affected by the different configurations of the epoxy coating layer (i.e. applied to the internal or external surface of the tubular capsule). The reason for that should rely on the cementitious shell preparation and coating procedure. In fact, the epoxy primer applied both to the internal and the external surfaces of the tubes was sufficient to isolate the healing agents from contact with the hardened capsule shell, and hence with the low residual humidity that might be present in it. The primary function of the epoxy coating was to offer protection solely against the high humidity and high alkalinity of the fresh mortar mix, which represents a major threat for the healing agents' retention. Therefore, *applying it either to the internal or the external surfaces of the capsule did not significantly change its performance* and allowed to provide a good barrier between the healing agents and the harsh environment of the matrix. As regards the sealing efficiency evaluated with water permeability and water absorption, good results were obtained in both tests using the polyurethane precursor, with sealing efficiency up to 79% and 41%, respectively. When water-repellent agent was used, excellent results were obtained in preventing the water absorption (namely, a sealing efficiency up to 92%), while detrimental effects were shown against water permeability (namely, a negative sealing efficiency up to -117%). On the contrary, silica gel immobilized *B. Sphaericus* showed the inverse behavior, with good results against water permeability (namely, a sealing efficiency up to 78%) and bad results during water absorption (namely, a negative sealing efficiency up to -145%). It can be assumed from these results that, while the PU precursor is well suited in mitigating both mechanisms, the water-repellent agent is well suited when the self-sealing structure will mainly be exposed to the ingress of deleterious substances governed by capillary forces, but not when the pressure is the driving force. On the other end, the bacterial healing agent seems more suited when the water leakage, also in pressure, could be the cause of the ingress of deleterious substances and losses of serviceability. For instance, this is the case of submerged structures, water tanks, or tunnel segments. In light of these considerations, it can be concluded that the self-sealing systems should be tailor-made for the real operating conditions that the structure will meet during its service life, by choosing the correct healing agent, the correct location for the self-sealing system, and by taking advantage of the synergy between different self-sealing mechanisms. Nevertheless, it has to be underlined that *the polyurethane*

Table 9.1: Summary of the different characteristics and the corresponding results obtained with the self-healing series.

			WRA_INT	WRA_EXT	PUR_INT	PUR_EXT	BAC_INT	BAC_EXT	CEM_SI	CEM_LI	CEM_LE	CEM_L	CEM_S	CEM_A	CEM_B
	Chapter		5	5	5	5	5	5	6	6	6	7	7	8	8
CHARACTERISTICS	• Manufacturing process of the capsule's shell		Extrusion	Extrusion	Extrusion	Extrusion	Extrusion	Extrusion	Rolling	Extrusion	Extrusion	Extrusion	Rolling	Rolling	Rolling
	• Mix design of the shell's cement paste		Mix 1	Mix 1	Mix 1	Mix 1	Mix 1	Mix 1	Mix 2	Mix 2	Mix 2	Mix 2	Mix 2	Mix 2	Mix 2
	• Healing agent		WRA	WRA	PU[1]	PU[1]	BS+DM	BS+DM	PU[2]	PU[2]	PU[2]	PU[1,*]	PU[1,*]	PU[2]	PU[2]
	• Surface of the shell coated with epoxy		Internal	External	Internal	External	Internal	External	Internal	Internal	External	Internal	Internal	Internal	Internal
	• Average internal diameter of the shell	(mm)	7.5	7.5	7.5	7.5	7.5	7.5	5	7.5	7.5	7.5	5	6	6
	• Average external diameter of the shell	(mm)	10	10	10	10	10	10	8	10	10	10	8	8.5	8.5
	• Average length of the capsule	(mm)	50	50	50	50	50	50	60	45	45	45	60	50	50
	• Average thickness of the epoxy coating	(mm)	1	1	1	1	1	1	1	1	1	1	1	1	1
	• Average internal diameter after coating	(mm)	5.5	7.5	5.5	7.5	5.5	7.5	3	5.5	7.5	5.5	3	4	4
	• Volume of cargo healing agent	(mL)	1	1.5	1	1.5	1	1.5	0.3	0.6	0.9	0.6	0.3	0.7	0.7
	• Number of capsules per specimen	(-)	1	1	1	1	2	2	2	1	1	1	2	2	2
RESULTS	• Average Crack width (measured through microscope)	(µm)	315	302	300	295	305	309	-	-	-	300	303	$\gtrsim$500	$\gtrsim$500
	• Average Surface coverage	(-)	36%	40%	37%	47%	17%	36%	-	-	-	13%	2%	62%	61%
	• Average Water flow	(g/min)	35	28	3	12	6	4	-	-	-	15	43	0	1
	• Average Sealing efficiency (*water permeability*)	(-)	-117%	-70%	79%	28%	64%	78%	-	-	-	74%	54%	100%	99%
	• Average Sorptivity index	(mm/s$^{0.25}$)	0.02	0.02	0.15	0.20	0.46	0.64	-	-	-	-	-	-	-
	• Average Sealing efficiency (*water absorption*)	(-)	92%	92%	41%	20%	-81%	-145%	-	-	-	-	-	-	-
	• Average Load Recovery Index	(-)	-	-	-	-	-	-	36%	31%	47%	-	-	86%	70%
	• Maximum Total Number of Cycles to failure	(-)	-	-	-	-	-	-	27625[a]	77797[b]	10921[c]	-	-	-	-

[1]Low viscosity polyurethane precursor (HA Flex SLV AF); [2]Highly expansive polyurethane precursor (CarboStop U); [*]Addition of fluorescent powder dye (EpoDye).
[a]At a Maximum Load Level S=0.80; [b]At a Maximum Load Level S=1.05; [c]At a Maximum Load Level S=0.75.

precursor allowed to obtain always positive results both in terms of reduction of water permeability and water absorption, never showing detrimental effects such as in the case of the other type of healing agents. Moreover, the polyurethane allows a very fast curing in presence of humidity, without requiring high quantity of water as for the bacterial healing agents. In addition, several types of polyurethane precursors can cause the formation of expansive foam, allowing the autonomous repair of larger cracks. Due to these positive aspects, *this type of healing agent was selected as the most promising* to obtain the desired self-healing system and it was decided to focus the subsequent study on its use.

The investigation of the self-healing performances concerned not only the recovery in terms of durability, but also in terms of mechanical behavior. This aspect was studied through the use of the cementitious capsules produced either by extrusion or by rolling and filled with a highly expansive polyurethane precursor. Their self-healing effect was evaluated in terms of mechanical recovery under static flexural loading and number of cycles to failure under cyclic flexural loading. This was an aspect of novelty since the fatigue behavior of cementitious self-healing systems is a seldom studied aspect. However, cyclic loadings can cause additional detrimental effects on self-healing cementitious materials with the continuous opening and closing of healed cracks, subjecting the composite materials formed by the cementitious matrix and the repairing agent to strains that could cause not only damages in the matrix or in the repairing material, but also debonding between these two different materials. This is an issue of fundamental importance for understanding and characterizing the behavior of these materials in real field conditions, and consequently allowing their use by ensuring the structural safety. The results were not significantly affected by the capsule manufacturing procedure (nor by the sequence of application of the epoxy coating layers as already previously ascertained); conversely, the internal diameter of the capsules and the overall amount of cargo healing agent may have influenced the release of the polyurethane precursor upon pre-cracking and hence the final mechanical performances, that were very satisfactory in any case. In general, bigger internal diameter and higher volume of cargo healing agent fostered the mechanical recovery, providing inputs for the development of the final self-healing system.

Once that the efficiency in recovery of both durability-related and mechanical properties was assessed, the self-healing performances obtained with cementitious capsules filled with a polyurethane precursor were compared with those obtained using glass capsules filled with the same healing agent. This comparison was performed by applying an inter-laboratory testing procedure developed in the framework of the EU COST Action SARCOS. Two series of self-healing mortar prisms were produced: one with a single large capsule manufactured by extrusion, the other with two smaller capsules manufactured with the rolling procedure developed in the framework of this thesis. The latter were comparable with the glass capsules used in the inter-laboratory testing in terms of internal diameter and volume of

cargo healing agent. In general, cementitious capsules offered comparable or better performance with respect to glass capsules, for the same healing agent type and content. This result confirmed the possibility to use the cementitious capsules as a valid alternative, offering additional advantages such as reduced fragility, reduced risk of alkali-silica reaction, and higher compatibility with the surrounding matrix.

Finally, the positive and negative aspects highlighted throughout the campaign were taken as basis for the improvement and testing of the *final autonomous self-healing system* based on the use of cementitious capsules.

The capsules for the final self-healing system were manufactured using the *rolling procedure* in such a way to achieve a better control over the capsule diameter. In fact, in order to *reduce the effect of capillary action*, the dimensions of the capsules were modified: namely, shorter capsules (50 mm versus 60 mm) with a slightly larger internal diameter (6 mm versus 5 mm) were produced. Moreover, the *highly expansive polyurethane precursor* was selected in order to boost the release of the healing agent due to its expansive action and for the good results obtained in the preliminary studies and in the study regarding the mechanical behavior of the system.

In order to characterize the self-healing performances of the system, first a controlled pre-cracking method in CMOD control was adopted. The capsule breakage was clearly identifiable by load drops and visual polyurethane leakage for CMOD inferior to 160 mu.

The durability improvement against the ingress of fluid-borne substances was investigated through two types of water flow tests: one well-established in literature and already used in the previous steps of the research, and one developed during this last part of the research. This novel water flow test was developed to provide a comparison with the other water permeability test under stricter testing conditions. The results with both testing configurations were highly positive and comparable, since an average sealing efficiency of 100% and 99% were obtained respectively, showing a *perfect sealing offered by the polyurethane*.

Subsequently, the mechanical recovery was investigated through the quasi-static reloading of the healed system. Also in this case, the results were highly positive, showing in some cases *a complete recovery of the mechanical properties*, with *load-bearing capacity even slightly higher than that of the intact system*. Average Load Recovery Indexes LRI of 86% and 70% were obtained for the self-healing specimen configurations adopted for the two water flow tests mentioned above.

In conclusion, the main objective set for this doctoral thesis was achieved, namely the development and characterization of an efficient self-healing system for cementitious materials based on the encapsulation of polyurethane in newly-designed cementitious capsules. Such system allowed to obtain almost full recovery in both durability-related and mechanical properties after damage occurrence, proving that the system is mature to be upscaled in real concrete structures.

9.2 Future perspectives

Even though the system allowed to obtain good recovery performances both on the mechanical and durability-related properties, further research is needed to meet the remaining challenges to implement the system in practice.

First, all the tests were performed using cement mortar specimens as a prototypal cementitious material instead of concrete. Due to the positive results obtained throughout the study, the next natural development step will be to test the efficiency of the system in concrete. It would be of particular relevance to test the system in full-scale reinforced concrete elements. In fact, this would represent the final condition in which the system should work and the presence of structural reinforcement could have an effect on the crack development, with consequent different behavior of the healing agent release and effect inside the cracks.

Another aspect of paramount importance is the stability in time of the healing agent, both inside the capsule and once released in the crack. Specifically, it is important to guarantee the protection and efficacy of the healing agent until crack occurrence. The crack occurrence could happen even after years, especially the large cracks addressed by the macro-encapsulation system, while the healing agents' shelf life is often much shorter. Other than the stability of the healing agent before its release, another aspect that requires more research is the stability and durability of the bonding between the agent and the cementitious matrix, which can be degraded by several actions during a real structure service life. For example, a first attempt in this direction was described in Chapter 6, where the behavior of a pre-cracked and autonomously healed cementitious prototype subjected to dynamic loading was studied. Further research is needed on this aspect and on other degradation mechanisms such as freeze and thaw cycles, thermal cycles, impacts, resistance to chloride diffusion and carbonation, etc.

Since the tests were performed on small scale specimens, a limited number of capsules (i.e. one or two per specimen) was adopted. However, another important aspect is the correct dosage and distribution of the capsules in a real structural element. It was demonstrated that the cementitious capsules can be added directly in the mixer without premature breakage of the capsules when subjected to the mixing loading action. Nevertheless, the limitations related to the random orientation of the macro-capsules in the concrete mix when added during the casting and the consequent effect on the healing performances should be addressed in the future. Also, the overall efficiency of the random capsule distribution during mixing should be compared with that of pre-placing before casting, in order to assess the most suitable way of application for this type of macro-capsules. Moreover, when macro-capsules are embedded into the concrete matrix, it is important to take into account the possible reduction of the mechanical properties of the element, hence to define the correct dosage to have a good balance between possible mechanical loss, durability increase, and overall cost. The latter should include not only the

cost of the material but also the cost related to the increase of service life and reduction of maintenance of the structure, following a life cycle assessment approach. Consequently, it is important to develop design criteria to take into account the addition of the capsules in the structural elements.

Finally, to effectively realize the scale-up of the system, a last aspect to be taken into account should be the industrialization of the processes involved in the production of the cementitious capsules and their coating, filling, and sealing.

Bibliography

[1] P. J. M. Monteiro, S. A. Miller, and A. Horvath. "Towards sustainable concrete". *Nature Materials* 16.7 (2017), pp. 698–699. DOI: 10.1038/nmat4930.

[2] I. Vázquez-Rowe, K. Ziegler-Rodriguez, J. Laso, I. Quispe, R. Aldaco, and R. Kahhat. "Production of cement in Peru: Understanding carbon-related environmental impacts and their policy implications". *Resources, Conservation and Recycling* 142 (2018), pp. 283–292. DOI: 10.1016/j.resconrec.2018.12.017.

[3] B. Lothenbach, K. Scrivener, and R. D. Hooton. "Supplementary cementitious materials". *Cement and Concrete Research* 41 (2011), pp. 1244–1256. DOI: 10.1016/j.cemconres.2010.12.001.

[4] E. Özbay, M. Erdemir, and H. İ. Durmuş. "Utilization and efficiency of ground granulated blast furnace slag on concrete properties – A review". *Construction and Building Materials* 105 (2016), pp. 423–434. DOI: 10.1016/J.CONBUILDMAT.2015.12.153.

[5] N. Alderete, Y. Villagrán, A. Mignon, D. Snoeck, and N. De Belie. "Pore structure description of mortars containing ground granulated blast-furnace slag by mercury intrusion porosimetry and dynamic vapour sorption". *Construction and Building Materials* 145 (2017), pp. 157–165. DOI: 10.1016/j.conbuildmat.2017.03.245.

[6] P. Palmero, A. Formia, J.-M. Tulliani, and P. Antonaci. "Valorisation of alumino-silicate stone muds: From wastes to source materials for innovative alkali-activated materials". *Cement and Concrete Composites* 83 (2017), pp. 251–262. DOI: 10.1016/j.cemconcomp.2017.07.011.

[7] S. Matthews, I. Holton, J. Morlidge, and R. Pool. "CON REP NET - A thematic network on performance-based rehabilitation of reinforced concrete structures". *Concrete* 37.8 (2003), pp. 58–59.

[8] C. L. Freyermuth. "Life-cycle cost analysis for large segmental bridges". *Concrete International* 23.2 (2001), pp. 89–95.

[9] M. Sánchez, P. Faria, L. Ferrara, E. Horszczaruk, H. Jonkers, A. Kwiecień, J. Mosa, A. Peled, A. Pereira, D. Snoeck, M. Stefanidou, T. Stryszewska, and B. Zając. "External treatments for the preventive repair of existing constructions: A review". *Construction and Building Materials* 193 (2018), pp. 435–452. DOI: 10.1016/j.conbuildmat.2018.10.173.

[10] K. van Breugel. "Is there a market for self-healing cement-based materials?" In: *Proceedings of the First International Conference on Self Healing Materials*. Ed. by A. J. M. Schmets and S. van der Zwaag. Noordwijk aan Zee, the Netherlands: Springer, 2007, pp. 1–9.

[11] P. K. Metha and P. J. M. Monteiro. *Concrete: Microstructure, Properties, and Materials*. Third Edit. New York, NY, USA: Mc Graw-Hill, 2006.

[12] C. Leahy, E. OBrien, and A. O'Connor. "The Effect of Traffic Growth on Characteristic Bridge Load Effects". In: *Transportation Research Procedia*. Vol. 14. Elsevier B.V., 2016, pp. 3990–3999. DOI: 10.1016/j.trpro.2016.05.496.

[13] I. Bayane, A. Mankar, E. Brühwiler, and J. D. Sørensen. "Quantification of traffic and temperature effects on the fatigue safety of a reinforced-concrete bridge deck based on monitoring data". *Engineering Structures* 196 (2019). DOI: 10.1016/j.engstruct.2019.109357.

[14] Y. Yu, C. S. Cai, W. He, and H. Peng. "Prediction of bridge maximum load effects under growing traffic using non-stationary bayesian method". *Engineering Structures* 185 (2019), pp. 171–183. DOI: 10.1016/j.engstruct.2019.01.085.

[15] B. Van Belleghem. "Effect of capsule-based self-healing on chloride induced corrosion of reinforced concrete". PhD Thesis. Ghent University, 2018.

[16] N. De Belie, E. Gruyaert, A. Al-Tabbaa, P. Antonaci, C. Baera, D. Bajare, A. Darquennes, R. Davies, L. Ferrara, T. Jefferson, C. Litina, B. Miljevic, A. Otlewska, J. Ranogajec, M. Roig-Flores, K. Paine, P. Lukowski, P. Serna, J.-M. Tulliani, S. Vucetic, J. Wang, and H. M. Jonkers. "A Review of Self-Healing Concrete for Damage Management of Structures". *Advanced Materials Interfaces* 5.17 (2018), p. 1800074. DOI: 10.1002/admi.201800074.

[17] K. Van Tittelboom, D. Snoeck, P. Vontobel, F. H. Wittmann, and N. De Belie. "Use of neutron radiography and tomography to visualize the autonomous crack sealing efficiency in cementitious materials". *Materials and Structures* 46.1-2 (2013), pp. 105–121. DOI: 10.1617/s11527-012-9887-1.

[18] M. de Rooij, K. Van Tittelboom, N. De Belie, and E. Schlangen, eds. *Self-healing phenomena in cement-based materials : State-of-the-Art Report of RILEM Technical Committee 221-SHC: Self-Healing Phenomena in Cement-Based Materials*. Springer, 2013.

[19] L. Ferrara, T. Van Mullem, M. C. Alonso, P. Antonaci, R. P. Borg, E. Cuenca, A. Jefferson, P.-L. Ng, A. Peled, M. Roig-Flores, M. Sanchez, C. Schroefl, P. Serna, D. Snoeck, J. M. Tulliani, and N. De Belie. "Experimental characterization of the self-healing capacity of cement based materials and its effects on the material performance: A state of the art report by COST Action SARCOS WG2". *Construction and Building Materials* 167 (2018), pp. 115–142. DOI: 10.1016/J.CONBUILDMAT.2018.01.143.

[20] A. Kanellopoulos, T. Qureshi, and A. Al-Tabbaa. "Glass encapsulated minerals for self-healing in cement based composites". *Construction and Building Materials* 98 (2015), pp. 780–791. DOI: 10.1016/J.CONBUILDMAT.2015.08.127.

[21] K. Van Tittelboom, J. Wang, M. Araújo, D. Snoeck, E. Gruyaert, B. Debbaut, H. Derluyn, V. Cnudde, E. Tsangouri, D. Van Hemelrijck, and N. De Belie. "Comparison of different approaches for self-healing concrete in a large-scale lab test". *Construction and Building Materials* 107 (2016), pp. 125–137. DOI: 10.1016/J.CONBUILDMAT.2015.12.186.

[22] T. Qureshi, A. Kanellopoulos, and A. Al-Tabbaa. "Encapsulation of expansive powder minerals within a concentric glass capsule system for self-healing concrete". *Construction and Building Materials* 121 (2016), pp. 629–643. DOI: 10.1016/J.CONBUILDMAT.2016.06.030.

[23] H. Huang, G. Ye, and Z. Shui. "Feasibility of self-healing in cementitious materials – By using capsules or a vascular system?" *Construction and Building Materials* 63 (2014), pp. 108–118. DOI: 10.1016/j.conbuildmat.2014.04.028.

[24] L. Souza and A. Al-Tabbaa. "Microfluidic fabrication of microcapsules tailored for self-healing in cementitious materials". *Construction and Building Materials* 184 (2018), pp. 713–722. DOI: 10.1016/J.CONBUILDMAT.2018.07.005.

[25] C. Dry and W. McMillan. "Three-part methylmethacrylate adhesive system as an internal delivery system for smart responsive concrete". *Smart Materials and Structures* 5.3 (1996), pp. 297–300. DOI: 10.1088/0964-1726/5/3/007.

[26] K. Van Tittelboom, N. De Belie, D. Van Loo, and P. Jacobs. "Self-healing efficiency of cementitious materials containing tubular capsules filled with healing agent". *Cement and Concrete Composites* 33.4 (2011), pp. 497–505. DOI: 10.1016/J.CEMCONCOMP.2011.01.004.

[27] B. Hilloulin, K. Van Tittelboom, E. Gruyaert, N. De Belie, and A. Loukili. "Design of polymeric capsules for self-healing concrete". *Cement and Concrete Composites* 55 (2015), pp. 298–307. DOI: 10.1016/J.CEMCONCOMP.2014.09.022.

[28] M. Araújo, S. Chatrabhuti, S. Gurdebeke, N. Alderete, K. Van Tittelboom, J.-M. Raquez, V. Cnudde, S. Van Vlierberghe, N. De Belie, and E. Gruyaert. "Poly(methyl methacrylate) capsules as an alternative to the ''proof-of-concept" glass capsules used in self-healing concrete". *Cement and Concrete Composites* 89 (2018), pp. 260–271. DOI: 10.1016/J.CEMCONCOMP.2018.02.015.

[29] J. Feiteira, E. Gruyaert, and N. De Belie. "Self-healing of moving cracks in concrete by means of encapsulated polymer precursors". *Construction and Building Materials* 102 (2016), pp. 671–678. DOI: 10.1016/j.conbuildmat.2015.10.192.

[30] P. Van den Heede, B. Van Belleghem, N. Alderete, K. Van Tittelboom, and N. De Belie. "Neutron Radiography Based Visualization and Profiling of Water Uptake in (Un)cracked and Autonomously Healed Cementitious Materials." *Materials* 9.5 (2016). DOI: 10.3390/ma9050311.

[31] J. Wang, K. Van Tittelboom, N. De Belie, and W. Verstraete. "Use of silica gel or polyurethane immobilized bacteria for self-healing concrete". *Construction and Building Materials* 26.1 (2012), pp. 532–540. DOI: 10.1016/J.CONBUILDMAT.2011.06.054.

[32] K. Van Tittelboom, N. De Belie, F. Lehmann, and C. U. Grosse. "Acoustic emission analysis for the quantification of autonomous crack healing in concrete". *Construction and Building Materials* 28.1 (2012), pp. 333–341. DOI: 10.1016/J.CONBUILDMAT.2011.08.079.

[33] M. Maes, K. Van Tittelboom, and N. De Belie. "The efficiency of self-healing cementitious materials by means of encapsulated polyurethane in chloride containing environments". *Construction and Building Materials* 71 (2014), pp. 528–537. DOI: 10.1016/J.CONBUILDMAT.2014.08.053.

[34] B. Van Belleghem, P. Van den Heede, K. Van Tittelboom, and N. De Belie. "Quantification of the Service Life Extension and Environmental Benefit of Chloride Exposed Self-Healing Concrete". *Materials* 10.1 (2016), p. 5. DOI: 10.3390/ma10010005.

[35] K. Van Tittelboom, E. Tsangouri, D. Van Hemelrijck, and N. De Belie. "The efficiency of self-healing concrete using alternative manufacturing procedures and more realistic crack patterns". *Cement and Concrete Composites* 57 (2015), pp. 142–152. DOI: 10.1016/j.cemconcomp.2014.12.002.

[36] E. Gruyaert, K. Van Tittelboom, J. Sucaet, J. Anrijs, S. Van Vlierberghe, P. Dubruel, B. G. De Geest, J. P. Remon, N. De Belie, and N. D. Belie. "Capsules with evolving brittleness to resist the preparation of self-healing concrete". *Materiales de Construcción* 66.323 (2016), e092. DOI: 10.3989/mc.2016.07115.

[37] J. Feiteira. "Self-Healing Concrete Encapsulated Polymer Precursors as Healing Agents for Active Cracks". PhD Thesis. Ghent University, 2017.

[38] A. Formia, S. Terranova, P. Antonaci, N. M. Pugno, and J. M. Tulliani. "Setup of extruded cementitious hollow tubes as containing/releasing devices in self-healing systems". *Materials* 8.4 (2015), pp. 1897–1923. DOI: 10.3390/ma8041897.

[39] A. Formia, S. Irico, F. Bertola, F. Canonico, P. Antonaci, N. M. Pugno, and J.-M. Tulliani. "Experimental analysis of self-healing cement-based materials incorporating extruded cementitious hollow tubes". *Journal of Intelligent Material Systems and Structures* (2016), pp. 1–20. DOI: 10.1177/1045389X16635847.

[40] S. Irico. "Study and development of multifunctional cement-based materials". PhD Thesis. Università del Piemonte Orientale "A. Avogadro", 2016.

[41] T. Van Mullem, E. Gruyaert, B. Debbaut, R. Caspeele, and N. De Belie. "Novel active crack width control technique to reduce the variation on water permeability results for self-healing concrete". *Construction and Building Materials* 203 (2019), pp. 541–551. DOI: 10.1016/j.conbuildmat.2019.01.105.

[42] S. van der Zwaag, ed. *Self Healing Materials: An Alternative Approach to 20 Centuries of Materials Science*. Springer Netherlands, 2007, pp. 1–388.

[43] R. D. Doherty, D. A. Hughes, F. J. Humphreys, J. J. Jonas, D. Juul Jensen, M. E. Kassner, W. E. King, T. R. McNelley, H. J. McQueen, and A. D. Rollett. "Current issues in recrystallization: A review". *Materials Science and Engineering A* 238.2 (1997), pp. 219–274. DOI: 10.1016/S0921-5093(97)00424-3.

[44] K. K. Alaneme and E. A. Okotete. "Recrystallization mechanisms and microstructure development in emerging metallic materials: A review". *Journal of Science: Advanced Materials and Devices* 4.1 (2019), pp. 19–33. DOI: 10.1016/j.jsamd.2018.12.007.

[45] K. R. Lauer and F. O. Slate. "Autogenous Healing of Cement Paste". *ACI Journal Proceedings* 52.6 (1956), pp. 1083–1098. DOI: 10.14359/11661.

[46] M. Wu, B. Johannesson, and M. Geiker. "A review: Self-healing in cementitious materials and engineered cementitious composite as a self-healing material". *Construction and Building Materials* 28.1 (2012), pp. 571–583. DOI: 10.1016/j.conbuildmat.2011.08.086.

[47] K. Van Tittelboom and N. De Belie. "Self-healing in cementitious materials-a review". *Materials* 6.6 (2013), pp. 2182–2217. DOI: 10.3390/ma6062182.

[48] C. Joseph, D. Gardner, T. Jefferson, B. Isaacs, and B. Lark. "Self-healing cementitious materials: a review of recent work". *Proceedings of the Institution of Civil Engineers - Construction Materials* 164.1 (2011), pp. 29–41. DOI: 10.1680/coma.900051.

[49] K. Vijay, M. Murmu, and S. V. Deo. "Bacteria based self healing concrete – A review". *Construction and Building Materials* 152 (2017), pp. 1008–1014. DOI: 10.1016/J.CONBUILDMAT.2017.07.040.

[50] S. K. Ghosh. *Self-Healing Materials: Fundamentals, Design Strategies, and Applications*. John Wiley and Sons, 2009. DOI: 10.1002/9783527625376.

[51] A. Witze. "Seawater is the secret to long-lasting Roman concrete". *Nature* (July 2017). DOI: 10.1038/nature.2017.22231.

[52] H. Mihashi and T. Nishiwaki. "Development of engineered self-healing and self-repairing concrete-state-of-the-art report". *Journal of Advanced Concrete Technology* 10.5 (2012), pp. 170–184. DOI: 10.3151/jact.10.170.

[53] H. Huang, G. Ye, and D. Damidot. "Effect of blast furnace slag on self-healing of microcracks in cementitious materials". *Cement and Concrete Research* 60 (2014), pp. 68–82. DOI: 10.1016/j.cemconres.2014.03.010.

[54] D. Snoeck. "Self-healing and microstructure of cementitious materials with microfibres and superabsorbent polymers". PhD Thesis. Ghent University, 2015.

[55] Y. Yang, M. D. Lepech, E. H. Yang, and V. C. Li. "Autogenous healing of engineered cementitious composites under wet-dry cycles". *Cement and Concrete Research* 39.5 (2009), pp. 382–390. DOI: 10.1016/j.cemconres.2009.01.013.

[56] C. Edvardsen. "Water Permeability and Autogenous Healing of Cracks in Concrete". *ACI Materials Journal* 96.4 (1999), pp. 448–454. DOI: 10.14359/645.

[57] D. Homma, H. Mihashi, and T. Nishiwaki. "Self-Healing Capability of Fibre Reinforced Cementitious Composites". *Journal of Advanced Concrete Technology* 7.2 (2009), pp. 217–228.

[58] H. Ma, S. Qian, and Z. Zhang. "Effect of self-healing on water permeability and mechanical property of Medium-Early-Strength Engineered Cementitious Composites". *Construction and Building Materials* 68 (2014), pp. 92–101. DOI: 10.1016/j.conbuildmat.2014.05.065.

[59] C. A. Clear. *The effects of autogenous healing upon the leakage of water through cracks in concrete*. Cement and Concrete Association, 1985, p. 31.

[60] E. F. Wagner. *Autogenous Healing of Cracks in Cement-Mortar Linings for Gray-Iron and Ductile-Iron Water Pipe*. 1974. DOI: 10.2307/41267080.

[61] D. J. Hannant and J. G. Keer. "Autogenous healing of thin cement based sheets". *Cement and Concrete Research* 13.3 (1983), pp. 357–365. DOI: 10.1016/0008-8846(83)90035-2.

[62] S. Jacobsen, J. Marchand, and H. Hornain. "Sem observations of the microstructure of frost deteriorated and self-healed concretes". *Cement and Concrete Research* 25.8 (1995), pp. 1781–1790. DOI: 10.1016/0008-8846(95)00174-3.

[63] S. Jacobsen and E. J. Sellevold. "Self healing of high strength concrete after deterioration by freeze/thaw". *Cement and Concrete Research* 26.1 (1996), pp. 55–62. DOI: 10.1016/0008-8846(95)00179-4.

[64] S. Granger, G. Pijaudier Cabot, A. Loukili, D. Marlot, and J. Lenain. "Monitoring of cracking and healing in an ultra high performance cementitious material using the time reversal technique". *Cement and Concrete Research* 39.4 (2009), pp. 296–302. DOI: 10.1016/J.CEMCONRES.2009.01.004.

[65] B. Hilloulin, D. Hilloulin, F. Grondin, A. Loukili, and N. De Belie. "Mechanical regains due to self-healing in cementitious materials: Experimental measurements and micro-mechanical model". *Cement and Concrete Research* 80 (2016), pp. 21–32. DOI: 10.1016/j.cemconres.2015.11.005.

[66] L. Ferrara, V. Krelani, and F. Moretti. "Autogenous healing on the recovery of mechanical performance of High Performance Fibre Reinforced Cementitious Composites (HPFRCCs): Part 2 – Correlation between healing of mechanical performance and crack sealing". *Cement and Concrete Composites* 73 (2016), pp. 299–315. DOI: 10.1016/j.cemconcomp.2016.08.003.

[67] L. Ferrara, V. Krelani, F. Moretti, M. Roig Flores, and P. Serna Ros. "Effects of autogenous healing on the recovery of mechanical performance of High Performance Fibre Reinforced Cementitious Composites (HPFRCCs): Part 1". *Cement and Concrete Composites* 83 (2017), pp. 76–100. DOI: 10.1016/j.cemconcomp.2017.07.010.

[68] V. C. Li and E. Herbert. "Robust Self-Healing Concrete for Sustainable Infrastructure". *Journal of Advanced Concrete Technology* 10.6 (2012), pp. 207–218. DOI: 10.3151/jact.10.207.

[69] T. Nishiwaki, M. Koda, M. Yamada, H. Mihashi, and T. Kikuta. "Experimental study on self-healing capability of FRCC using different types of synthetic fibers". *Journal of Advanced Concrete Technology* 10.6 (2012), pp. 195–206. DOI: 10.3151/jact.10.195.

[70] D. Snoeck and N. De Belie. "Mechanical and self-healing properties of cementitious composites reinforced with flax and cottonised flax, and compared with polyvinyl alcohol fibres". *Biosystems Engineering* 111.4 (2012), pp. 325–335. DOI: 10.1016/j.biosystemseng.2011.12.005.

[71] D. Snoeck, K. Van Tittelboom, S. Steuperaert, P. Dubruel, and N. De Belie. "Self-healing cementitious materials by the combination of microfibres and superabsorbent polymers". *Journal of Intelligent Material Systems and Structures* 25.1 (2014), pp. 13–24. DOI: 10.1177/1045389X12438623.

[72] D. Snoeck and N. De Belie. "Repeated Autogenous Healing in Strain-Hardening Cementitious Composites by Using Superabsorbent Polymers". *Journal of Materials in Civil Engineering* 28.1 (2016), p. 04015086. DOI: 10.1061/(ASCE)MT.1943-5533.0001360.

[73] L. Ferrara, S. R. Ferreira, V. Krelani, M. della Torre, F. Silva, and R. D. Toledo Filho. "Natural Fibres As Promoters Of Autogeneous Healing In HPFRCCS: Results From On-Going Brazil-Italy Cooperation". In: *Durability and Sustainability of Concrete Structures — Workshop Proceedings*. Ed. by M. A. Chiorino, L. Coppola, C. Mazzotti, R. Realfonzo, and P. Riva. Vol. 305. American Concrete Institute, 2015, pp. 11.1–11.10.

[74] J. A. Barros, L. Ferrara, and E. Martinelli, eds. *Recent Advances on Green Concrete for Structural Purposes. The contribution of the EU-FP7 Project EnCoRe*. 1. Springer, Cham, 2017, pp. 1–2. DOI: 10.1007/978-3-319-56797-6.

[75] M. Sahmaran, G. Yildirim, and T. K. Erdem. "Self-healing capability of cementitious composites incorporating different supplementary cementitious materials". *Cement and Concrete Composites* 35.1 (2013), pp. 89–101. DOI: 10.1016/j.cemconcomp.2012.08.013.

[76] J. Qiu, H. S. Tan, and E. H. Yang. "Coupled effects of crack width, slag content, and conditioning alkalinity on autogenous healing of engineered cementitious composites". *Cement and Concrete Composites* 73 (2016), pp. 203–212. DOI: 10.1016/j.cemconcomp.2016.07.013.

[77] K. Van Tittelboom, E. Gruyaert, H. Rahier, and N. De Belie. "Influence of mix composition on the extent of autogenous crack healing by continued hydration or calcium carbonate formation". *Construction and Building Materials* 37 (2012), pp. 349–359. DOI: 10.1016/J.CONBUILDMAT.2012.07.026.

[78] K. Olivier, A. Darquennes, F. Benboudjema, and R. Gagné. "Early-Age Self-Healing of Cementitious Materials Containing Ground Granulated Blast-Furnace Slag under Water Curing". *Journal of Advanced Concrete Technology* 14.11 (2016), pp. 717–727. DOI: 10.3151/jact.14.717.

[79] H. Huang, G. Ye, C. Qian, and E. Schlangen. "Self-healing in cementitious materials: Materials, methods and service conditions". *Materials and Design* 92 (2016), pp. 499–511. DOI: 10.1016/j.matdes.2015.12.091.

[80] C. C. Hung and Y. F. Su. "Medium-term self-healing evaluation of Engineered Cementitious Composites with varying amounts of fly ash and exposure durations". *Construction and Building Materials* 118 (2016), pp. 194–203. DOI: 10.1016/j.conbuildmat.2016.05.021.

[81] E. Gruyaert, K. V. Tittelboom, H. Rahier, and N. D. Belie. "Activation of Pozzolanic and Latent-Hydraulic Reactions by Alkalis in Order to Repair Concrete Cracks". *Journal of Materials in Civil Engineering* 27.7 (2015), p. 04014208. DOI: 10.1061/(ASCE)MT.1943-5533.0001162.

[82] J. Qiu, X. N. Lim, and E. H. Yang. "Fatigue-induced deterioration of the interface between micro-polyvinyl alcohol (PVA) fiber and cement matrix". *Cement and Concrete Research* 90 (2016), pp. 127–136. DOI: 10.1016/j.cemconres.2016.08.021.

[83] D. Palin, H. M. Jonkers, and V. Wiktor. "Autogenous healing of sea-water exposed mortar: Quantification through a simple and rapid permeability test". *Cement and Concrete Research* 84 (2016), pp. 1–7. DOI: 10.1016/j.cemconres.2016.02.011.

[84] S. H. Na, Y. Hama, M. Taniguchi, O. Katsura, T. Sagawa, and M. Zakaria. "Experimental Investigation on Reaction Rate and Self-healing Ability in Fly Ash Blended Cement Mixtures". *Journal of Advanced Concrete Technology* 10.7 (2012), pp. 240–253. DOI: 10.3151/jact.10.240.

[85] D. Jóźwiak-Niedźwiedzka. "Microscopic observations of self-healing products in calcareous fly ash mortars". *Microscopy Research and Technique* 78.1 (2015), pp. 22–29. DOI: 10.1002/jemt.22440.

[86] H. Siad, A. Alyousif, O. K. Keskin, S. B. Keskin, M. Lachemi, M. Sahmaran, and K. M. Hossain. "Influence of limestone powder on mechanical, physical and self-healing behavior of Engineered Cementitious Composites". *Construction and Building Materials* 99 (2015), pp. 1–10. DOI: 10.1016/j.conbuildmat.2015.09.007.

[87] G. Yildirim, M. Sahmaran, and H. U. Ahmed. "Influence of Hydrated Lime Addition on the Self-Healing Capability of High-Volume Fly Ash Incorporated Cementitious Composites". *Journal of Materials in Civil Engineering* 27.6 (2015), p. 04014187. DOI: 10.1061/(ASCE)MT.1943-5533.0001145.

[88] Z. Jiang, W. Li, Z. Yuan, and Z. Yang. "Self-healing of cracks in concrete with various crystalline mineral additives in underground environment". *Journal Wuhan University of Technology, Materials Science Edition* 29.5 (2014), pp. 938–944. DOI: 10.1007/s11595-014-1024-2.

[89] K. A. Shahid, M. F. M. Jaafar, and F. M. Yahaya. "Self-Healing Behaviour of Pre-Cracked POFA-Concretes in different Curing Conditions". *Journal of Mechanical Engineering and Sciences* 7 (2014), pp. 1227–1235. DOI: 10.15282/jmes.7.2014.22.0120.

[90] T. Qureshi, A. Kanellopoulos, and A. Al-Tabbaa. "Autogenous self-healing of cement with expansive minerals-I: Impact in early age crack healing". *Construction and Building Materials* 192 (2018), pp. 768–784. DOI: 10.1016/J.CONBUILDMAT.2018.10.143.

[91] T. Qureshi, A. Kanellopoulos, and A. Al-Tabbaa. "Autogenous self-healing of cement with expansive minerals-II: Impact of age and the role of optimised expansive minerals in healing performance". *Construction and Building Materials* 194 (2019), pp. 266–275. DOI: 10.1016/J.CONBUILDMAT.2018.11.027.

[92] L. Ferrara, V. Krelani, and M. Carsana. "A "fracture testing" based approach to assess crack healing of concrete with and without crystalline admixtures". *Construction and Building Materials* 68 (2014), pp. 535–551. DOI: 10.1016/j.conbuildmat.2014.07.008.

[93] L. Ferrara, V. Krelani, and F. Moretti. "On the use of crystalline admixtures in cement based construction materials: from porosity reducers to promoters of self healing". *Smart Materials and Structures* 25.8 (2016), p. 084002. DOI: 10.1088/0964-1726/25/8/084002.

[94] ACI Committee 212. *Report on Chemical Admixtures for Concrete*. Tech. rep. American Concrete Institute (ACI), 2010.

[95] The Concrete Society. *The Influence of Integral Water-Resisting Admixtures on the Durability of Concrete — Report CS174*. Tech. rep. 2013.

[96] K. Sisomphon, O. Copuroglu, and E. Koenders. "Effect of exposure conditions on self healing behavior of strain hardening cementitious composites incorporating various cementitious materials". *Construction and Building Materials* 42 (2013), pp. 217–224. DOI: 10.1016/J.CONBUILDMAT.2013.01.012.

[97] C. De Nardi, S. Bullo, L. Ferrara, L. Ronchin, and A. Vavasori. "Effectiveness of crystalline admixtures and lime/cement coated granules in engineered self-healing capacity of lime mortars". *Materials and Structures* 50.4 (2017), pp. 1–12. DOI: 10.1617/s11527-017-1053-3.

[98] R. P. Borg, E. Cuenca, E. M. Gastaldo Brac, and L. Ferrara. "Crack sealing capacity in chloride-rich environments of mortars containing different cement substitutes and crystalline admixtures". *Journal of Sustainable Cement-Based Materials* 7.3 (2018), pp. 141–159. DOI: 10.1080/21650373.2017.1411297.

[99] E. Cuenca, G. Cislaghi, M. Puricelli, and L. Ferrara. "Influence of Self-Healing Stimulated via Crystalline Admixtures on Chloride Penetration". *ACI Special Publication* 326 (2018).

[100] E. Cuenca, E. M. Gastaldo Brac, S. Rigamonti, V. Violante, and L. Ferrara. "Self-healing Stimulated by Crystalline Admixtures in Chloride Rich Environments: Is It Possible to Extend the Structure Service Life?" In: *Concrete Durability and Service Life Planning. ConcreteLife 2020. RILEM Bookseries*. Ed. by K. Kovler, S. Zhutovsky, S. Spatari, and O. Jensen. Vol. 26. Springer, Cham, 2020, pp. 141–147. DOI: 10.1007/978-3-030-43332-1_28.

[101] E. Cuenca and L. Ferrara. "Repeatability of Self-Healing in Fiber Reinforced Concretes with and without Crystalline Admixtures: Preliminary Results". *ACI Special Publication* 319 (2017), pp. 11.1–11.18.

[102] L. Ferrara, E. Cuenca, A. Tejedor, and E. G. Brac. "Performance of concrete with and without crystalline admixtures under repeated cracking/healing cycles". *MATEC Web of Conferences* 199 (2018), p. 02016. DOI: 10.1051/MATECCONF/201819902016.

[103] E. Cuenca, A. Tejedor, and L. Ferrara. "A methodology to assess crack-sealing effectiveness of crystalline admixtures under repeated cracking-healing cycles". *Construction and Building Materials* 179 (2018), pp. 619–632. DOI: 10.1016/j.conbuildmat.2018.05.261.

[104] M. Roig-Flores, S. Moscato, P. Serna, and L. Ferrara. "Self-healing capability of concrete with crystalline admixtures in different environments". *Construction and Building Materials* 86 (2015), pp. 1–11. DOI: 10.1016/j.conbuildmat.2015.03.091.

[105] M. Roig-Flores, F. Pirritano, P. Serna, and L. Ferrara. "Effect of crystalline admixtures on the self-healing capability of early-age concrete studied by means of permeability and crack closing tests". *Construction and Building Materials* 114 (2016), pp. 447–457. DOI: 10.1016/j.conbuildmat.2016.03.196.

[106] L. Ferrara, P. Bamonte, C. Suesta, F. Animato, C. Pascale, A. Tretjakov, E. Camacho, P. Deegan, S. Sideri, E. M. Gastaldo, P. Serna, V. Mechtcherine, M. Cruz Alonso, A. Peled, and R. P. Borg. "An Overview on H2020 Project ReSHEALience". In: *Proceedings of the IABSE Symposium 2019 "Towards a Resilient Built Environment - Risk and Asset Management"*. Guimarães, Portugal, 2019, pp. 174–181.

[107] K. Kabiri, H. Omidian, S. A. Hashemi, and M. J. Zohuriaan-Mehr. "Synthesis of fast-swelling superabsorbent hydrogels: Effect of crosslinker type and concentration on porosity and absorption rate". *European Polymer Journal* 39.7 (2003), pp. 1341–1348. DOI: 10.1016/S0014-3057(02)00391-9.

[108] D. Buenger, F. Topuz, and J. Groll. *Hydrogels in sensing applications*. 2012. DOI: 10.1016/j.progpolymsci.2012.09.001.

[109] C. Schröfl, D. Snoeck, and V. Mechtcherine. "A review of characterisation methods for superabsorbent polymer (SAP) samples to be used in cement-based construction materials: report of the RILEM TC 260-RSC". *Materials and Structures* 50.4 (2017), pp. 1–19. DOI: 10.1617/s11527-017-1060-4.

[110] D. Snoeck, L. Pel, and N. De Belie. "The water kinetics of superabsorbent polymers during cement hydration and internal curing visualized and studied by NMR". *Scientific Reports* 7.1 (2017), pp. 1–14. DOI: 10.1038/s41598-017-10306-0.

[111] V. Mechtcherine, C. Schröfl, M. Wyrzykowski, M. Gorges, P. Lura, D. Cusson, J. Margeson, N. De Belie, D. Snoeck, K. Ichimiya, S. I. Igarashi, V. Falikman, S. Friedrich, J. Bokern, P. Kara, A. Marciniak, H. W. Reinhardt, S. Sippel, A. Bettencourt Ribeiro, J. Custódio, G. Ye, H. Dong, and J. Weiss. "Effect of superabsorbent polymers (SAP) on the freeze–thaw resistance of concrete: results of a RILEM interlaboratory study". *Materials and Structures* 50.1 (2017), pp. 1–19. DOI: 10.1617/s11527-016-0868-7.

[112] Y. Yao, Y. Zhu, and Y. Yang. "Incorporation superabsorbent polymer (SAP) particles as controlling pre-existing flaws to improve the performance of engineered cementitious composites (ECC)". *Construction and Building Materials* 28.1 (2012), pp. 139–145. DOI: 10.1016/j.conbuildmat.2011.08.032.

[113] H. X. Lee, H. S. Wong, and N. R. Buenfeld. "Potential of superabsorbent polymer for self-sealing cracks in concrete". *Advances in Applied Ceramics* 109.5 (2010), pp. 296–302. DOI: 10.1179/174367609X459559.

[114] A. Mignon, D. Snoeck, P. Dubruel, S. Van Vlierberghe, N. De Belie, A. Mignon, D. Snoeck, P. Dubruel, S. Van Vlierberghe, and N. De Belie. "Crack Mitigation in Concrete: Superabsorbent Polymers as Key to Success?" *Materials* 10.3 (2017), p. 237. DOI: 10.3390/ma10030237.

[115] D. P. Bentz and J. Weiss. *Internal Curing: A 2010 State-of-the-Art Review*. Tech. rep. Gaithersburg, MD: National Institute of Standards and Technology, 2011. DOI: 10.6028/NIST.IR.7765.

[116] S.-i. Igarashi and A. Watanabe. "Experimental study on prevention of autogenous deformation by internal curing using super-absorbent polymer particles". In: *International RILEM Conference on Volume Changes of Hardening Concrete: Testing and Mitigation*. Ed. by O. M. Jensen, P. Lura, and K. Kovler. RILEM Publications SARL, 2006, pp. 77–86. DOI: 10.1617/2351580052.009.

[117] J. Justs, M. Wyrzykowski, D. Bajare, and P. Lura. "Internal curing by superabsorbent polymers in ultra-high performance concrete". *Cement and Concrete Research* 76 (2015), pp. 82–90. DOI: 10.1016/j.cemconres.2015.05.005.

[118] D. Snoeck, D. Schaubroeck, P. Dubruel, and N. De Belie. "Effect of high amounts of superabsorbent polymers and additional water on the workability, microstructure and strength of mortars with a water-to-cement ratio of 0.50". *Construction and Building Materials* 72 (2014), pp. 148–157. DOI: 10.1016/j.conbuildmat.2014.09.012.

[119] J. Pelto, M. Leivo, E. Gruyaert, B. Debbaut, D. Snoeck, and N. D. Belie. "Application of encapsulated superabsorbent polymers in cementitious materials for stimulated autogenous healing". *Smart Materials and Structures* 26.10 (2017), p. 105043. DOI: 10.1088/1361-665X/AA8497.

[120] E. Gruyaert, B. Debbaut, D. Snoeck, P. Díaz, A. Arizo, E. Tziviloglou, E. Schlangen, and N. De Belie. "Self-healing mortar with pH-sensitive superabsorbent polymers: testing of the sealing efficiency by water flow tests". *Smart Materials and Structures* 25.8 (2016), p. 084007. DOI: 10.1088/0964-1726/25/8/084007.

[121] A. Mignon, D. Snoeck, D. Schaubroeck, N. Luickx, P. Dubruel, S. Van Vlierberghe, and N. De Belie. "pH-responsive superabsorbent polymers: A pathway to self-healing of mortar". *Reactive and Functional Polymers* 93 (2015), pp. 68–76. DOI: 10.1016/j.reactfunctpolym.2015.06.003.

[122] D. Snoeck, S. Steuperaert, K. Van Tittelboom, P. Dubruel, and N. De Belie. "Visualization of water penetration in cementitious materials with superabsorbent polymers by means of neutron radiography". *Cement and Concrete Research* 42.8 (2012), pp. 1113–1121. DOI: 10.1016/J.CEMCONRES.2012.05.005.

[123] H. X. Lee, H. S. Wong, and N. R. Buenfeld. "Self-sealing of cracks in concrete using superabsorbent polymers". *Cement and Concrete Research* 79 (2016), pp. 194–208. DOI: 10.1016/j.cemconres.2015.09.008.

[124] G. Lefever, D. Snoeck, D. G. Aggelis, N. De Belie, S. Van Vlierberghe, and D. Van Hemelrijck. "Evaluation of the Self-Healing Ability of Mortar Mixtures Containing Superabsorbent Polymers and Nanosilica". *Materials* 13.2 (2020), p. 380. DOI: 10.3390/ma13020380.

[125] A. Mignon, D. Snoeck, K. D'Halluin, L. Balcaen, F. Vanhaecke, P. Dubruel, S. Van Vlierberghe, and N. De Belie. "Alginate biopolymers: Counteracting the impact of superabsorbent polymers on mortar strength". *Construction and Building Materials* 110 (2016), pp. 169–174. DOI: 10.1016/J.CONBUILDMAT.2016.02.033.

[126] A. Mignon, D. Devisscher, G. J. Graulus, B. Stubbe, J. Martins, P. Dubruel, N. De Belie, and S. Van Vlierberghe. "Combinatory approach of methacrylated alginate and acid monomers for concrete applications". *Carbohydrate Polymers* 155 (2017), pp. 448–455. DOI: 10.1016/j.carbpol.2016.08.102.

[127] A. E. M. Abd-Elmoaty. "Self-healing of polymer modified concrete". *Alexandria Engineering Journal* 50.2 (2011), pp. 171–178. DOI: 10.1016/j.aej.2011.03.002.

[128] N. Z. Muhammad, A. Shafaghat, A. Keyvanfar, M. Z. A. Majid, S. K. Ghoshal, S. E. Mohammadyan Yasouj, A. A. Ganiyu, M. Samadi Kouchaksaraei, H. Kamyab, M. M. Taheri, M. Rezazadeh Shirdar, and R. McCaffer. "Tests and methods of evaluating the self-healing efficiency of concrete: A review". *Construction and Building Materials* 112 (2016), pp. 1123–1132. DOI: 10.1016/j.conbuildmat.2016.03.017.

[129] P. Lukowski and G. Adamczewski. "Self-repairing of polymer-cement concrete". *Bulletin of the Polish Academy of Sciences: Technical Sciences* 61.1 (2013), pp. 195–200. DOI: 10.2478/bpasts-2013-0018.

[130] G. F. Huseien, J. Mirza, N. F. Ariffin, and M. W. Hussin. "Synthesis and characterization of shelf-healing mortar with modified strength". *Jurnal Teknologi* 76.1 (2015), pp. 195–200.

[131] A. R. Mohd Sam, N. F. Ariffin, M. W. Hussin, H. S. Lee, M. A. Ismail, N. H. Abdul Shukor Lim, N. H. A. Khalid, M. Samadi, J. Mirza, and M. Z. A. Majid. "Performance of epoxy resin as self-healing agent". *Jurnal Teknologi* 77.16 (2015), pp. 9–13. DOI: 10.11113/jt.v77.6386.

[132] B. R. Reddy, F. Liang, and R. Fitzgerald. "Self-healing cements that heal without dependence on fluid contact: A laboratory study". *SPE Drilling and Completion* 25.3 (2010), pp. 309–313. DOI: 10.2118/121555-PA.

[133] X. Z. Yuan, W. Sun, and X. B. Zuo. "Study of Feasibility of Heat Melt Adhesive Being Used in Crack Self-Healing of Cement-Based Materials". In: *Architecture and Building Materials*. Vol. 99. Applied Mechanics and Materials. Trans Tech Publications Ltd, 2011, pp. 1087–1091. DOI: 10.4028/www.scientific.net/AMM.99-100.1087.

[134] C. Romero Rodríguez, S. Chaves Figueiredo, B. Chiaia, and E. Schlangen. "Induction healing of concrete reinforced by bitumen-coated steel fibres". In: *9th International Conference on Fracture Mechanics of Concrete and Concrete Structures*. International Association for Fracture Mechanics of Concrete and Concrete Structures, 2016. DOI: 10.21012/fc9.134.

[135] J. Leng, X. Lan, Y. Liu, and S. Du. "Shape-memory polymers and their composites: Stimulus methods and applications". *Progress in Materials Science* 56.7 (2011), pp. 1077–1135. DOI: 10.1016/j.pmatsci.2011.03.001.

[136] A. Jefferson, C. Joseph, R. Lark, B. Isaacs, S. Dunn, and B. Weager. "A new system for crack closure of cementitious materials using shrinkable polymers". *Cement and Concrete Research* 40.5 (2010), pp. 795–801. DOI: 10.1016/j.cemconres.2010.01.004.

[137] S. van der Zwaag, N. van Dijk, H. Jonkers, S. Mookhoek, and W. Sloof. "Self-healing behaviour in man-made engineering materials: bioinspired but taking into account their intrinsic character". *Philosophical Transactions of the Royal Society A: Mathematical, Physical and Engineering Sciences* 367.1894 (2009), pp. 1689–1704. DOI: 10.1098/rsta.2009.0020.

[138] O. Teall, M. Pilegis, R. Davies, J. Sweeney, T. Jefferson, R. Lark, and D. Gardner. "A shape memory polymer concrete crack closure system activated by electrical current". *Smart Materials and Structures* 27.7 (2018), p. 075016. DOI: 10.1088/1361-665X/AAC28A.

[139] T. Hazelwood, A. D. Jefferson, R. J. Lark, and D. R. Gardner. "Long-term stress relaxation behavior of predrawn poly(ethylene terephthalate)". *Journal of Applied Polymer Science* 131.23 (2014). DOI: 10.1002/app.41208.

[140] R. Davies, O. Teall, M. Pilegis, A. Kanellopoulos, T. Sharma, A. Jefferson, D. Gardner, A. Al-Tabbaa, K. Paine, and R. Lark. "Large Scale Application of Self-Healing Concrete: Design, Construction, and Testing". *Frontiers in Materials* 5 (2018), p. 51. DOI: 10.3389/fmats.2018.00051.

[141] B. Balzano, R. Davies, J. Sweeney, G. Thompson, and A. Jefferson. "Enhanced concrete crack closure with hydrid shape memory polymer tendons". In: *10th International Conference on Fracture Mechanics of Concrete and Concrete Structures (FraMCoS-X)*. Ed. by G. Pijaudier-Cabot, P. Grassl, and C. La Borderie. Bayonne, France, 2019. DOI: 10.21012/FC10.235142.

[142] E. Mostavi, S. Asadi, M. M. Hassan, and M. Alansari. "Evaluation of Self-Healing Mechanisms in Concrete with Double-Walled Sodium Silicate Microcapsules". *Journal of Materials in Civil Engineering* 27.12 (2015), p. 04015035. DOI: 10.1061/(ASCE)MT.1943-5533.0001314.

[143] W. Mao, C. Litina, and A. Al-Tabbaa. "Development and Application of Novel Sodium Silicate Microcapsule-Based Self-Healing Oil Well Cement". *Materials* 13.2 (2020), p. 456. DOI: 10.3390/ma13020456.

[144] J. Wang, H. Soens, W. Verstraete, and N. De Belie. "Self-healing concrete by use of microencapsulated bacterial spores". *Cement and Concrete Research* 56 (2014), pp. 139–152. DOI: 10.1016/J.CEMCONRES.2013.11.009.

[145] A. Kanellopoulos, P. Giannaros, and A. Al-Tabbaa. "The effect of varying volume fraction of microcapsules on fresh, mechanical and self-healing properties of mortars". *Construction and Building Materials* 122 (2016), pp. 577–593. DOI: 10.1016/J.CONBUILDMAT.2016.06.119.

[146] A. Kanellopoulos, P. Giannaros, D. Palmer, A. Kerr, and A. Al-Tabbaa. "Polymeric microcapsules with switchable mechanical properties for self-healing concrete: synthesis, characterisation and proof of concept". *Smart Materials and Structures* 26.4 (2017), p. 045025. DOI: 10.1088/1361-665X/aa516c.

[147] L. Lv, E. Schlangen, Z. Yang, and F. Xing. "Micromechanical Properties of a New Polymeric Microcapsule for Self-Healing Cementitious Materials". *Materials* 9.12 (2016), p. 1025. DOI: 10.3390/ma9121025.

[148] L. Ribeiro de Souza. "Design and synthesis of microcapsules using microfluidics for autonomic self-healing in cementitious materials". PhD Thesis. University of Cambridge, 2017.

[149] L. Lv, Z. Yang, G. Chen, G. Zhu, N. Han, E. Schlangen, and F. Xing. "Synthesis and characterization of a new polymeric microcapsule and feasibility investigation in self-healing cementitious materials". *Construction and Building Materials* 105 (2016), pp. 487–495. DOI: 10.1016/j.conbuildmat.2015.12.185.

[150] A. Guerrero, J. L. G. Calvo, P. Carballosa, G. Perez, V. R. Allegro, E. Erkizia, and J. J. Gaitero. "An Innovative Self-Healing System in Ultra-high Strength Concrete Under Freeze-Thaw Cycles". In: *Nanotechnology in Construction*. Springer International Publishing, 2015, pp. 357–362. DOI: 10.1007/978-3-319-17088-6_46.

[151] G. Perez, J. J. Gaitero, E. Erkizia, I. Jimenez, and A. Guerrero. "Characterisation of cement pastes with innovative self-healing system based in epoxy-amine adhesive". *Cement and Concrete Composites* 60 (2015), pp. 55–64. DOI: 10.1016/j.cemconcomp.2015.03.010.

[152] G. Perez, E. Erkizia, J. J. Gaitero, I. Kaltzakorta, I. Jiménez, and A. Guerrero. "Synthesis and characterization of epoxy encapsulating silica microcapsules and amine functionalized silica nanoparticles for development of an innovative self-healing concrete". *Materials Chemistry and Physics* 165 (2015), pp. 39–48. DOI: 10.1016/j.matchemphys.2015.08.047.

[153] G. Pérez, J. L. G. Calvo, P. Carballosa, V. R. Allegro, J. J. Gaitero, E. Erkizia, and A. Guerrero. "Efficiency of an Innovative Self-Healing System in Ultra-High-Strength Concrete under a Salt Spray Test". In: *CONCREEP 10*. Reston, VA: American Society of Civil Engineers, Sept. 2015, pp. 919–928. DOI: 10.1061/9780784479346.110.

[154] J. L. García Calvo, G. Pérez, P. Carballosa, E. Erkizia, J. J. Gaitero, and A. Guerrero. "Development of ultra-high performance concretes with self-healing micro/nano-additions". *Construction and Building Materials* 138 (2017), pp. 306–315. DOI: 10.1016/j.conbuildmat.2017.02.015.

[155] G. Pérez, J. L. García Calvo, P. Carballosa, R. Tian, V. R. Allegro, E. Erkizia, J. J. Gaitero, and A. Guerrero. "Durability of self-healing ultra-high-strength reinforced micro-concrete under freeze–thaw or chloride attack". *Magazine of Concrete Research* 69.23 (2017), pp. 1231–1242. DOI: 10.1680/jmacr.17.00075.

[156] B. Dong, Y. Wang, W. Ding, S. Li, N. Han, F. Xing, and Y. Lu. "Electrochemical impedance study on steel corrosion in the simulated concrete system with a novel self-healing microcapsule". *Construction and Building Materials* 56 (2014), pp. 1–6. DOI: 10.1016/j.conbuildmat.2014.01.070.

[157] Y. Wang, G. Fang, W. Ding, N. Han, F. Xing, and B. Dong. "Self-immunity microcapsules for corrosion protection of steel bar in reinforced concrete". *Scientific Reports* 5.1 (2015), pp. 1–8. DOI: 10.1038/srep18484.

[158] B. Dong, Y. Wang, G. Fang, N. Han, F. Xing, and Y. Lu. "Smart releasing behavior of a chemical self-healing microcapsule in the stimulated concrete pore solution". *Cement and Concrete Composites* 56 (2015), pp. 46–50. DOI: 10.1016/j.cemconcomp.2014.10.006.

[159] W. Xiong, J. Tang, G. Zhu, N. Han, E. Schlangen, B. Dong, X. Wang, and F. Xing. "A novel capsule-based self-recovery system with a chloride ion trigger". *Scientific Reports* 5.1 (2015), pp. 1–6. DOI: 10.1038/srep10866.

[160] B. Dong, W. Ding, S. Qin, G. Fang, Y. Liu, P. Dong, S. Han, F. Xing, and S. Hong. "3D visualized tracing of rebar corrosion-inhibiting features in concrete with a novel chemical self-healing system". *Construction and Building Materials* 168 (2018), pp. 11–20. DOI: 10.1016/j.conbuildmat.2018.02.094.

[161] B. Dong, W. Ding, S. Qin, N. Han, G. Fang, Y. Liu, F. Xing, and S. Hong. "Chemical self-healing system with novel microcapsules for corrosion inhibition of rebar in concrete". *Cement and Concrete Composites* 85 (2018), pp. 83–91. DOI: 10.1016/j.cemconcomp.2017.09.012.

[162] X. Wang, F. Xing, M. Zhang, N. Han, and Z. Qian. "Experimental Study on Cementitious Composites Embedded with Organic Microcapsules". *Materials* 6.9 (2013), pp. 4064–4081. DOI: 10.3390/ma6094064.

[163] B. Dong, G. Fang, W. Ding, Y. Liu, J. Zhang, N. Han, and F. Xing. "Self-healing features in cementitious material with urea-formaldehyde/epoxy microcapsules". *Construction and Building Materials* 106 (2016), pp. 608–617. DOI: 10.1016/j.conbuildmat.2015.12.140.

[164] X. Wang, P. Sun, N. Han, and F. Xing. "Experimental Study on Mechanical Properties and Porosity of Organic Microcapsules Based Self-Healing Cementitious Composite". *Materials* 10.1 (2017), p. 20. DOI: 10.3390/ma10010020.

[165] D. Palin, V. Wiktor, and H. M. Jonkers. "A bacteria-based bead for possible self-healing marine concrete applications". *Smart Materials and Structures* 25.8 (2016), p. 084008. DOI: 10.1088/0964-1726/25/8/084008.

[166] Y. S. Lee and J. S. Ryou. "Self healing behavior for crack closing of expansive agent via granulation/film coating method". *Construction and Building Materials* 71 (2014), pp. 188–193. DOI: 10.1016/j.conbuildmat.2014.08.045.

[167] P. W. Chen, R. M. Erb, and A. R. Studart. "Designer polymer-based microcapsules made using microfluidics". *Langmuir* 28.1 (2012), pp. 144–152. DOI: 10.1021/la203088u.

[168] C. Litina, A. Kanellopoulos, and A. Al-Tabbaa. "Alternative repair system for concrete using microencapsulated healing agents". In: *Proceedings of Concrete Solutions, 5th International Conference on Concrete Repair*. Ed. by M. Grantham, M. Basheer, B. Magee, and M. Soutsos. Belfast, UK, 2014, pp. 97–103.

[169] J. Wang, A. Mignon, D. Snoeck, V. Wiktor, S. Van Vliergerghe, N. Boon, and N. De Belie. "Application of modified-alginate encapsulated carbonate producing bacteria in concrete: A promising strategy for crack self-healing". *Frontiers in Microbiology* 6 (2015). DOI: 10.3389/fmicb.2015.01088.

[170] H. Huang and G. Ye. "Application of sodium silicate solution as self-healing agent in cementitious materials". In: *International RILEM Conference on Advances in Construction Materials Through Science and Engineering*. Ed. by C. Leung and K. T. Wan. Hong Kong, China: RILEM Publications SARL, Sept. 2011, pp. 530–536.

[171] M. M. Pelletier, R. Brown, A. Shukla, and A. Bose. *Self-healing concrete with a microencapsulated healing agent*. Tech. rep. Kingston. University of Rhode Island, 2011.

[172] J. Gilford, M. M. Hassan, T. Rupnow, M. Barbato, A. Okeil, and S. Asadi. "Dicyclopentadiene and Sodium Silicate Microencapsulation for Self-Healing of Concrete". *Journal of Materials in Civil Engineering* 26.5 (2014), pp. 886–896. DOI: 10.1061/(ASCE)MT.1943-5533.0000892.

[173] P. Giannaros, A. Kanellopoulos, and A. Al-Tabbaa. "Sealing of cracks in cement using microencapsulated sodium silicate". *Smart Materials and Structures* 25.8 (Aug. 2016), p. 084005. DOI: 10.1088/0964-1726/25/8/084005.

[174] N. P. B. Tan, L. H. Keung, W. H. Choi, W. C. Lam, and H. N. Leung. "Silica-based self-healing microcapsules for self-repair in concrete". *Journal of Applied Polymer Science* 133.12 (2016). DOI: 10.1002/app.43090.

[175] C. Dry. "Matrix cracking repair and filling using active and passive modes for smart timed release of chemicals from fibers into cement matrices". *Smart Materials and Structures* 3.2 (1994), pp. 118–123. DOI: 10.1088/0964-1726/3/2/006.

[176] V. C. Li, Y. M. Lim, and Y. W. Chan. "Feasibility study of a passive smart self-healing cementitious composite". *Composites Part B: Engineering* 29.6 (1998), pp. 819–827. DOI: 10.1016/S1359-8368(98)00034-1.

[177] C. Joseph, A. Jefferson, B. Isaacs, R. Lark, and D. Gardner. "Experimental investigation of adhesive-based self-healing of cementitious materials". *Magazine of Concrete Research* 62.11 (2010), pp. 831–843. DOI: 10.1680/macr.2010.62.11.831.

[178] L. Restuccia, A. Reggio, G. A. Ferro, and J. M. Tulliani. "New self-healing techniques for cement-based materials". In: *Procedia Structural Integrity*. Vol. 3. Elsevier B.V., 2017, pp. 253–260. DOI: 10.1016/j.prostr.2017.04.016.

[179] T. Van Mullem, K. Van Tittelboom, E. Gruyaert, R. Caspeele, and N. De Belie. "Development of an improved cracking method to reduce the variability in testing the healing efficiency of self-healing mortar containing encapsulated polymers". *MATEC Web of Conferences* 199 (2018). Ed. by M. Alexander, H. Beushausen, F. Dehn, and P. Moyo, p. 02017. DOI: 10.1051/matecconf/201819902017.

[180] J. Feiteira, V. Couvreur, E. Gruyaert, and N. De Belie. "Resistance to fatigue of self-healed concrete based on encapsulated polymer precursors". In: *Concrete Solutions - Proceedings of Concrete Solutions, 6th International Conference on Concrete Repair*. Ed. by M. G. Grantham, I. Papayianni, and K. Sideris. Thessaloniki, Greece: Taylor & Francis Group, 2016, pp. 585–590.

[181] J. Feiteira, E. Tsangouri, E. Gruyaert, C. Lors, G. Louis, and N. De Belie. "Monitoring crack movement in polymer-based self-healing concrete through digital image correlation, acoustic emission analysis and SEM in-situ loading". *Materials and Design* 115 (2017), pp. 238–246. DOI: 10.1016/j.matdes.2016.11.050.

[182] K. Van Tittelboom. "Self-Healing Concrete through Incorporation of Encapsulated Bacteria- or Polymer-Based Healing Agents". PhD Thesis. Ghent University, 2012.

[183] K. Van Tittelboom, E. Gruyaert, P. De Backer, W. Moerman, and N. De Belie. "Self-repair of thermal cracks in concrete sandwich panels". *Structural Concrete* 16.2 (2015), pp. 273–288. DOI: 10.1002/suco.201400055.

[184] B. Šavija, J. Feiteira, M. Araújo, S. Chatrabhuti, J.-M. Raquez, K. Van Tittelboom, E. Gruyaert, N. De Belie, and E. Schlangen. "Simulation-Aided Design of Tubular Polymeric Capsules for Self-Healing Concrete". *Materials* 10.1 (2016), p. 10. DOI: 10.3390/ma10010010.

[185] G. Anglani, P. Antonaci, S. I. Carillo Gonzales, G. Paganelli, and J.-M. Tulliani. "3D printed capsules for self-healing concrete applications". In: *10th International Conference on Fracture Mechanics of Concrete and Concrete Structures (FraMCoS-X)*. Ed. by G. Pijaudier-Cabot, P. Grassl, and C. La Borderie. Bayonne, France, 2019. DOI: 10.21012/fc10.235356.

[186] C. De Nardi, D. Gardner, and A. D. Jefferson. "Development of 3D Printed Networks in Self-Healing Concrete". *Materials* 13.6 (2020), p. 1328. DOI: 10.3390/ma13061328.

[187] K. Sisomphon, O. Copuroglu, and A. Fraaij. "Application of encapsulated lightweight aggregate impregnated with sodium monofluorophosphate as a self-healing agent in blast furnace slag mortar". *Heron* 56.1-2 (2011), pp. 17–36.

[188] R. Alghamri, A. Kanellopoulos, and A. Al-Tabbaa. "Impregnation and encapsulation of lightweight aggregates for self-healing concrete". *Construction and Building Materials* 124 (2016), pp. 910–921. DOI: 10.1016/J.CONBUILDMAT.2016.07.143.

[189] E. Tziviloglou, V. Wiktor, H. Jonkers, and E. Schlangen. "Bacteria-based self-healing concrete to increase liquid tightness of cracks". *Construction and Building Materials* 122 (2016), pp. 118–125. DOI: 10.1016/J.CONBUILDMAT.2016.06.080.

[190] B. J. Blaiszik, S. L. B. Kramer, S. C. Olugebefola, J. S. Moore, N. R. Sottos, and S. R. White. "Self-Healing Polymers and Composites". *Annual Review of Materials Research* 40 (2010), pp. 179–211. DOI: 10.1146/annurev-matsci-070909-104532.

[191] C. M. Dry. "Repair and prevention of damage due to transverse shrinkage cracks in bridge decks". In: *Smart Structures and Materials 1999: Smart Systems for Bridges, Structures, and Highways*. Ed. by S.-C. Liu. Vol. 3671. International Society for Optics and Photonics. SPIE, 1999, pp. 253–256. DOI: 10.1117/12.348675. URL: https://doi.org/10.1117/12.348675.

[192] H. Mihashi, Y. Kaneko, T. Nishiwaki, and K. Otsuka. "Fundamental Study on Development of Intelligent Concrete Characterized by Self-Healing Capability for Strength". *Transactions of the Japan Concrete Institute* 22 (2000), pp. 441–450. DOI: 10.3151/crt1990.11.2_21.

[193] T. Selvarajoo, R. E. Davies, D. R. Gardner, B. L. Freeman, and A. D. Jefferson. "Characterisation of a vascular self-healing cementitious material system: Flow and curing properties". *Construction and Building Materials* 245 (2020), p. 118332. DOI: 10.1016/j.conbuildmat.2020.118332.

[194] P. Minnebo, G. Thierens, G. De Valck, K. Van Tittelboom, N. De Belie, D. Van Hemelrijck, E. Tsangouri, P. Minnebo, G. Thierens, G. De Valck, K. Van Tittelboom, N. De Belie, D. Van Hemelrijck, and E. Tsangouri. "A Novel Design of Autonomously Healed Concrete: Towards a Vascular Healing Network". *Materials* 10.1 (2017), p. 49. DOI: 10.3390/ma10010049.

[195] T. Selvarajoo, R. E. Davies, B. L. Freeman, and A. D. Jefferson. "Mechanical response of a vascular self-healing cementitious material system under varying loading conditions". *Construction and Building Materials* 254 (2020), p. 119245. DOI: 10.1016/j.conbuildmat.2020.119245.

[196] S. Pareek, K. C. Shrestha, Y. Suzuki, T. Omori, R. Kainuma, and Y. Araki. "Feasibility of externally activated self-repairing concrete with epoxy injection network and Cu-Al-Mn superelastic alloy reinforcing bars". *Smart Materials and Structures* 23.10 (2014), p. 105027. DOI: 10.1088/0964-1726/23/10/105027.

[197] S. Sangadji and E. Schlangen. "Self Healing of Concrete Structures - Novel Approach Using Porous Network Concrete". *Journal of Advanced Concrete Technology* 10.5 (2012), pp. 185–194. DOI: 10.3151/jact.10.185.

[198] Z. Li, L. R. de Souza, C. Litina, A. E. Markaki, and A. Al-Tabbaa. "Feasibility of Using 3D Printed Polyvinyl Alcohol (PVA) for Creating Self-Healing Vascular Tunnels in Cement System". *Materials* 12.23 (2019), p. 3872. DOI: 10.3390/ma12233872.

[199] Z. Li, L. R. de Souza, C. Litina, A. E. Markaki, and A. Al-Tabbaa. "A novel biomimetic design of a 3D vascular structure for self-healing in cementitious materials using Murray's law". *Materials and Design* 190 (2020), p. 108572. DOI: 10.1016/j.matdes.2020.108572.

[200] T. Nishiwaki, H. Mihashi, B.-K. Jang, and K. Miura. "Development of Self-Healing System for Concrete with Selective Heating around Crack". *Journal of Advanced Concrete Technology* 4.2 (2006), pp. 267–275. DOI: 10.3151/jact.4.267.

[201] U. K. Gollapudi, C. L. Knutson, S. S. Bang, and M. R. Islam. "A new method for controlling leaching through permeable channels". *Chemosphere* 30.4 (1995), pp. 695–705. DOI: 10.1016/0045-6535(94)00435-W.

[202] J. Dick, W. De Windt, B. De Graef, H. Saveyn, P. Van Der Meeren, N. De Belie, and W. Verstraete. "Bio-deposition of a calcium carbonate layer on degraded limestone by Bacillus species". *Biodegradation* 17 (2006), pp. 357–367. DOI: 10.1007/s10532-005-9006-x.

[203] W. De Muynck, K. Cox, N. De Belie, and W. Verstraete. "Bacterial carbonate precipitation as an alternative surface treatment for concrete". *Construction and Building Materials* 22 (2008), pp. 875–885. DOI: 10.1016/j.conbuildmat.2006.12.011.

[204] H. M. Jonkers and E. Schlangen. "Crack repair by concrete-immobilized bacteria". In: *1st International Conference on Self Healing Materials*. Noordwijk aan Zee, The Netherlands, 2007, p. 32.

[205] E. Boquet, A. Boronat, and A. Ramos-Cormenzana. "Production of calcite (Calcium carbonate) crystals by soil bacteria is a general phenomenon". *Nature* 246.5434 (1973), pp. 527–529. DOI: 10.1038/246527a0.

[206] R. Zeebe and D. Wolf-Gladrow. *CO2 in Seawater: Equilibrium, Kinetics, Isotopes*. First Edition. Vol. 65. Elsevier Science, 2001, pp. 1–84.

[207] R. Ludwig, F. A. Al-Horani, D. de Beer, and H. M. Jonkers. "Photosynthesis-controlled calcification in a hypersaline microbial mat". *Limnology and Oceanography* 50.6 (2005), pp. 1836–1843. DOI: 10.4319/lo.2005.50.6.1836.

[208] V. Wiktor and H. M. Jonkers. "Quantification of crack-healing in novel bacteria-based self-healing concrete". *Cement and Concrete Composites* 33.7 (2011), pp. 763–770. DOI: 10.1016/j.cemconcomp.2011.03.012.

[209] H. M. Jonkers, V. A. C. Wiktor, M. G. Sierra-Beltran, R. M. Mors, E. Tziviloglou, and D. Palin. *Limestone-producing bacteria make concrete self healing*. Ed. by S. van der Zwaag and E. Brinkman. IOS Press, 2015.

[210] M. G. S. Beltran and H. M. Jonkers. *Ceramic Processing Research Crack self-healing technology based on bacteria*. Tech. rep. 1. 2015, pp. 33–39.

[211] V. Wiktor and H. M. Jonkers. "Field performance of bacteria-based repair system: Pilot study in a parking garage". *Case Studies in Construction Materials* 2 (2015), pp. 11–17. DOI: 10.1016/j.cscm.2014.12.004.

[212] M. D. Hager, S. van der Zwaag, and U. S. Schubert, eds. *Self-healing Materials*. Vol. 273. Advances in Polymer Science. Cham: Springer International Publishing, 2016. DOI: 10.1007/978-3-319-32778-5.

[213] R. M. Mors and H. M. Jonkers. "Feasibility of lactate derivative based agent as additive for concrete for regain of crack water tightness by bacterial metabolism". *Industrial Crops and Products* 106 (2017), pp. 97–104. DOI: 10.1016/j.indcrop.2016.10.037.

[214] H. M. Jonkers, A. Thijssen, G. Muyzer, O. Copuroglu, and E. Schlangen. "Application of bacteria as self-healing agent for the development of sustainable concrete". *Ecological Engineering* 36 (2010), pp. 230–235. DOI: 10.1016/j.ecoleng.2008.12.036.

[215] K. Van Tittelboom, N. De Belie, W. De Muynck, and W. Verstraete. "Use of bacteria to repair cracks in concrete". *Cement and Concrete Research* 40.1 (2010), pp. 157–166. DOI: 10.1016/j.cemconres.2009.08.025.

[216] J. Y. Wang, N. De Belie, and W. Verstraete. "Diatomaceous earth as a protective vehicle for bacteria applied for self-healing concrete". *Journal of Industrial Microbiology & Biotechnology* 39.4 (2012), pp. 567–577. DOI: 10.1007/s10295-011-1037-1.

[217] J. Wang, D. Snoeck, S. Van Vlierberghe, W. Verstraete, and N. De Belie. "Application of hydrogel encapsulated carbonate precipitating bacteria for approaching a realistic self-healing in concrete". *Construction and Building Materials* 68 (2014), pp. 110–119. DOI: 10.1016/J.CONBUILDMAT.2014.06.018.

[218] Y. Ç. Erşan, F. B. Da Silva, N. Boon, W. Verstraete, and N. De Belie. "Screening of bacteria and concrete compatible protection materials". *Construction and Building Materials* 88 (2015), pp. 196–203. DOI: 10.1016/J.CONBUILDMAT.2015.04.027.

[219] I. Karatas. "Microbiological improvement of the physical properties of soils". PhD Thesis. Arizona State University, 2008.

[220] L. A. van Paassen, C. M. Daza, M. Staal, D. Y. Sorokin, W. van der Zon, and M. C. van Loosdrecht. "Potential soil reinforcement by biological denitrification". *Ecological Engineering* 36.2 (2010), pp. 168–175. DOI: 10.1016/j.ecoleng.2009.03.026.

[221] Y. Ç. Erşan, N. de Belie, and N. Boon. "Microbially induced $CaCO_3$ precipitation through denitrification: An optimization study in minimal nutrient environment". *Biochemical Engineering Journal* 101 (2015), pp. 108–118. DOI: 10.1016/j.bej.2015.05.006.

[222] Y. Ç. Erşan, H. Verbruggen, I. De Graeve, W. Verstraete, N. De Belie, and N. Boon. "Nitrate reducing $CaCO_3$ precipitating bacteria survive in mortar and inhibit steel corrosion". *Cement and Concrete Research* 83 (2016), pp. 19–30. DOI: 10.1016/j.cemconres.2016.01.009.

[223] Y. Ç. Erşan, E. Hernandez-Sanabria, N. Boon, and N. De Belie. "Enhanced crack closure performance of microbial mortar through nitrate reduction". *Cement and Concrete Composites* 70 (2016), pp. 159–170. DOI: 10.1016/j.cemconcomp.2016.04.001.

[224] T. A. Söylev and M. G. Richardson. "Corrosion inhibitors for steel in concrete: State-of-the-art report". *Construction and Building Materials* 22.4 (2008), pp. 609–622. DOI: 10.1016/j.conbuildmat.2006.10.013.

[225] F. B. da Silva, N. Boon, N. De Belie, and W. Verstraete. "Industrial Application of Biological Self-healing Concrete: Challenges and Economical Feasibility". *Journal of Commercial Biotechnology* 21.1 (2015). DOI: 10.5912/jcb662.

[226] F. B. da Silva, N. De Belie, N. Boon, and W. Verstraete. "Production of non-axenic ureolytic spores for self-healing concrete applications". *Construction and Building Materials* 93 (2015), pp. 1034–1041. DOI: https://doi.org/10.1016/j.conbuildmat.2015.05.049.

[227] Y. Ç. Erşan, E. Gruyaert, G. Louis, C. Lors, N. De Belie, and N. Boon. "Self-protected nitrate reducing culture for intrinsic repair of concrete cracks". *Frontiers in Microbiology* 6 (2015), p. 1228. DOI: 10.3389/fmicb.2015.01228.

[228] J. Zhang, A. Zhou, Y. Liu, B. Zhao, Y. Luan, S. Wang, X. Yue, and Z. Li. "Microbial network of the carbonate precipitation process induced by microbial consortia and the potential application to crack healing in concrete". *Scientific Reports* 7.1 (2017), pp. 1–10. DOI: 10.1038/s41598-017-15177-z.

[229] H. M. Jonkers and A. Thijssen. "Bacteria mediated remediation of concrete structures". In: *2nd International Symposium on Service Life Design for Infrastructures*. Ed. by K. Van Breugel, G. Ye, and Y. Yuan. Delft, the Netherlands: RILEM Publications SARL, 2010, pp. 833–840.

[230] B. Liu, J. L. Ke, X. Deng, G. M. Zhu, Y. C. Luo, N. X. Han, and F. Xing. "A waterproof epoxy resin microcapsule for the encapsulation of self healing bacterium". In: *Proceedings of the Fifth International Conference on Self-Healing Materials*. Durham, NC, USA, June 2015, pp. 22–24.

[231] N. De Belie, J. Wang, Z. B. Bundur, and K. Paine. "Bacteria based concrete". In: *Eco-efficient Repair and Rehabilitation of Concrete Infrastructures*. Ed. by F. Pacheco-Torgal, R. E. Melchers, X. Shi, N. De Belie, K. Van Tittelboom, and A. Sáez. 1st Edition. Woodhead Publishing, 2017. DOI: 10.1016/c2016-0-04100-1.

[232] E. Tziviloglou, V. Wiktor, J. Wang, K. Paine, M. Alazhari, A. Richardson, M. Gueguen, N. De Belie, E. Schlangen, and H. Jonkers. "Evaluation of experimental methodology to assess the sealing efficiency of bacteria-based self-healing concrete: Round Robin test". In: *International RILEM Conference on Microorganisms-Cementitious Materials Interactions*. Ed. by V. Wiktor, H. Jonkers, and A. Bertron. RILEM Publications SARL, 2016, pp. 156–170.

[233] Y. Ç. Erşan, N. De Belie, and N. Boon. "Resilient denitrifiers wink at microbial self-healing concrete". *International Journal of Environmental Engineering* 2.1 (2015), pp. 28–32.

[234] S. Bhaskar, K. M. Anwar Hossain, M. Lachemi, G. Wolfaardt, and M. Otini Kroukamp. "Effect of self-healing on strength and durability of zeolite-immobilized bacterial cementitious mortar composites". *Cement and Concrete Composites* 82 (2017), pp. 23–33. DOI: 10.1016/j.cemconcomp.2017.05.013.

[235] J. Zhang, Y. Liu, T. Feng, M. Zhou, L. Zhao, A. Zhou, and Z. Li. "Immobilizing bacteria in expanded perlite for the crack self-healing in concrete". *Construction and Building Materials* 148 (2017), pp. 610–617. DOI: 10.1016/j.conbuildmat.2017.05.021.

[236] Z. B. Bundur, M. J. Kirisits, and R. D. Ferron. "Use of pre-wetted lightweight fine expanded shale aggregates as internal nutrient reservoirs for microorganisms in bio-mineralized mortar". *Cement and Concrete Composites* 84 (2017), pp. 167–174. DOI: 10.1016/j.cemconcomp.2017.09.003.

[237] S. Gupta, H. W. Kua, and S. D. Pang. "Healing cement mortar by immobilization of bacteria in biochar: An integrated approach of self-healing and carbon sequestration". *Cement and Concrete Composites* 86 (2018), pp. 238–254. DOI: 10.1016/j.cemconcomp.2017.11.015.

[238] H. Chen, C. Qian, and H. Huang. "Self-healing cementitious materials based on bacteria and nutrients immobilized respectively". *Construction and Building Materials* 126 (2016), pp. 297–303. DOI: 10.1016/j.conbuildmat.2016.09.023.

[239] M. Alazhari, T. Sharma, A. Heath, R. Cooper, and K. Paine. "Application of expanded perlite encapsulated bacteria and growth media for self-healing concrete". *Construction and Building Materials* 160 (2018), pp. 610–619. DOI: 10.1016/j.conbuildmat.2017.11.086.

[240] M. Seifan, A. Ebrahiminezhad, Y. Ghasemi, A. K. Samani, and A. Berenjian. "Amine-modified magnetic iron oxide nanoparticle as a promising carrier for application in bio self-healing concrete". *Applied Microbiology and Biotechnology* 102.1 (2018), pp. 175–184. DOI: 10.1007/s00253-017-8611-z.

[241] M. Seifan, A. K. Sarmah, A. Ebrahiminezhad, Y. Ghasemi, A. K. Samani, and A. Berenjian. "Bio-reinforced self-healing concrete using magnetic iron oxide nanoparticles". *Applied Microbiology and Biotechnology* 102.5 (2018), pp. 2167–2178. DOI: 10.1007/s00253-018-8782-2.

[242] R. Mors and H. Jonkers. "Effect on Concrete Surface Water Absorption upon Addition of Lactate Derived Agent". *Coatings* 7.4 (2017), p. 51. DOI: 10.3390/coatings7040051.

[243] L. Mercuri, C. Romero Rodríguez, Y. Xu, S. Chaves Figueiredo, R. Mors, E. Rossi, G. Anglani, P. Antonaci, B. Šavija, and E. Schlangen. "On the role of soft inclusions on the fracture behaviour of cement paste". In: *10th International Conference on Fracture Mechanics of Concrete and Concrete Structures (FraMCoS-X)*. Ed. by G. Pijaudier-Cabot, P. Grassl, and C. La Borderie. Bayonne, France, 2019. DOI: 10.21012/fc10.235271.

[244] C. Romero Rodriguez, F. F. de Mendonca Filho, L. Mercuri, Y. Gan, E. Rossi, G. Anglani, P. Antonaci, E. Schlangen, and B. Šavija. "Chemo-physico-mechanical properties of the interface zone between bacterial PLA self-healing capsules and cement paste". *Cement and Concrete Research* (Submitted).

[245] J. Wang, J. Dewanckele, V. Cnudde, S. Van Vlierberghe, W. Verstraete, and N. De Belie. "X-ray computed tomography proof of bacterial-based self-healing in concrete". *Cement and Concrete Composites* 53 (2014), pp. 289–304. DOI: 10.1016/j.cemconcomp.2014.07.014.

[246] D. Palin, V. Wiktor, and H. M. Jonkers. "A Bacteria-Based Self-Healing Cementitious Composite for Application in Low-Temperature Marine Environments". *Biomimetics* 2.4 (2017), p. 13. DOI: 10.3390/biomimetics2030013.

[247] R. Mors and H. M. Jonkers. "Bacteria-based self-healing concrete: evaluation of full scale demonstrator projects". *RILEM Technical Letters* 4 (2020), pp. 138–144. DOI: 10.21809/rilemtechlett.2019.93.

[248] N. de Belie, T. Van Mullem, E. Gruyaert, and P. Van den Heede. "Self-healing concrete to increase service life of a roof plate for an inspection pit in the Oosterweel link : healing efficiency and preliminary service life estimation". In: *Proceedings of the 4th International Conference on Service Life Design for Infrastructures (SLD4)*. Ed. by G. Ye, Y. Yuan, C. Romero Rodriguez, H. Zhang, and B. Šavija. Delft, the Netherlands: RILEM Publications S.A.R.L., 2018, pp. 429–436.

[249] T. Van Mullem, E. Gruyaert, R. Caspeele, and N. De Belie. "First Large Scale Application with Self-Healing Concrete in Belgium: Analysis of the Laboratory Control Tests". *Materials* 13.4 (2020), p. 997. DOI: 10.3390/ma13040997.

[250] G. Anglani, P. Antonaci, G. Idone, and J.-M. Tulliani. "Self-healing of cementitious materials via embedded macro-capsules". In: *Proceedings of the 4th International Conference on Service Life Design for Infrastructures (SLD4)*. Ed. by G. Ye, Y. Yuan, C. Romero Rodriguez, H. Zhang, and B. Šavija. Delft, the Netherlands: RILEM Publications S.A.R.L., 2018, pp. 385–388.

[251] G. Anglani, P. Antonaci, J.-M. Tulliani, K. Van Tittelboom, J. Wang, and N. De Belie. "Self-healing efficiency of cement-based materials containing extruded cementitious hollow tubes filled with bacterial healing agent". In: *Final Conference of RILEM TC 253-MCI: Microorganisms-Cementitious Materials Interactions*. Ed. by A. Bertron and H. Jonkers. Toulouse, France: RILEM Publications S.A.R.L., 2018, pp. 425–431.

[252] G. Anglani, J.-M. Tulliani, and P. Antonaci. "Behaviour of Pre-Cracked Self-Healing Cementitious Materials under Static and Cyclic Loading". *Materials* 13.5 (2020), p. 1149. DOI: 10.3390/MA13051149.

[253] G. Anglani, T. Van Mullem, X. Zhu, J. Wang, P. Antonaci, N. De Belie, J. M. Tulliani, and K. Van Tittelboom. "Sealing efficiency of cement-based materials containing extruded cementitious capsules". *Construction and Building Materials* 251 (2020), p. 119039. DOI: 10.1016/j.conbuildmat.2020.119039.

[254] S. Tsivilis, E. Chaniotakis, G. Kakali, and G. Batis. "An analysis of the properties of Portland limestone cements and concrete". *Cement and Concrete Composites* 24.3-4 (2002), pp. 371–378. DOI: 10.1016/S0958-9465(01)00089-0.

[255] N. Voglis, G. Kakali, E. Chaniotakis, and S. Tsivilis. "Portland-limestone cements. Their properties and hydration compared to those of other composite cements". *Cement and Concrete Composites* 27.2 (2005), pp. 191–196. DOI: 10.1016/j.cemconcomp.2004.02.006.

[256] T. Matschei, B. Lothenbach, and F. P. Glasser. "The role of calcium carbonate in cement hydration". *Cement and Concrete Research* 37.4 (2007), pp. 551–558. DOI: 10.1016/j.cemconres.2006.10.013.

[257] H. Paiva, L. M. Silva, J. A. Labrincha, and V. M. Ferreira. "Effects of a water-retaining agent on the rheological behaviour of a single-coat render mortar". *Cement and Concrete Research* 36.7 (2006), pp. 1257–1262. DOI: 10.1016/j.cemconres.2006.02.018.

[258] B. Mu, Z. Li, S. N. Chui, and J. Peng. "Cementitious composite manufactured by extrusion technique". *Cement and Concrete Research* 29.2 (1999), pp. 237–240. DOI: 10.1016/S0008-8846(98)00097-0.

[259] H. Lombois-Burger, P. Colombet, J. Halary, and H. Van Damme. "Kneading and extrusion of dense polymer–cement pastes". *Cement and Concrete Research* 36.11 (2006), pp. 2086–2097. DOI: 10.1016/J.CEMCONRES.2006.08.001.

[260] A. M. Rashad. "Metakaolin as cementitious material: History, scours, production and composition-A comprehensive overview". *Construction and Building Materials* 41 (2013), pp. 303–318. DOI: 10.1016/j.conbuildmat.2012.12.001.

[261] Y. Ohama. *Handbook of Polymer-Modified Concrete and Mortars*. First Edition. Elsevier, 1995, p. 246.

[262] L. K. Aggarwal, P. C. Thapliyal, and S. R. Karade. "Properties of polymer-modified mortars using epoxy and acrylic emulsions". *Construction and Building Materials* 21.2 (2007), pp. 379–383. DOI: 10.1016/j.conbuildmat.2005.08.007.

[263] A. Passuello, G. Moriconi, and S. P. Shah. "Cracking behavior of concrete with shrinkage reducing admixtures and PVA fibers". *Cement and Concrete Composites* 31.10 (2009), pp. 699–704. DOI: 10.1016/j.cemconcomp.2009.08.004.

[264] M. Safiuddin and K. A. Soudki. "Sealer and coating systems for the protection of concrete bridge structures". *International Journal of Physical Sciences* 6.37 (2011), pp. 8188–8199. DOI: 10.5897/IJPSX11.005.

[265] K. Sisomphon, O. Çopuroğlu, and A. Fraaij. "Durability of blast-furnace slag mortars subjected to sodium monofluorophosphate application". *Construction and Building Materials* 25.2 (2011), pp. 823–828. DOI: 10.1016/J.CONBUILDMAT.2009.09.010.

[266] J. LaRosa Thompson, P. Gill, B. Scheetz, and M. Silsbee. "Sodium silicate applications for cement and concrete". In: *Proceeding of the 10th International Congress on the Chemistry of Cement*. Gothenburg, Sweden, 1997, p. 8.

[267] J. LaRosa Thompson, M. Silsbee, P. Gill, and B. Scheetz. "Characterization of silicate sealers on concrete". *Cement and Concrete Research* 27.10 (1997), pp. 1561–1567. DOI: 10.1016/S0008-8846(97)00167-1.

[268] S. S. Kouassi, M. T. Tognonvi, J. Soro, and S. Rossignol. "Consolidation mechanism of materials obtained from sodium silicate solution and silica-based aggregates". *Journal of Non-Crystalline Solids* 357.15 (2011), pp. 3013–3021. DOI: 10.1016/j.jnoncrysol.2011.04.006.

[269] N. Latifi, A. Eisazadeh, and A. Marto. "Strength behavior and microstructural characteristics of tropical laterite soil treated with sodium silicate-based liquid stabilizer". *Environmental Earth Sciences* 72.1 (2014), pp. 91–98. DOI: 10.1007/s12665-013-2939-1.

[270] F. Pakir, A. Marto, N. Z. M. Yunus, S. A. A. Tajudin, and C. S. Tan. "Effect of Sodium Silicate as Liquid based Stabilizer on Shear Strenght of Marine Clay". *Jurnal Teknologi* 2 (2015), pp. 45–50.

[271] P. Palmero, A. Formia, J.-M. Tulliani, and P. Antonaci. "Processing and applications of geopolymers as sustainable alternative to traditional cement". In: *5th International Conference on Development, Energy, Environment, Economics (DEEE '14)*. Ed. by F. Batzias, N. Mastorais, and C. Giarnaccia. Florence, Italy, 2014, pp. 213–221.

[272] P. Palmero, A. Formia, P. Antonaci, S. Brini, and J.-M. Tulliani. "Geopolymer technology for application-oriented dense and lightened materials. Elaboration and characterization". *Ceramics International* 41.10 (2015), pp. 12967–12979. DOI: 10.1016/j.ceramint.2015.06.140.

[273] M. McDonald and J. LaRosa Thompson. "Sodium silicate a binder for the 21st century". *The PQ Corporation* (2003).

[274] E. McGettigan. "Silicon-based weatherproofing materials". *Concrete International* 14.6 (1992), pp. 52–56.

[275] L. Jiang, X. Xue, W. Zhang, J. Yang, H. Zhang, Y. Li, R. Zhang, Z. Zhang, L. Xu, J. Qu, J. Song, and J. Qin. "The investigation of factors affecting the water impermeability of inorganic sodium silicate-based concrete sealers". *Construction and Building Materials* 93 (2015), pp. 729–736. DOI: 10.1016/j.conbuildmat.2015.06.001.

[276] I. Prasetia. "The Ineffectiveness of Sodium Based Surface Treatment on the Mitigation of Alkali Silica Reaction". *International Journal of Advances in Engineering & Technology* 8.4 (2015), pp. 466–474.

[277] Z. Song, X. Xue, Y. Li, J. Yang, Z. He, S. Shen, L. Jiang, W. Zhang, L. Xu, H. Zhang, J. Qu, W. Ji, T. Zhang, L. Huo, B. Wang, X. Lin, and N. Zhang. "Experimental exploration of the waterproofing mechanism of inorganic sodium silicate-based concrete sealers". *Construction and Building Materials* 104 (2016), pp. 276–283. DOI: 10.1016/j.conbuildmat.2015.12.069.

[278] A. Negro, J. M. Tulliani, and L. Montanaro. *Scienza e Tecnologia dei Materiali*. Turin, Italy: CELID, 2001, p. 264.

[279] W. J. McCoy and A. G. Caldwell. "New Approach to Inhibiting Alkali-Aggregate Expansion". *ACI Journal Proceedings* 47.5 (1951). DOI: 10.14359/12030.

[280] M. Ait Ouarabi, P. Antonaci, F. Boubenider, A. Gliozzi, and M. Scalerandi. "Ultrasonic Monitoring of the Interaction between Cement Matrix and Alkaline Silicate Solution in Self-Healing Systems". *Materials* 10.1 (2017), p. 46. DOI: 10.3390/ma10010046.

[281] G. Anglani, P. Antonaci, A. S. Gliozzi, and M. Scalerandi. "Ultrasonic investigation on the fracture-healing mechanism due to alkaline silicate solutions". In: *ICF 2017 - 14th International Conference on Fracture*. Ed. by E. E. Gdoutos. Vol. 1. Rhodes, Greece: International Conference on Fracture, 2017, pp. 120–121.

[282] A. S. Gliozzi, M. Scalerandi, G. Anglani, P. Antonaci, and L. Salini. "Correlation of elastic and mechanical properties of consolidated granular media during microstructure evolution induced by damage and repair". *Physical Review Materials* 2.1 (2018), p. 013601. DOI: 10.1103/PhysRevMaterials.2.013601.

[283] M. Roos and S. Giessler-Blank. "Keeping moisture at bay - Sustainable concrete protection with siloxane based admixtures". *European Coatings Journal* 4 (2012), pp. 10–14.

[284] A. M. U. B. Attanayaka, O. Duyar, X. Liang, H. Aktan, and K. Ng. "Fundamentals of Use of Penetrating Sealants for Concrete Bridge Deck Protection". In: *82nd Annual Meeting of the Transportation Research Board (TRB)*. Washington, D.C., USA, 2003, p. 19.

[285] J.-G. Dai, Y. Akira, F. Wittmann, H. Yokota, and P. Zhang. "Water repellent surface impregnation for extension of service life of reinforced concrete structures in marine environments: The role of cracks". *Cement and Concrete Composites* 32.2 (2010), pp. 101–109. DOI: 10.1016/j.cemconcomp.2009.11.001.

[286] H. Y. Sun, Z. Yang, G. L. Shan, N. Xu, and G. X. Sun. "Current situation of research and application of silicone water repellent for protecting reinforced concrete". In: *Bridge Maintenance, Safety, Management and Life Extension - Proceedings of the 7th International Conference of Bridge Maintenance, Safety and Management, IABMAS 2014*. Taylor and Francis - Balkema, 2014, pp. 2495–2502.

[287] K. Bilba, M. A. Arsene, and A. Ouensanga. "Sugar cane bagasse fibre reinforced cement composites. Part I. Influence of the botanical components of bagasse on the setting of bagasse/cement composite". *Cement and Concrete Composites* 25.1 (2003), pp. 91–96. DOI: 10.1016/S0958-9465(02)00003-3.

[288] M. A. Sawpan, K. L. Pickering, and A. Fernyhough. "Effect of various chemical treatments on the fibre structure and tensile properties of industrial hemp fibres". *Composites Part A: Applied Science and Manufacturing* 42.8 (2011), pp. 888–895. DOI: 10.1016/j.compositesa.2011.03.008.

[289] D. Snoeck, P. A. Smetryns, and N. De Belie. "Improved multiple cracking and autogenous healing in cementitious materials by means of chemically-treated natural fibres". *Biosystems Engineering* 139 (2015), pp. 87–99. DOI: 10.1016/j.biosystemseng.2015.08.007.

[290] A. Ravve. *Principles of Polymer Chemistry*. Third Edition. New York, NY, USA: Springer, 2012, pp. 1–801. DOI: 10.1007/978-1-4614-2212-9.

[291] F. Hammes and W. Verstraete. "Key roles of pH and calcium metabolism in microbial carbonate precipitation". *Reviews in Environmental Science and Biotechnology* 1.1 (2002), pp. 3–7. DOI: 10.1023/A:1015135629155.

[292] T. Nishiwaki, J. de B. Leite, and H. Mihashi. "High performance fibre reinforced cementitious composites: a sustainable building material for controlling water permeability". In: *International RILEM Symposium on Environment-Conscious Materials and Systems for Sustainable Development*. Koriyama, Japan, 2004, pp. 279–286.

[293] B. Van Belleghem, K. Van Tittelboom, and N. De Belie. "Efficiency of self-healing cementitious materials with encapsulated polyurethane to reduce water ingress through cracks". *Materiales de Construccion* 68.330 (2018), e159. DOI: 10.3989/mc.2018.05917.

[294] Y. A. Villagrán Zaccardi, N. M. Alderete, and N. De Belie. "Improved model for capillary absorption in cementitious materials: Progress over the fourth root of time". *Cement and Concrete Research* 100 (2017), pp. 153–165. DOI: 10.1016/j.cemconres.2017.07.003.

[295] K. J. Shin, W. Bae, S.-W. Choi, M. W. Son, and K. M. Lee. "Parameters influencing water permeability coefficient of cracked concrete specimens". *Construction and Building Materials* 151 (2017), pp. 907–915. DOI: 10.1016/j.conbuildmat.2017.06.093.

[296] S. Jacobsen, J. Marchand, and L. Boisvert. "Effect of cracking and healing on chloride transport in OPC concrete". *Cement and Concrete Research* 26.6 (1996), pp. 869–881. DOI: 10.1016/0008-8846(96)00072-5.

[297] J. Ollivier, J. Maso, and B. Bourdette. "Interfacial transition zone in concrete". *Advanced Cement Based Materials* 2.1 (1995), pp. 30–38. DOI: 10.1016/1065-7355(95)90037-3.

[298] K. L. Scrivener, A. K. Crumbie, and P. Laugesen. "The Interfacial Transition Zone (ITZ) Between Cement Paste and Aggregate in Concrete". *Interface Science* 12.4 (2004), pp. 411–421. DOI: 10.1023/B:INTS.0000042339.92990.4c.

[299] D. Snoeck and N. De Belie. "From straw in bricks to modern use of microfibers in cementitious composites for improved autogenous healing – A review". *Construction and Building Materials* 95 (2015), pp. 774–787. DOI: 10.1016/J.CONBUILDMAT.2015.07.018.

[300] B. Pang, Z. Zhou, P. Hou, P. Du, L. Zhang, and H. Xu. "Autogenous and engineered healing mechanisms of carbonated steel slag aggregate in concrete". *Construction and Building Materials* 107 (2016), pp. 191–202. DOI: 10.1016/j.conbuildmat.2015.12.191.

[301] Z. Yang, J. Hollar, X. He, and X. Shi. "A self-healing cementitious composite using oil core/silica gel shell microcapsules". *Cement and Concrete Composites* 33.4 (2011), pp. 506–512. DOI: 10.1016/J.CEMCONCOMP.2011.01.010.

[302] V. M. C. F. Cunha, J. A. O. Barros, and J. M. Sena-Cruz. "Pullout Behavior of Steel Fibers in Self-Compacting Concrete". *Journal of Materials in Civil Engineering* 22.1 (2010), pp. 1–9. DOI: 10.1061/(ASCE)MT.1943-5533.0000001.

[303] G. Ferrara, B. Coppola, L. Di Maio, L. Incarnato, and E. Martinelli. "Tensile strength of flax fabrics to be used as reinforcement in cement-based composites: experimental tests under different environmental exposures". *Composites Part B: Engineering* 168 (2019), pp. 511–523. DOI: 10.1016/j.compositesb.2019.03.062.

[304] A. E. Naaman and H. Hammoud. "Fatigue characteristics of high performance fiber-reinforced concrete". *Cement and Concrete Composites* 20.5 (1998), pp. 353–363. DOI: 10.1016/S0958-9465(98)00004-3.

[305] S. P. Singh and S. K. Kaushik. "Fatigue strength of steel fibre reinforced concrete in flexure". *Cement and Concrete Composites* 25.7 (2003), pp. 779–786. DOI: 10.1016/S0958-9465(02)00102-6.

[306] A. G. Graeff, K. Pilakoutas, K. Neocleous, and M. V. N. Peres. "Fatigue resistance and cracking mechanism of concrete pavements reinforced with recycled steel fibres recovered from post-consumer tyres". *Engineering Structures* 45 (2012), pp. 385–395. DOI: 10.1016/j.engstruct.2012.06.030.

[307] T. D. P. Thao, T. J. S. Johnson, Q. S. Tong, and P. S. Dai. "Implementation of self-healing in concrete – Proof of concept". *The IES Journal Part A: Civil & Structural Engineering* 2.2 (2009), pp. 116–125. DOI: 10.1080/19373260902843506.

[308] CEN - European Committee for Standardization. *Eurocode 2. Design of Concrete Structures—Part 1–1: General Rules and Rules for Buildings*. 2004.

[309] X. Chen, J. Bu, X. Fan, J. Lu, and L. Xu. "Effect of loading frequency and stress level on low cycle fatigue behavior of plain concrete in direct tension". *Construction and Building Materials* 133 (2017), pp. 367–375. DOI: 10.1016/j.conbuildmat.2016.12.085.

[310] E. Poveda, G. Ruiz, H. Cifuentes, R. C. Yu, and X. Zhang. "Influence of the fiber content on the compressive low-cycle fatigue behavior of self-compacting SFRC". *International Journal of Fatigue* 101 (2017), pp. 9–17. DOI: 10.1016/j.ijfatigue.2017.04.005.

[311] L. Sui, Q. Zhong, K. Yu, F. Xing, P. Li, and Y. Zhou. "Flexural fatigue properties of ultra-high performance engineered cementitious composites (UHP-ECC) reinforced by polymer fibers". *Polymers* 10.8 (2018). DOI: 10.3390/polym10080892.

[312] Z. Jun and H. Stang. "Fatigue performance in flexure of fiber reinforced concrete". *ACI Materials Journal* 95.1 (1998), pp. 58–67. DOI: 10.14359/351.

[313] B. T. Huang, Q. H. Li, and S. L. Xu. "Fatigue Deformation Model of Plain and Fiber-Reinforced Concrete Based on Weibull Function". *Journal of Structural Engineering (United States)* 145.1 (2019). DOI: 10.1061/(ASCE)ST.1943-541X.0002237.

[314] D. M. Carlesso, A. de la Fuente, and S. H. P. Cavalaro. "Fatigue of cracked high performance fiber reinforced concrete subjected to bending". *Construction and Building Materials* 220 (2019), pp. 444–455. DOI: 10.1016/j.conbuildmat.2019.06.038.

[315] F. Germano, G. Tiberti, and G. Plizzari. "Post-peak fatigue performance of steel fiber reinforced concrete under flexure". *Materials and Structures* 49.10 (2016), pp. 4229–4245. DOI: 10.1617/s11527-015-0783-3.

[316] B. Coppola, L. Di Maio, P. Scarfato, and L. Incarnato. "Use of polypropylene fibers coated with nano-silica particles into a cementitious mortar". In: *AIP Conference Proceedings*. Vol. 1695. 1. American Institute of Physics Inc., 2015, p. 020056. DOI: 10.1063/1.4937334.

[317] J. Qiu, X. N. Lim, and E. H. Yang. "Fatigue-induced in-situ strength deterioration of micro-polyvinyl alcohol (PVA) fiber in cement matrix". *Cement and Concrete Composites* 82 (2017), pp. 128–136. DOI: 10.1016/j.cemconcomp.2017.06.002.

[318] T. Jefferson, E. Javierre, B. Freeman, A. Zaoui, E. Koenders, and L. Ferrara. "Research Progress on Numerical Models for Self-Healing Cementitious Materials". *Advanced Materials Interfaces* 5.17 (2018), p. 1701378. DOI: 10.1002/admi.201701378.

[319] T. Van Mullem, G. Anglani, M. Dudek, H. Vanoutrive, G. Bumanis, C. Litina, A. Kwiecień, A. Al-Tabbaa, D. Bajare, T. Stryszewska, R. Caspeele, K. Van Tittelboom, J. M. Tulliani, E. Gruyaert, P. Antonaci, and N. De Belie. "Addressing the need for standardization of test methods for self-healing concrete: an inter-laboratory study on concrete with macrocapsules". *Science and Technology of Advanced Materials* (2020). DOI: 10.1080/14686996.2020.1814117.

[320] I. Arganda-Carreras, V. Kaynig, J. Schindelin, A. Cardona, and H. S. Seung. "Trainable Weka Segmentation : A Machine Learning Tool for Microscopy Image Segmentation". *Bioinformatics* 33.15 (2016), pp. 2424–2426. DOI: 10.1111/exd.12463.

[321] J. Schindelin, I. Arganda-Carreras, E. Frise, V. Kaynig, M. Longair, T. Pietzsch, S. Preibisch, C. Rueden, S. Saalfeld, B. Schmid, J. Y. Tinevez, D. J. White, V. Hartenstein, K. Eliceiri, P. Tomancak, and A. Cardona. *Fiji: An open-source platform for biological-image analysis*. 2012. DOI: 10.1038/nmeth.2019.

[322] C. Romero Rodríguez, S. Chaves Figueiredo, M. Deprez, D. Snoeck, E. Schlangen, and B. Šavija. "Numerical investigation of crack self-sealing in cement-based composites with superabsorbent polymers". *Cement and Concrete Composites* 104 (2019), p. 103395. DOI: 10.1016/j.cemconcomp.2019.103395.

[323] C. Romero Rodriguez, M. Deprez, F. F. de Mendonca Filho, S. van Offenwert, V. Cnudde, E. Schlangen, and B. Šavija. "X-Ray Micro Tomography of Water Absorption by Superabsorbent Polymers in Mortar". In: *3rd International Conference on the Application of Superabsorbent Polymers (SAP) and Other New Admixtures Towards Smart Concrete. SAP 2019. RILEM Bookseries*. Ed. by W. P. Boshoff, V. Mechtcherine, R. Combrinck, and M. Wyrzykowsk. Vol. 24. Skukuza, South Africa: Springer, Cham, 2020, pp. 29–37. DOI: https://doi.org/10.1007/978-3-030-33342-3_4.

[324] The GIMP Development Team. *GIMP*. Version 2.10.4. URL: https://www.gimp.org.

[325] C. M. Aldea, W. J. Song, J. S. Popovics, and S. P. Shah. "Extent of healing of cracked normal strength concrete". *Journal of Materials in Civil Engineering* 12.1 (2000), pp. 92–96. DOI: 10.1061/(ASCE)0899-1561(2000)12:1(92).

[326] K. Van Tittelboom, K. Adesanya, P. Dubruel, P. Van Puyvelde, and N. De Belie. "Methyl methacrylate as a healing agent for self-healing cementitious materials". *Smart Materials and Structures* 20.12 (2011), p. 125016. DOI: 10.1088/0964-1726/20/12/125016.

[327] V. Mechtcherine and M. Lieboldt. "Permeation of water and gases through cracked textile reinforced concrete". *Cement and Concrete Composites* 33.7 (2011), pp. 725–734. DOI: 10.1016/j.cemconcomp.2011.04.001.

[328] S. T. Yi, T. Y. Hyun, and J. K. Kim. "The effects of hydraulic pressure and crack width on water permeability of penetration crack-induced concrete". *Construction and Building Materials* 25.5 (2011), pp. 2576–2583. DOI: 10.1016/j.conbuildmat.2010.11.107.

[329] G. Z. Voyiadjis and P. I. Kattan. "Healing and super healing in continuum damage mechanics". *International Journal of Damage Mechanics* 23.2 (2014), pp. 245–260. DOI: 10.1177/1056789513491773.

[330] C. Oucif, G. Z. Voyiadjis, P. I. Kattan, and T. Rabczuk. "Nonlinear Superhealing and Contribution to the Design of a New Strengthening Theory". *Journal of Engineering Mechanics* 144.7 (2018), p. 04018055. DOI: 10.1061/(ASCE)EM.1943-7889.0001484.

[331] C. Oucif and L. M. Mauludin. "Continuum damage-healing and super healing mechanics in brittle materials: A state-of-the-art reviews". *Applied Sciences* 8.12 (2018), p. 2350. DOI: 10.3390/app8122350.

This Ph.D. thesis has been typeset by means of the TEX-system facilities. The typesetting engine was pdfLATEX. The document class was `toptesi`, by Claudio Beccari, with option `tipotesi=scudo`. This class is available in every up-to-date and complete TEX-system installation.